Aspects of the distribution of Na^+,K^+ ATPase in cultured cells with particular reference to the effects of fluid shear stress

Cindy Lazarus

A thesis submitted in partial fulfilment of the requirements for the degree of Doctor of Philosophy at the University of St Andrews

School of Biomedical Sciences

University of St Andrews,

December, 2000

ABSTRACT

A two-part study was conducted into aspects of the distribution of Na^+,K^+ ATPase α-1 and β-1subunits in HeLa and bovine aortic endothelial cells (BAECs). The primary experimental emphasis was to examine Na^+,K^+ ATPase distribution in relation to cell type, cell morphology and age using immunocytochemical, Western blot analysis, ^3H ouabain assays and various cell permeabilisation techniques. This forms Part I of the study. Part II of the study focussed on the potential up/down regulation in addition to changes in Na^+K^+ATPase distribution throughout the cytoskeleton under the influence of laminar fluid shear stress.

Initially aspects of HeLa cell morphology were examined using anthroylouabain, a fluorescence derivative of the cardiac glycoside ouabain. It was discovered that affinity for ouabain in HeLa cells decreases for cells that are actively dividing whereas confluent cells exhibit a 3-fold increase in sensitivity to ouabain. Initial findings by Lamb (1996) showed that the dissociation constant K_d for ouabain binding to the sodium pump of HeLa cells is dependent on cell morphology. Results of this study show that rounder cells take up more anthroylouabain compared to flatter cells. Laser scanning confocal microscopy reveals this was not an artefact of differing depth of cells, but a real difference of *ca.* 5-fold. Further studies examined BAECs in addition to HeLa cells in order to compare the quantity of ouabain binding between young and old cells. The results demonstrate that both HeLa cells and BAECs used for experimentation at Day 4 after plating have similar levels of ouabain binding, whereas BAECs harvested at Day 14 show less ouabain binding in comparison to younger cells (one-way ANOVA $F_{2,56}=8.60$, $p<0.001$). Different pre-treatments were used before BAEC cells were stained for the α-1 subunit of the Na pump and actin. These were permeabilising with SDS (sodium dodecylsulphate) and hypotonically rupturing the cell membrane. The aim was to expose antigenic sites in intra-cellular compartments leading to the augmentation of α-1 subunit staining. Results of this experiment showed α-1 subunits a similar distribution pattern to actin. However it is difficult to state with certainty that there is an actual co-localisation.

BAECs were subjected to steady laminar shear stresses using specialised parallel plate chambers of 15 and 50 dyn cm^{-2}. Immunocytochemical techniques were used to reveal any physical differences in pump distribution after exposure to flow stresses. In addition Western blot analysis was used to explore possible up or down regulation of the α-1 subunit. Results indicate that under a flow stress of 50 dyn cm^{-2} for 4 hours there is a marked change in sodium pump distribution from the cell periphery to the cytoplasm. In addition, there are concurrent and specific morphological changes in BAECs i.e. reorganisation and alignment of actin stress fibres with the direction of flow. Protein estimations derived from gel densitometry analysis of ECLs for cells sheared at 15 and 50 cm^{-2} over a time course experiment showed no significant difference with either time or flow stress (two-way ANOVA without replication: df=1, F=32.85 $p=0.001$). Additional experiments were designed to expose cells to the same shear magnitude but then incubate them for 8 hours at 37°C to look for down or up-regulation of sodium pump protein over time. Shearing under a flow stress of 50 cm^{-2} produced a characteristic bell-shaped distribution over time. Statistical analysis showed a significant difference with time and flow stress (two-way ANOVA with replication df=7, F=4.47, $p=0.033$) indicating possible up-regulation of pump protein after incubation.

Acknowledgements

This thesis is a product of a long, uphill struggle and no-one could be more please to see the end of their PhD thesis than I.

I shall never forget the day I set out on my journey to travel 3,500 miles across the Atlantic to embark on one of the most special, exciting and hopefully inspiring periods in my life. The tearful goodbye to my parents in the airport, with my life packed up into two of the biggest suitcases imaginable there was no turning back as I headed towards the gate. Full of nervous anticipation as the plane took off, the last of the New York sunshine was beaming on my face so brightly I could barely keep my eyes open to view the final images of home. My eyes fell shut to a movie-like visual of pictures, places, and faces of everyone, everywhere, and everything I had just given up to take on this challenge. It was sad. The sorrow of leaving family and friends as well as the uncertainty of what was to come reminded me of a song, which will always stick in my mind and still takes me back to that very point time.

> "Lost in thought and lost in time, while the seeds of life and the seeds of change were planted – I took a heavenly ride through our silence I knew the waiting had begun - And headed straight... into the shining sun."
>
> *-Pink Floyd, Division Bell.*

The next series of events shattered any romantic illusions I might have had! My initial greeting into the Bute School of Biomedical Sciences was non-existent, with my 'initial' supervisor not showing up to the department until one month after my arrival. His personal technician was not there at the time, nor was anyone in the department expecting an overseas student. This leads me to my first acknowledgement and my very first friend in the department, Iain Laurie. Iain is the senior technician on "D-Floor" who noticed me rattling around with no direction and no supervisor. Promptly taking me under his wing, I had my first tour of the department as well as my first kind words. Over my time on D-floor in the Bute 'Uncle Iain' has really fought my corner, supporting me through times where I felt totally isolated, unwanted and under scrutiny for use of laboratory space and equipment. Over the years Iain has called me his "wee angel". He has always been a listening ear, and he wiped away many tears of frustration. Such a sterling chap shall always be heartily remembered.

From my lab, I would like to start by thanking my biggest in-lab support, Dr. Rebecca Pritchard. A woman after me own heart – I shall never forget "operation rescue Stinky" (AKA Jacque Mouzole), a wise decision I must say! You and I have a time tested friendship and I thank you for all of your support! A 'thank you' to Dr. Eric Flitney for his efforts and for providing me with a facility to carry out this research and for stimulating my interest in fluid shear stress. Also, from his lab I would like to thank Mrs. Jean Melville, an excellent technician and overall lovely woman who provided daily motivation and structure to my days, as well as broadened my technical experience. And lastly Catherine Beers - for calibrating the chambers and making available all the relevant data.

There are a few others in the department I would like to mention. Dr. Colin Nicol for finding me a functional lab to use radioactive material in, as well as a tissue culture hood when I was officially booted out of the D-floor facility. I appreciate your support in the department. Dr. Jeff Graves for all of his statistical advice. Dr. Brian Cohen for helping to sort out a very big 'gel-problem'. With my time swiftly running short your expert buffer advice really saved my PhD! Dr. Amanda Fleet... where do I start? Finding me teaching in the department, copious cups of tea, advice, use of Eyes-higha the good luck lizard and the lovely new addition 'Hey-Zeus', always having an E.G.S on standby, and not to mention NACHOS... The list could go on. I thank you for ALL your friendship and support! Mr. John Mackie for his skill and patience on the confocal, the ever-so skilled Mr. Murray Coutes whose calming mannerism took charge with a sweet smile to the panic of "MURRAY-FIX"! (your picture and phone extension still remains above the gel electrophoresis rig). A thank you to all the porters and cleaners in the Bute who always greeted me with big smiles and big hearts over the years, the Bute building would have been a pretty lonely place without you! Thank you to the lads in the photographic unit (Sean, Dave and Jim) for all your expertise and help! And a brief thank you to Professor Dave Paterson for accepting me into the Gatty Marine Laboratory as a refugee, and never throwing me off the computer or scanner in my times of panic. A special thank you to Dr. Ali Mobasheri (Liverpool University) for all your support and advice along the way and for providing me with a bit of inspiration regarding Na+,K+ ATPase.

To my friends from home I can't thank you enough for all your loving support. Through all of the letters, calls, and many, many e-mails over the years I can't begin to tell you how I appreciate the words, 'I miss you, I can't wait to see you, and I love you.' In leaving the world you know you swiftly learn who the people are at your side.

I am a very fortunate young lady! A special mention to those of you who traversed the Atlantic to visit me, the New York invasion of Britain will long be remembered.

> "When you can't find the light to guide you through a cloudy day, when the stars ain't shining bright and you feel like you've lost your way, when the candle light from home burns so very far away, ahhh ya gotta let your soulshine just like my daddy used to say. He used to say soulshine, it's better then sunshine, it's better then the moonshine, it's damn sure better then rain! Yea now people don't mind, we all get this way sometimes, ya gotta let your soulshine, shine till the break of day."
>
> *- The Allman Brothers Blues Band*

And the good Lord knows it sure does rain here! Being so far away from home for so long has been hard. A special mention to Dr. Gus Xhudo who has been like a brother to me over the years, and I think the very person I should blame/thank? for my decision to undertake this task. Miss Paula Briscoe my surrogate sister (and Jen E.Dawg) and Dr. Colin Davidson (Coin-Raghrrrr) I thank you for the endless loving support you give me!

To the friends I have made in the UK, I hope to hold onto you from the other side of the pond! You have really helped make my time here. Your assistance in refining my taste for fine whisky and warm beers will be everlasting in my memory (not to mention coining the term To Shayler a Pint). There are many people actively on the forefront in my life here, and I have become good-friends with them and their families. I shall always warmly remember our time spent together. A special mention to The St. Andrews Ju Jitsu Club (Sensei Robert Ross and Family) and the St. Andrews Water Polo Club. A BIG thank you to a fellow countryman Dr. Scot Hagerthey for your statistical advice, use of your computer, desk, chair, office, you name it? You have been so very understanding throughout my write up I can't thank you enough for your support. I will never forget your 'hoover–patrol' or the crazed sheep incident. Thank God for those cattle grids!

A very special acknowledgement goes to Dr. Kevin Black, who is (and has been) my best friend, and a stalwart in my life throughout my whole PhD experience! I couldn't possibly put to words in the amount of space I have here all you have done for me, but I will certainly take this opportunity to graciously thank you! You are my fondest memory of the UK and in our travels you have shown me some of the most amazing little corners of the world I otherwise would never have seen. You have filled my memory banks with castles, cathedrals and mystery, not to mention some of Britains most beautiful landscapes and scenery. As well you have supported me through, and helped me over, some of my toughest hurdles. You have been my sounding board, [and punching bag on the Ju Jitsu mats], you have calmed my worries, distributed many hugs and certainly wiped away many tears of frustration. I thank you for your patience support over
the years - you are an amazing friend - Rwy'n dy garu di.

I would like to dedicate this thesis to my family Lester, Julia and Wendy Lazarus.

In September 1996 my parents were in a near-fatal car accident, leaving my mother relatively immobile for several months and my father on a respirator for six-months with a long road to recovery ahead. At the time of the accident my sister selflessly put her PhD on academic suspension and returned to the states to pull the family together. If it were not for my sister's sacrifice, I would not have completed this PhD. I admire your strength Wendy, you have always been the biggest inspiration to me! I am very fortunate to have all of my family, who has faithfully and lovingly supported me over the years. I thank my family for giving me courage and for the tremendous amounts of faith they have in me. You have all been 'the wind beneath my wings'. I love you!

Declarations

I, Cindy Lazarus, hereby certify that this thesis, which is approximately 48,895 words in length, has been written by me, that it is the record of work carried out by me and that it has not been submitted in any other previous application for a higher degree.

Date 21/04/00 Signature of Candidat

I was admitted as a research student in October, 1995 and as a candidate degree of Ph.D. in October, 1996; the higher study for which this is a record was carried out in the University of St. Andrews between 1995 and 2000

Date 21/04/00 Signature of Candic

I hereby certify that the candidate has fulfilled the conditions of the Resolution and Regulations appropriate for the degree of Ph.D. in the University of St. Andrews and that the candidate is qualified to submit this thesis in application for that degree.

Date 21/04/00 Signature of Supervisor

Unrestricted

In submitting this thesis to the University of St. Andrews I understand that I am giving permission for it to be made available for use in accordance with the regulations of the University Library for the time being in force, subject to any copyright vested in the work not being affected thereby. I also understand that the title and abstract will be published, and that a copy of the work may be made and supplied to any *bona fide* library or research worker.

Date 21/04/00 Signature of Candi

Table of Contents

Part I

Part II

Part III

List of Figures

Part I

Part II

List of Tables

Part I

Part II

Notation

a	Half the plate spacing
α	Alpha subunit
ADPKD	Autosomal dominant polysistic kidney disease
AE-1(2)	Anion exchanger –1(2)
AMOG	Adhesion molecule on glial
Aϕ	Anthroylouabain
APS	Ammonium persulfate
ATPase	Adenosine triphosphatase
β	Beta subunit
b	half height of channel
BAEC's	Bovine aortic endothelial cells
bFGF	Basic fibroblast growth factor
B_{max}	Maximum number of binding sites
BME	Beta-mercaptoethanol
BSA	Bovine serum albumin
Ca^{+}	Calcium
CAM	Cell adhesion molecule
CD3(4)	Cytoplasmic domain 3(4)
CFTR	Cystic fibrosis transmembrane conductance
Dabco	1,4-diazabicyclo[2,2,2] octane
DAG	1,2-diacylglycerol
DMEM	Dulbecco's modification Eagels medium
DMSO	Dimethyl sulfoxide
dU/dz	Local velocity gradient
Dynes/cm^2	Units of flow shear
E	Enzyme
EBSS	Earle's based salt solution
ECACC	European collection of Animal cell cultures
EC's	Endothelial cells
ECL	Enhanced chemiluminescence
EDF	Epidermal growth factor
EDTA	Ethylenediaminetetraacetic acid
EGTA	Ethyleneglycoltetraacetic acid
eNOS	Endothelial nitric oxide synthase
ES	Enzyme-substrate complex
FBCS	Foetal bovine calf serum
F-actin	Filamentous actin
FITC	Fluorescein Isothiocyanate
FSS	Fluid shear stress
Fn	Fibrinectin
γ	Gamma subunit
G-actin	Golbular actin
GAMF	Goat anti-mouse fluorescein
G58K	Golgi apparatus antibody

H^+	Hydrogen
H_2O	Water
^{3}H-ouabain	Tritiated ouabain
HeLa cells	Henrietta Lacks cells
HSP-70	70kDa heat shock protein
ICAM-1	Intracellular adhesion molecule-1
IgG	Immunoglobulin
IP_3	Insoitol-1,4,5-triphosphate
$0K^+$	Zero potassium Krebs solution
$5K^+$	5mM potassium Krebs solution
K^+	Potassium
K_d	Dissociation constant
kD	Kilodalton (1 Dalton = mass of 1 hydrogen atom)
K_m	Michaelis Menten constant of an enzyme for a particular substrate
l	distance between pressure ports (cm)
LSC	Liquid scintillation counting
MAP	Mitogen-activated pathway
MDCK	Madin-Darby canine kidney cells
MCP-1	Monocyte chemoattractant protein-1
min.	Minutes
Mg^{2+}	Magnesium
MTOC	Microtubule organising centre
mRNA	Messenger ribonucleic acid
Na^+, K^+, ATPase	The sodium potassium pump
Na^+	Sodium
NFκB	Nuclear factor kappa B
NGS	Normal goat serum
nM	Nanomolar
NO	Nitric oxide
NP-40	Nonidet P-40
η	Viscosity (molecular)
ϕ	Ouabain
°C	Degrees centigrade
ΔP	Pressure drop (cm of H_2O)
ΔP/l	Pressure drop per unit length
PBS	Phosphate buffered saline
PBSc	Phosphate buffered saline (complete)
PBSt	Phosphate buffered saline (tween)
PDGF-B	Platelet derived growth factor B chain
PGI_2	Prostaglandin I_2 (prostacyclin)
PKA	Protein kinase A
PKC	Protein kinase C
PMSF	Phenylmethylsulfonyl fluoride
Q	Volumetric flow

R	Radial location outward from the
centre	of the artery
r=0	At the centreline
r=a	At the wall
RNA	Ribonucleic acid
S	Substrate
SAMP	Sheep anti-mouse peroxidase
SDS	Sodium Dodecyl Sulphate
SHR	Spontaneously hypertensive rats
SHHR	Stroke-prone spontaneously hypertensive rats
SSRE	Shear stress response element
τ	Shear stress
T_3	Triiodothyronine
T_4	Thyroxine
TC	Tissue culture
TEMED	N,N,N',N'-tetramethylenediamide
TM	Thrombomodulin
TMRITC	Tetramethylrhodamine
Isothiocynate/	rhodamine
tPA	Tissue plasminogen activator
Tween-20	Polyoxyethylene-sorbitan monolaurate
μ (or ν or η)	Dynamic viscosity
V_0	Initial rate of substrate concentration [S]
V_{max}	Maximum rate
VSMC	Vascular smooth muscle cells
W	Width of channel
WKY	Wister-Kyoto rats
X	Concentration of ligand [^{3}H ouabain]

Part I

Part I

The sodium potassium pump

1.1 Introduction

The enzyme sodium - potassium adenosine triphosphatase (Na^+, K^+ ATPase) is an integral membrane protein found in virtually all cells (Shull and Lingrel, 1987). Also known as the sodium pump, the enzyme translocates three Na^+ ions and two K^+ ions across the plasma membrane against their electrochemical gradients, and is responsible for maintaining ionic balance across the plasma membrane of the cell (Glynn and Karlish, 1975). Each cycle of translocation is dependent on magnesium (Mg^+) and the hydrolysis of ATP (DeWeer, 1985).

One of the earliest studies of the cell membrane demonstrated the capacity of the cell to regulate volume based on the osmotic strength of the surrounding medium (Nageli, 1855, cited in Overton, 1902). In 1902, Overton expanded on these observations and developed ideas about the permeability of plant and animal membranes to Na^+ and K^+ (reviewed by Glynn, 1993). Studies by Dean (1941) demonstrated the active movement of Na^+ and K^+ ions against their concentration gradients. In experiments on muscle recovering from periods of activity or cold storage, Dean noted that Na^+ and K^+ ions moved in an "uphill" fashion and was the first to term this process a "pump" mechanism (Dean, 1941). In experiments using the crab nerve, Skou isolated an ATP hydrolysing enzyme which required the presence of Mg^{2+}, Na^+ and K^+ (Skou, 1957). Together, this fundamental work demonstrated the prime function of the sodium pump: namely, to effect the movement of sodium and potassium ions

against their concentration gradients using the hydrolysis of ATP as an energy source.

1.2 The function of the sodium pump

Na^+, K^+ ATPase is found ubiquitously in the plasma membrane of animal cells and plays an essential role in the life of the cell (Sweadner, 1989). The principle function of the protein is to maintain high intracellular levels of K^+ (~140mM) and a low intracellular concentration of Na^+ (~ 5-15mM) against a large chemical gradient. Extracellular concentrations of K^+ and Na^+ are ~ 5mM and ~145mM respectively (Alberts *et al.*, 1989). The process of translocating ions against their concentration gradients requires energy that is provided by the hydrolysis of one molecule of ATP to ADP and P_i. This maintains a steep concentration gradient for the ions (Schwartz *et al.*, 1975; Sweadner, 1995). The chemical gradients created by the pump are fundamental to fulfil a range of physiological functions. These functions include: volume regulation; Na^+ and water reabsorption from the glomerular filtrates in kidney cells; the maintenance of resting membrane potential and intracellular pH through Na-H exchange (Rindler and Saier, 1981; Rossier *et al.*, 1987; Skou and Essmann, 1992).

The pump operates with a stoichiometry of $3Na^+$: $2K^+$ and is electrogenic through the export of one net positive charge for each transport cycle (DeWeer and Rakowski; 1984, Glynn, 1985). The maintenance of cellular ionic homeostasis via Na^+, K^+ ATPase requires large quantities of energy from the cell (see Figure 1.1). Non-excitable cells use approximately a third of the cell's

total energy requirement. In electrically active tissues, Na^+, K^+ ATPase consumes nearly two-thirds (Mercer, 1993).

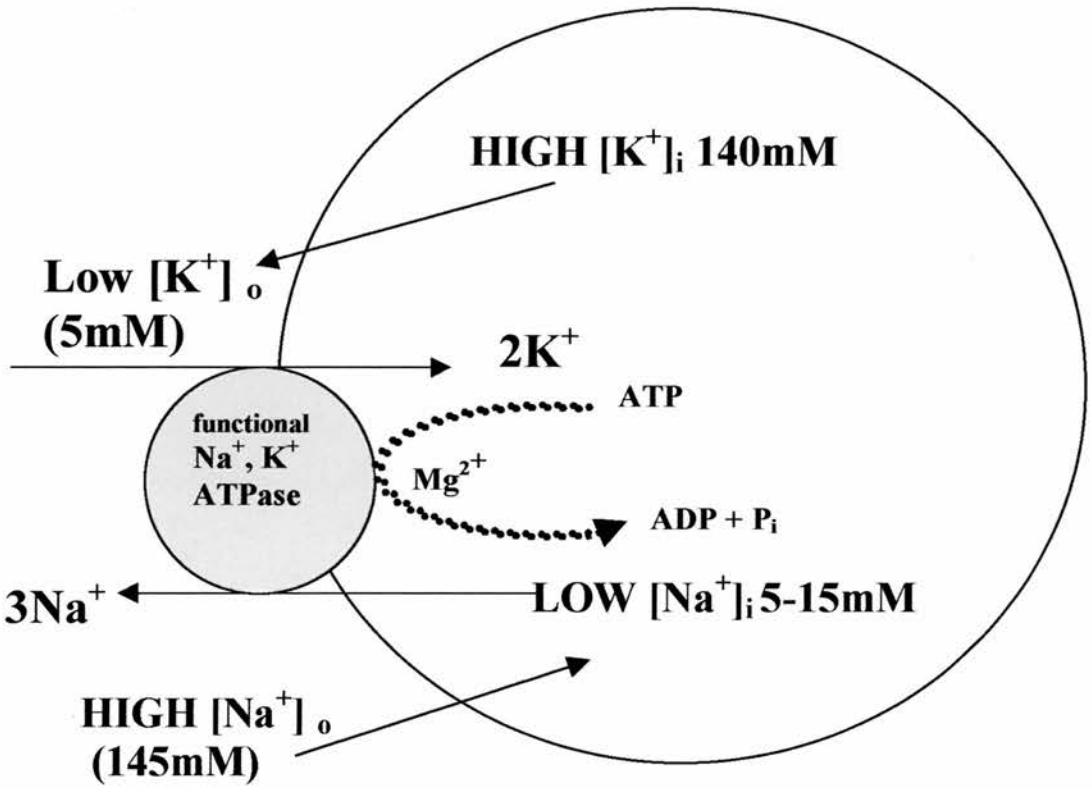

Figure 1.1 A schematic diagram (adapted from Vander *et al.*, 1994) showing the comparison of intracellular and extracellular ion concentrations in a typical mammalian cell. The concentration of Na^+ ions is approximately 10 times higher extracellularly, whereas the concentration of K^+ is higher intracellularly. Energy derived from the hydrolysis of ATP by Na^+, K^+ ATPase maintains these electrochemical gradients (Jorgensen, 1986, Alberts *et al*, 1994). The arrows indicate a steep concentration gradient.

1.3 Structure of the sodium pump

1.3.1. Subunit structure.

Na^+, K^+ ATPase is a heterodimer consisting of two polypeptide chains, α and β. The α subunit (110 –112 kD) is noncovalently linked to a smaller β subunit (35 kD). The β subunit is glycosylated in up to three positions showing molecular weights of approximately 40-60kD (Rossier *et al.*, 1987). Both subunits are essential for enzymatic activity (Lytton *et al.*, 1985; Tamkun and Fambrough, 1986; Pressley, 1992; Mc Donough *et al.*, 1990; Sweadner, 1995). In some cell types (for example, renal epithelial cells), a third subunit has been isolated (γ subunit) with molecular weight of approximately 10kD. The function of the γ subunit is poorly understood. Initially it was suggested that it may be a breakdown product of the α and β subunits and was not required for normal functioning of the pump (Collins and Leszyk, 1987; Harris and Stahl, 1988; Sweadner, 1989; McDonough *et al.*, 1990). Now it is believed that the γ subunit is an important component of renal Na^+, K^+ ATPase. Topological models of the pump are still in question. The α subunit spans the membrane approximately 10 times with both the COOH and NH_2-terminus in the cytosol (Lingrel *et al.*, 1994; Shainskaya and Karlish, 1994). The α subunit plays the key functional role in the catalytic cycle. It carries specific binding sites for nucleotides, cations, and cardiac glycosides (Schwartz *et al.*, 1975). Present models depict little of the α subunit to be exposed on the extracellular surface. The β subunit is an N-linked glycoprotein (three asparagine-linked carbohydrate groups) with three disulfide bridges, and spans the membrane only once leaving the NH_2-terminus in the cytosol. Unlike the α subunit, the majority of the β subunit is

extracellular (Sweadner, 1995). The role of the β subunit is not clearly defined, and little is known about its function in the catalytic cycle. However, it is essential for functioning of the pump, since separation from the α subunit leads to irreversible loss of function (Sweadner, 1989; Chow and Forte, 1995). It is believed that enzymatic activity is initiated when the α and β subunits form a heterodimer, however there is much controversy as to whether this is actually the active form of the enzyme (Glynn, 1985; Jorgensen, 1982). Lamb (personal communication, 1995) suggests that there may be non-functional pumps in the membrane. The actual enzymatic activity of newly synthesised pumps is still poorly understood. It is suggested that the β subunit may play a role in the biosynthesis and targeting of the enzyme to the plasma membrane (McDonough *et al.*, 1990; Geering, 1991; Sweadner, 1995). Evidence shows the β subunit acts as a receptor or a stabiliser for newly synthesised α subunits escorting their transport out of the endoplasmic reticulum (Martinez *et al.*, 1994; Lecuona *et al.*, 1996). Synthesis of the subunits occurs when mRNAs are co-translationally inserted into the membrane of the rough endoplasmic reticulum. Assembled subunits are exported from the endoplasmic reticulum and sent to the Golgi apparatus for further modifications before they are sent to the plasma membrane (Lescale-Matys *et al.*, 1993; Scheiner-Bobis *et al.*, 1994; Chow and Forte, 1995). Experiments on turnover and degradation of both newly synthesised and mature α and β subunits indicate that intracellular accumulation of the β subunit exceeds the amount of the intracellular α subunit. This shows that the subunits are not synthesised in a 1:1 α to β stoichiometry (Lescale-Matys *et al.*, 1993) with the excess intracellular pools of the β subunit presumably degraded.

There has been controversy throughout the literature about the number of times the α subunit spans the membrane (Goldshleger *et al*, 1995). The amino acid sequences of the α and β subunits are arranged into three groups according to the properties of their side chains; hydrophobic side-chains, uncharged hydrophilic side-chains and ionic side-chains (Jorgensen, 1982). A large portion of the subunits' hydrophobicity comes from residues with large aromatic side chains. In the α subunit the hydrophobic region comprises approximately 45% and approximately 42% in the β (Jorgensen, 1982). Hydropathy analysis estimates the average hydrophobicity of groups of amino acids sequentially along the length of a polypeptide (Kyte and Doolittle 1982). Based on this type of analysis, the α subunit is thought to traverse the membrane approximately 6-11 times (Lingrel *et al.*, 1990; Arzamazova *et al.*, 1988) whereas the β subunit is found to span the membrane only once (Shull *et al.*, 1986). Antibody labelling of different amino acid sequences of the α and β subunit has been used to determine cellular locations of membrane spanning regions. From these experiments, it has been suggested that the N terminus of the α subunit is located in the cytosol, with the C terminus on the extracellular surface (Arzamazova *et al.*, 1988; Bayer, 1990; Goldshleger *et al*, 1995). These results suggest that the α subunit traverses the membrane an uneven number of times locating the C terminus in the cytosol. Further experiments using proteolysis techniques suggest that there could be approximately seven trans-membrane domains. However, results from X-ray crystallography and protease digestion indicate approximately 25-50% of the enzyme is located in the membrane (Karlish *et al.*, 1977; Maunsbach *et al.*, 1988). A model has been suggested with eight membrane spanning domains that shows only 15% of the protein inside the membrane (Jorgensen, 1988). A more

recent model for topological and spatial organisation predicts approximately 10 membrane spanning regions (Goldshleger *et al*, 1995). Hydropathy analysis of the primary sequence of the β subunit shows one segment spanning the membrane (Kawakami *et al.*, 1986). A full understanding of the membrane-spanning organisation may help elucidate the active transport mechanisms (Glynn and Karlish 1990). Figure 1.2 shows a recently accepted model of the trans-membrane segments for each subunit.

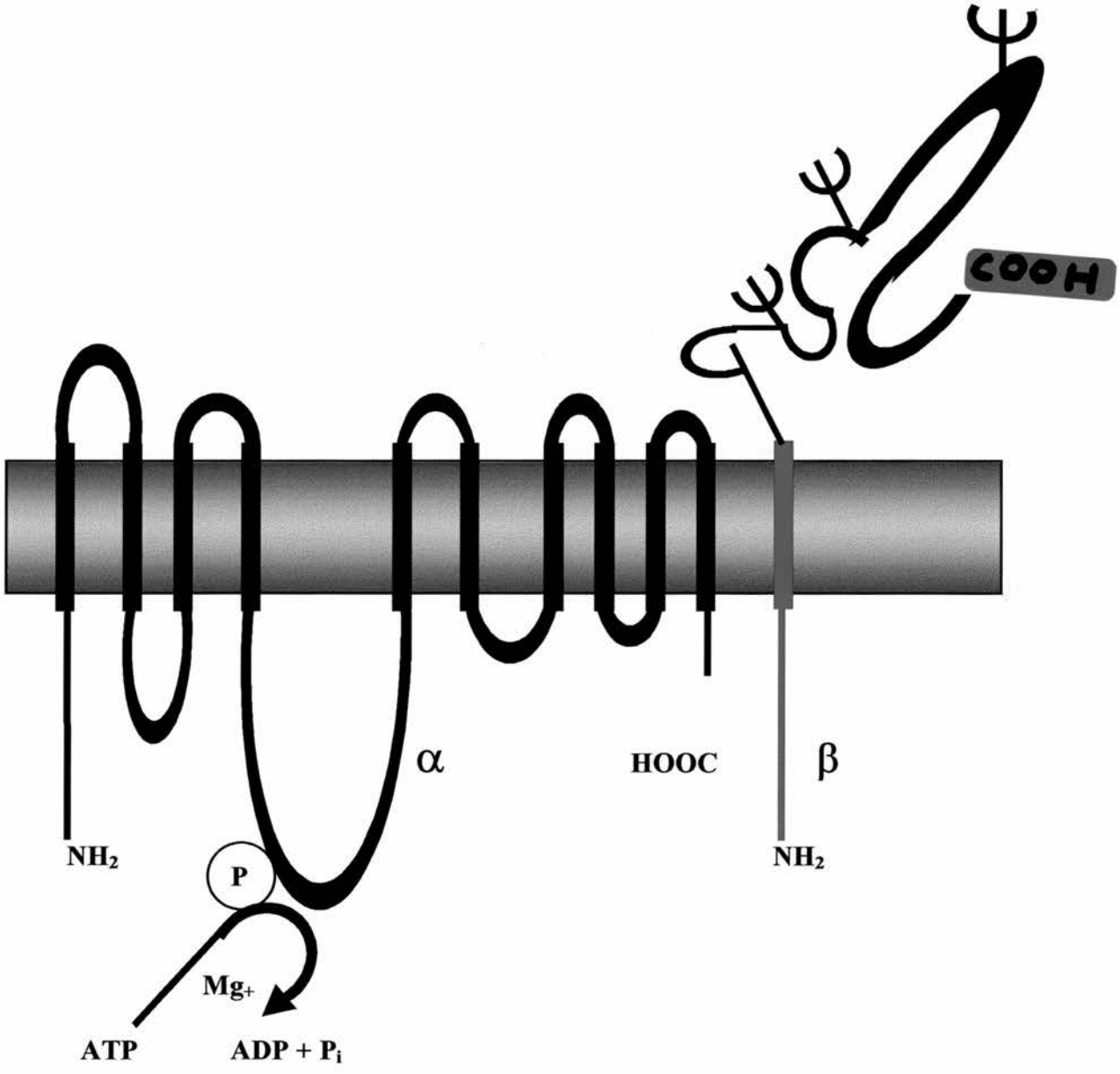

Figure 1.2 Topological model for the membrane insertion of α and β subunits in the plasma membrane (from Fambrough *et al.*, 1994). This model depicts the α subunit spanning the membrane 10 times, leaving both the NH_2 and COOH terminal in the cytosol. The β subunit spans the membrane only once with the NH_2 in the cytosol (Jorgensen, 1975; Felsenfeld and Sweadner, 1988). The sites of glycosylation (represented by ψ) are located on the extracellular side of the membrane and are thought to be associated with the mature β peptide (Geering, 1990).

Subunit	Function
α subunit	Catalytic subunit containing binding sites for cations, nucleotides and cardiac glycosides. The α subunit can be synthesised without the β subunit, however it will remain inactive (Schwartz *et al.*, 1975; Jorgensen, 1982)
β subunit	The functional role of the β subunit in enzymatic activity is unclear, however, it may assist in biosynthesis and insertion of the αβ complex into the plasma membrane Both α and β subunit are essential for enzymatic activity. The subunits are active when they exist as dimers and evidence suggests potential association of these dimers to form fully functional tetramers. Reduction of disulfide bonds leads to inactivation of the enzyme, indicating the β subunit plays an essential role in Na^+, K^+ ATPase activity (Kawamura and Nagano, 1984; McDonough *et al.*, 1990;Geering, 1991; Skou and Esmann, 1992; Sweadner, 1995).
γ subunit	The γ subunit is a distinct protein not related to the α or β subunit. Although it is not necessary for enzymatic function of the pump, the possibility of the γ subunit influencing development, regulation, and polarised sorting is being examined (DeTomaso *et al.*, 1991; Mercer, 1993).

Table 1.1 Summary of α and β subunit assembly and the functional roles of each subunit.

1.3.2 Isoforms of the sodium pump

Multiple isoforms of both α and β subunits exist depending on tissue type and species. Sequences of isoforms from both subunits have been determined by cloning and sequencing from rat brain and kidney cDNA libraries (Shull *et al.*, 1986; Noguchi *et al.*, 1987). The α subunit cDNAs isolated from the kidney were derived from a single mRNA, whereas the brain cDNA is encoded for by three classes of mRNA (Shull *et al.*, 1986).

In vertebrates, the α subunit has three well-characterised isoforms which are encoded by different genes localised on different chromosomes (Shull *et al*, 1986; Lingrel *et al.,* 1990). They have been termed α–1 (~1018 amino acids in length, ~112,573 kD), α–2 (~ 1015 amino acids, ~111,736 kD), and α–3 (~ 1013 amino acids, ~111,727kD) (Orlowski and Lingrel, 1988). The isoforms are also referred to in the literature as α, α(+), and αIII respectively. (Shull and Lingrel, 1987; Sweadner, 1989). A fourth isoform has also been identified in human and rat testis (1021 amino acids, ~112,904kD) (Shamaraj and Lingrel, 1994). The isoforms have remained highly conserved throughout evolution: although encoded for by different genes (Lingrel *et al.*, 1990), there is approximately 85% homology between the isoforms and 90 to 99% identity between vertebrate species (Takeyasu *et al.*, 1990). The main area of amino acid divergence is in the NH_2 terminus (between amino acids 60 –70) with higher degrees of similarity expressed around a site of phosphorylation and the major hydrophobic regions (Mercer, 1993). The NH_2 terminal region is also thought to be involved in determining the rate of ion transport. Tryptic cleavage at this region results in an increase in the amount of the enzyme in the E1 conformation (see section 1.5), and reduced enzymatic activity (Jorgensen and Collins, 1988). This suggests that the E1-E2 conformation is reduced by tryptic cleavage (which compromises the translocation of Na^+ ions to the extracellular surface) (Lytton *et al.,* 1985). Isoform expression is tissue/species specific and found to be regulated developmentally (Emmanuel *et al.*, 1987; Jewell and Lingrel, 1991). In the adult rat brain, α subunits 1-3 are expressed in relatively equal amounts, however in foetal rat brain, α–3 is the most abundant isoform (Mercer, 1993). During the first 7 days of development, levels of α–3 mRNA increase approximately 10-

fold. The amount of α–2 and α–3 mRNA increase gradually, reaching approximately the same level of α–3 mRNA after 25 days (Orlowski and Lingrel, 1988).

Vertebrates have at least four genes encoding the β subunit, and again, distribution is based upon tissue specificity and developmental stage (Jewell and Lingrel, 1991). It was originally assumed that the β subunit existed in one form (β–1) since other isoforms were not initially detected due to the high divergence in their amino acid sequences (~30-40%) (Martin-Vasallo *et al.*, 1989; Sweadner, 1995). In mammals only two isoforms of the β–subunit have been identified (β–1 and β –2) (Hernando *et al.*, 1994). The β subunit does not contain any binding sites. Interestingly, β –2 has been shown to be identical to an adhesion molecule on glial cells (AMOG) which is a protein specifically involved in neuronal-astrocyte adhesion (Schmalzing *et al.*, 1992; Mueller-Husmann *et al.*, 1993). β–1 shows no evidence of cell adhesion properties. It has been shown in studies on gene knockout mice that β–2 isoform (AMOG) expression is necessary for the development of the central nervous system (Magyar *et al.*, 1994). These studies showed that the mutant started to exhibit a lack in muscle co-ordination after 15 days of age. Examples of other notable symptoms at this age were enlarged ventricles, degeneration in photoreceptor cells, and swelling and degeneration of astrocytic endfeet. The animals died at approximately day 17-18 after birth. Tissue homogenates from the animals at day 16-17 showed no change of expression of the β-1 subunit of other neural adhesion molecules (such as L1, CAM and MAG). The results of this study suggest that the symptoms expressed by the mutants were related to a decrease in pump activity, with neural

degeneration as a consequence of osmotic imbalance (Isenmann *et al.*, 1994; Magyar *et al.*, 1994). Table 1.2 summarises the properties of the various pump isoforms.

SUBUNIT	TISSUE SPECIFICITY
α –1	Ubiquitously distributed (Sweadner. 1989; Skou and Esmann, 1992).
α –2	Brain, skeletal muscle, adipose tissue and cardiac muscle (Ghosh *et al.*, 1990; Mcgrail *et al.*, 1991; Sweadner, 1995).
α –3	Brain and cardiac muscle (Fambrough *et al.*, 1994 Sweadner, 1995).
α –4	Testis of human and rat (Shamraj and Lingrel, 1994).
β–1	Ubiquitously distributed (Lingrel *et al.*, 1990; Skou and Esmann, 1992).
β –2	Brain, kidney, lungs and heart tissue of adult rats (Martin – Vasallo, 1989).
β –3	Developmentally regulated, brain specific in the *Xenpus Laevis* embryo, *Bufo marinus* and newly found in mammalian epithelium (Good *et al.*, 1990; Jassier *et al.*, 1992; Schmalzing *et al.*, 1992; Malik *et al.*, 1996).
β –4	Toad bladder epithelium and mammalian epithelium (Jassier *et al.*, 1994; Malik *et al.*, 1996; Pestor *et al.*, 1999).

Table 1.2. A summary of the α and β isoforms. Various combinations of subunit isoforms can form functional Na^+, K^+ ATPase molecules. Little is known about the effect of the different isoforms on the overall function of the Na^+, K^+ ATPase enzyme.

1.4 Turnover of the Na^+, K^+ ATPase

Virtually all components of cells are in a continual state of molecular flux (Pollack *et al.*, 1981), being synthesised, metabolised, degraded or released from the cell (Palade, 1975). Integral proteins found in all cell membranes play an important functional purpose during the life of the cell (Von Heijne, 1995). The

turnover of cellular proteins is determined by the synthesis and degradation rates of proteins. Although cells expend metabolic energy in the turnover process the advantage may be for correctional purposes, such as replacing damaged molecules with newly synthesised functional molecules, or perhaps the upregulation or downregulation as a response to altered environmental conditions. Hence turnover determines the level at which molecules may found in the cell. Na^+, K^+ ATPase is an integral membrane protein synthesised in the endoplasmic reticulum, sent to the Golgi apparatus for terminal glycosylation and ultimately the proteins are inserted into the membrane.

Turnover also involves the endocytotic internalisation of proteins and their presumed degradation in the lysosomal compartments. Observations about the rates of turnover vary. It has been suggested that after the Na^+, K^+ ATPase heterodimer is internalised, it is either immediately degraded or possibly stored (Fambrough *et al*, 1991). Experiments in cultured avian neurones suggest that both α and β subunits are degraded at the same rate (Tamkun and Fambrough, 1986). In the pig kidney it has been observed that after synthesis the degradation rates of the α and β subunit differ, although after a period of approximately four hours the rates of degradation became the same. This suggests that this was the degradation of the heterodimer (Lescale-Matys *et al.*, 1993). The main function of turnover is to keep an appropriate number of working pumps in the plasma membrane in order to maintain transmembrane Na^+ and K^+ gradients; the rate of internalisation is slow suggesting the possibility that the pump only cycles once (Strous *et al.*, 1988). However, evidence now shows that there is recycling of Na^+, K^+ ATPase (Fambrough *et al.*, 1991).

1.5 Conformational changes of Na^+, K^+ ATPase

The hydrolysis of ATP to ADP is accompanied by a series of conformational changes that translocate Na^+ and K^+ across the plasma membrane (Figure 1.3 and 1.4; Jorgensen, 1986). The two major conformational states are known as E1 and E2. These states determine which ion-binding site is exposed to the internal or external environment. A detailed structural model is important for the identification of conformational changes which are coupled to energy conversion and translocation of ions across the membrane (Jorgensen, 1981).

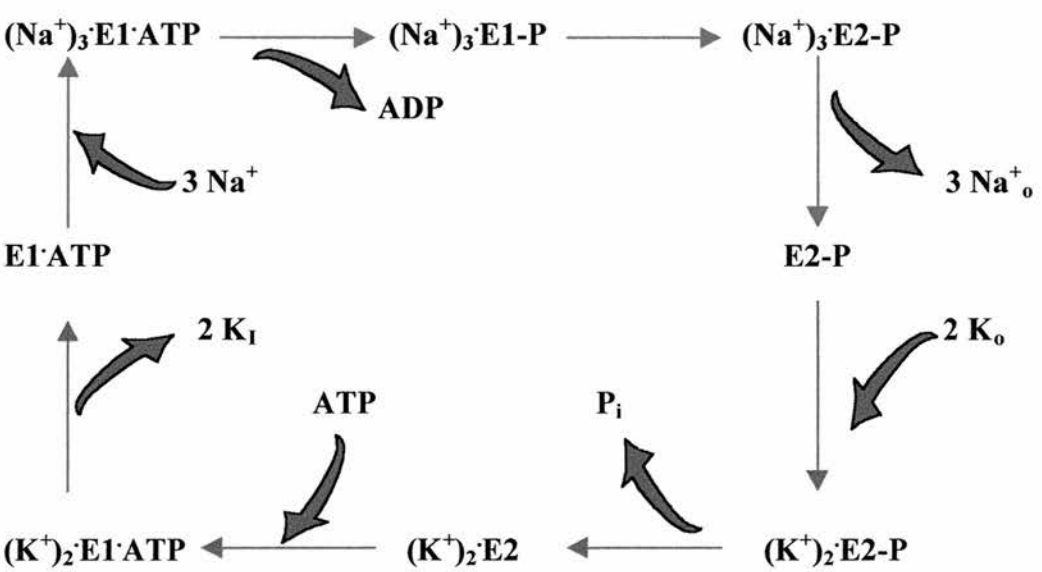

Figure 1.3. (from Sweadner, 1995) shows the enzymatic activity of Na^+, K^+ ATPase utilising the energy of ATP hydrolysis to move ions across the membrane.

E1 is found in the presence of Na^+; **$(Na^+)_3$·E1·ATP** represents the three high affinity binding sites for Na^+ ions which are exposed to on the inside of the cell (Figure 1.3). Binding of three Na^+ ions stimulates the hydrolysis of ATP **[$(Na^+)_3$·E1-P]**. The binding accelerates the transfer of the terminal phosphate of

ATP to an aspartyl side chain in the active site. This leads to a conformational change which transfers Na^+ ions to the outside of the cell, which then expose the Na^+ binding sites to the extracellular face **[$(Na^+)_3$·E2-P]** (Figure 1.4). The E2 conformation is found in the presence of K^+; at the same time as the **[$(Na^+)_3$·E2-P]** is formed, two high affinity binding sites for two K^+ ions become exposed on the extracellular surface of the cell **[$(K^+)_2$·E2-P]**. Binding of two K^+ ions at these sites stimulates hydrolysis of the phosphate group bound to the pump **[$(K^+)_2$·E2]**, leading to a second conformational change. This restores the pump to its original configuration, with the K^+ binding sites exposed to the cytosol, lowering their binding affinity and releasing K^+ ions into the cell. This completes one transport cycle (Jorgensen, 1986; Glynn and Karlish, 1990; Lingrel, 1992; Sweadner, 1995).

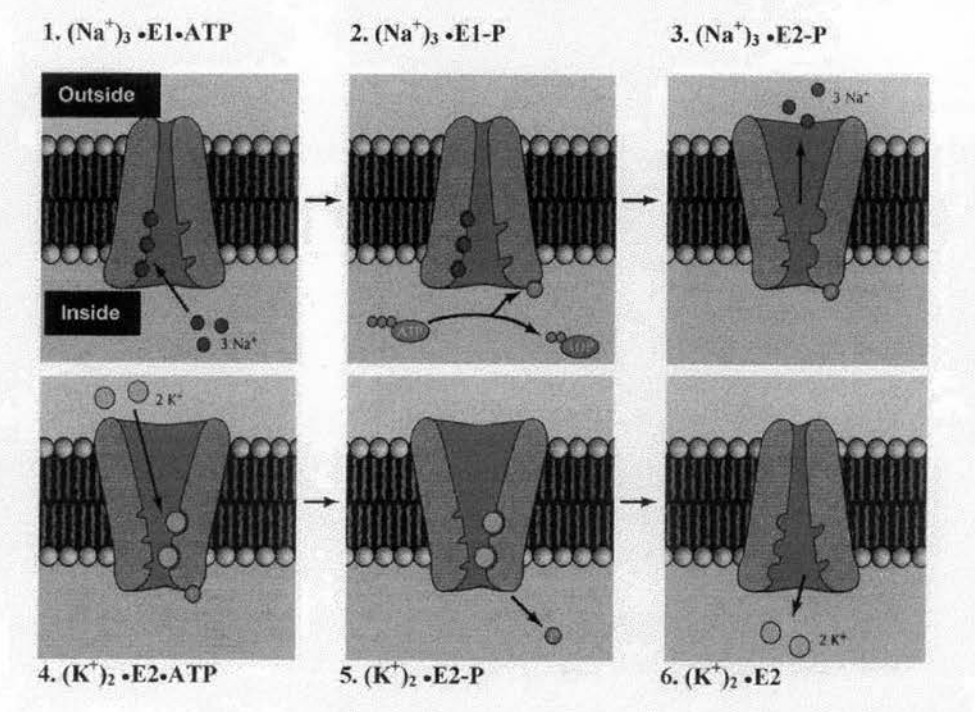

Figure 1.4 Model for the operation of Na^+, K^+ ATPase during one cycle (From Cooper, 1997)

1.6 Other ion translocating ATPases

Cell membranes contain several membrane-bound enzymatic systems that function to actively move ions against their concentration gradients (Chow and Forte, 1995). There are four categories among this family of primary active transport systems. They are: Na^+, K^+ ATPase; Ca^{2+}ATPase; H^+, K^+ATPase; and H^+ATPase. These are termed P-Type ATPases because they all commonly form an aspartyl phosphate intermediate during the hydrolysis of ATP and cation translocation (Horisberger *et al.*, 1991; Chow and Forte, 1995).

The α subunit of the H^+-K^+ ATPase shows a close relation to α subunit of the Na^+, K^+ ATPase cloned from the rat and pig, with an overall homology of 62% (Shull and Lingrel, 1986). Although the H^+, K^+ ATPase and Na^+, K^+ATPase show large regions of homology, the H^+, K^+ ATPase does not require a β subunit to function. However, it is found non-covalently associated with a protein of approximately the same molecular weight as the core β subunit of the Na^+, K^+ATPase. There is also homology between Ca^{2+}ATPase and Na^+, K^+ATPase, and like the H^+, K^+ ATPase, has a non-covalently linked protein (Leberer *et al.*, 1989) Both Ca^{2+}ATPase, and H^+ ATPase show structural similarity to Na^+, K^+ATPase, as they all have similar hydropathy profiles.

1.7 Cardiac glycosides

Cardiac glycosides are extensively used for clinical prophylactic management and treatment of congestive heart failure (Mason *et al*, 1971; Shamraj *et al.*,

1993). Cardiac glycosides function by inhibiting the Na^+, K^+ ATPase (Skou *et al.*, 1957; Chatterjee, 1989). Initial evidence of pump inhibition was first demonstrated in 1953 by Schatzmann, who showed the effects of cardiac glycoside inhibition on the active transport of Na^+ and K^+ ions in red blood cells (Baker and Willis 1972; Skou and Esmann 1992). Cardiac glycosides bind to specific sites on the extracellular surface of the α subunit and function by inhibiting the effects of Na^+, K^+ ATPase. Intracellular levels of Na^+ are increased due to pump inhibition and intracellular levels of Ca^{2+} are also increased via Na^+/Ca^{2+} exchange producing a positive inotropic effect (increased contractility) on the heart (Shamraj *et al.*, 1993; Woolfson *et al*, 1993). The effect of glycoside binding to the α subunit is due to the increased intracellular levels of cytosolic Ca^{2+}, leading to increased contractility through enhanced interaction of actin and myosin.

Cardiac glycosides, such as digitalis, digoxin and ouabain, are found widely in nature and also made synthetically (Allen *et al.*, 1985). It was first shown in 1960 that ouabain is a specific inhibitor of the sodium pump and via radiolabelling techniques ouabain and digoxin bind directly to the sodium pump (Albers *et al.*, 1968). Glycosides have a characteristic ring structure, known as an aglycone, which is associated with one or more sugars (Schwartz, 1988). The aglycone is associated with a α,β 5-6-membered lactone ring structure. The binding of cardiac glycosides is useful when studying the mechanisms of Na^+, K^+ ATPase. Initially, it was thought that the binding site of cardiac glycosides to the Na^+, K^+ ATPase enzyme involved three separate regions interacting with the sugar, steroid and lactone ring (Schwartz, 1988). Determination of the amino acid

sequence of the α subunit of Na^+, K^+ ATPase has helped to pinpoint possible binding sites. The extracellular loops near the N-terminal of the α polypeptide (Herrera *et al.*, 1987), and a site located near the C-terminal have been identified as possible regions involved in glycoside binding, though precise locations are still under dispute (Sweadner, 1995).

Binding affinities of cardiac glycosides can vary among the isoforms both within and between different species (Schwatrz, *et al.*, 1988). The extracellular loops from the first and second trans- membrane spanning domains (starting from the NH_2 terminus) are important for glycoside binding. Site directed mutagenesis showed that changes in specific amino acids on the extracellular domain of the α - subunit affected ouabain binding affinity (Price and Lingrel, 1988). Using site directed mutagenesis the expressions of two amino acids within the extracellular domain were altered. Glutamine and asparagine residues located at positions 111 and 122 of the amino acid sequence of the human α–1, and arginine and aspartic acid residues in the same position were altered in the rat α–1. These changes converted ouabain resistant α–1 to ouabain sensitive α–1 in cultured cells (Price *et al.*, 1989). Changes in the experimental conditions, such as the concentrations of ions and substrates in the experimental medium, can also alter ouabain-binding affinities. In analysis of ouabain binding assays, two components of binding are shown: *specific binding* which shows the association of ouabain binding to Na^+, K^+ ATPase, and *non-specific binding*, which represents the amount of ouabain binding and uptake into the cell (Baker and Willis, 1972). Affinity of ouabain binding is reduced under conditions of high K^+ (Sweadner, 1995), indicating that ouabain and K^+ compete with each other for binding in the

E2P conformation of the enzyme (Jorgensen, 1986). Non-specific binding can be determined when high levels of K^+ inhibit specific glycoside binding to the Na^+, K^+ ATPase. Total glycoside binding is the ouabain binding determined under conditions of a K^+ free medium (Baker and Willis, 1972). Based on these results, the amount of specific ouabain binding can be determined by subtracting the non-specific binding from total binding (Baker and Willis, 1972).

1.8 Regulators of Na^+, K^+ ATPase

1.8.1. Drugs that regulate Na^+, K^+ ATPase

A. Monensin. Monensin is a Na^+ ionophore known to upregulate the Na^+, K^+ ATPase (Smith and Rozengurt, 1978; Rapeport *et al.*, 1985; Unkles *et al.*, 1988; Cramb *et al* 1989; Kennedy *et al.*, 1990). The mechanisms underlying upregulation are unclear, but it is thought that they involve a rise in intracellular [Na^+] (Unkles *et al.*, 1988). Experiments on HeLa (human cervical carcinoma cells) cells incubated with monensin showed that an increase in pump density was due to an increased rate of protein synthesis, rather then a decreased rate of internalisation (Cramb *et al.*, 1989).

B. Nystatin. Nystatin increases the number of Na^+, K^+ ATPase in rat kidney epithelial cells. This was found to be independent of *de novo* protein synthesis, since neither actinomycin D blocking RNA synthesis nor cycloheximide which inhibits cytosolic protein synthesis but not organelle protein synthesis abolished it. It was suggested that pumps were recruited from intracellular pools, an opposite effect to that of monensin (Barlet-Bas *et al.*, 1990).

C. Veratradine. Veratradine increases intracellular Na^+ concentrations by opening voltage-sensitive Na^+ channels, allowing leakage of Na^+ into the cell. Closure of voltage-sensitive Na^+ channels with tetrodotoxin reverses this effect (Wolitzky and Fambrough, 1986; Taormino and Fambrough, 1990).

D. Ethacrynic acid. Ethacrynic acid increases the number of Na^+, K^+ ATPase *in vitro* in HeLa cells and lymphocytes (Lamb and Newton, 1973; Boardman *et al.*, 1974,1975; Rapaport *et al.*, 1986; Oh, 1987). This may be initiated by an increase in intracellular Na^+, however, the exact mechanism is not yet known. It is possible that ethacrynic acid could affect the pump through the phosphoinositide system, as it inhibits inositol phosphate turnover (Guiramand *et al.*, 1990; Bartolami *et al.*, 1993).

1.8.2. Ionic regulation

Na^+, K^+ ATPase is subject to a variety of regulatory controls in response to the environment, leading to an alteration in the number and activity of pumps. This type of regulation has been identified in two ways: short-term regulation and long-term regulation. Using measurements of increased intracellular [Na^+], short-term regulation was defined as an acute increase in Na^+, K^+ ATPase activity, and long-term regulation was identified as a change in the number of pumps in the membrane (Pollack *et al.*, 1981; Pressley, 1988).

Studies on the binding affinities for substrates (Na^+, K^+ and Mg^{2+}ATP) show that Na^+ is most likely to be the rate-limiting point for enzyme activity (Sweadner, 1995). Increased levels of intracellular Na^+ accelerate the rate of Na^+, K^+ ATPase activity, causing internal levels of Na^+ to return to their normal concentration

(~5-15mM). Long-term regulation of Na^+, K^+ ATPase activity has been examined by experimentally altering the $[Na]_i$. in cells grown in culture. This can be achieved in a number of different ways. Cells grown in ouabain have increased levels of Na^+, K^+ ATPase in the membrane, as estimated by ^3H-ouabain binding (Lamb and McCall, 1972). Other methods of increasing $[Na]_i$ include: increasing external $[Na^+]$ in the culture media, through the use of compounds such as nystatin or monensin (Cramb *et al.*, 1989); or by using Na^+ channel activators such as veratradine (Jorgensen, 1986). If the stimulus is sustained for long periods the cell produces and inserts more pumps into the plasma membrane. The increase in Na^+, K^+ ATPase is due to alterations in subunit transcription and translation. The pathways that bring about these signals to the genome are unknown (Pollack *et al.*, 1981). Experiments using HeLa cells showed that under conditions of prolonged growth in low extracellular $[K^+]$ showed an increase in Na^+, K^+ ATPase synthesis. Lamb's group (Boardman *et al.*, 1974) suggested that up-regulation of Na^+, K^+ ATPase is triggered by an initial increase in intracellular $[Na^+]$. By manipulating concentrations of Na^+ and K^+ in the medium, and maintaining osmolarity with sorbitol, they showed that low extracellular K^+ had no direct effect on pumps unless the internal Na^+ concentration rose (Boardman *et al.*, 1974; Vaughan and Cook, 1972 Pollack *et al.*, 1981). Under these conditions, the increase in Na^+, K^+ ATPase units in the membrane is possibly due to a decrease in the rate of degradation or removal of the pumps (Pressley, 1988). The concept of intracellular pools of Na^+, K^+ ATPase is still under dispute (Caplan *et al.*, 1985). In cells where rapid changes in response to an increase in $[Na^+]_i$ are possible, such as epithelial cells engaged in vectorial Na^+ transport, an increase in Na^+, K^+ ATPase pumps is required. However, it has been suggested that the recruitment of intracellular pools of pre-

of intracellular pools of pre-formed Na^+, K^+ ATPase sub-units (referred to as 'inactive', 'cryptic', or 'masked') can rapidly restore normal ionic concentrations (Bowen and McDonough 1987, Verrey *et al.*, 1989). Recruitment of intracellular pools of Na^+, K^+ ATPase inserted into the plasma membrane would result in a rapid increase in enzyme activity, as opposed to the more lengthy procedure of producing pumps *de novo* (Wolitzky and Fambrough, 1986). Barlet-Bas and Doucet (1988) have shown that an increase in $[Na^+]_i$, caused by nystatin, resulted in a large increase in Na^+, K^+ ATPase units that was not dependent upon protein synthesis. The intracellular pool of Na^+, K^+ ATPase units represented 60% of the total enzyme in chick myotubes (Tankum and Fambrough, 1986). In other experiments on chick myotubes, cells grown in veratradine (a Na^+ channel activator) led to the intracellular pools not being depleted, but increasing instead, suggesting that the increase in Na^+, K^+ ATPase found at the membrane was not through recruitment of intracellular pools (Wolitzky and Fambrough, 1986). Subcellular fractionation studies have shown that most of the intracellular pool of Na^+, K^+ ATPase is associated with the Golgi complex (Mircheff *et al.*, 1989).

1.8.3. Hormonal regulation

The expression of Na^+, K^+ ATPase activity is modulated by a variety of different hormones that are implicated in the long-term regulation Na^+, K^+ ATPase units. These include aldosterone, progesterone (Verrey *et al.*, 1987), cortisol, corticosterone, deoxymethasone, thyroid hormone (triiodothyronine (T3) and possibly thyroxine (T4) (Horowitz *et al.*, 1990; Giannella *et al.*, 1993). Peptide hormones, such as insulin (Lytton et al., 1985) glucagon, epidermal growth factor (EGF), vasopressin and catecholamines (Clausen and Flatman, 1987) have a short-term effect on Na^+, K^+ ATPase (Rossier *et al.*, 1987). The action of

hormones and growth factors are mediated via membrane receptors and second messengers (Rossier *et al.*, 1987).

A. Thyroid hormone. Thyroid hormone (T3) causes upregulation of Na^+, K^+ ATPase and increased ouabain binding in several tissues, including rat heart, kidney, liver, skeletal muscle and intestine. Guinea pig brain has also been examined, but no increase in Na^+, K^+ ATPase activity was observed (Ismail-Begi and Edelman, 1970; Lo *et al.*, 1976; Lin and Akera, 1978). The action of T3 on Na^+, K^+ ATPase has been studied by removal of the thyroid gland accompanied by an injection of T3, thus removing any effect of other thyroid hormones. In kidney tissue of thyroidectomized rats, injected T3 caused an increased synthesis of both α and β subunits after 8-22 hours (Lo and Lo, 1980). The rates of degradation between the hypothyroid rats and the T3 treated rats were unchanged, supporting the role of *de novo* synthesis. Increases in mRNA levels for the subunits in response to T3 depend on the cell type. For example, in the rat kidney cortex, T3 increased α and β-mRNA, whereas in rat liver, it increased α mRNA levels only (Gick *et al.*, 1988). In heart and skeletal muscle from hyperthyroid rats, α-1 mRNA is increased, whereas α-2 mRNA is unchanged (Horowitz *et al.*, 1990). Skeletal muscle expresses α-1, α-2, β–1 and β–2 isoforms. In the hyperthyroid state, only the α-2 and β–2 are upregulated. In the kidney, both in control and T3 treated situations, only the α-1and β–2 isoforms were expressed (Azuma *et al.*, 1993).

B. Steroid hormones. Steroid hormones bind to DNA receptors that are encoded by the same gene family which encodes/controls the production of thyroid

receptors (Evans 1988). It would therefore be expected that they have the same mechanism of action, namely targeting transcription rates leading to protein synthesis. The increase in Na^+, K^+ ATPase activity in the toad bladder, seen after aldosterone treatment, is insensitive to amiloride (an inhibitor of the Na^+/H^+ exchanger). This implies that upregulation does not depend on an increase in the intracellular sodium concentration *per se,* but on a direct action of the hormone (Verrey *et al.*, 1987). Lamb (1988) also suggested that there is a direct effect of the hormone on the levels of a subfraction of Na^+, K^+ ATPase in cultured cells, and in addition, a secondary effect due to ionic leakage into the cells has been proposed (Paccolat *et al.*, 1987).

Progesterone has been shown to inhibit Na^+, K^+ ATPase activity in *Xenopus* oocytes during their maturation process (Richter *et al.*, 1984). The mechanism is unknown, although regulation of gene transcription is one possibility. In contrast, oxytocin stimulates Na^+ transport in the toad bladder in a synergistic fashion with aldosterone. Oxytocin had a non-additive effect (compared to aldosterone) on the rate of biosynthesis of Na^+, K^+ ATPase α and β subunits (Girardet *et al.*, 1986).

C. Insulin. Insulin stimulates Na^+, K^+ ATPase activity in muscle, liver, and kidney (Lavoie *et al.*, 1996). This is an important action because it compensates for the gain in intracellular Na^+ caused by hormonal activation of Na^+ -coupled amino acid uptake and Na^+/H^+ exchange (Klip *et al.*, 1986). Upregulation of Na^+, K^+ ATPase in response to insulin differs depending on cell types. Insulin also shows an affect on the different isoforms of Na^+, K^+ ATPase. It increases the expression of the α-2 isoform (Russo and Sweadner, 1993) and also increases its affinity for Na^+ (Lytton, 1985). In experiments using rat adipocytes, which

express α-1 and α-2 isoforms, Lytton (1985) demonstrated that insulin treatment produced a shift in the Na^+ inside to 14mM (from 17mM) for α-1 and a shift to 33mM (from 52mM) for the α-2. The explanation for this change is selective stimulation of α-2 by insulin (Clausen and Flatman, 1987). Sargeant *et al.,* (1995) examined the effects of insulin on Na^+, K^+ ATPase in adipocytes and concluded that insulin activation of Na^+, K^+ ATPase is mediated by a bumetanide-sensitive elevation of intracellular [Na^+]. Hence, it is probable that this is the consequence of activation of Na^+/ K^+ /Cl^- cotransporter.

1.9 Regulation by phosphorylation/dephosphorylation

ATP phosphorylates the Na+, K+ ATPase (Albers *et al.*, 1968) on the side-chain of the α subunit in the presence of Na^+ and Mg^+, on a specific aspartate residue. Determination of the amino acid sequence surrounding this site indicates that aspartate 372 is phosphorylated. Na^+, K^+ ATPase is also phosphorylated on other sites that regulate the activity of the pump (Mercer, 1993). Reversible phosphorylation/dephosphorylation, mediated by kinases/phosphatases (respectively), may play a role in regulation of Na^+, K^+ ATPase activity (Bertorello and Katz, 1995). There are 38 sites that could qualify as protein kinase C (PKC) motifs in rat α-1 subunit. However, there are species-specific differences in the phosphorylation of the Na^+, K^+ ATPase by PKC which have been shown to have a structural basis (Freschenko *et al.*, 1995). In purified preparations of Na^+, K^+ ATPase from the rat kidney it has been found that 25% ^{32}P incorporated into the phosphorylated protein was found on serine 11. The remaining 75% was found on serine 18, a site which is absent from the amino acid sequence of many species. Current research on the rat kidney shows

modulation of Na^+, K^+ ATPase activity by a tyrosine phosphorylation (Féraille, 1997). Epidermal growth factor (EGF) and insulin have been implicated in increase Na^+ reabsorption in the rat proximal convoluted tubule (PCT). Both of these growth factor receptors become phosphorylated themselves, and have effects on cell processes that are mediated through tyrosine phosphorylation of key proteins (for example MAP kinase). Féraille and his colleagues investigated the possibility that effects on Na^+ reabsorption were also produced via a process of tyrosine phosphorylation. They examined changes in Na^+ reabsorption in the rat PCT stimulated by insulin and EGF under different conditions. Tyrosine kinase activity was blocked by genistein, and tryosine phosphatases were blocked by orthovanadate. Their results indicate that both activation of receptor tyrosine kinases and inhibition of tyrosine phosphatases stimulate Na^+, K^+ ATPase activity, suggesting that tyrosine phosphorylation is involved in the control of pump activity (Féraille *et al.*, 1997). It is also shown that vanadyl ions stimulate K^+ uptake into isolated perfused rat liver via the sodium pump by a tyrosine kinase-dependant mechanism (Bruck *et. al.*, 1998).

Internalisation of the sodium pump studied using anthroylouabain a fluorescent derivative of ouabain

2.1 Introduction

The aim of this study was to investigate the relationship of Na^+, K^+ ATPase and the cytoskeleton in cultured HeLa cells using anthroylouabain, a fluorescent derivative of ouabain. This study was prompted by initial findings by Lamb (1996), showing that the dissociation constant (K_d) for ouabain binding to the sodium pump of HeLa cells is dependent on cell morphology. Results of this study show that rounder cells take up more anthroylouabain then flatter cells having a prominent cytoskeleton. Laser scanning confocal microscopy in the proper UV range confirmed that this was not an artefact of differing depth of cells, but a real difference of *ca.*3-5 fold in uptake between round and flat cells. HeLa cells were used in these experiments as they serve as a good physiological model for other cells *in vivo*, as well as having a highly sensitive α- subunit (Shull, 1987). The function of cardiac glycosides will be reviewed along with that of some key "linking" cytoskeletal proteins.

2.1a. Cardiac Glycosides

The group of drugs known as cardiac glycosides, including digoxin, ouabain and other digitalis-like compounds (Hinson *et al.,* 1995), is widely used in the treatment of certain forms of heart disease. These compounds belong to a class of steroids termed cardenolides, which were originally obtained from plants. For example, foxglove (*Digitalis purpurea*) was initially used in the treatment of heart failure (Allen *et al.*, 1985). The initial step in their role of action is to bind

to and partially block the sodium pumps of cells. This causes an increase in $[Na^+]_i$. In the myocardium, this stimulates the sarcolemmal Na^+-Ca^+ exchange, increasing intracellular calcium concentrations ($[Ca^{2+}]_i$). The increase in $[Ca^{2+}]_i$ is responsible for the generation of extra force during myocardical contraction, referred to as a positive inotropic effect (Schwartz *et al.*, 1988 Shamraja *et al.*, 1993, Woolfson *et al.*,1993).

Ouabain is a highly polar crystalline compound and has been used extensively in experimental research e.g. in binding assays and enzyme kinetics, which have helped explain the function of the sodium pump to date. A fluorescent derivative of ouabain, called anthroylouabain, has also been synthesised and provides another approach to investigate the properties of Na^+, K^+ ATPase. Anthroylouabain exhibits the same inhibitory activity and binding affinity for the α-subunit for Na^+, K^+ ATPase as ouabain (Fortes, 1977). Like ouabain, its binding to the Na^+, K^+ ATPase is antagonised by K^+ (Yoda and Yoda, 1988) and its fluorescence is reported to increase upon binding to purified membrane preparations (Fortes, 1977; McCormick, 1990).

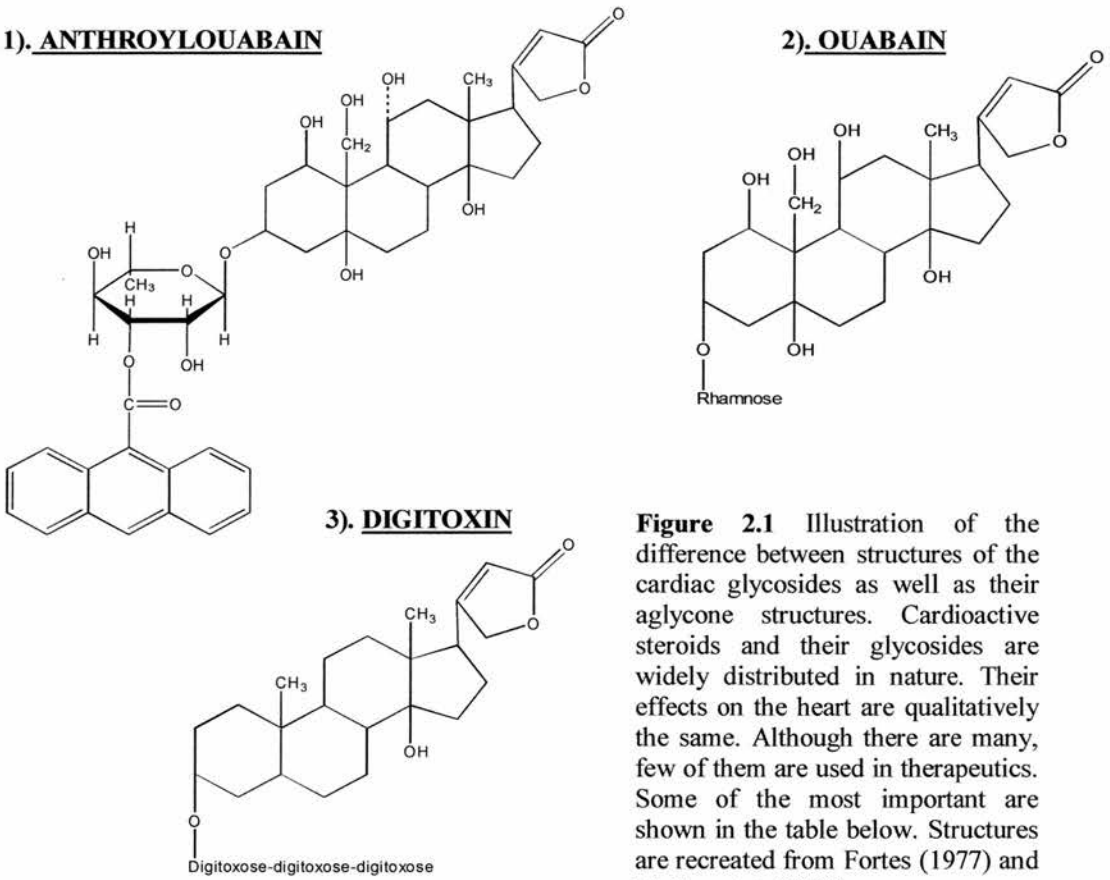

Figure 2.1 Illustration of the difference between structures of the cardiac glycosides as well as their aglycone structures. Cardioactive steroids and their glycosides are widely distributed in nature. Their effects on the heart are qualitatively the same. Although there are many, few of them are used in therapeutics. Some of the most important are shown in the table below. Structures are recreated from Fortes (1977) and McCormick (1990).

Table 2.1 Cardiac glycosides

Digitalis purpurea	*Digitalis lanta*	*Strophanthus gratus*
Digitoxin	Digoxin	Ouabain
Digoxin	Lanatoside C	
Digitalis leaf	Deslanoside	

2.1b. Enzyme Kinetics

Experiments by Lamb (1996) showed that there is a large turnover of sodium pumps in HeLa cells following a medium change. Results from ^{3}H-ouabain binding assays and ^{86}Rb uptake related the results to the uptake of anthroylouabain (Fortes, 1977). The density of the Na^{+}, K^{+} ATPase on the plasma membrane was measured by ^{3}H-ouabain binding. In Lamb's experiments, ouabain was used rather than digoxin, because although they have similar total binding and K_d values, ouabain has much lower non-specific binding than digoxin, reducing the errors in measurement. ^{3}H-ouabain binding is specific to

the α subunit of the Na^+, K^+ ATPase receptor. This is a time and temperature-dependant process following the laws of mass action (Erdmann and Hasse, 1975).

The Michaelis-Menten Equation describes the relationship between rate and substrate concentration for an enzyme reaction. Enzyme-catalysed reactions normally proceed by formation of an enzyme-substrate complex (ES complex) in which the substrate is bound to a specific region of the enzyme called the active site. The ES complex then dissociates to yield the products of the catalysed reaction. Experimentally, it has been found that the rates of many enzyme-catalysed reactions are directly proportional to substrate concentration when substrate concentration is low, and become independent of substrate concentration as substrate concentration increases

The accepted kinetic mechanism accounting for this behaviour is expressed as:

$$E+S \underset{k_{-1}}{\overset{k_{+1}}{\rightleftharpoons}} ES$$

(E) is the enzyme that first combines reversibly with its substrate (S) to form an enzyme-substrate (ES) complex as a necessary step in enzyme catalysis. k_{+1} is the temperature-dependent association and k_{-1} the dissociation rate constant. The theory behind the Michaelis-Menten equation is that the rate-limiting step in the enzymatic reactions is the break down of the ES complex to form the product a free enzyme. The Michaelis-Menten equation is used to determine the equilibrium binding of a ligand (^{3}H-ouabain) to a receptor (Na^+, K^+ ATPase) .

The "modern" derivation is:

$$V_o = \frac{V_{max}[S]}{K_m + [S]}$$

Where,
[S]= the concentration of the ligand
V_0 = the initial rate at substrate concentration [S]
V_{max} = the maximum rate
K_m = Michaelis-Menten constant of enzyme for a particular substrate

For examining Na^+, K^+ ATPase in the membrane using ouabain binding assays, ^{3}H-ouabain binding curves are fitted using the "one site binding" curve and formula:

$$Y = \frac{B_{max} \cdot X}{K_d + X}$$

Where,
Y= zero initially then increases to a maximum plateau value B_{max}
X= the concentration of ligand (^{3}H-ouabain)
B_{max} = maximum number of binding sites (Na^+, K^+ ATPase on the plasma membrane).

In this case the B_{max} is the V_{max} the maximum activity, and is expressed in the same units as the Y-axis (^{3}H-ouabain bound or sites per cell)

K_d = The dissociation constant expressed in the same units as the X-axis (^{3}H-ouabain concentration). When the ^{3}H-ouabain concentration equals the K_d, half the binding sites are occupied at equilibrum ($K_d = K_m$) the Michaelis-Menten constant.

Experiments by Lamb (1996) compared the K_d of the Na^+, K^+ ATPase of HeLa cells for ouabain at equilibrium using cells grown on plates in the presence of 10% foetal calf serum. His findings support that of Griffiths (1991), showing a K_d (nM) of approximately 5.6±1.4. In subsequent experiments, Lamb compared plated cells with cells brought into suspension (cells that had rounded up) and found the K_d was much higher (K_d 29±6). These findings prompted him to investigate the difference between flattened cells, having a well-defined

cytoskeletal structure, and cells that were rounded up in suspension having a more disorganised cytoskeleton. He used conventional fluorescence microscopy on cells labelled with anthroylouabain. Anthroylouabain is a good fluorescence label for of Na^+, K^+ ATPase as it has been shown to have similar kinetic parameters as ouabain (Moczydlowski and Fortes, 1980).

2.1c. Interaction between the Na^+, K^+ ATPase and the cytoskeleton

The cytoskeleton is the internal protein skeleton of eukaryotic cells, responsible for many important functions e.g. maintaining cell shape, cell motility, anchoring cells together, cell division, and response to environmental changes. Actin makes up approximately 5% of the total protein in most cell types. Actin binding proteins bind to or interact with forms of actin such as globular actin (G-actin) or filamentous actin (F-actin), therefore regulating actin polymerisation (Wong *et al.,* 1983). The cell cortex (cortical layer) is composed of an actin-rich layer located beneath the cell membrane. Actin is arranged into a stiff network by attachment to several actin-binding proteins, the most abundant being filamin, providing mechanical support to the membrane (Edelstein *et al.*, 1988; Cantiello, 1995b). This "meshwork" is resilient to deformative forces but allows changes in cell shape through actin reorganisation. Gelsolin is a 90kD protein that acts as an actin "capping" or "severing protein" which breaks down, or caps, actin in the presence of high cytosolic concentrations of free Ca^{2+}, allowing the reorganisation of short-actin filaments under conditions of mechanical stress (Cantiello, 1995a). Transmembrane proteins, such as voltage sensitive Na^+ channels, volume regulating Na^+/ K^+/$2Cl^-$ cotransporter (Jorgensen *et al.*, 1986), and the pH regulating Na^+/H^+ antiporter (Watson *et al.*, 1992), are all associated with the cytoskeleton. In endothelial cells, haemodynamic forces acting upon the

lining of a vessel causes the to membrane "stretch". The cortical cytoskeleton is consequently stretched and this is responsible for activating membrane ion channels (Davies, 1988). Patch clamp studies by Davies (1995) showed that the electrical activity of the membrane is related to the degree of stretch and, more specifically, to the opening of transmembrane cation channels.

Actin and spectrin co-localise with the third cytoplasmic domain (CD3) of the α-subunit of Na^+, K^+ ATPase in epithelial cells and rat brain, and with band 3 protein in erythrocytes, also called the anion exchanger 1 (or AE-1) responsible for HCO_3-/Cl^- exchange (Cantiello, 1995a). Na^+, K^+ ATPase and AE-1are found to interact with the actin cytoskeleton via the linking protein ankyrin (Nelson and Veshnock, 1987; Morrow *et al.*, 1989). Ankyrin is a 195 kD protein which helps bind spectrin to the cell membrane. Spectrin tetramers (also called fodrin in other tissues) are non-covalently associated with the cytoplasmic surface of erythrocytes, along with other linking proteins, allowing red blood cells to maintain their distinctive biconcave shape (Alberts *et al.*, 1989). Figure 2.2 illustrates the location of the cortical linking proteins.

Linkage of integral membrane proteins to the membrane cytoskeleton is important for confining membrane proteins to specialised domains of the cell surface. Restriction of the Na^+, K^+ ATPase to either the apical or basolateral domain of polarised epithelial cells is fundamental to vectorial ion and solute transport in many tissues and organs (Hammerton *et al.*, 1991). In the choroid plexus, Na^+, K^+ ATPase is located to the apical (luminal) membrane. The fodrin-ankyrin cytoskeleton colocalises with the apical Na^+, K^+ ATPase rather then the

basolateral anion exchanger AE-2 (Alper *et al.*, 1994). Administration of colchicine, which prevents microtubule function and intracellular trafficking, did not alter the polarity of apical cytoskeletal and transport proteins or basolateral AE-2 in the choroid plexus, suggesting that the localisation of these proteins is not microtubule dependent.

Vectorial transport requires the establishment and maintenance of a non-random distribution of Na^+, K^+-ATPase on the cell surface. In many epithelia, the Na^+, K^+-ATPase is located at the basal-lateral domain of the plasma membrane (Rodriguez-Boulan, 1989). The mechanisms involved in the spatial organisation of the Na, K-ATPase in these cells is poorly understood (Nelson *et al.*, 1991). The role of regulated cell-cell contacts and assembly of the membrane-cytoskeleton in the development of the cell surface polarity of Na^+, K^+-ATPase has been investigated in polarised Madin-Darby canine kidney (MDCK) cells. Results show directly that Na^+, K^+-ATPase has a high affinity binding site for the membrane-cytoskeletal proteins ankyrin and fodrin, and that all three proteins exist in a high molecular weight protein complex that also contains the cell adhesion molecule (CAM) uvomorulin. It is suggested that these interactions are important in the assembly at sites of cell-cell contact of the membrane-cytoskeleton, which in turn initiates the development of the non-random distribution of the Na^+, K^+-ATPase. Further studies of the of the Na^+, K^+-ATPase in fibroblasts transfected with a cDNA encoding uvomorulin, showed that expression of uvomorulin is sufficient to induce a redistribution of Na^+,K^+-ATPase, from an unrestricted distribution over the entire cell surface in non-transfected cells to a restricted distribution at sites of uvomorulin-mediated cell-cell contacts in transfected cells. This distribution is similar to that in polarised

epithelial cells. This restricted distribution of the Na^+, K^+-ATPase occurred in the absence of tight junctions, but coincided with reorganisation of the membrane-cytoskeleton. These results support a model in which uvomorulin functions as an inducer of cell surface polarity of Na^+, K^+-ATPase through cytoplasmic linkage to the membrane-cytoskeleton (Nelson *et al.*, 1991).

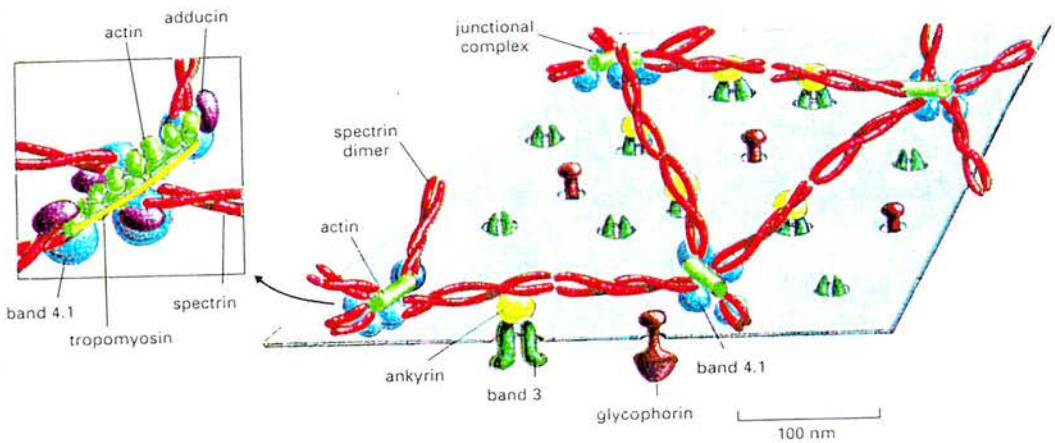

Figure 2.2 Schematic diagram showing the location of cortical linking proteins. This example shows the "head-to-head" association of spectrin dimers to form tetramers that are linked together by junctional complexes composed of short actin filaments (containing 13 actin monomers). The cytoskeleton is linked to the membrane by the indirect binding of spectrin tetramers to some band 3 proteins linked via ankyrin molecules (Adapted from Alberts, 1994).

A good illustration of the importance of Na^+, K^+ ATPase location is in the genetic disorder autosomal dominant polyscystic kidney disease (ADPKD), a disease in which the renal tubules become enlarged due to fluid accumulation (Wilson, *et al.*, 1991). Tests examined normal versus cystic regions of whole kidney, in confluent primary cultures of micro-dissected renal tubule and cyst-lining epithelia. Immunostaining with antibodies directed against the α-subunit

of the Na^+, K^+ ATPase showed the Na^+, K^+ ATPase is confined to the apical membranes of ADPKD epithelia, which is the reverse of its normal location in the basolateral membrane. This results in overall vectorial transport of Na^+ ions from the tubule lumen into the blood (Perrone, 1989; Wilson *et al.*, 1991; Avner *et al.*, 1992). Na^+ ions are the major osmotic determinant in the kidney. The activity and location of Na^+, K^+ ATPase controls the direction of reabsorptive osmotic fluid flow, implying that the altered polarity of Na^+, K^+ ATPase, resulting in the secretion of Na^+ ions may account for cyst development. Intracellular protein sorting defect is proposed as the cause of this defect (Wilson *et al.*, 1991).

Since intracellular cortical proteins have been implicated in Na^+, K^+ ATPase regulation this study investigated the morphological state of HeLa cells in relation to Na^+, K^+ ATPase uptake, using anthroylouabain as a fluorescent marker for the pump.

2.2 Methods

2.2.1 Tissue culture

HeLa cells (human epithelial cervical carcinoma cells) were cultured routinely in tissue culture flasks in minimal Essential Medium (MEM) with Earle's salts containing 10% foetal calf serum, 1% non-essential amino acids, 1% glutamine and 0.5% kanamycin. Cells were sub-cultured routinely and grown for 4 days on $22cm^2$ borosciliate glass coverslips at a seeding density of $2x10^4$cells cm^{-2}. Ouabain uptake was monitored directly using the fluorescent form of ouabain, anthroylouabain (Fortes, 1977). The cells were loaded with anthroylouabain for 1 hour in K^+ free Krebs (0 K^+) solution to measure the ouabain-pump uptake directly; others were stained for actin with FITC-labelled phalloidin. Cells were fixed with 1.0% formaldehyde for 10 minutes and coverslips mounted in Gelvatol Mountant.

2.2.2 Materials and Drugs

Tissue culture flasks and Petri dishes were supplied by Nunc, and were 75 cm^2 tissue culture grade and 30 mm diameter, respectively. $22cm^2$ borosciliate glass coverslips were obtained from BDH. Culture media were obtained from Gibco BRL. $2x10^{-3}$M anthroylouabain (in methanol, BDH) was bought from Sigma. All other chemicals used were Analar grade from BDH. The modified Krebs solution (refer to Appendix 2 for composition) was adjusted to pH 7.4 for both Krebs solutions (Corning™, 120 pH meter).

Chemicals for cell fixation and actin staining were as follows: 1.0 % EM grade formaldehyde (TAAB Lab) in methanol (BDH), 0.1% Nonidet P40 [NP40] (Sigma), 0.1% Bovine serum albumin [BSA] (BDH), actin was labelled using phalloidin Rhodamine Isothiocyanate [RITC] or Fluorescein Isothiocyanate [FITC] (FLUKA). Gelvatol Mountant (Airvol) containing 100mg/ml 1,4 Diazabicyclo [222] octane [DABCO] (Sigma) was used to prevent fluorescence fading. Coverslips were sealed with nail varnish and stored in the dark at 4°C.

2.2.3 Microscopy

Cells were examined and photographed using Zeiss™ Axioplan Universal Microscope (Carl Zeiss Inc.) with x40 and x100 (oil immersion) objective lenses. For fluorescence microscopy, specific filters were used to view different fluorochromes (Table 2.2). Black and white micrographs were taken on Kodak™ T-max 100 (TMX) film at ASA 800 and colour micrographs on Kodak EPH colour slide film ASA 800. The scale bar represents 25 μm at x40 magnification and 10 μm at x100.

FLUOROCHROME	EXCITATION FILTER	BARRIER FILTER
FITC	BP485/20	LP 520
RITC	BP 546/12	LP 590
AMCA	G 365	LP 420

Table 2.2 The filters used to view different fluorochromes using a Zeiss™ Axioplan Universal microscope.Cells were also analysed using a Bio-Rad MRC - 600 series laser scanning confocal microscope; the UV excitation was at 360nm and the emission read at 480 nm. The optical slice thickness was approximately 1μm.

2.3 Results

Cells grown on coverslips showed two types of morphology; rounded cells, presumably involved in cell division, and flattened cells which appear to have a more prominent cytoskeleton.

2.3.1 A morphological study between round and flat cells via actin staining

HeLa cells were cultured for 3-4 days or until sub-confluent. They were stained with FITC tagged phalloidin and examined via conventional fluorescence microscopy. Figure 2.3a is an example of a rounded up cell, which is presumably undergoing cell division. The yellow arrow points to an area of thin "whisker-like" filaments known as filopodia. These parallel bundles of actin are enriched with fimbrin and responsible for the tight parallel bundles of actin. The arrays of filapodia extend out from the cell to contact other cells. At this stage of development, prominent stress fibres are not seen in the cell. After cell attachment, spherical cells normally flatten out. In Figure 2.3b, the cells have migrated over the coverslip and become attached. The arrows, point to parallel aligned stress fibres that are uniformly distributed throughout the cytoplasm, but were not necessarily parallel to those in neighbouring cells. In viewing cells grown to subconfluence, approximately 95% of the cells are attached with only few rounded up cells.

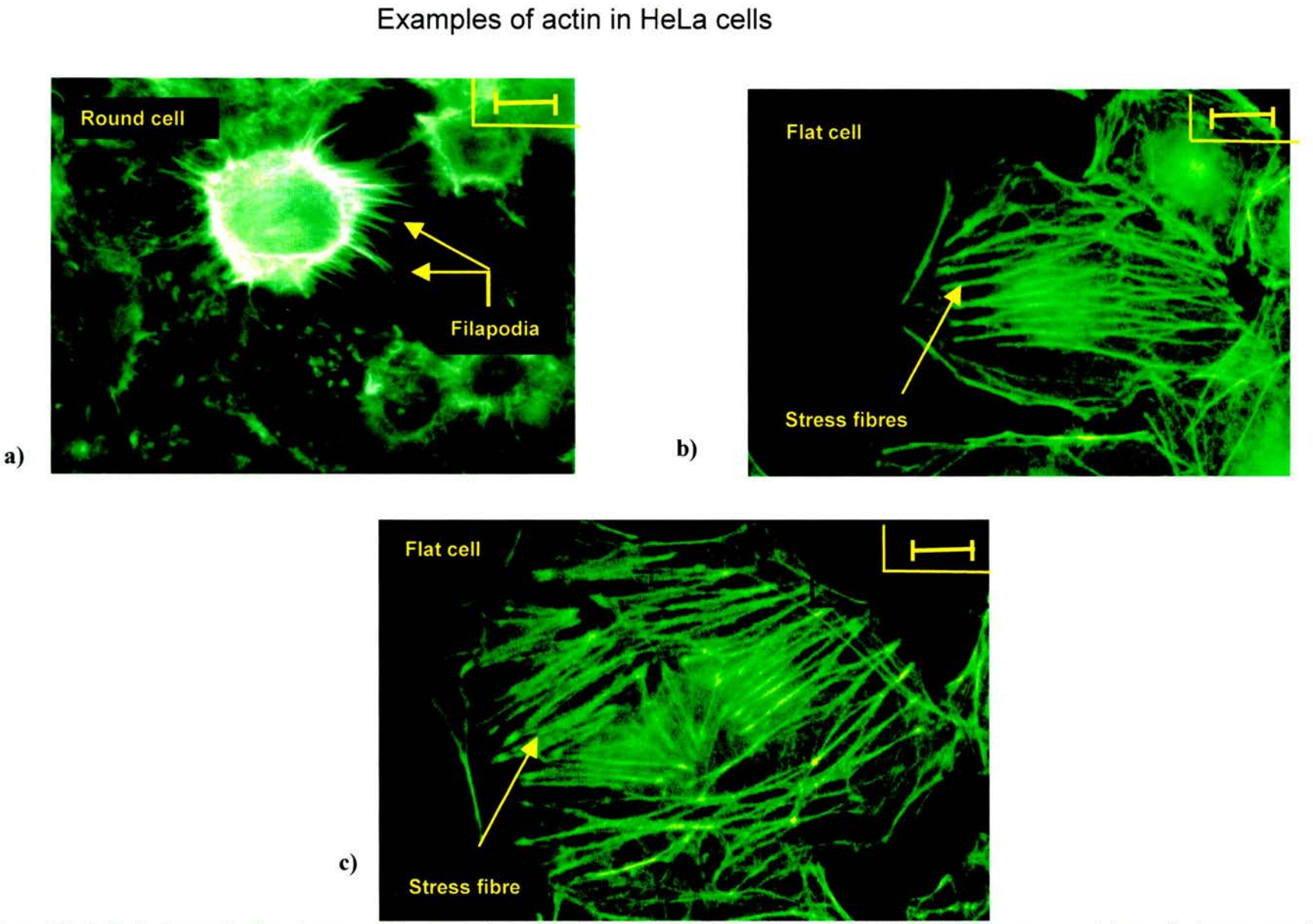

Figure 2.3 a), b) & c) are cells from the same slide preparation of day 4 HeLa cells stained with phalloidin-FITC a) illustrates a rounded up cell, the arrows point to whisker-like fibres called filapodia. b) & c) illustrate flattened cells in static culture, the arrows point to different patterns of stress fibres. Scale bar = 10 μm.

2.3.2 Anthroylouabain uptake in HeLa cells

Figure 2.4 shows rounded cells (red) and flattened cells (blue) in the same field of view. They are represented by a false colour intensity scheme using a "hot-cold" coding scale. "Cool" colours (blue, green) indicate a low concentration of anthroylouabain whereas "hot" colours (white, red and yellow) indicate a high concentration. The concentration of anthroylouabain in two of the cells was analysed using associated software. Figure 2.5 is a black and white pixel intensity diagram The intensity has been sampled along the line shown transecting the cells (x-x). The overlaid graph gives a pixel intensity reading of anthroylouabain through a micron slice through the cells. The concentration of anthroylouabain in the rounded cells is 3x greater than that in the flattened cell.

2.3.3 Anthroylouabain concentrations in HeLa cells

Figure 2.6 shows cells from the same preparation, but with the concentration of anthroylouabain represented by the numbers associated with each cell. Figure 2.7 shows a pixel intensity profile, concentrating on three cells in the centre of the field of view (cells labelled 140, 90, and 80). Again, the rounded cell with a greater concentration of anthroylouabain then the flattened cells.

Anthroylouabain uptake by HeLa

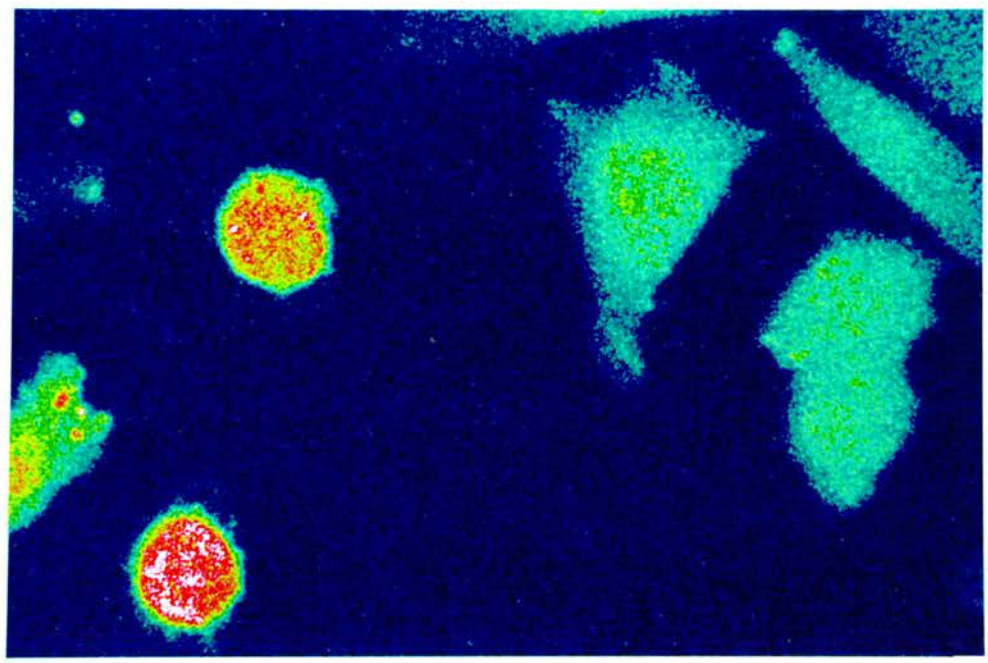

Figure 2.4 Photograph showing an example of two different cell morphologies viewed under the laser scanning confocal microscope.

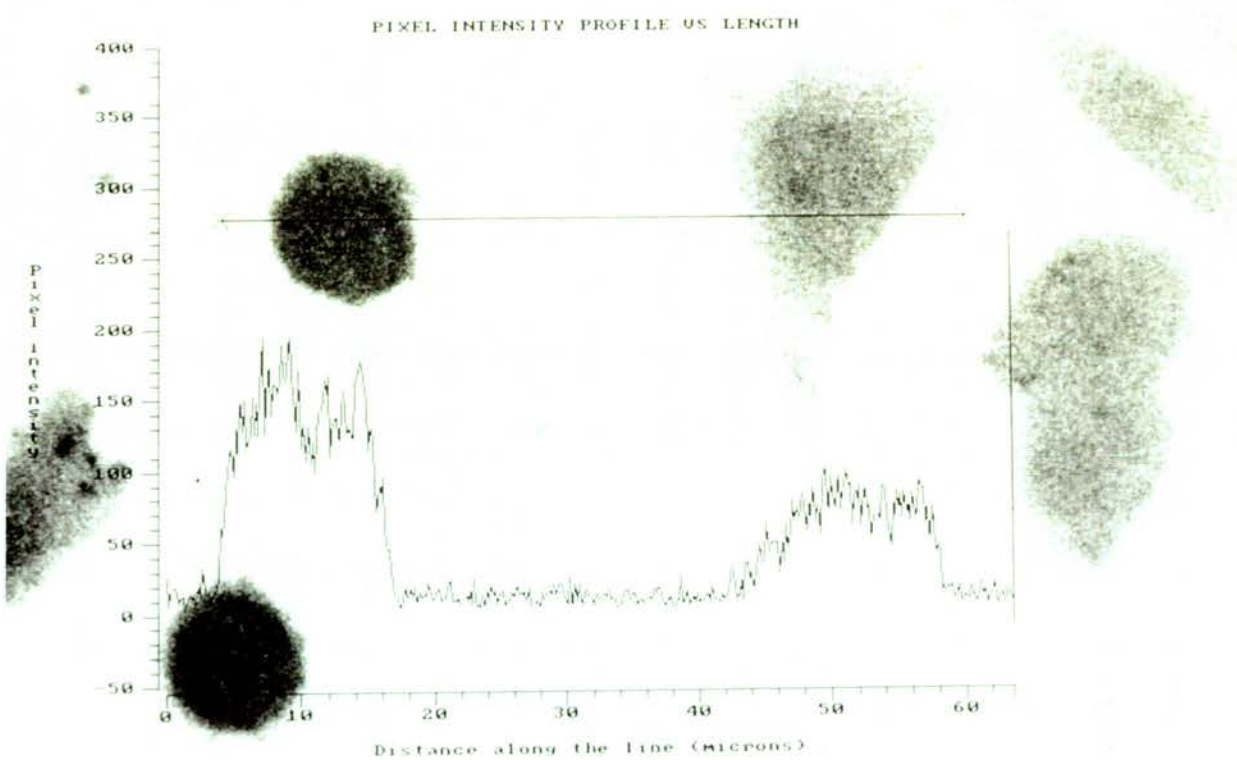

Figure 2.5 This is a photograph of cells in the same field of view as Figure 2.6 showing a black and white pixel intensity graph.

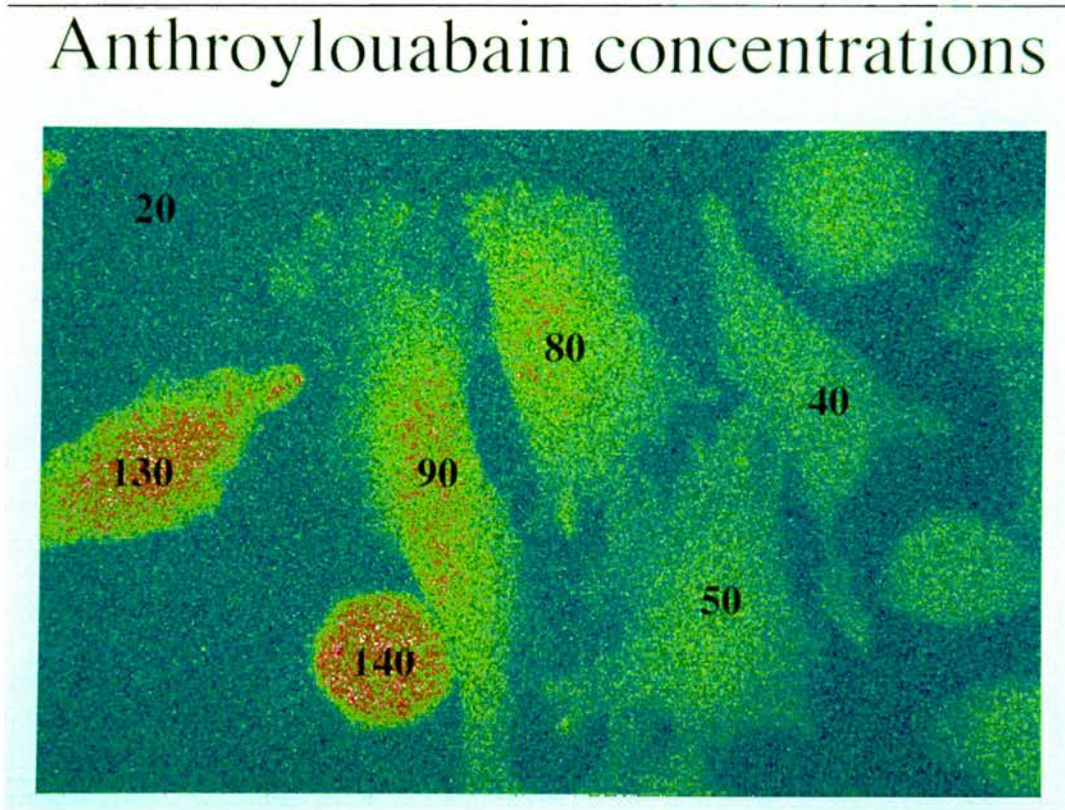

Figure 2.6 b For legend see below

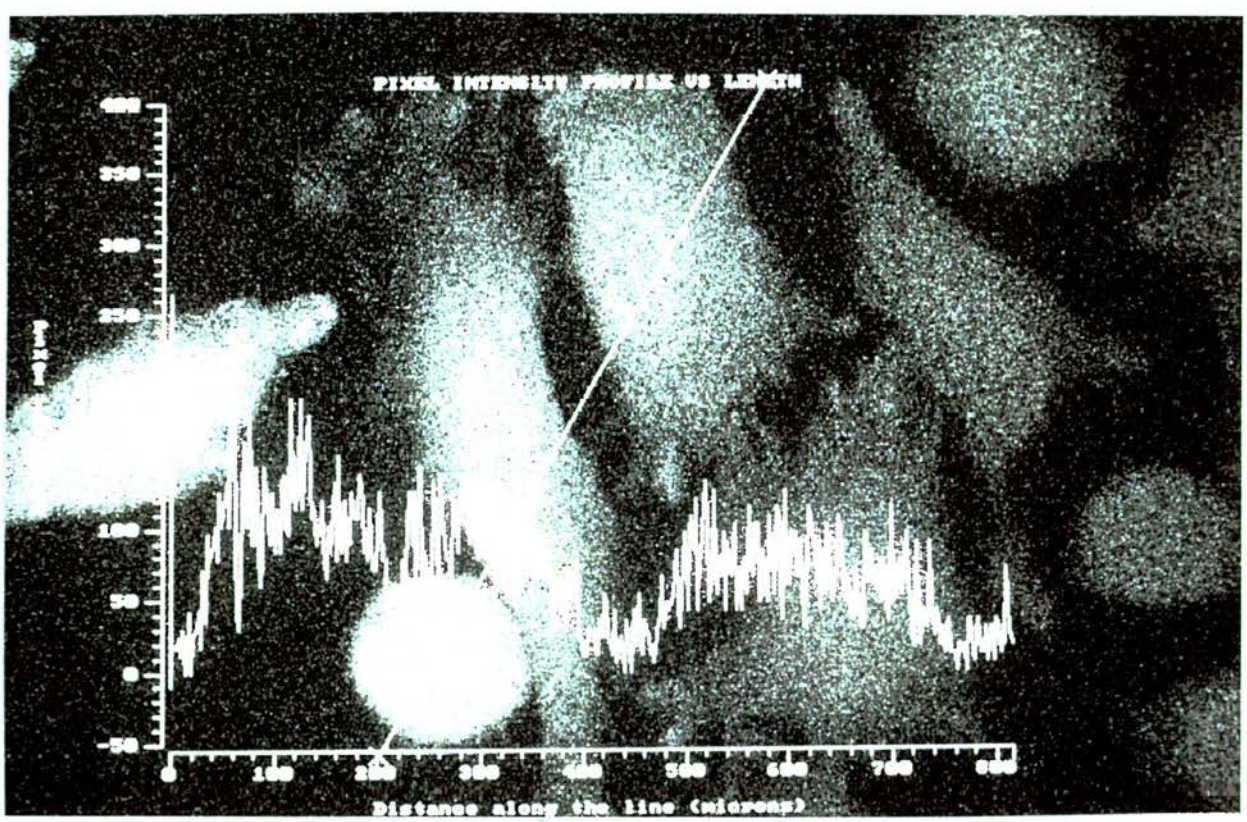

Figure 2.7 Photographs 2.6 & 2.7 are laser scanning confocal images of sub-confluent cells treated with anthroylouabain. 2.6 gives anthroylouabain concentrations through an area of the cell with photograph 2.7 showing a pixel intensity graph from a micron slice through the cells.

2.4 Discussion

Initial findings by Lamb (1996) show that affinity for ouabain (measured as the K_d) of the sodium pump in HeLa cells varies with growth conditions. He found that the affinity for ouabain falls while cells are actively dividing. Conversely, in confluent cells, the affinity rises, showing a three-fold increase in sensitivity to ouabain than dividing cells. Reasons for this have not fully been explored, however it is understood that during cell division pumps are rapidly internalised from the surface into the cell, taking attached ouabain with them. Recovery to the plasma membrane is equally as rapid. The ability of Na^+, K^+ ATPase of the dividing cell to transport potassium ions was also briefly investigated. A high affinity for ouabain is associated with a higher ability to transport potassium. This implies that when pumps are less able to transport ions, the cell inserts more of them into the plasma membrane. It has been shown that isolated Na^+, K^+ ATPase is much more active in the presence of actin (Cantiello, 1995). There is much evidence that cytoskeletal elements of cells in culture changes when they reach confluence (Wong, 1983). For example, in endothelial cells the specific microfilament structure lying below the plasma membrane (the 'dense peripherial bands') only appears at confluence.

The membrane surface of polarised epithelial cells can be divided in apical and basolateral domains that differ in molecular composition and function. Components of the cytoskeleton are involved in critical steps of both generation and maintenance of cell polarity. Generation of polarity is controlled by microtubules that serve as uniformly aligned and polarised cytoplasmic guiding structures for the vectorial and selective transport of Golgi-derived carrier vesicles to the apical cell surface. Targeting of membrane proteins to the

basolateral cell surface does not depend on microtubules but follows the constitutive bulk flow of membranes. Once inserted into the lipid bilayer several membrane proteins such as the kidney anion exchanger 1 (AE-1) and the sodium pump become immobilised at specialised microdomains of the lateral cell surface. Evidence is provided that both membrane proteins are linked via ankyrin to the spectrin-based membrane cytoskeleton that underlies the basolateral membrane domain. Linkage of these and other integral membrane proteins to the cytoskeleton may not only place them to specialised sites of the plasma membrane but may also prevent these transporters from clustering and endocytosis, thus helping them to stay at the cell surface (Drenckhahn *et al.*, 1993). Associations with the plasma membrane proteins and Na^+, K^+ ATPase is of interest in cells reaching confluence. Research by Morrow *et al.* (1989) examines the cortical cytoskeleton (composed of fodrin/spectrin) in MDCK cells, which have been previously shown to co-distribute at the basolateral domain. Fodrin distribution is regulated post-translationally after monolayer confluence is attained, but this is a regulatory process that is poorly understoond (Nelson &Veshnock 1987). Morrow's findings show in MDCK cells and cells of the kidney proximal tubule, Na^+, K^+ ATPase, fodrin and human analogues of ankyrin (specific to erythrocytes) co-localise ultrasturcturally only after confluence is attained. In erythrocytes, binding of ankyrin to Na^+, K^+ ATPase is found in a molar ratio of 1:4. Ankyrin is an important key protein transferring the signal between the inside and outside of eukaryotic cells, because of its ability to bind both to ionic channels of the plasma membranes and to cytoskeletal proteins. Investigations by Davis & Bennett (1990) demonstrate via affinity chromatography new ankyrin binding protein in the rat cerebral membrane. Five proteins in the extract of demyelinated membranes were bound to erythrocyte

ankyrin. One of the proteins distinguished had a molecular weight of 97 KDa that was almost identical with that of the α subunit of Na^+, K^+ ATPase. ^{125}I-labeled erythrocyte ankyrin was bound to the α subunit of cerebral Na^+, K^+ ATPase, which contains both α-1 and α-2 subunits. Results of these binding experiments show 70% of total erythrocyte ankyrin bound to cerebral Na^+, K^+ ATPase (Morrow *et al.* 1989; Davis & Bennett (1990). Experiments by Morrow *et al.* (1989) also identify a second minor membrane protein of approximately 240 KDa that is associated with both erythrocyte and kidney membranes that binds ^{125}I-labeled ankyrin. The precise identity of this component is unknown. These results identify a molecular mechanism in the renal epithelial cell that may account for the polarised distribution of the fodrin-based cortical cytoskeleton (Morrow *et al.* 1989).

A hypothesis for the preliminary results from this Chapter is that some aspects of these cytoskeletal changes interact with Na^+, K^+ ATPase via ankyrin molecules (Jordan, 1995) altering its structure. This in turn, will effect the transport of ions and the ability to bind ouabain. Interaction between Na^+, K^+ ATPase and the actin cytoskeleton may prove to function as an intracellular and dynamic regulatory pathway by which the cytoskeletal proteins contribute to the regulation of intracellular [Na^+].

A comparison of Na^+, K^+ ATPase density and distribution in HeLa and bovine aortic endothelial cells.

The aim of this study is to compare the abundance of Na^+, K^+ ATPase in HeLa and bovine aortic endothelial cells [BAECs] and to examine the potential of BAECs for investigating the response of Na^+, K^+ ATPase to fluid shear stress. This study will examine any differences that exist between the two cell lines, but will also compare the amount of ouabain binding between young and old cells. The results demonstrate that HeLa cells and BAECs used for experimentation at day 4 growth (after plating) have similar levels of specific ouabain binding, whereas BAECs harvested at day 14 show less ouabain binding in comparison to the younger cells. Differences in the cell types will be reviewed, along with an immunocytochemical study of actin and the Na^+, K^+ ATPase α-1 and β-1 subunits in young and old cells.

3.1 Introduction

Ouabain is a potent inhibitor of Na^+, K^+ ATPase as previously discussed in Chapter 2. Radio-isotopically labelled ouabain (in this case labelled with ^3H) is used as a specific ligand of Na^+, K^+ ATPase kinetics to study ouabain association and dissociation, as well as ouabain uptake and intracellular processing. Under normal conditions, the relationship between ouabain binding and pump site inhibition is 1:1 (Sweadner, 1995) i.e. one molecule of ouabain binds to an external site on one sodium pump. Glycoside concentrations of 1 nM take approximately 24 hours to reach equilibrium. so the process is more difficult to study in human tissues. In cultured HeLa cells the α- subunit of Na^+, K^+ ATPase has the same composition as the most sensitive form of the α- subunit from other human tissues (Shull, 1987).

Experimentally, ouabain binding to cells has been shown to be composed of two components; a saturable *specific* component, associated with the binding and inhibition of Na^+, K^+ ATPase; and an unsaturable, component thought to represent non-specific binding and uptake of ouabain into the cell (Baker and Willis, 1972). The nature of the non-saturable cellular uptake mechanism for ouabain has not yet been characterised. The non-saturable component can be determined when specific glycoside binding to the Na^+, K^+ ATPase is inhibited in the presence of K^+ ions. Specific ouabain binding represents the total ouabain binding minus the non-specific binding, and can be used for quantification of the total number of Na^+, K^+ ATPase units (Baker and Willis, 1972).

3.1.1 HeLa and endothelial cells

3.1.1a HeLa cells

HeLa cells are human cervical carcinoma cells, named after **He**nrietta **La**cks, a young woman diagnosed with cervical cancer (Jones, 1997). The cells lining the cervix are stratified squamous epithelial cells. The tumour cells found (HeLa cells) proliferate rapidly and have proved to be a very robust cell line. Their initial discovery in 1951 opened many doors in research areas such as tissue culture, developments in protein synthesis, genetic engineering and the discovery of the polio vaccine. HeLa cells are still widely used throughout scientific research today. This cell line is found having only one α-subunit, shown to be equivalent to the rat α-1 isoform (Cutler, 1988; Griffiths *et al.*, 1991). The rat α-1 isoform is half maximally inhibited ($K_{0.5}$) by 40 μM ouabain (Erdmann *et al.*, 1980), whereas the human α-1 subunit has a $K_{0.5}$ of approximately 5 nM (Aiton, 1976). Although there are large differences in binding constants between species,

there is a good correlation between the percent inhibition of Na^+, K^+ ATPase and the percent increase in myocardial contractile force (Schwartz *et al.*, 1988).

HeLa cells grown in confluent monolayers do not contact-inhibit, meaning they continually grow. The term "confluent" describes a cultured population that occupies all available growth surfaces (depicted in the Figure 3.1).

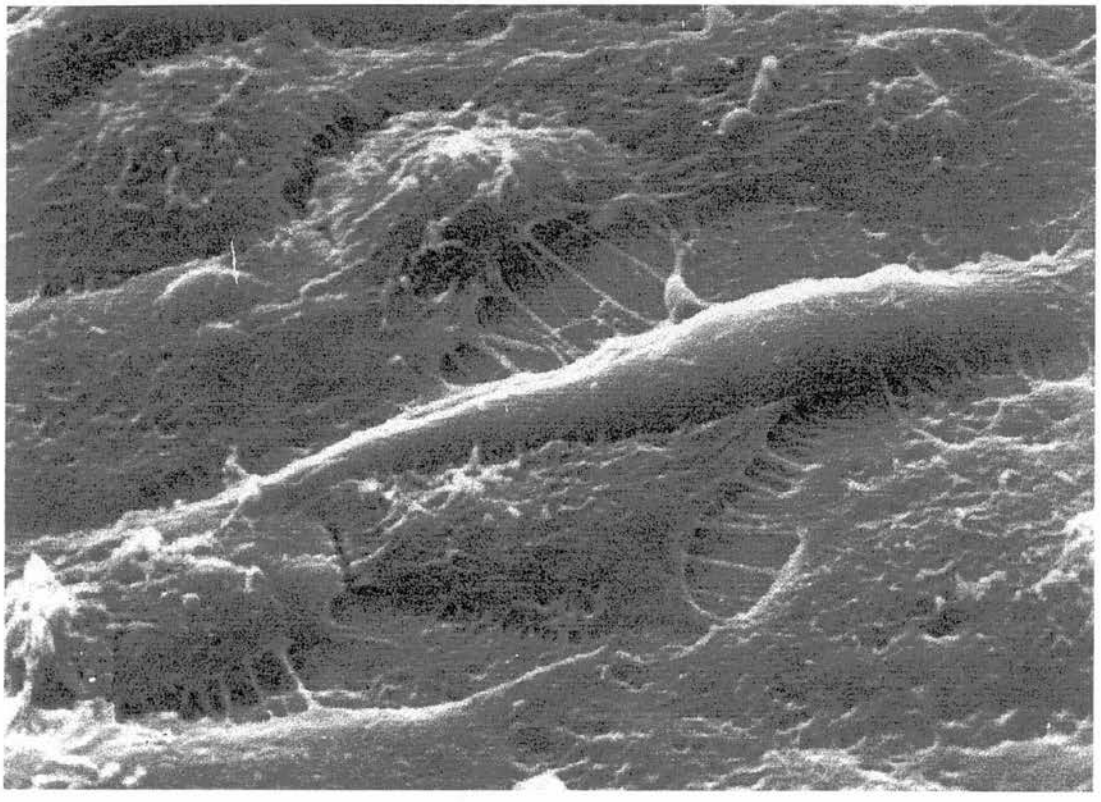

Figure 3.1 Scanning electron micrograph of HeLa cells in monolayer culture (courtesy of Dr. J. Aiton). HeLa cells grown in confluent monolayers do not contact-inhibit but grow continuously. The term "confluent" describes a cultured population that occupies all available growth surfaces as depicted in the micrograph.

3.1.1b Endothelial cells

Endothelial cells (EC) can be divided into two groups: those that line large vessels, and those that line the microvasculature. EC's are attached to blood vessel walls in a polarized fashion to form the luminal surface of the vascular system. Blood flow regulates the internal diameter of arteries in two ways; first, by acute regulation, by relaxation and contraction of the smooth muscle cells; and secondly, through chronic regulation, by the reorganization of the vascular wall cellular and extracellular components (Davis and Tripathi, 1993). Therefore, the endothelium functions as a mechanically sensitive signal transduction interface between the blood and artery wall.

EC's that line all blood vessels continually produce NO (via activity of eNOS) to maintain normal blood flow and blood pressure (Hecker *et al.*, 1994). In many cardiovascular diseases (hypertension, diabetes, atherosclerosis, heart failure), the ability of EC's to manufacture NO is impaired suggesting a defect in NOS enzymology and activation. Nitric oxide (NO) is an important second messenger in the nervous, cardiovascular and immune systems. In the brain and endothelium NO is produced from the guanidino nitrogen of L-arginine, by a constitutively expressed calcium/calmodulin-, tetrahydrobiopterin-, NADPH-requiring enzyme.

Vascular sodium pump activity was examined by Redondo *et al.,* (1996). The focus of his study was on the regulation of Na^+, K^+ ATPase by vasoactive agents. He examined endothelium and cultured aortic vascular smooth muscle cells from

normotensive Wistar-Kyoto rats (WKY) and spontaneously hypertensive rats (SHR)[1]. Baseline Na^+, K^+ ATPase activity (measured by ouabain-inhibitable $^{86}Rb^+$ influx) was similar in both rat strains. Ouabain effects vascular resistance by causing vasoconstriction by direct effect on the vascular smooth muscles, or indirectly by releasing norepinephrine from perivascular nerve endings (Redondo *et al.*, 1996). Contractile responses evoked by glycoside binding in SHR vasculature are enhanced. Along with vasoconstriction, the inhibition of Na^+, K^+ ATPase can increase vascular resistance by interfering with vasodilator endothelial factors (Rapoport *et al.*, 1985a and b). Hence, ouabain inhibits endothelium-dependant vasodilation by blocking NO release from EC's, by reducing the effects of NO on the underlying vascular smooth muscle cells, or by antagonizing the action of a still unidentified endothelium-derived hyperpolarizing factor.

Further experiments by Redondo, *et al.*, (1996) investigated other mechanisms involved in endothelial stimulation of VSMC using the rat strains mentioned in the previous studies and using the radioactive marker for K^+: $^{86}Rb^+$. Conditioned medium of bovine endothelial aortic cells was used to investigate the endothelial modulation of VSMC Na^+, K^+ ATPase activity. Results show that conditioned medium enhanced VSMC Na^+, K^+ ATPase activity, an effect that was greater in SHR cells. This stimulatory effect was neither modified in Na^+ loaded cells from both rat strains nor inhibited by the Na^+/H^+ exchange blocker amiloride. Permeable analogues of cyclic adenosine and guanosine monophosphates did not modify the baseline VSMC Na^+,

[1] SHR rats are an inbred strain. As the animal ages, it develops high blood pressure spontaneously. Another strain also exists called the SHHR (stroke-prone spontaneously hypertensive rat). The genetic background of the SHR rat is predominantly from the normotensive (i.e. does not develop hypertension like the SHR) Wistar-Kyoto strain. (Davidson pers. comm.) For further information see: Aitman, T.J. (1999) *Nat Genet*, **21**, 76-83.

monophosphates did not modify the baseline VSMC Na^+, K^+ ATPase activity of WKY rats and SHR. Subsequently, the guanylate cyclase inhibitor methylene blue did not alter the conditioned medium-induced stimulation of the pump. However, the Ca^{2+} channel inhibitor nifedipine reduced the Na^+, K^+ ATPase stimulation by conditioned medium, and this effect was greater in WKY than in SHR VSMC. Moreover, treatment with phorbol 12,13-dibutyrate for 24 h, or with the protein kinase C inhibitor staurosporine, for 15 min reduced the conditioned medium-induced Na^+, K^+ ATPase activation in both VSMC cultures. Conclusions show that Na^+, K^+ ATPase stimulation by conditioned medium of endothelial cells is mediated mainly via activation of protein kinase C in VSMC from either WKY or SHR VSMC. However, SHR VSMC shows some alterations in their intracellular signaling pathways (Redondo, *et al.*, 1996).

For the purpose of this study BAECs were grown and used for experimentation in confluent monolayers (Figure 3.2). Unlike HeLa cells, BAECS cells contact-inhibit when they touch other cells, with older monolayers showing a cobbled effect. HeLa cells continue to replicate in log phase growth[2] if nutritional conditions are adequate.

[2]The kinetics of cells grown in monolayer culture has a characteristic pattern of growth. After seeding, the cells undergo a quiescent or "**lag phase**" corresponding to a period when there is no cell division. The duration of this phase is dependent on cell type, seeding density, media composition and initial health of the cells. The cells then enter a "**log phase**" of growth where there is an exponential increase in cell number. It is during this phase that the cells exhibit their highest metabolic activity. When the culture conditions can no longer support cell division the population enters a "**stationary phase**" where the cells number remains constant (Jakoby and Pastan, 1979).

Figure 3.2 Confluent monolayer of BAECs under phase-contrast. Scale bar = 10μm

3.2 Methods

3.2.1 Epithelial cells

HeLa cells obtained from Imperial Laboratories were cultured in Dulbecco's modification of Eagles medium [DMEM]. DMEM was supplemented with 10% foetal calf serum [FBCS], 1% glutamine, 1% Non-essential amino acids, and 0.5% Kanamycin. Cells were routinely passaged under asceptic conditions and seeded at density of 2.7 x 10^4 per cm^2. Cells were stored in a sealed box and equilibrated with a 5% CO_2, 95% O_2 mixture to maintain pH at 7.4.and incubated at 37°C. A stock of HeLa cells was also kept in liquid N_2 to ensure continuity of the cell line.

3.2.2 Endothelial cells

Bovine aortic endothelial cells (BAECs) were obtained from the European Collection of Animal Cell Cultures (ECACC) for Applied Microbiology and Research, Salisbury, U.K. Confluent monolayers of endothelial cells consisted of a homogeneous population of tightly packed, polygonal cells. Cells were serially sub-cultured with DMEM and supplemented with 10% FBCS, 50 i.u./ml penicillin, 50μg ml^{-1} streptomycin and 29 mg ml^{-1} glutamine. Cells were plated at 2 x10^4 cells per cm^2, requiring a medium change twice a week. Routine passage was carried and cells were incubated at 37°C in an atmosphere of 5% CO_2 and 95% O_2. A stock of BAECs was also kept in liquid N_2 to ensure continuity of the cell line.

3.2.3 ^{3}H Ouabain binding

Ouabain binding was measured according to the methods of Baker and Willis (1970 and 1972) and of Boardman *et al.*, (1972). The previous studies describe

two components of ouabain binding in intact HeLa cells. First, non-specific binding which is non-saturable and insensitive to the extracellular potassium concentrations; second, specific ouabain binding, which is first order with respect to ouabain concentration, saturates at low concentrations of ouabain and is extremely sensitive to extracellular potassium concentrations. Results of several studies show that a proportional relationship exists between potassium sensitive specific ouabain binding and (a) inhibition of Na^+, K^+ ATPase activity; and (b) ouabain sensitive transport of either sodium efflux or potassium influx (Baker and Willis 1970, 1972; Boardman, *et.al.*, 1972, Esmann, 1988).

In the present study, specific binding of ouabain to Na^+, K^+ ATPase was measured. Since K^+ competes with ouabain for binding to Na^+, K^+ ATPase two types of Krebs solutions were used: $0K^+$ and $5K^+$ (chemicals and concentrations the same as in Section 2.6, pH 7.4). Ouabain solutions were made from $2x10^{-7}M$, non-radioactive ouabain plus between 0.5 and 6 $\mu Ci\ ml^{-1}$ [^{3}H]-ouabain made up in $0K^+$ Krebs with BSA (final concentration = $2\text{-}3x10^{-7}M$). After incubation with [^{3}H]-ouabain, the plates were rinsed with ice-cold Krebs solution to remove the extracellular isotope and the cells were then detached with trypsin/EDTA (0.25% trypsin, 2mM EDTA in basal salt solution without Ca^+ or Mg^{2+}) to obtain a cell suspension. Cell numbers and volumes were determined using a Coulter Counter. The amount of isotope was determined with a liquid scintillation spectrometer. [For a more detailed protocol see Part I Appendix 3]

3.2.4 Immunofluorescence

Cells were viewed under a light microscope (Olympus) to ensure desired cell confluence before experimenting. HeLa cells and BAECs cells grown on glass

coverslips were removed from culture medium and rinsed with phosphate buffered saline (PBSc) at room temperature (2x5 min). Cells were fixed for 10 minutes with 4% paraformaldehyde in distilled water at room temperature. The fixative was then removed and cells were washed in PBSc (3x5 min.) and permeabilised with 0.1% Nonidet P40 detergent in PBS (5 min.) at room temperature. Subsequently, the cells were washed in PBSc (3x5 min). Non-specific binding of antibody was blocked by incubating cells with PBSc containing 10% normal goat serum for one hour at room temperature.

3.2.4a Na^+, K^+ ATPase staining

Monoclonal antibodies for the α-1 and β-1 subunit of the sodium pump were diluted with 1.0% NGS. 50µl of antibody solution/coverslip was added and incubated overnight in a moist chamber at room temperature. After incubation with the primary antibody, cells were rinsed in 1.0% NGS (3x5 min) to remove all traces of the primary antibody. Cells were then incubated with 50µl of secondary antibody, a 1:200 dilution of goat anti-mouse Fluorescein Isothiocyanate (FITC/Fluorescein) for 30 minutes at 37°C. The cells were rinsed with PBSc (3x5 min) and mounted with Gelvatol on glass slides. Before using Gelvatol mountant, 100 mg ml^{-1} of 1,4 Diazabicyclo [2,2,2] octane was added to help preserve fluorescence. All antibodies were mixed well and then centrifuged in a micro-centrifuge (500 rpm x 15min) before use.

Na^+, K^+ -ATPase antibody dilutions

(Monoclonal)

1°Ab	Dilution	2° Ab	Dilution
α -1	1:30	GAMF	1:200
β1	1:50	GAMF	1:200

3.2.4b Actin staining

Cells were fixed with 1.0 % formaldehyde (10 min) in PBSc, permeabilised with 0.1% NP40 (20 min) and non-specific binding blocked using 0.1% BSA (20 min). Actin was labelled with phalloidin RITC or FITC. Phalloidin is a neurotoxin produced naturally by *Amanita phalloidies* [the toadstool] (Cooper, 1997). Precaution was taken by wearing gloves and properly discarding pipette tips.

3.2.4c Golgi staining

Cells were fixed in 1.0 % EM grade formaldehyde for 10 minutes, permeabilised in 0.1% NP40, blocked for 5 minutes in 10 % BSA and stained for the Golgi apparatus with the G58K antibody. Secondary antibody (GAMF) was used at 1:200.

3.2.4d Hoechst stain

Cells were also mounted using the Hoechst stain 33258 that binds directly to DNA. The fluorescent DNA staining technique is an effective way of checking to detect mycoplasma infection (Figure 3.3). It is important to ensure that cultures are free of infection to rule out the possibility of cross reactivity of antibodies with contaminant.

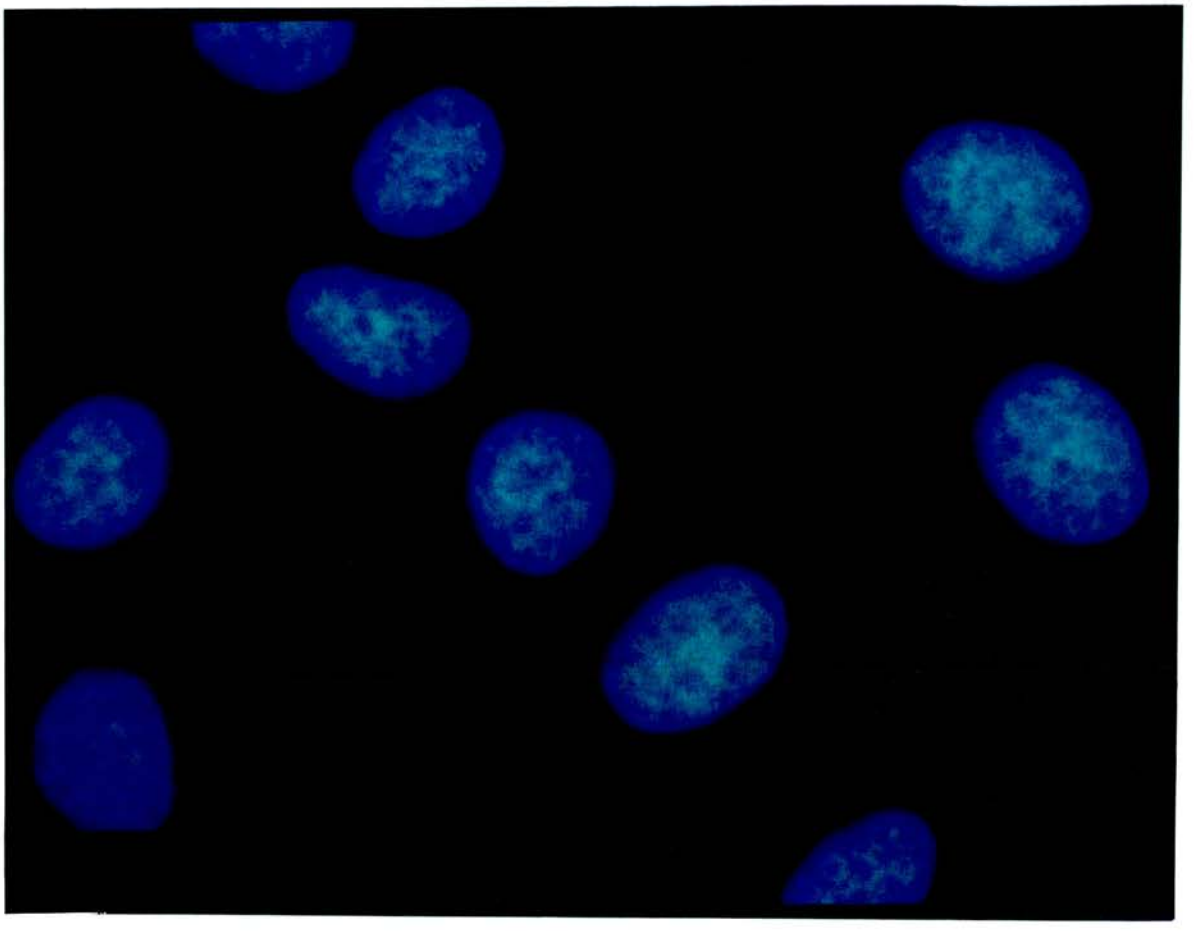

Figure 3.3 HeLa cells stained with the Hoechst 33258 stain. The nuclei fluoresce brightly from cellular DNA. There is no cytoplasmic background with this stain, extracellular fluorescence would mean the cells are infected with mycoplasma. Immunofluorescence of Na^+, K^+ ATPase yields a very particulate stain. It is important to rule out cross reactivity of the antibody with existing colonies. The cells for the following experiments have been checked for mycoplasmas and are reported negative for infection. All HeLa and bovine cell cultures are healthy in the following experiments

3.2.5 One dimensional gel electrophoresis

HeLa and BAECs were grown in Nunc 90mm diameter TC grade petri dishes for cell lysate preparation.

3.2.5a Cold Lysis buffer for HeLa cell preparations

Cells were lysed in ice cold lysis buffer (pH 6.8 50mM Tris-HCL, 0.25% sodium deoxycholate detergent, 150 mM NaCl, 1.0mM EGTA, 1.0 mM PMSF [phenylmethylsulfonyl fluoride protease inhibitor in methanol], 1.0 mM Na_3VO_4, 1.0 mM NaF, and 1μg/ml of each of aprotonin, leupeptin and pepstain). Total protein was assayed using Bio-Rad DC (detergent compatible) kit. The proteins were diluted with 5 x laemmli buffer.

3.2.5b Hot Lysis Buffer for whole cell lysate

Passage 21 cells (P21) BAECs were harvested at 1, 2, 3, 4 and 14 days incubation. Cells were removed by treatment with 0.5% trypsin in PBS-EDTA for 3 minutes at 37°C. Trypinisation was halted by the addition of 10 ml of serum-containing medium and the resulting cell suspension was centrifuged for 10 minutes at 1000rpm at 4°C. The supernatant was decanted and the cells washed twice with cold PBSa (without calucim and magnesium). An aliquot was removed for cell counting before final centrifugation.

An appropriate volume of 3% beta-mercaptoethanol (BME) was added to the dried pellet to give the sample containing 10^7 cells ml^{-1}. This was pipetted into an eppendorf tube and placed in a boiling water bath for 5-10 min. and cooled to

room temperature, centrifuged for at 12,000rpm x 5 min. and the supernatant stored at –20°C.

3.2.5c Gel electrophoresis and Western blotting

Proteins were resolved on 6.0 % SDS polyacrylamide gel [Running buffer used 10x Tris/Glycine: Tris (Analar) 0.025 M, SDS (Sigma MB) 0.1%, glycine (Sigma MB) 0.24 M pH 8.0] using an Anachem Model MV2-DC gel rig [providing a discontinuous buffer system] and power pack run between 70-100volts. The proteins were transferred to nitrocellulose membrane using a semi-dry horizontal transfer Blotter at 10 volts for 45 minutes to 1 hour with Bio-Rad Power pac. Towbins buffer (25 mM Tris, 192 mM glycine, 20% v:v methanol, pH 8.3) was used for electrophoretic transfer. The membranes were blocked in 5% powdered fat free milk in PBS-T. Membranes were incubated with primary antibody [α-1 and β-1 subunits of Na^+, K^+ -ATPase used at 1:1000], with agitation overnight at 4°C. After x 4 washes with PBS-T (phosphate buffered saline with 0.1% Tween-20 pH 7.6), the membrane was incubated with sheep anti-mouse peroxidase [SAMP] at 1:1000, at room temperature with agitation. The protein bands in Western blotting were visualised using enhanced chemiluminescence (ECL, Amersham). ECL Western blotting is a light emitting non-radioactive method for detection of immobilized specific proteins/antigens conjugated directly with horseradish peroxidase-labelled antibodies.

3.2.5d Coomassie blue staining of cells

Protein bands in the gel were detected using Coomassie blue stain which non-specifically binds to the proteins. The detection limit is 0.3 μg to 1mg/protein

band. After leaving the gel in Coomassie blue overnight at 4°C the entire gel was stained blue. By putting the gel into destain solution for several hours then changing the destain solution, blue bands appear against a clear background. The gels were photographed immediately or stored for up to a week before the colour faded.

3.2.6 Materials and Drugs

3.2.6a Tissue Culture

HeLa cell tissue culture materials: 10% foetal calf serum [FBCS], 1% glutamine, 1% Non-essential amino acids, and 0.5% Kanamycin. For BAECs: FBCS (Globepharm), penicillin (Sigma), streptomycin (Sigma), glutamine (ICN/Flow). Both cell types require use of: Corning 30mm diameter x6 multiwell TC grade petri dishes, 19.76 cm^2 glass microscope slides (BDH), 22mm^2 boroscilicate glass coverslips (BDH), Nunc 90mm diameter, hot water bath (Tempate® Junior TE-8J), Coulter Counter™ (ZM model), isoton® II (Azide-free electrolyte solution), Microflow™ Biological safety cabinet Model M51424/2, LEEC incubator.

3.2.6b ^{3}H-ouabain binding

^{3}H-ouabain (Sigma), non-radioactive ouabain (Sigma), Bovine serum ablumin [BSA] (BDH), Foetal bovine calf serum [FBCS] (Globepharm), Coulter Counter™ (ZM model) and channelyzer (Model 256), [LSC] Packard, Tri-Carb 2000CA Liquid scintillation analyzer, liquid scintillant (Sigma), trypsin (DIFCO), Vortex [Autovortex Mixer SA2] (Stuart Scientific), pony vials (Sterilin) for radioactive cell counts.

3.2.6c Immunofluorescence

Monoclonal antibodies for the α-1 and β1 subunit of the sodium pump were purchased from Upstate Biotechnology Inc (Lake placid, New York, U.S.A.), G58K antibody for the Golgi apparatus (Sigma), goat anti mouse antibody labelled with fluorescein isothiocyanate (Jackson Immuno. research labs), phalloidin RITC or FITC (FLUKA), Hoechst stain 33258 (Sigma), sheep anti mouse peroxidase, (Sigma) phosphate buffered saline (BDH), 4% paraformaldehyde (Fisions), 1.0 % EM grade formaldehyde (TAAB Lab), 0.1% Nonidet P40 detergent (Sigma), normal goat serum (Sigma), bovine serum albumin (BDH), PBSa and PBS-T (Gibco), 37°C incubator (Hearsan), Gelvatol (Airvol), 1,4 Diazabicyclo [2,2,2] octane (Sigma), Microcentrifuge, (ScotLab Micro Centaur).

3.2.7 One dimensional gel electrophoresis

3.2.7a Lysis buffers

Tris-HCL, NaCl (BDH), sodium deoxycholate detergent, EGTA, PMSF [phenylmethylsulfonyl fluoride protease inhibitor in methanol], Na_3VO_4, NaF, aprotonin, leupeptin and pepstain. (All the aforementioned chemicals were obtained from Sigma unless otherwise specified. Total protein was assayed using Bio-Rad DC (detergent compatable) kit.

3.2.7b Gel Rig

Model MV2-DC gel rig and PSU 400/200 power pack (Anachem), enhanced chemiluminescence reagents (ECL, Amersham). nitrocellulose membrane

(Amersham), transfer Blotter (Bio-Rad Trans-blot® Semi-dry Electrophoretic transfer cell) with Bio-Rad Power pack 200.

3.3 Results

3.3.1 Indirect immunofluorescence staining of the αand β-1 Na+, K+-ATPase in HeLa cells

Black and white photographs taken by conventional microscopy in Figure 3.4 a and b show the differences in the expression of the α-1 subunit of the pump in cells that were newly seeded (Figure 3.4 a day 1) and cells at day 4 growth (Figure 3.4 b).

a)

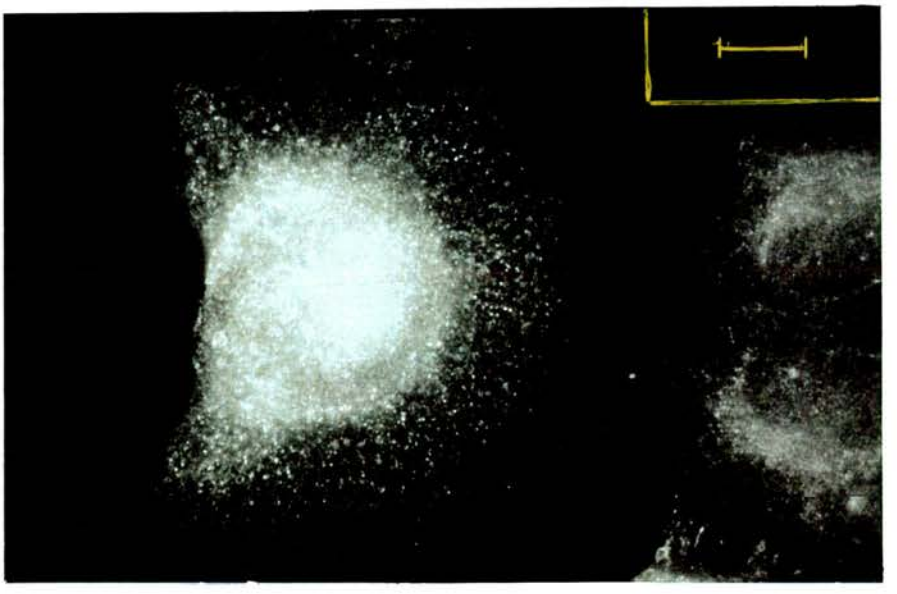

b)

Figure 3.4 Indirect immunofluorescence stain showing distribution of the Na^+, K^+ ATPase α-1 subunit in HeLa cells. a) HeLa cells at day 1 growth. b) HeLa cells at day 4 growth. Scale bar = 10μm.

Cells harvested for experimentation at day 1 are sub-confluent. The cell in the field of view of Figure 3.4 a shows that the α-1 subunit does not appear to be distributed in a particular pattern. The pumps seem to be randomly distributed over the cell with areas towards the edges of the cell appearing as if they are starting to align with filopodia extending out from the cell. The more confluent day 4 cells in Figure 3.4 b show a slightly different α–1 subunit distribution, whereas the pumps appear to be in more distinct rows clearly extending out on areas of filapodia and concentrated around the nucleus of the cells.

a)

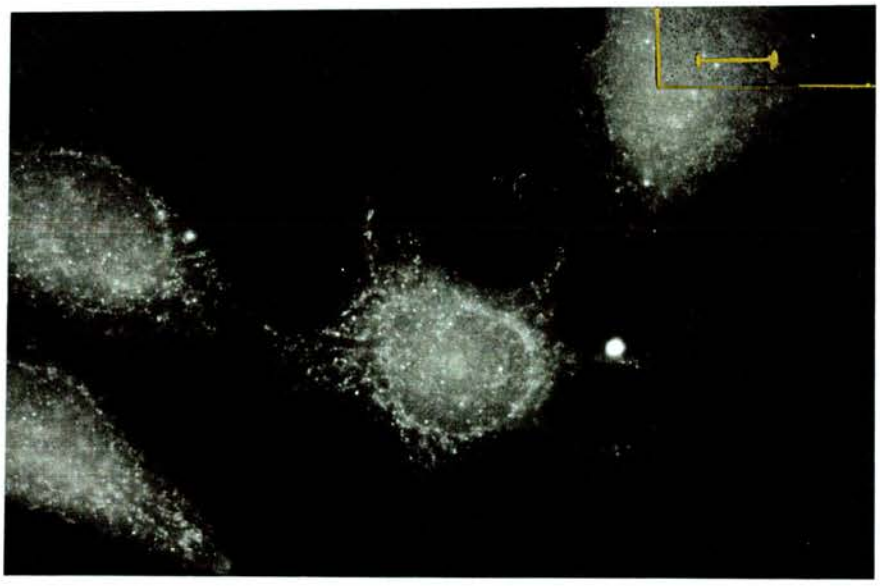

b)

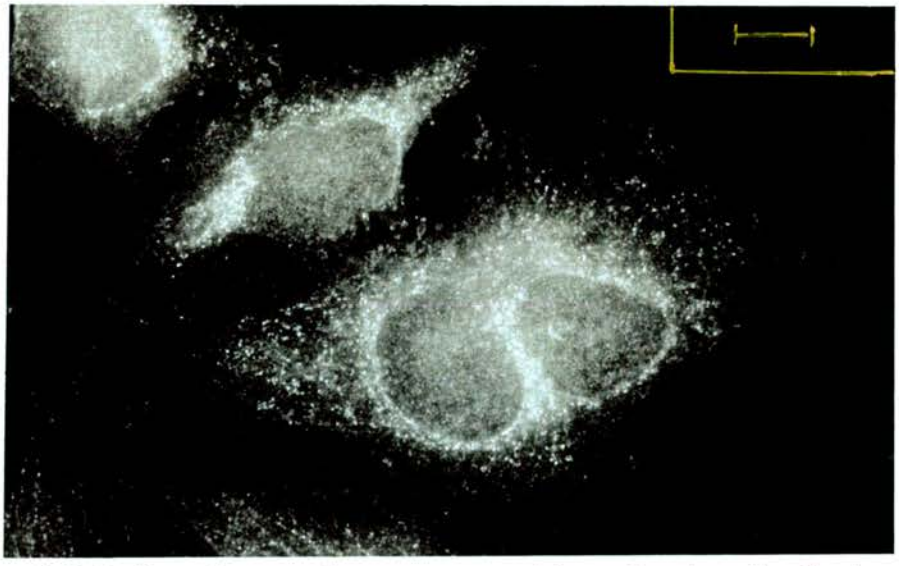

Figure 3.5 Indirect immunofluorescence staining showing distribution of the Na^+, K^+ ATPase β-1 subunit in HeLa cells. a) HeLa cells at day 1 growth. b) HeLa cells at day 4 growth. Scale bar = 10μm.

Figure 3.5 a and b show the distribution of the β-1 antibody in cells after day one growth (Figure 3.5 a) and cells after day 4 of growth (Figure 3.5 b). There is a similar pattern of β-1 antibody distribution between days 1-4, showing large amounts of intracellular staining around the nucleus of the cells as well as alignment with cell filapodia. Expression of the β-1 subunit in day 1-4 cells also shows a similar distribution and abundance of pumps to the α-1 subunit in HeLa cells.

3.3.2 Indirect immunofluorescence staining of the α-1 Na^+, K^+ ATPase in BAECs in young and old cells

BAECs were labelled with antibody to the α-subunit of Na+, K+ ATPase at day 1-4 growth (Figure 3.6 a and b). Expression of the antibody was similar in distribution over the cell membrane. Black and white photographs were taken using conventional microscopy, focusing down on the slide preparation to examine pumps on the surface of the cell membrane. Cells at day 4 growth (Figure 3.6 b) are more confluent, however pump abundance in the membrane appears to be consistent with the cells examined one day after seeding (Figure 3.6 a).

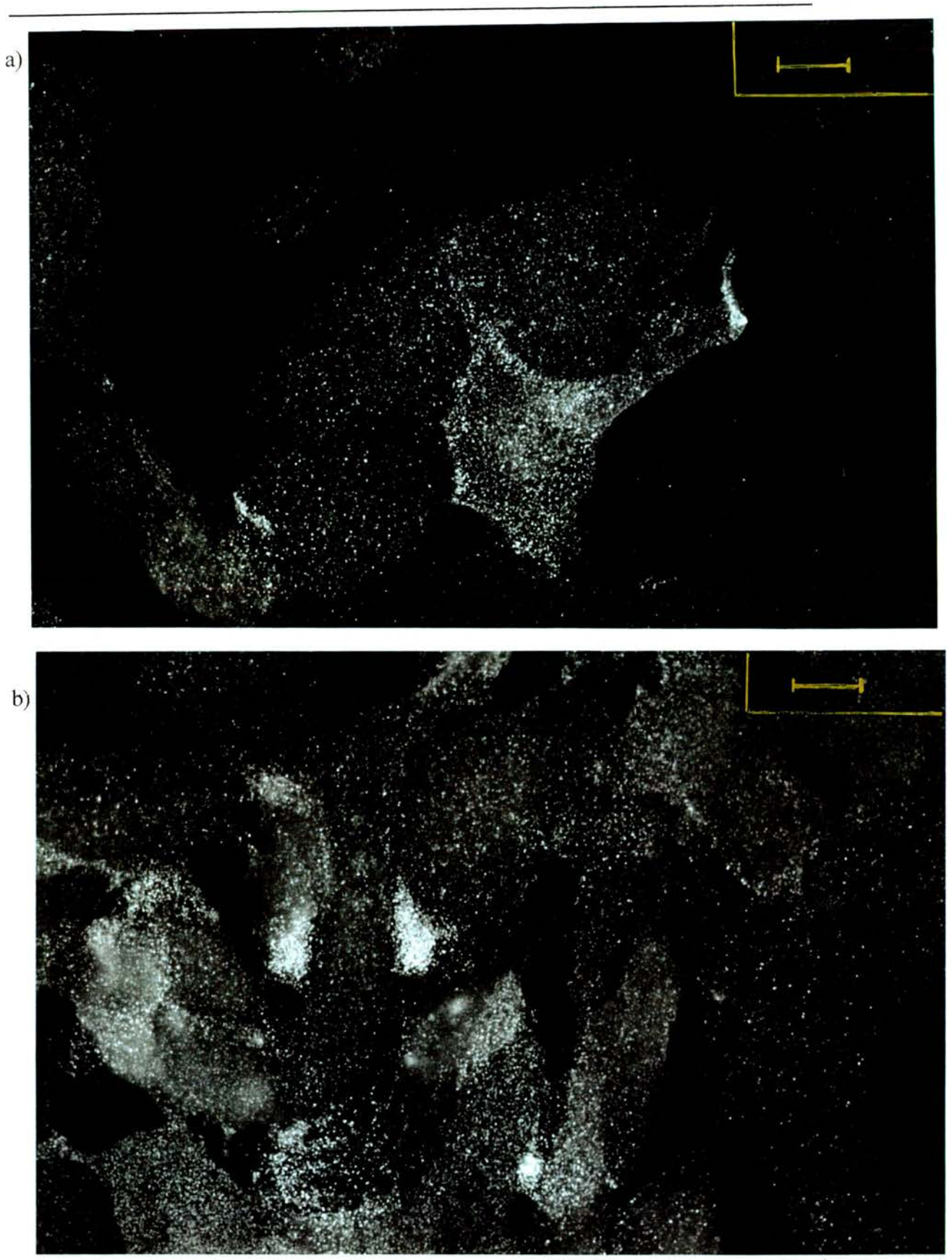

Figure 3.6 Indirect immunofluorescence stain showing distribution of the Na^+, K^+ ATPase α-1 subunit in BAECs. a) BAECs day 1 growth. b) BAECs at day 4 growth. The pattern of Na^+, K^+ ATPase staining is randomly distributed in the cell membrane. Scale bar = 10μm.

An interesting finding is shown in older BAECs. Figure 3.7 a and b show fully confluent cells having a similar distribution of staining between days 11-14, but a vast contrast compared to days 1-4.

Figure 3.7 a) NB Legend below Figure 3.7 b).

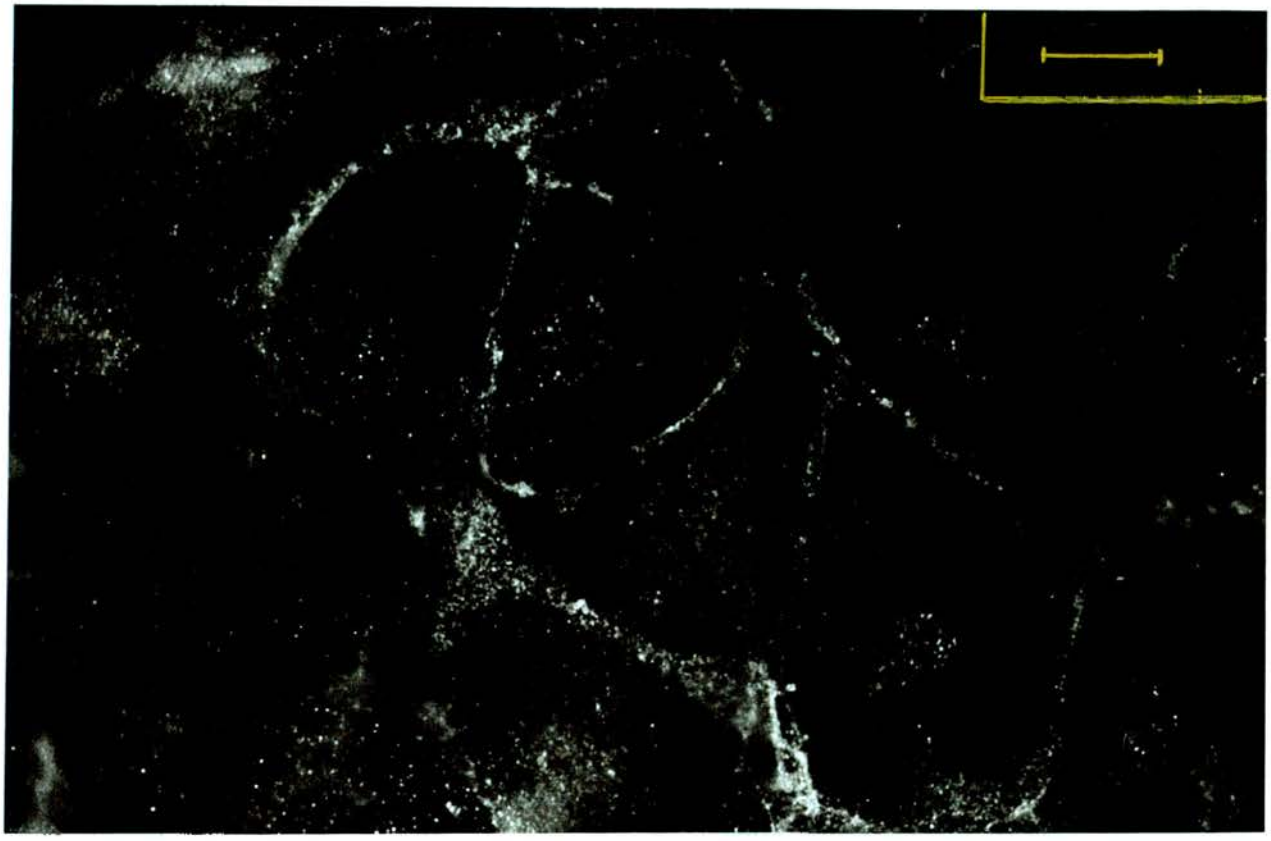

b)

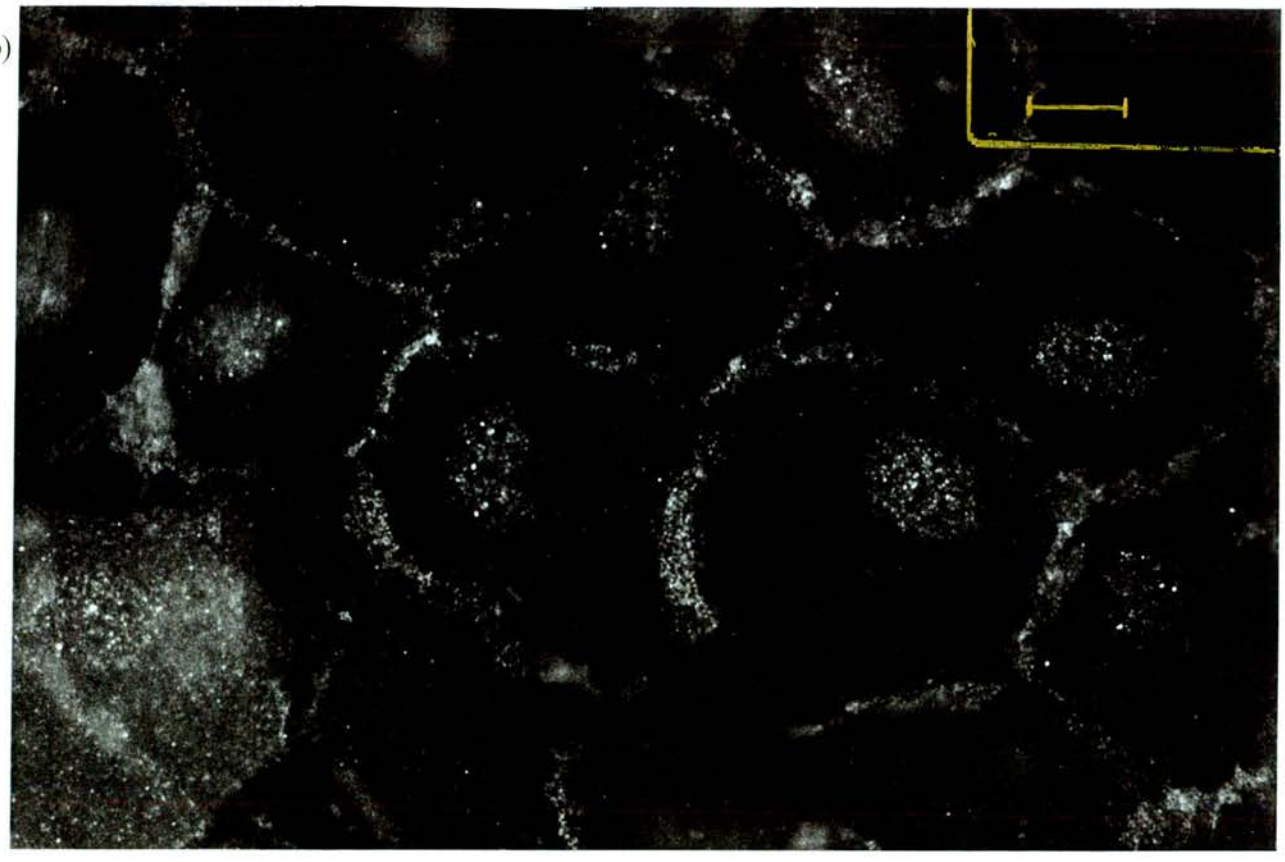

Figure 3.7 Indirect immunofluorescence staining showing distribution of the Na^+, K^+ ATPase α-1 subunit in BAECs. a) BAECs at day 11 growth. b) BAECs at day 14 growth. Notice the difference in pump distribution, as the cells become older and more confluent the pump staining appears to be strongly concentrated between adjacent cells. Scale bar = 10μm.

In days 11-14 cells the α-1 subunit of Na^+, K^+ ATPase is heavily concentrated between adjacent cells which are now in contact with each other. This pattern closely resembles the distribution of dense peripheral bands of actin that appear when the cells become fully confluent. Figure 3.13 d shows dense peripheral bands of actin in day 14 cells. In day 11-14 cells there also appears to be nuclear staining, however these pumps may not be in the nucleus. When focusing through the cell at x100 (oil immersion) pumps are seen distributed throughout the cell in intracellular pools situated between the nucleus and the plasma membrane, possibly on stand by for recruitment into the cell membrane.

3.3.3 Indirect immunofluorescence staining of the β-1 Na^+, K^+ ATPase in the BAECs in young cells

Indirect immunofluorescence staining with a monoclonal antibody against β-1 in young cells (Figure 3.8 a and b days 1-2) revealed the distribution of the β-1 sub-unit to be strongly nuclear and juxta-nuclear with some staining throughout the cell. The juxta-nuclear staining appears to be in a similar position to the Golgi apparatus. To verify that the densely staining nucleus is not necessarily pumps in the nucleus day 2 cells were analysed using laser scanning confocal microscopy.

Figure 3.8 a Legend below Figure 3.8 b.

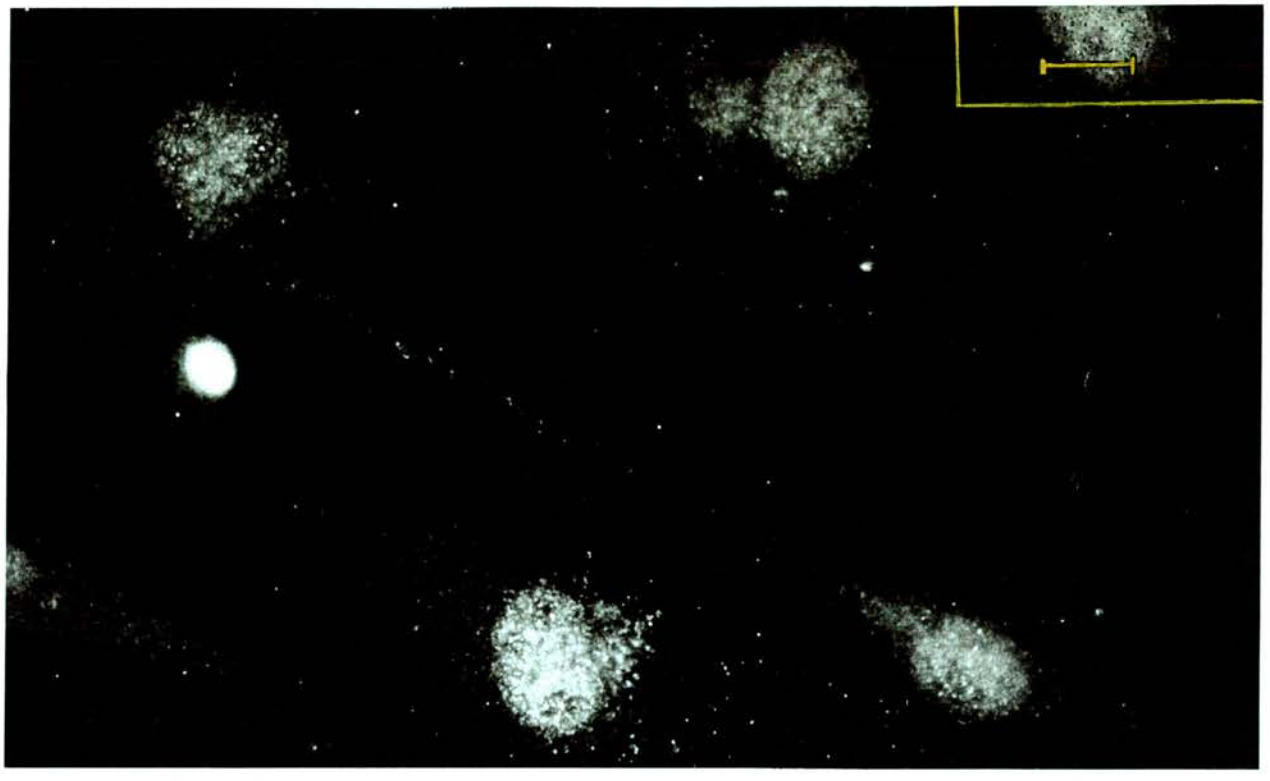

b)

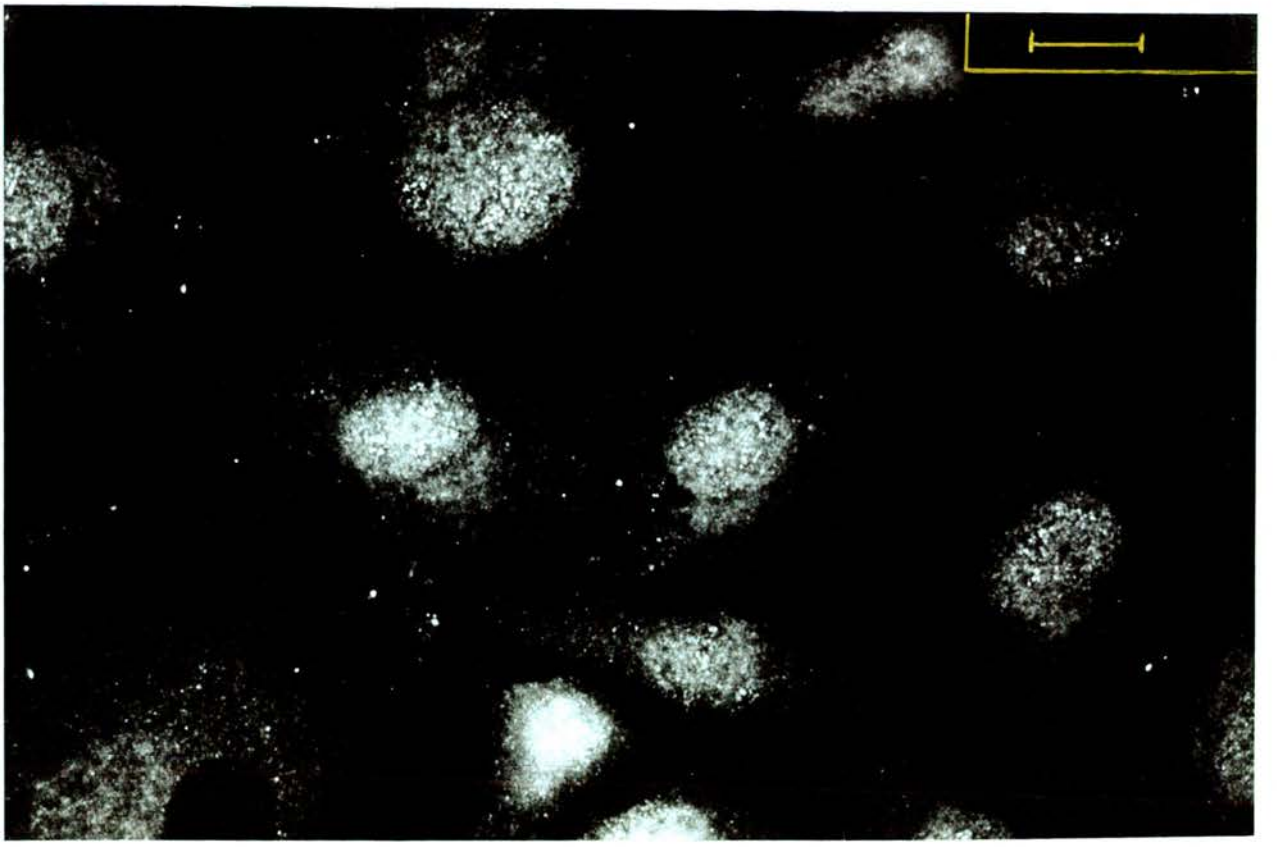

Figure 3.8 Indirect immunofluorescence stain showing distribution of the Na^+, K^+ ATPase β-1 subunit in BAECs. a) BAECs at day 1 growth. b) BAECs at day 2 growth. This illustrates strong nuclear and juxta-nuclear staining in a similar position as the Golgi apparatus. Scale bar = 10μm.

Figure 3.9 a shows a micron slice through the cell surface. The pumps appear to be very brightly staining in this area of the cell.

Figure 3.9 a) Legend below Figure 3.9 b)

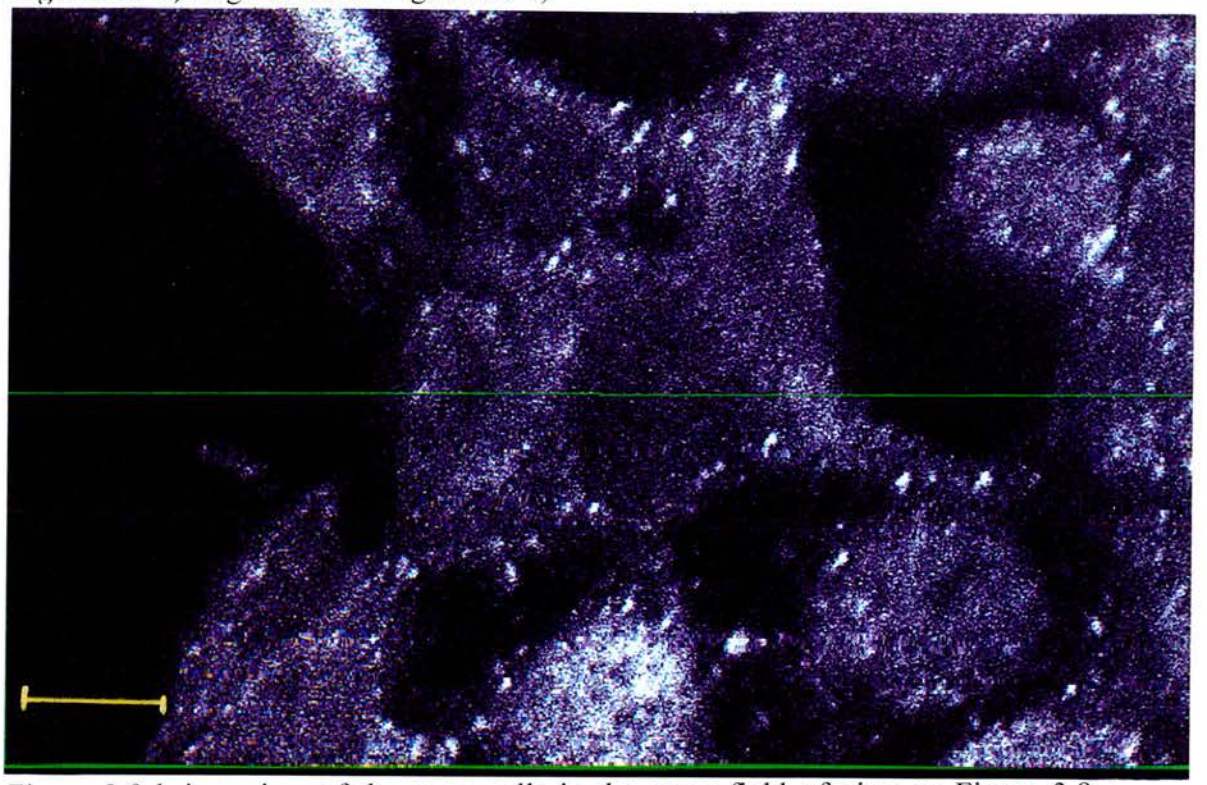

Figure 3.9 b is a view of the same cells in the same field of view as Figure 3.9 a. Focusing down through the cells the pixel intensity reading along a micron slice through the cell (represented by the green line) gives a very low intensity reading as shown by the yellow superimposed pixel intensity graph. This indicates that the majority of the pumps are located on the cell surface, rather than inside the cell. Note the area through the nucleus has a low intensity as well proving the pumps are located in the cell membrane and not the nucleus.

b)

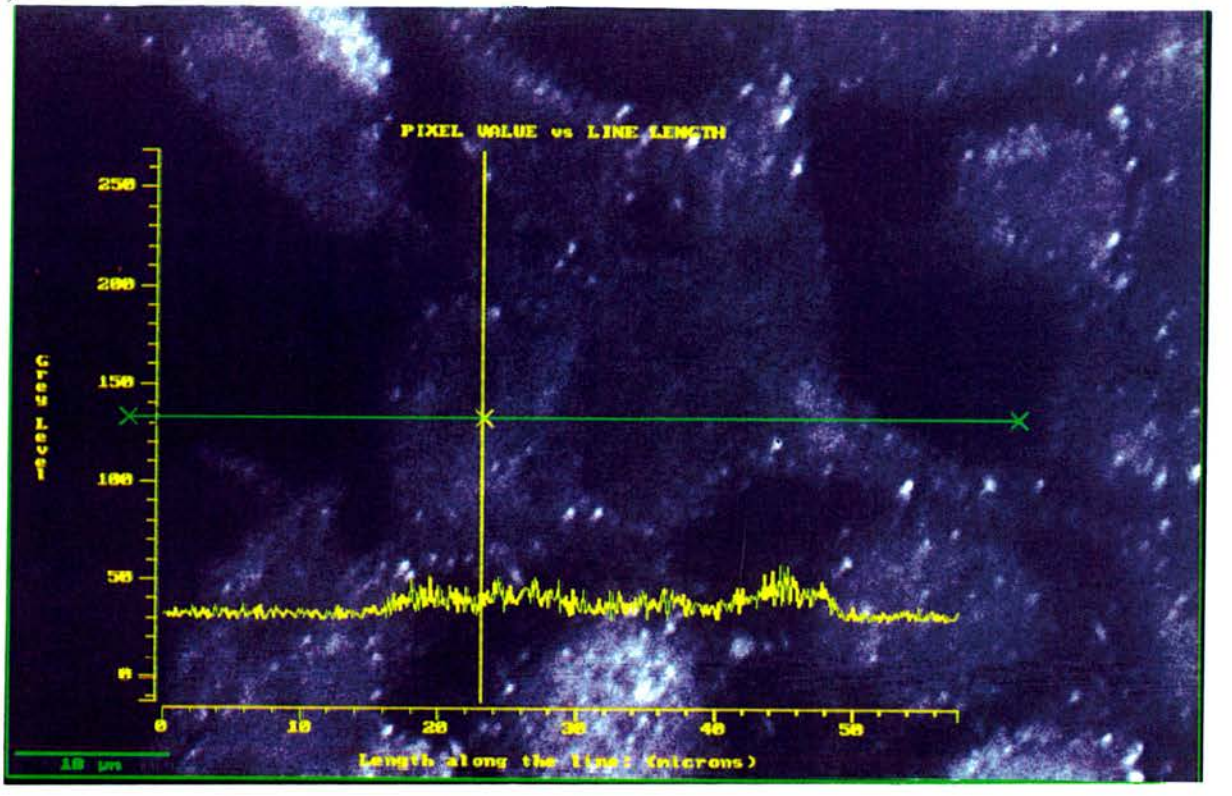

Figure 3.9 Confocal images of day 2 BAECs. The cells are stained for the β-1 subunit of Na^+, K^+ ATPase. a) This photo shows a micron slice through the cell surface. b) focusing down through the cells in the same field of view the pixel intensity reading along a micron slice through the cell gives a very low reading. This indicates that the majority of the pumps are located on the cell surface rather then inside the cell. Note the area through the nucleus has a low reading indicating pumps are in the cell membrane not the nucleus.

Figure 3.10 a and b illustrate BAECs stained with β-1 subunit day 3 and 4 cells.

a)

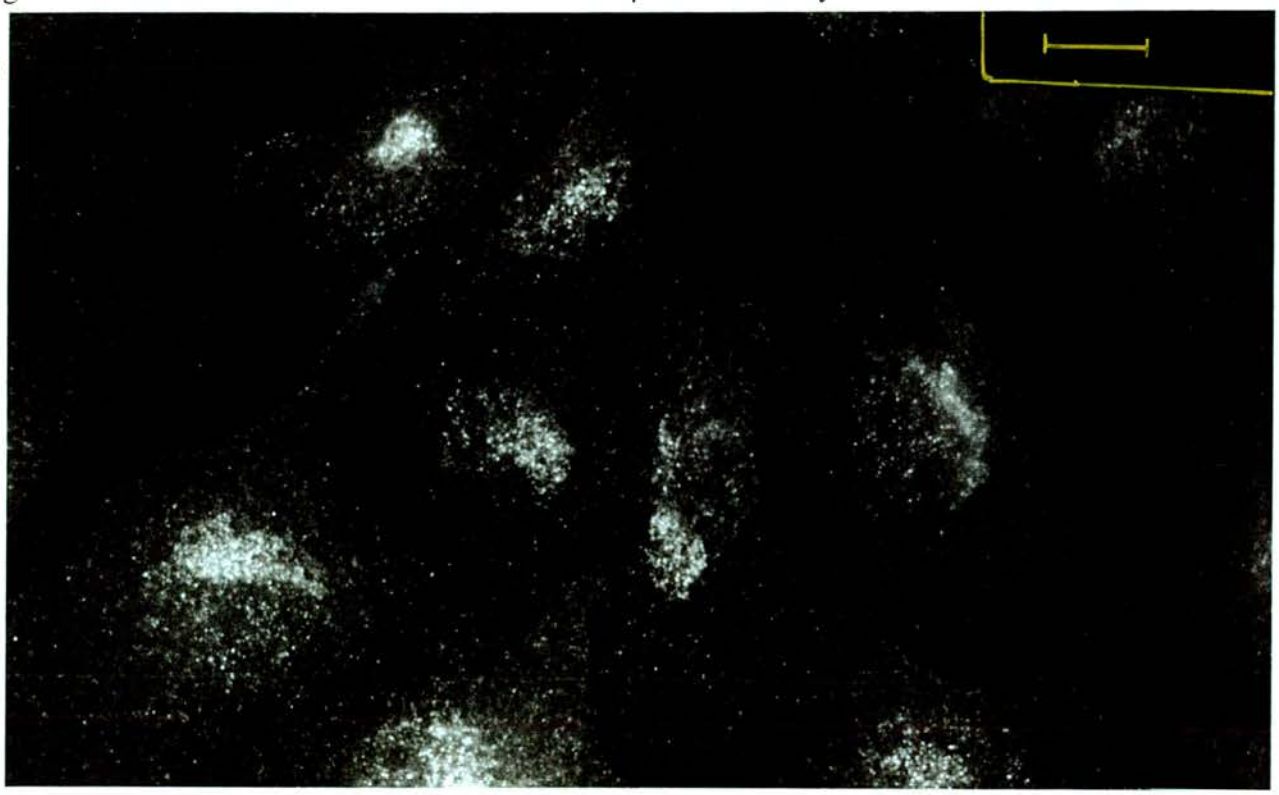

b)

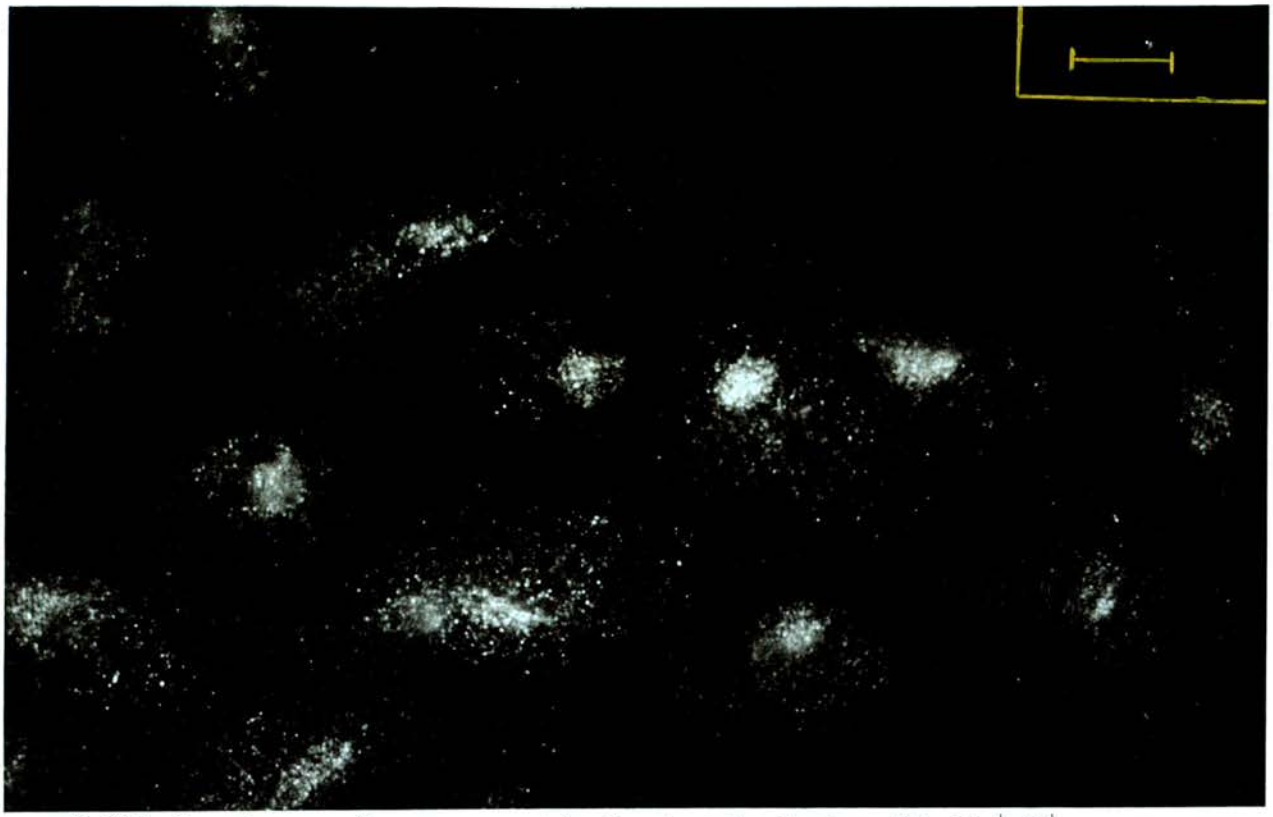

Figure 3.10 Indirect immunofluorescence stain showing distribution of the Na^+, K^+ ATPase β-1 subunit in BAECs. a) BAECs at day 3 growth. b) BAECs at day 4 growth. Note the "nuclear staining" seems to disappear but the cells still have strong juxtanuclear staining which appears to be in alignment with the Golgi apparatus. Scale bar = 10μm.

The pattern of staining is more prominent than the cells in day 1 and 2, however the juxta-nuclear staining (in the area of the Golgi) seems better defined. Note, though, that the dense staining around the nucleus (what appeared to be nuclear staining in younger cells) is no longer seen. Much older cells at days 11-14 stained with the β-1 subunit (Figure 3.11) show a comparable yet slightly different pattern of staining to the younger cells. A distinct ring of β-1 subunit around the nucleus is seen, with a strongly juxta-nuclear stain located in the same region as the Golgi apparatus.

Figure 3.11 a) NB Legend below Figure 3.11 b.

b)

Figure 3.11 Indirect immunofluorescence stain showing perinuclear distribution of the Na^+, K^+ ATPase β-1 subunit in BAECs. a) BAECs at day 11 growth. b) BAECs at day 14 growth. Scale bar = 10μm.

Figure 3.12 shows the Golgi staining, showing the location of the Golgi apparatus in comparison to the β-1 subunit of distribution.

Figure 3.12 a) NB Legend below Figure 3.12 b).

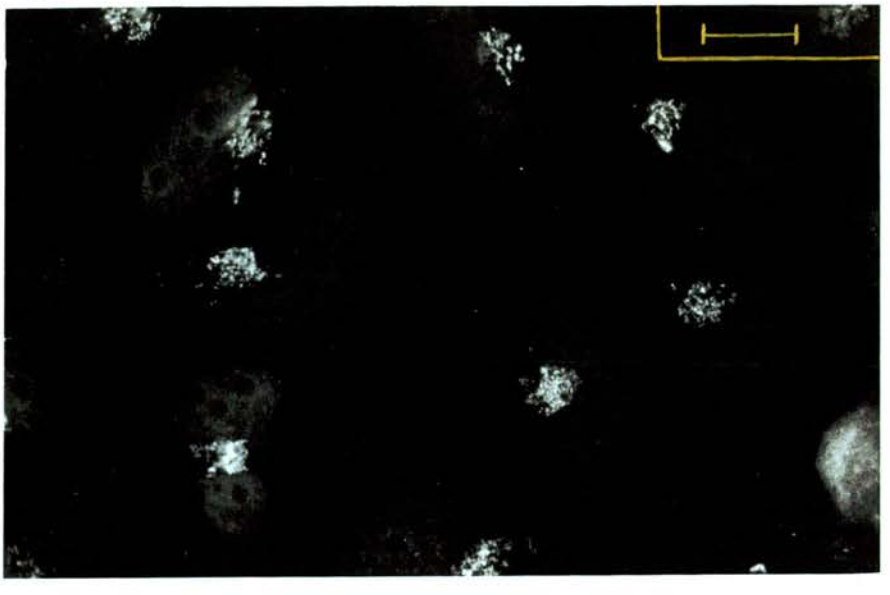

b)

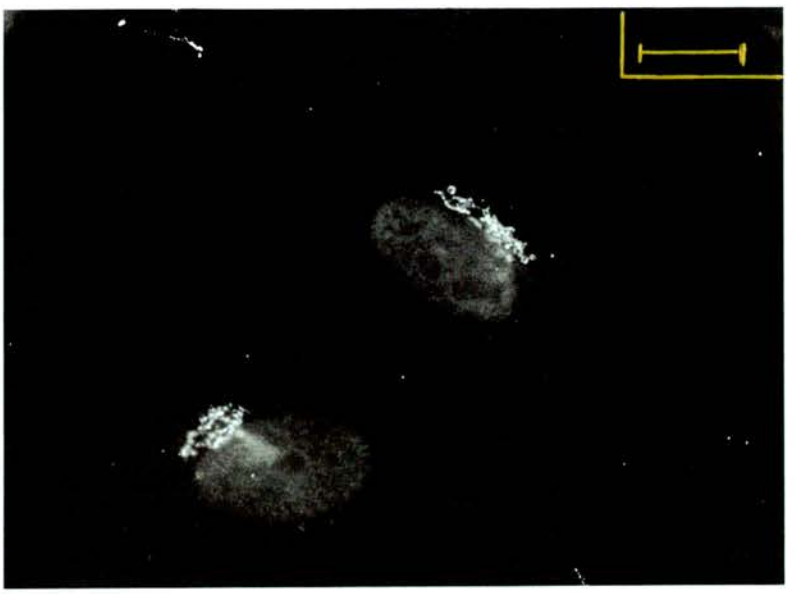

Figure 3.12 Indirect immunofluorescence stain of BAECs. a) and b) BAECs at day 4 labelled with G58K to illustrates the location of the Golgi apparatus in comparison to the β-1 subunit seen in Figures 3.8, 3.10 and 3.11. Scale bar = 10μm.

The series of photographs in Figure 3.13 compare actin staining between the HeLa and BAECs in young and old cells. HeLa cells processed at day 4 after seeding demonstrate near parallel arrays of intracellular stress fibres (Figure 3.13 a) with filapodia extending out from the subconfluent cells to contact neighbouring cells. A similar pattern of actin distribution is found in BAECs stained for actin during days 1-4 after seeding (Figure 3.13 b & c). Figure 3.13 b illustrates a similar pattern of staining to HeLa cells, however as cells become more confluent (in this case cells are near by day 4; Figure 3.13 c) stress fibres are more abundant and begin to change their pattern of organisation. As cells reach full confluence the actin fully changes from near linear bundles throughout the cytoplasm to dense peripheral bands concentrated between cells (Figure 3.13 d).

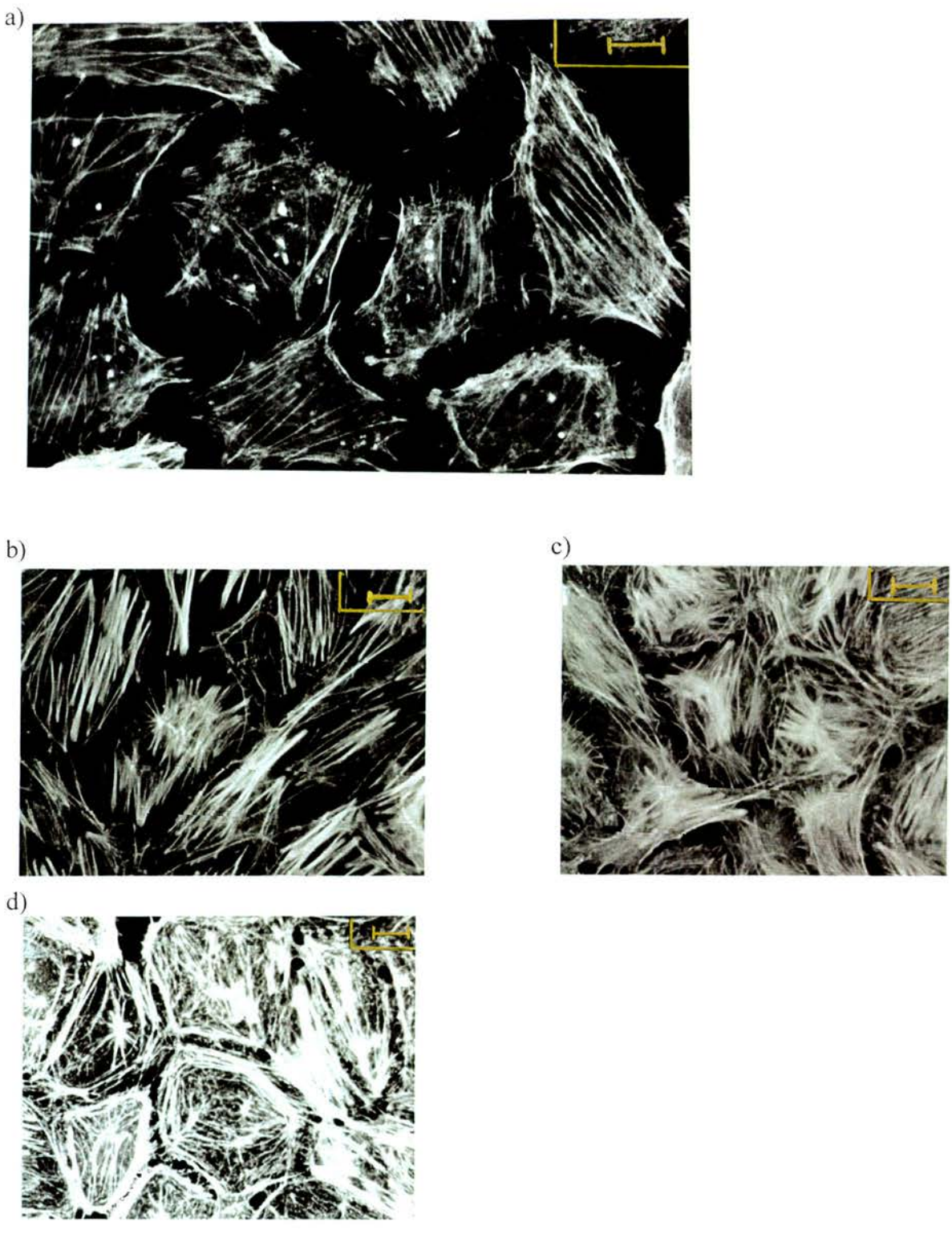

Figure 3.13 Illustrates actin staining. a) day 4 HeLa cells. b) BAECs day 2. c) BAECs day 4. d) BAECs day 14. The actin in HeLa cells is relatively similar in days 1-4. The stress fibres in young cells become more prominent as the cells age. The BAECs show a large difference in actin staining as the cells age. Note the dense peripherial bands in (d) that start to form around day 3-4 of cell growth. The α-1 Na^+, K^+ ATPase staining in Figure 3.7 appears shows a very similar pattern of staining. Scale-bar= 10μm.

3.3.4 Expression of the α-1 and β-1 isoforms of Na^+, K^+ -ATPase in young and old HeLa and BAECs

Detection of the isoforms of Na^+, K^+ -ATPase using monoclonal antibodies to the α-1 and β-1 subunit of the pump demonstrates the absence or presence of the particular isoform. This method is also a good measure of the abundance of the isoform. Figure 3.14 a is a Coomassie blue stain showing levels of protein in young and old HeLa and BAECs. Similar amounts of protein were loaded into each well: HeLa ~ 15.7 μg protein/well and BAECs ~ 20.3 μg protein/well. Both HeLa and BAECs show the banding pattern becoming darker in older cells, signifying higher protein levels in older cells. The Coomassie stains give overall protein level, but do not show exactly what happens to Na^+, K^+ -ATPase. Figure 3.14 b shows an ECL from a nitrocellulose membrane probed for the 112 KDa α-1 subunit of the pump. A slight decrease was observed in the α-1 subunit of HeLa cells for days 3-4. BAECs display similar protein levels in day 1-2 and decreasing over time, and show weaker signal in day 14 cells compared to day 1. Nitrocellulose membranes were also probed for the 55 KDa β-1 subunit of cells, although the β-1 subunit gives a weaker signal compared to the α-subunit. Both HeLa and BAECs showed a decrease in expression of the β-1 protein with time.

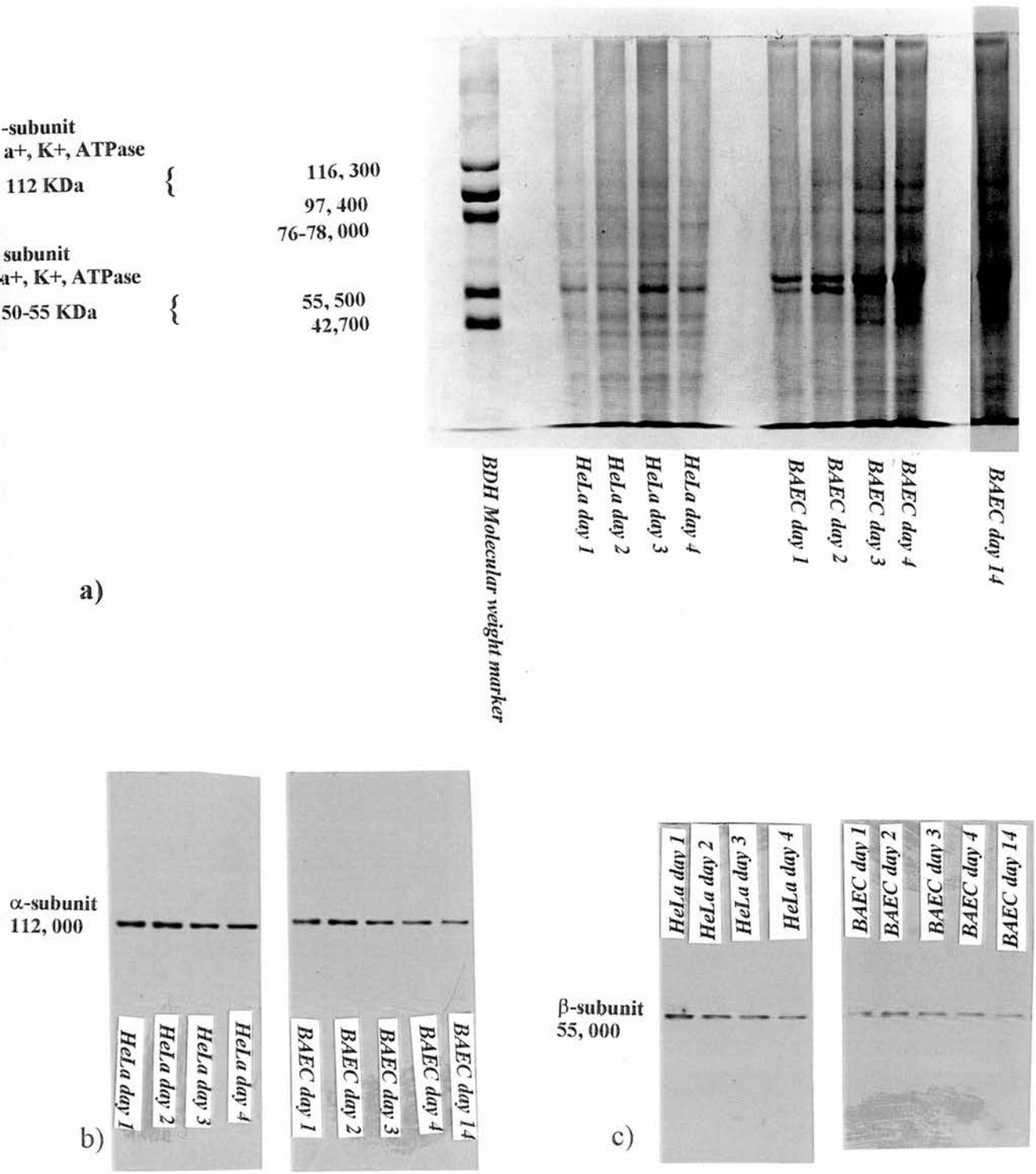

Figure 3.14 6% SDS polyacrylamide gel of HeLa and BAEC, showing expression of the Na^+, K^+ ATPase α-1 and β-1 subunit. a) HeLa cells lysates contain ~15.7μg protein/well, BAE whole cell lysates contain ~20.3μg protein/well stained with coomassie blue stain. b) Membrane probed with α-1 antibody used at 1:500, secondary (SAMP) used at 1:1000. c) Membrane probed with β-1 antibody used at 1:500, secondary (SAMP) used at 1:1000.

A statistical analysis of this data (One way ANOVA and Tukey's pairwise comparison) shows that the mean number of sodium pumps per μm^2 for BAEC day 14 cells was significantly lower than both HeLa day 4 and BAEC day 4 treatments ($F_{2,56}$=8.60, $p<0.001$, Tukey's comparison $p<0.05$).

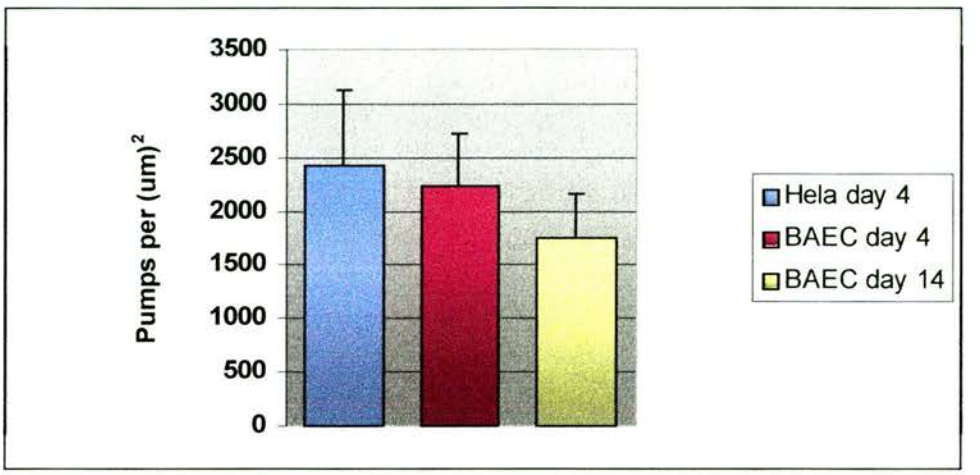

Figure 3.15 The density of Na^+, K^+ ATPase in HeLa cells and BAECs at different ages, measured by ^{3}H-ouabain binding. Error bars are ± 1 standard deviation.

3.4 Discussion

The α-subunit of Na^+, K^+ ATPase has three well-characterised isoforms (discussed in detail in Introduction 1.1 Section 1.3.1), known as the α-1, α-2, α-3 (Sweadner, 1989). The α-1 contains the binding sites for ATP and ouabain on the external side of the membrane (Sweadner, 1989). Each isoform is a product of different a gene on different chromosomes (Lingrel *et al.,* 1990). The β-subunit is also found having multiple isoforms derived from separate genes. The distribution of the different isoforms of the subunits is dependent of tissue, species, cell type and stage of development (Glynn, 1993). A γ-subunit has also been identified, which may be involved in pump development, regulation, or polarised sorting of Na^+, K^+ ATPase (Mercer, 1993). Both the α and the β-subunit is essential for the expression of enzymatic activity, which the γ-subunit is understood to have some function in the hydrolysis of ATP or ion transport (DeTomaso *et al.*, 1991, Mercer, 1993; Beguin *et al.*, 1997).

In this study the expression of α and β-subunit of Na^+, K^+ ATPase was examined in HeLa cells and BAECs. The main purpose of this study was to determine if BAECs served as a good model for further experiments in comparison to HeLa cells. Older cells were also examined, BAECs can be maintained confluent monolayers under adequate growth conditions (mentioned in Section 3.2). As HeLa cells can not be maintained past confluence (about day 4 growth), this study was to identify if it is critical to use the same age cells and if the use of older cells would affect pump estimation in future experiments.

A qualitative examination using conventional fluorescence microscopy of the cell lines showed the α -1 and the β-1 subunit of HeLa cells day 1-4 having little noticeable difference between the age of the cell and the subunit staining. In most cells the staining of both subunits appears to be randomly distributed however, a fine ring of pumps is identifiable around the nucleus as well as areas that appear to line up in rows. This could suggest possible colocalisation of actin with Na^+, K^+ ATPase. BAECs of the same age (day 1-4) also appear to have a random distribution of sodium pumps with no obvious difference between cells of different ages however, the pattern of staining differs slightly from cells HeLa cells day 1-4. Immunofluroescence of the α -1 subunit in older BAECs (day 11-14) showed a very different pattern. Figures 3.7 a&b show strong staining around the perimeter of the adjacent cells. This pattern coincides with dense peripheral bands of actin (shown in Figure 3.13 d.) F-actin microfilaments are located in two areas of the cell: they are found more centrally in linear arrays termed stress fibres (the suggested pattern of staining seen in HeLa cells day 1-4 for the α -1 and β-1), or at the cell periphery in dense peripheral bands. It has been hypothesised that the dense peripheral bands of each individual cell are linked via adherens type junctions to form a network of microfilaments which maintains the physical integrity of the cell (Wong and Gotlieb 1986). It is known that the spectrin cytoskeleton colocalises with Na^+ channels as discussed in Chapter Two. It has been shown that the actin filaments colocalise with Na^+ channels leading to a possible regulatory role in ion activity (Cantiello, 1995). Cantiello concluded from the following study that Na^+, K^+ ATPase may serve as an important component of transepithelial ion transport response, to also be functionally

controlled by the actin cytoskeleton. Neither monomeric nor prepolymerised actin are responsible for the stimulatory effect on Na^+, K^+ ATPase. The results of his study suggest that the activation process may be mediated by "short" actin filaments. Located in the main cytoplasmic loop of the α - subunit, a putative actin-binding site in of the Na^+, K^+ ATPase was also found sharing many similarities to the putative actin-binding domains of a different actin-binding protein family including gelsolin and severin (also mentioned in Chapter two). The putative actin-binding domain corresponds to the actin-binding domain of ankyrin (Morrow, 1989), and is also found in the various α - subunit isoforms indicating actin activation of Na^+, K^+ ATPase may apply to all three well characterised isoforms (Cantiello, 1995).

Detection of the β-1 by immunofluorescence showed nuclear and strong juxta-nuclear staining using conventional fluorescence microscopy. However, further examination via laser scanning confocal microscopy demonstrated that the staining was not inside the nucleus. Cells observed at days 11-14 show obvious juxta-nuclear and perinuclear rings of pump staining in the same location as the Golgi complex, as seen in Figure 3.1 2a&b. Most animal cells move newly synthesised proteins through an interlocking organelle system characterised by different compartments, and selective transport pathways. These compartments include the endoplasmic reticulum (ER) and Golgi apparatus. Membrane proteins translated into the (ER) are processed further in the Golgi complex before they are inserted into the membrane. The β-1 subunit is glycosylated at three sites (Fambrough *et al.*, 1994) and the α - subunit is N-glycosylated by the addition of a single sugar residue, N-acetyl glucosamine (Pedemonte and Kaplan, 1992). The

subunits are not synthesised in a 1:1 stoichiometry (Matys *et al.*, 1993) but subunits stored in intracellular pools. It is found in chick skeletal muscle that 60% of total detectable Na^+, K^+ ATPase is found in intracellular sites (Wolitzky and Fambrough, 1986). Immunofluorescent studies by Mobasheri *et al.*, (1995, 1996) show primary bone-derived osteobalsts and bovine articular chondrocytes have a large amount of intracellular Na^+, K^+ ATPase β-subunits with some α. In isolated bovine chondrocytes the β-2 isoform showed highest intracellular staining (Mobasheri, *et al.*, 1996).

Western blot analysis showed the α- subunit of HeLa cells having a relatively strong consistent signal. BAECs have a similar signal up to day 3, by day 4 and 14 the signal weakens. Experiments by Lamb (unpublished) showed an association between the K_d and the degree of cell confluence. Sub-confluent cells showed a high K_d, whereas in cells approaching confluence the K_d falls to low values. Although there is little published data, the accepted theory is that confluent cells have more cell-cell junctions allowing a greater transfer of ions between neighbouring cells. Or another possibly is that cells at confluence divide at a slower rate and few newer sodium pumps are created so the mean age of the sodium pumps in the samples is likely to be greater (pers. comm. Mobasheri, Cutler, Lamb). β-subunit staining appeared weak in both membrane blots.

α-1 subunit staining of bovine aortic endotheilal cells using different permeabilisation techniques.

4.1 Introduction

This Chapter will look the pattern of Na^+,K^+ ATPase staining of BAECs grown in static culture. Different pre-treatments were used before the cells were stained for the α-1 subunit of the pump and actin. BAECs permeabilised with either sodium dodecyl sulphate (SDS), or (in other experiments) via a method of lysing and refilling cells, showed the α-1 subunit staining to have a similar distribution to actin. These experiments show a strong association between the two cellular components, however it is difficult to state definitively that there is a direct co-localisation of Na^+,K^+ ATPase and actin.

4.1a Actin

F-actin microfilament bundles in endothelial cells are present in two distinct areas of the cell: organised into linear bundles throughout the cytoplasm, termed stress fibres (SF; Wong & Gotlieb, 1986), and at the cell periphery as dense peripheral bands (DPB;Wong & Pollard, 1983). Actin is also found associated with other proteins beneath the cell membrane.

The establishment of cell to cell contacts may be the signal responsible initiating the formation of dense peripheral bands. Stress fibres have a functional role in cellular adhesion to the substrate. Most stress fibres in cultured cells extend in straight paths throughout the cytoplasm terminating at focal adhesion sites. Focal adhesions are specialized sites consisting of extracellular matrix receptors (integrins) that span the plasma membrane interacting on the outside with the

extracellular matrix, and on the inside with bundles of actin filaments (stress fibres; Burridge & Wodnicka, 1996).

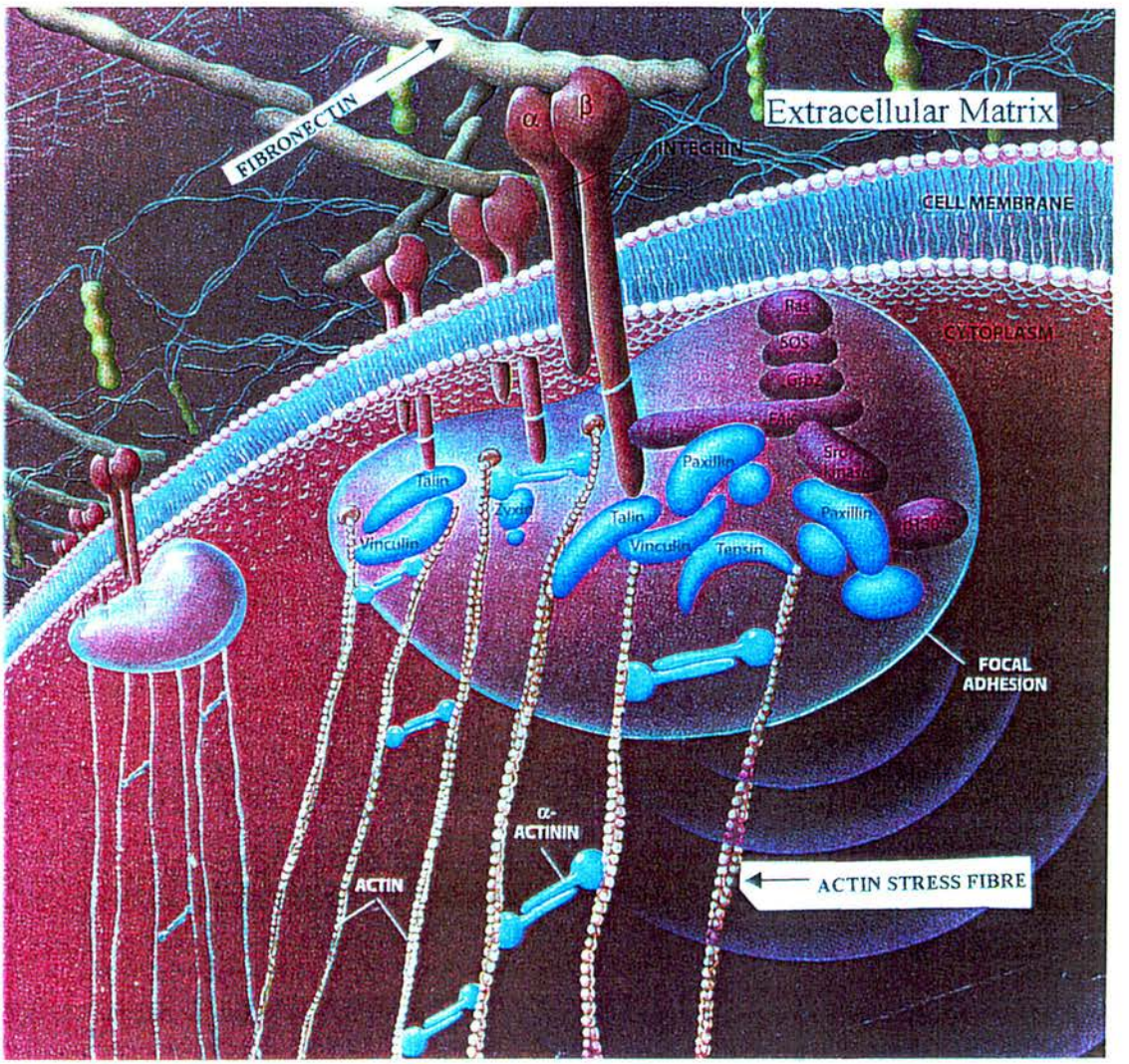

Figure 4.1 The schematic illustrates the attachment of the extracellular matrix to focal adhesion sites on the intracellular surface by integrins spanning the plasma membrane. This illustration also shows the location of actin and other cytoskeletal proteins (modified from Horowitz, 1997).

4.1b Sodium dodecylsulphate

Sodium dodecylsulphate (SDS) is an anionic detergent that denatures protein by binding to the hydrophobic regions of the protein molecule causing them to

unfold into extended polypeptide chains. Many antibodies recognise denatured proteins resulting in positive staining of bands by Western blotting after SDS-polyacrlyamide gel electrophoresis (PAGE). However, some antibodies will not recognise a native protein and may give a negative result by immunocytochemisty (Brown *et al.*, 1996). Several techniques can be used to increase the sensitivity of indirect immunostaining protocols and to enhance the detection of proteins by immunocytochemistry. These include denaturing agents, protease treatment, exposure to varying pH, and microwave methods of tissue section preparation (McQuaid *et al.*, 1995; Brown *et al.*, 1996).

Experiments on renal cell cultures (MDCK) by Brown *et al.*, (1996) showed an increase in Na^+,K^+ ATPase, anion exchanger 1 (AE1) and H^+, ATPase immunostaining after 5 minute pre-treatment with 1.0% SDS. They also showed that AE2 and caveolin were undetectable without SDS pre-treatments, with rab4, gp330, aquaporin 1 and 2 immunostaining having no change with this treatment.

Experiments in this Chapter were modified from Brown *et al.*, (1996) to examine if SDS pre-treatment would expose antigen binding sites for Na^+,K^+ ATPase in cultured BAECs. The association between Na^+,K^+ ATPase and actin was also examined.

4.1c Environmental conditions affecting cells

Hypotonic solutions contain a low concentration of solute relative to another solution. When a cell is placed in a hypotonic solution, the water diffuses into the cell due to osmosis, causing the cell to swell and possibly burst. Na^+,K^+ ATPase plays an indirect role on the regulation of cell volume, wherein the pump controls

the solute concentration inside the cell, thereby regulating the osmotic forces that can make the cell swell or shrink.

It is well known that increased levels of extracellular Na^+ result in upregulation of Na^+,K^+ ATPase, and that increasing osmolarity of the solution has a drastic effect on volume (Hall, 1996). In articular chondrocytes, increased extracellular osmolarity causes cell shrinkage, which in turn increases intracellular concentration of Na^+ (Mobasheri, 1996). Cell shrinkage also activates $Na^+/K^+/2Cl^-$ co-transport, resulting in Na^+ influx, (as well as K^+ and Cl^-; or KCl). KCl accumulation will lead to volume recovery or cell swelling through regulatory volume increase (Hoffman and Simonsen, 1989).

Experiments on *Helix pomatia* (snail) neurons show changes in cell volume is dependant upon Na^+,K^+ ATPase activity when levels of intracellular sodium ion concentration are altered (Ayrapetyan *et al.*, 1984). Hypertonic solutions (using increased glucose to increase osmolarity) caused hyperpolarisation of the membrane and increased membrane resistance in cells with low sodium content. The activity of the Na^+,K^+ ATPase (measured via patch clamp) in hypertonic solutions was increased, compared to the activity when bathed in low sodium content, hypotonic solutions. It was also noted that swelling of neurons bathed in hypotonic solutions was accompanied by an increase in the number of binding sites for ouabain, while shrinkage due to a hypertonic extracellular solution led to the opposite effect i.e. a decrease in binding sites (Ayrapetyan *et al.*, 1984).

Membrane potential responses of cultured oligodendrocytes and astrocytes were compared during changes in the osmolarity of the bathing solution (Kimelberg &

Kettenmann, 1990). Results showed that oligodendrocytes responded with depolarisation in a hypotonic solution and hyperpolarisation in hypertonic solution. These findings remained consistent depending on the concentration of intracellular K^+. Astrocytes were found having a similar response (hyperpolarisation) in a hypertonic solution, however, in a hypotonic medium a much larger depolarisation was observed. These results imply that swelling activates specific channels that may be involved in volume control in astrocytes, in contrast to oligodendrocytes (Kimelberg & Kettenmann 1990). Channels were studied in cell-attached patches of the basolateral membrane of cells isolated from frog kidneys using the patch clamp technique. Channels were found to open following the application of negative pressure to the rear of the patch pipette or by bathing the cells in hypotonic solution. (Hunter, 1990). In addition, the channels are voltage-sensitive, such that depolarisation increases channel opening. In these experiments the channels were found to be cation non-selective. Inward currents were observed at resting potential with Na^+ or K^+ being the dominant ion in the pipette solution. This excludes the possibility of channels serving a role as the route for solute exit from the cell during a volume regulatory decrease response and suggests that they may act as the transduction mechanism sensing changes in cell volume (Hunter, 1990).

Other studies demonstrated that sarcolemmal Na^+,K^+ ATPase current in cardiac myocytes is stimulated by cell swelling induced by exposure to hypotonic solutions. However, the underlying mechanism has not been examined (Bewick, *et al.*, 1999). Cell swelling activates stretch-sensitive ion channels and intracellular messenger pathways (Hug *et al.*, 1995). Bewick's group examined the exposure of rabbit ventricular myocytes to a hypotonic solution and

investigated their role in mediating Na^+,K^+ ATPase current stimulation (measured by the whole cell patch-clamp technique). Swelling-induced pump stimulation altered the voltage dependence of Na^+,K^+ ATPase current. Pump stimulation persisted in the absence of extracellular Na^+ and under conditions designed to minimise changes in intracellular Ca^{2+}, excluding an indirect influence on Na^+,K^+ ATPase current mediated via fluxes through stretch-activated channels. Pump stimulation was protein kinase C independent. The tyrosine kinase inhibitor tyrphostin A25, a phosphatidylinositol 3-kinase inhibitor (LY-294002), and the protein phosphatase-1 and 2A inhibitor okadaic acid abolished Na^+,K^+ ATPase stimulation. These findings suggest that swelling-induced pump stimulation involves the activation of tyrosine kinase, phosphatidylinositol 3-kinase, and a serine/threonine protein phosphatase. Activation of this messenger cascade may cause activation by the dephosphorylation of pump units (Bewick, *et al.*, 1999).

Experiments in this Chapter were designed to disrupt the membrane of BAECs by a method of hypotonic lysing and resealing the cells (Lamb and Lindsey, 1971). This technique produces a "ghost cell[1]", where the nucleus, and cytoskeletal elements, and cell membrane remain, but the soluble components are lost. This enables further examination of Na^+,K^+ ATPase in the cell membrane. The association of Na^+,K^+ ATPase and actin was also examined.

[1] The term cell "ghost" is usually applied to red blood cells RBCs. Hypotonic lysis of RBCs expels haemoglobin and allows the membrane to be isolated. In these studies BAECs cells were lysed and promptly resealed. The nucleus remained in the majority of these cells, and although they are not true cell ghosts, for this study they are referred to as cell "ghosts".

4.2 Methods and Materials

4.2.1 SDS treated cells

BAECs were grown as previously described in Chapter 3. The cells were rinsed with PBSc (2x5 min.) at room temperature. Cells were fixed for 10 minutes with 0.1% EM grade paraformaldehyde. The fixative was then removed and cells were washed in PBSc (3x5 min.) and permeabilised with 0.1% SDS detergent in PBSc (5 mins). Subsequently, the SDS was removed by immersing the coverslips in PBSc (3x5 min) in a Coplin jar. It is important to wash the coverslips well otherwise residual SDS will denature antibodies applied to the cultured cells. Coverslips used for control groups were washed in a separate container to avoid any possible contact with diluted SDS. Non-specific binding of antibody was blocked by incubating cells with PBSc containing 10% normal goat serum for one hour at room temperature.

4.2.2 Hypotonic treatment

Hypotonic solution "A" consisted of 10mM NaCl, 1.2mM $MgCl_2$, 1mM Cysteine HCl and 2.5% foetal calf serum. The reconstitution solution "B" was made by taking 10ml of solution "A" and adding 1.6 ml 1M KCl in distilled water (Lamb and Lindsey, 1971). All chemicals used were molecular biology grade.

Cells were grown on glass coverslips until a sub-confluent monolayer was formed. They were rinsed x2 with PBSc to remove any medium, immersed in10ml of hypotonic solution A for 10 minutes. This was drained off and the coverslips were put directly into solution B for 3 minutes. This creates cell "ghosts" by expelling the soluble contents of the cells. Many cells became

detached during this procedure. Cells were then fixed for 5 minutes with 4.0% paraformaldehyde, blocked in 10% NGS for one hour and stained for the α-1 subunit of the sodium pump. Coverslips were mounted with Gelvatol or Hoechst stain. Hoechst staining showed that the nucleus was not lost after cells burst.

4.2.3 Microscopy

The α-1 subunit and actin were visualised in BAECs using the technique previously described in detail in Chapters 2 and 3.

4.2.4 One dimensional gel electrophoresis

Passage 23 cells (P23) BAECs were harvested at day 4 using a hot lysis buffer. The cell lysate was prepared and gel run according to the protocol in Chapter 3.2.5.

4.2.5 Materials and Drugs

Hypotonic and reconstitution solutions

NaCl (BDH), MgCl2 (BDH), Cysteine-HCL (Sigma), foetal bovine calf serum (Gibco), KCl (BDH).

Antibodies and other chemicals used are previously mentioned Chapters 2 and 3.

4.3 Results

4.3.1 SDS treated cells

Conventional fluorescence microscopy revealed an interesting pattern of staining for both cytoskeletal components after treatment. Figure 4.2 a illustrates un-treated cells stained for actin. The cells show dense peripheral bands of actin in the two cells in the field of view in addition to stress fibres inside the cell. After cells were treated with 0.1% SDS the pattern of actin changes slightly. Figure 4.2 b shows the pattern of actin staining after treatment with detergent. The stress fibres are still very clear, along with distorted dense peripheral bands (that appear to be condensed into thick bands rather then strand-like structures surrounding the individual cells as in photograph a). Figures 4.2 c and d illustrate cells treated with 0.1% SDS and stained for the α-1 subunit of Na^+,K^+ ATPase. The pattern of staining in both cells [photographs c and d are from different fields of view] appear to follow the similar pattern of staining as actin stress fibres. The sodium pump staining on the periphery of the cells strongly resembles dense peripheral bands of actin. Inside the cell, the pattern of Na^+,K^+ ATPase staining is in uniform rows which also resemble stress fibres. Figure 4.3 a and b are un-treated BAECs that are stained for actin. The photographs illustrate cells from two different fields of view from the same preparation, and show different patterns of actin stress fibre staining in the cells. Photograph c illustrates actin staining after treatment with 0.1% SDS. The stress fibres are still visible. Staining for α-1 subunit of Na^+,K^+ ATPase reveals the pattern of stress fibre staining (photograph d) arranged in uniform rows, which are arranged in parallel arrays.

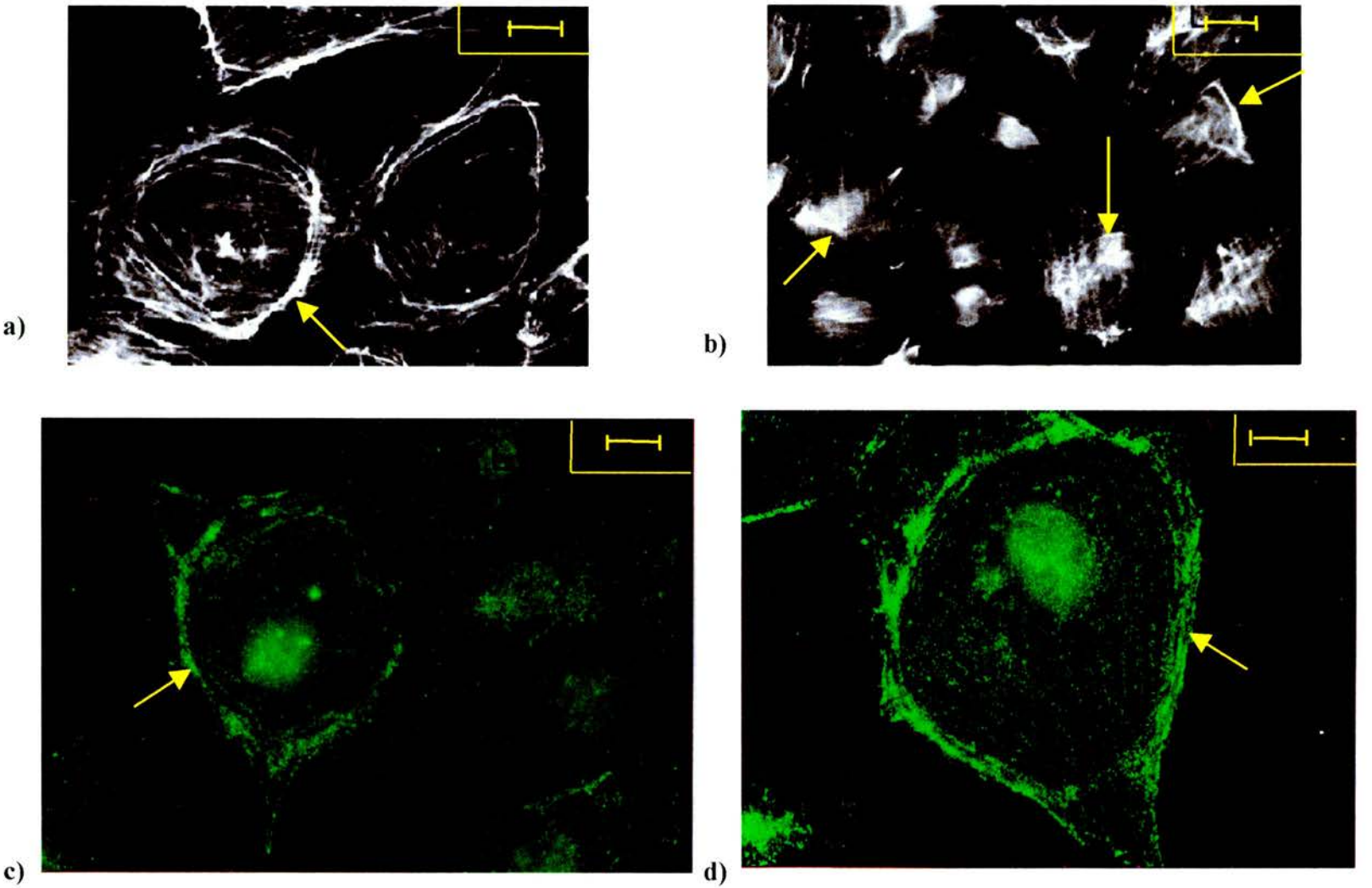

Figure 4.2 Photograph **a)** illustrates un-treated day 4 BAECs stained for actin, the yellow arrow pointing to dense peripheral bands. **b)** represents BAECs treated (permeabilised for 10mins.) with 0.1%SDS.The yellow arrows point to areas of actin. **c & d** illustrate BAECs that have been treated with 0.1% SDS and stained for the α-1 subunit of the sodium pump. The yellow arrows indicate areas that resemble dense peripheral bands of actin. Figures **a & b** also clearly show stress fibres throughout the cytoplasm. The pattern of the α-1 subunit staining in Figures **c & d** strongly resembles actin stress fibres. Scale bar = 10 μm

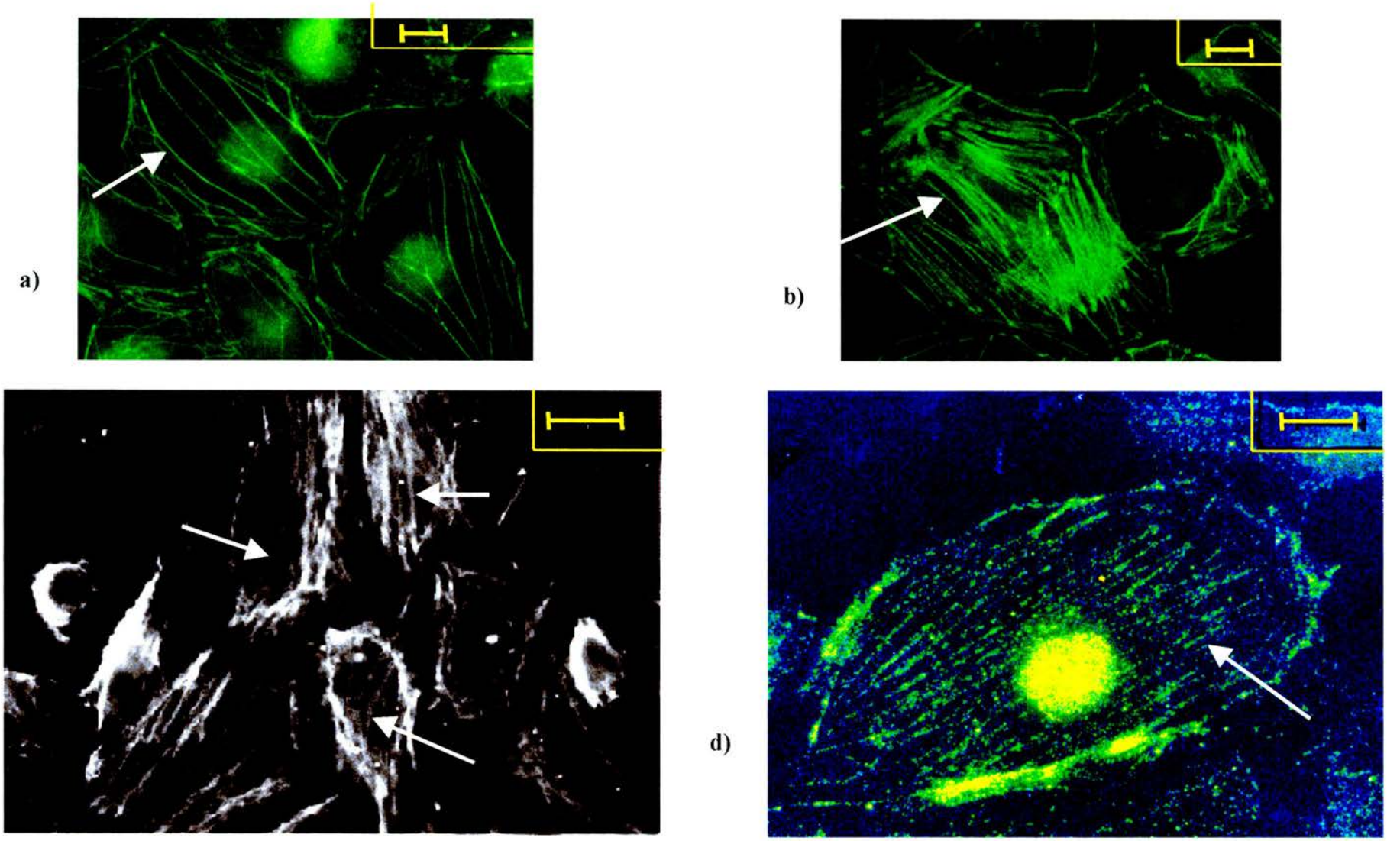

Figure 4.3 **a) & b)** are examples of un-treated BAECs stained for actin at day 4 growth (d4, p23). The arrows point to stress fibres in the cells. Figure **c)** shows BAECs (day 4, p23) treated with 0.1% SDS; the arrows point to stress fibres. Photograph **d)** shows a BAEC (day 4, p23) treated with 0.1% SDS and stained for the α-1 subunit of the sodium pump. The arrow is pointing to sodium pumps (stipple-like dots) distributed in uniform rows, which appear to have a similar pattern to the actin stained cells. Scale bar = 10 μm

4.3.2 Expression of the α-1 subunit of Na^+,K^+ ATPase in BAECs after hypotonic treatment.

BAECs were incubated in a hypotonic solution for 10 minutes, causing cell lysis, then incubated for 3 minutes in a reconstitution solution that refilled the cells. After this process the cells were immunostained for the α-1 subunit and labelled for actin. The slides were examined via fluorescence microscopy. The purpose of this series of experiments was to examine Na^+,K^+ ATPase isolated in the cell membrane. The cells were stained with a Hoechst stain to see if the nucleus was lost during hypotonic lysis. Figure 4.4 a illustrates α-1 subunit staining of an isolated cell that has also been mounted with Hoechst stain that stains the nucleus; b illustrates nuclear staining of the cell in photograph a. Cells were grown to sub-confluence for these experiments, and immunofluorescence analysis showed that some of the cells were detached from the coverslip after hypotonic incubation. The cells were immunostained for the α-1 subunit and labelled for actin and show pump staining in the cell "ghosts". Interestingly, cells that become detached leave behind patches of cell membrane where they were torn away from the coverslip. In areas where these patches of membrane are left behind, sodium pump staining and actin can be seen. The cell nucleus can not be detected in areas where there are patches of membrane. Figure 4.5 a and b are cells double labelled for the catalytic subunit and actin. Photograph c illustrates areas in the field of view where there are cell "ghosts" (labelled whole cells) and patches of membrane which have stained for the α-1 subunit of the pump. Photograph 4.5 b show the same cells as in photograph a double labelled for actin. The area that has stained for pumps also shows actin left behind after treatment. Figure 4.5 c & d, and photograph 4.6 a and b, c and d are other

illustrations of cell "ghosts" and membrane patches double labelled for the α-1 subunit and for actin.

Hypotonic treatment of bovine aortic endothelial cells

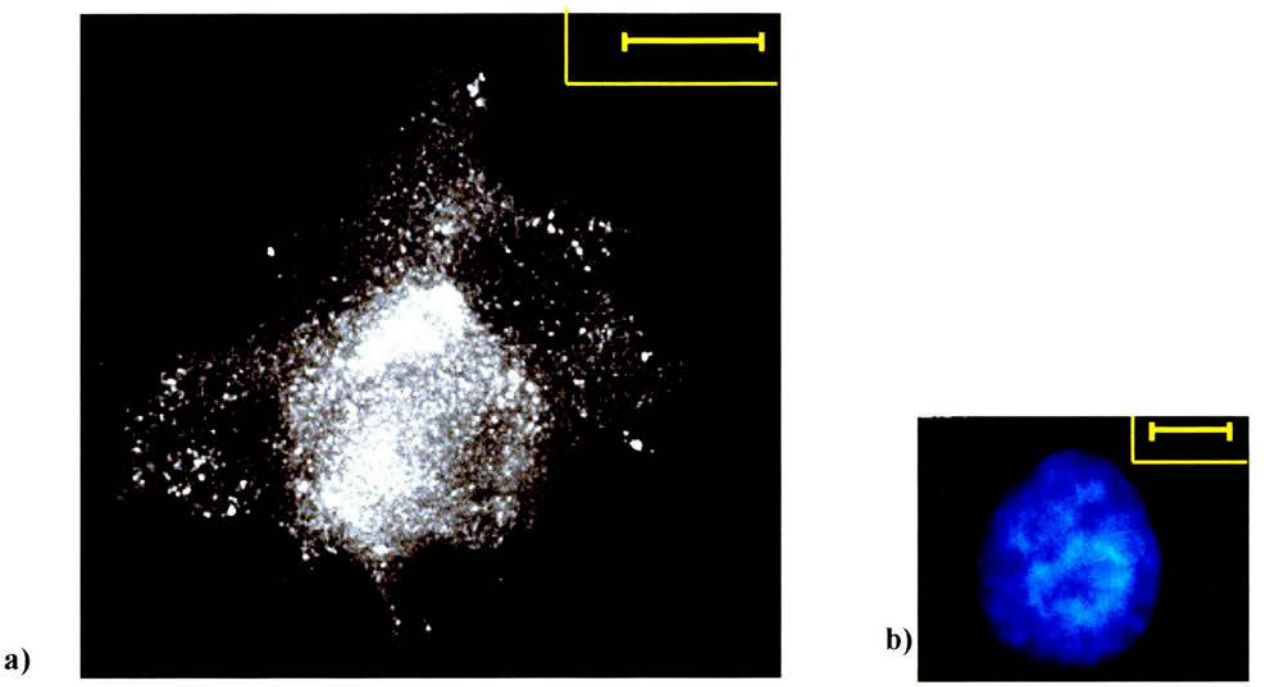

Figure 4.4 Photograph **a)** illustrates a cell "ghost" created by lysing BAECs with a hypotonic solution. Most of the contents of the cell are expelled, however, as shown by the Hoechst stain in photograph **b)** (taken of the same cell) the cell nucleus remains. This is apparent for the majority of cells that are remaining after the treatment. Scale bar = 10μm.

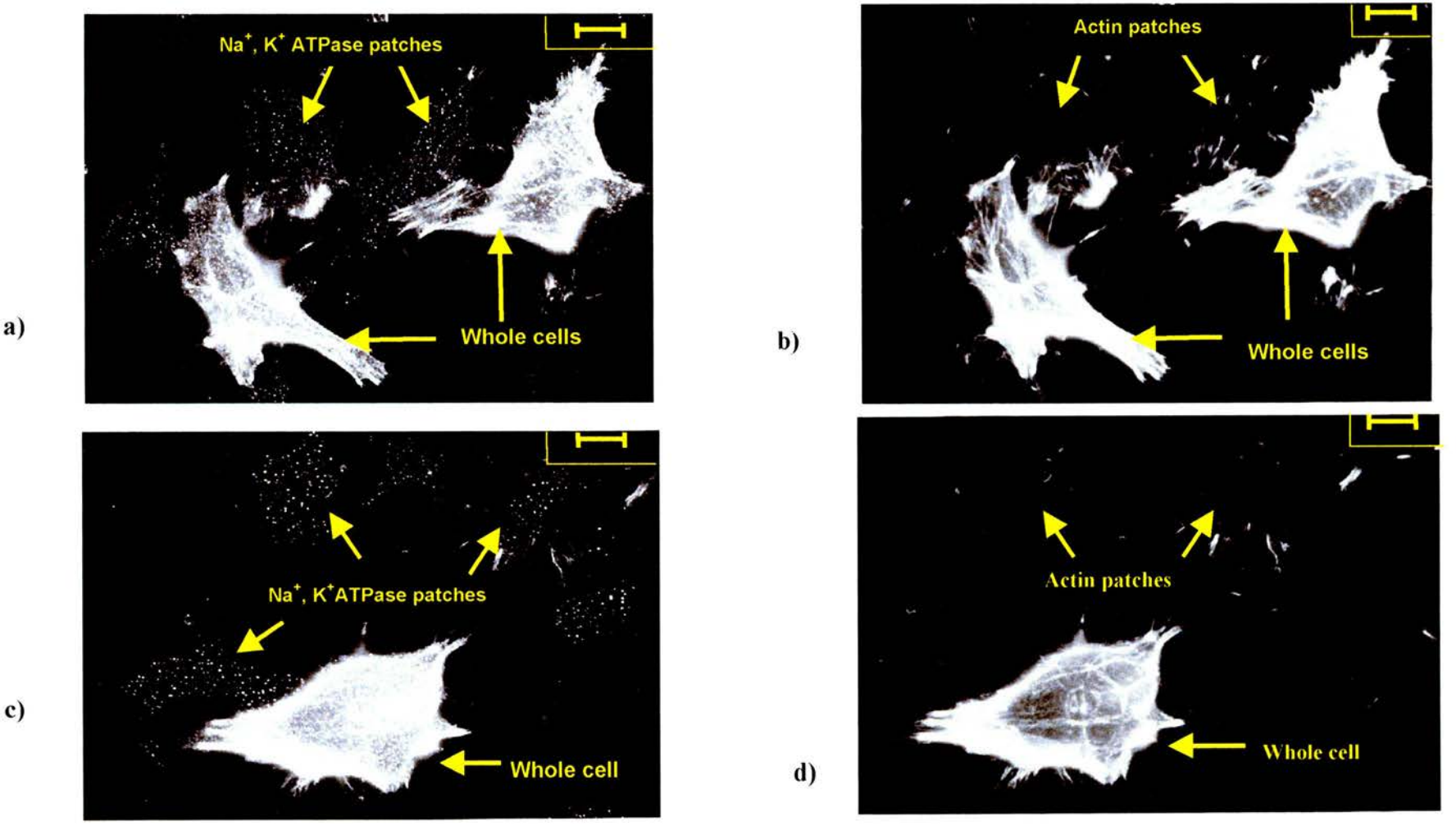

Figure 4.5 a) & b) are photographs of the same cells (BAECs d4, p23) after hypotonic lysing and refilling cells. Photograph **a)** shows staining of the α-1 subunit of Na^+,K^+ATPase, the arrows point to areas that appear to be patches of the cell membrane. **c) &d)** are also photographs of the same cells in a different field of view. **c)** shows α-1 subunit staining, photograph **d)** is actin staining. Scale bar=10um.

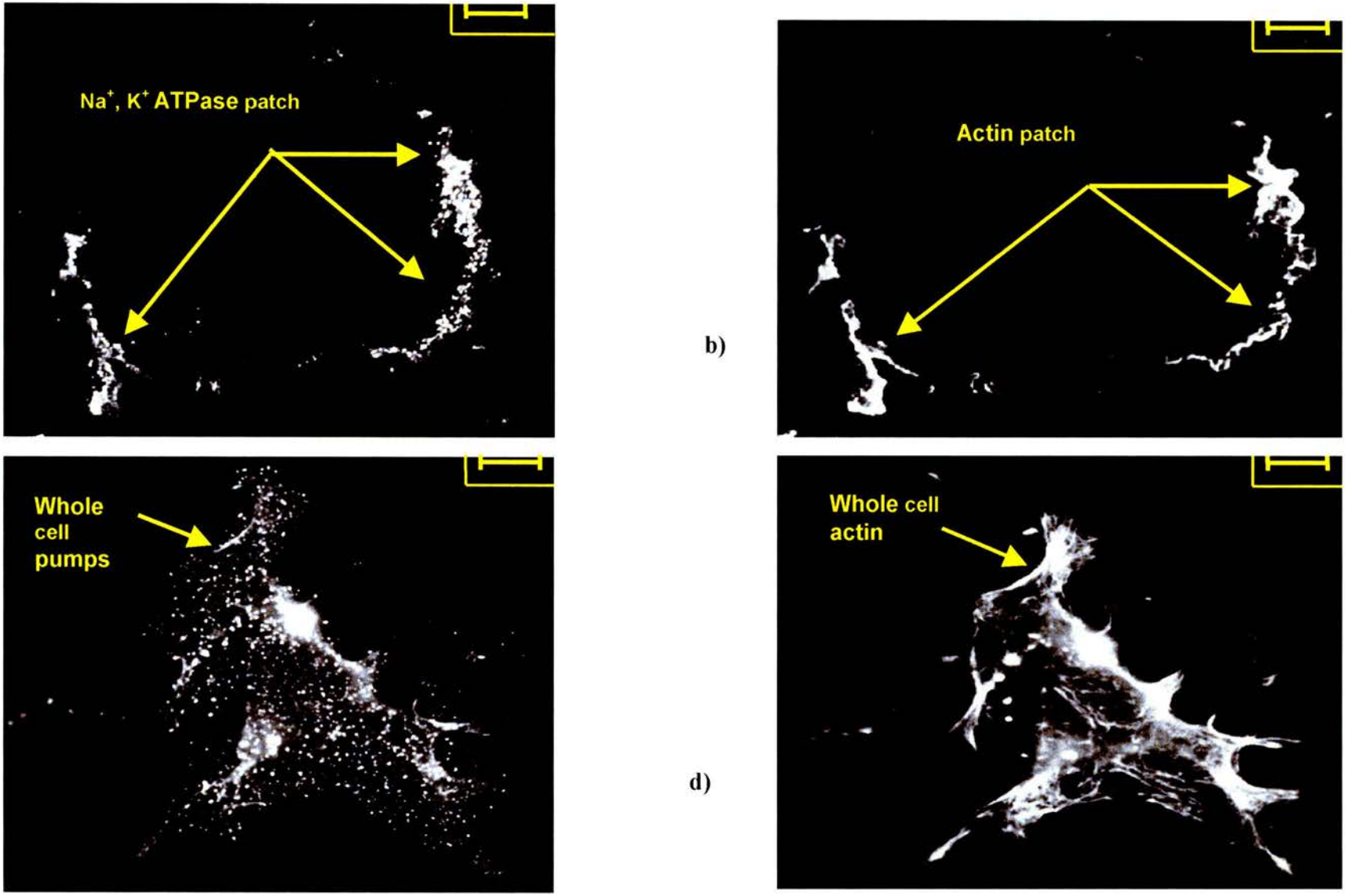

Figure 4.6 a) & b) are photographs of the same cell (BAECs d4, p23) illustrating a cell that was torn away from the coverslip during incubation in the hypotonic solution. **a)** shows sodium pump (α-1 subunit) staining and **b)** shows actin. Photograph **c) & d)** are pictures of the same cell (BAEC d4, p23) this is a whole cell in the field of view **c)** shows pump staining and **d)** shows actin. Scale bar=10μm.

BAECs used at confluence showed an interesting association of pump staining with actin. The cells were treated as previously described, and then labelled for the α-1 subunit and actin. The actin reformed into small rings, with Na^+,K^+ ATPase staining strongly around actin. Figure 4.7 a shows pump staining in treated cells. Arrows in this photograph point to small rings of pumps in individual cells which correspond to small rings of actin (shown in Figure 4.7 b), depicting the same cells as photograph a). Figure 4.7 c and d, 4.8 a and b, c and d are other illustrations of the pump staining that follows reformed actin after hypotonic lysing and refilling of cells.

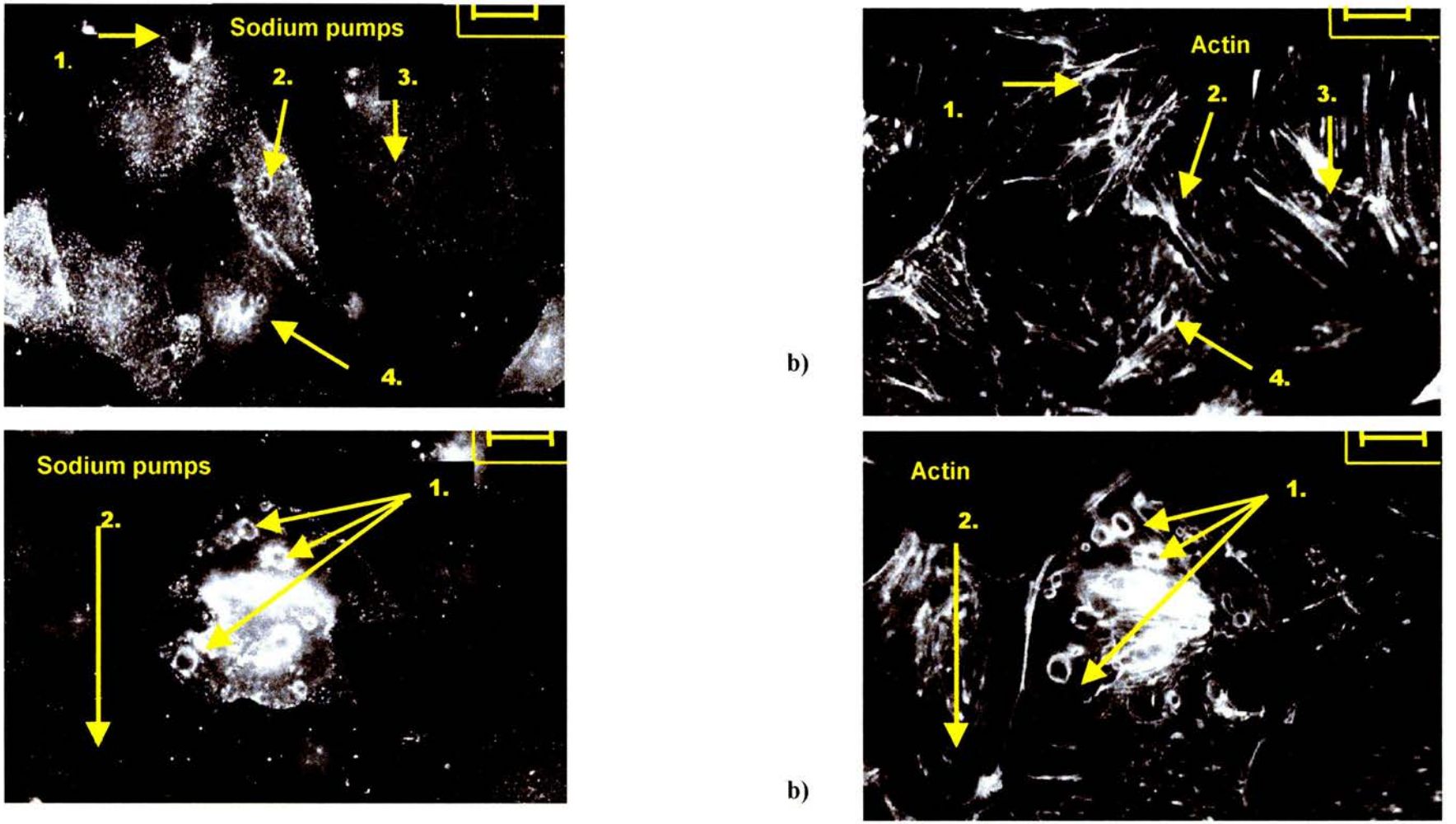

Figure 4.7 a) & b) are pictures of a more confluent monolayer of cells (BAECs d4, p23) double labelled for the α-1 subunit of Na^+,K^+ATPase and actin, respectively, after hypotonic lysing and refilling. **c) &d)** illustrate the same pattern of staining as photos **a) & b)** after the same treatment. **c)** is stained for the α-1 subunit of Na^+,K^+ATPase and **d)** is stained for actin. The numbers correspond to individual cells with the arrows pointing to areas where actin has reformed creating small rings. The sodium pumps follow this trend. Scale bar=10μm.

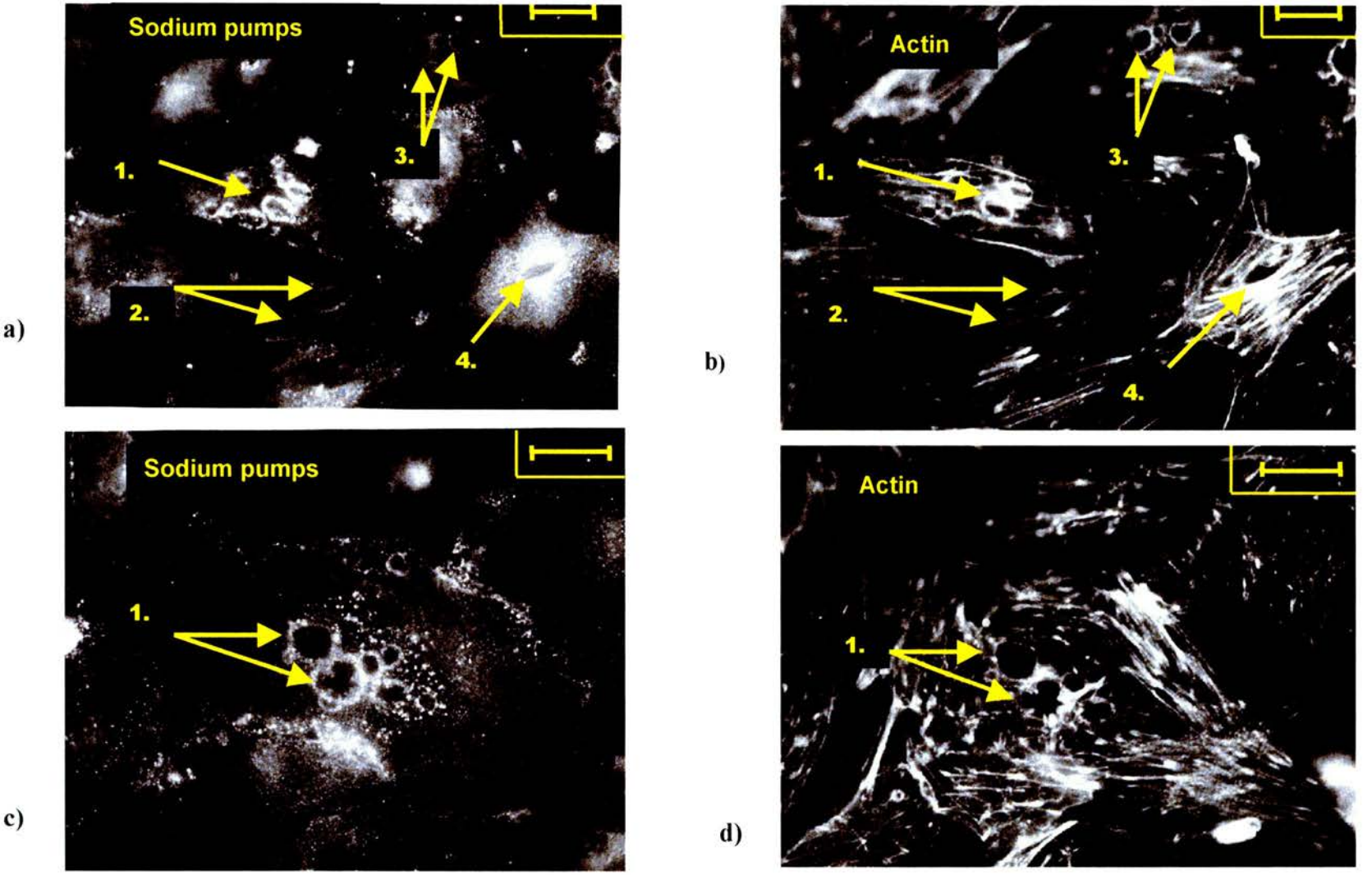

Figure 4.8 a) & b) are photographs of BAECs double labelled for the α-1 subunit of Na^+,K^+ATPase and actin, respectively. The cells were lysed with a hypotonic solution then resealed. The arrows point to areas of actin that reformed into rings with the sodium pumps following the same pattern of distribution. **c) & d)** illustrate a different field of view (the cells have been treated the same as in photograph **a) & b).** The scale bar =10μm.

4.3.3 Western blot analysis of actin

Western blot analysis was carried out using a monoclonal antibody against β-actin. Results (summarised in Figure 4.9) show the expression of the actin in bovine aortic endothelial cells. Cells were lysed in an appropriate volume of Leammli buffer so that each extract contained 10^7 cells cm^3. Figure 4.9 a illustrates a typical 8% SDS gel used to electrophoretically separate the proteins present in BAECs collected from static culture. The gel was subsequently stained with Coomassie Brilliant blue overnight, and rinsed several times with destain to show the protein bands. Lysates from BAECs grown from day 1 to day 5 were collected from passage 23 cells. 5μg of protein per well was loaded, along with Boehringer combithek molecular weight markers (the lane on the far right). The molecular weight of actin is approximately 43 KDa. On the gel, in days 1-5 cells a dark band appears between the 39 KDa and the 56 KDa molecular weight markers. This band represents actin staining on the Coomassie stained gel. From the known Rf values on the gel, this band is calculated to be approximately 43 KDa, which corresponds to actin.

A portion of the gel was transferred onto nitrocellulose. The membrane was probed with a monoclonal antibody against β-actin used at 1:2000. Secondary antibody was sheep anti-mouse peroxidase (SAMP) used at 1:1000. Expression of actin was confirmed using enhanced chemiluminescence (ECL), with one-minute exposure time. Figure 4.9 b illustrates the protein band detected by ECL. The molecular weight of the band was calculated to be approximately 43 KDa.

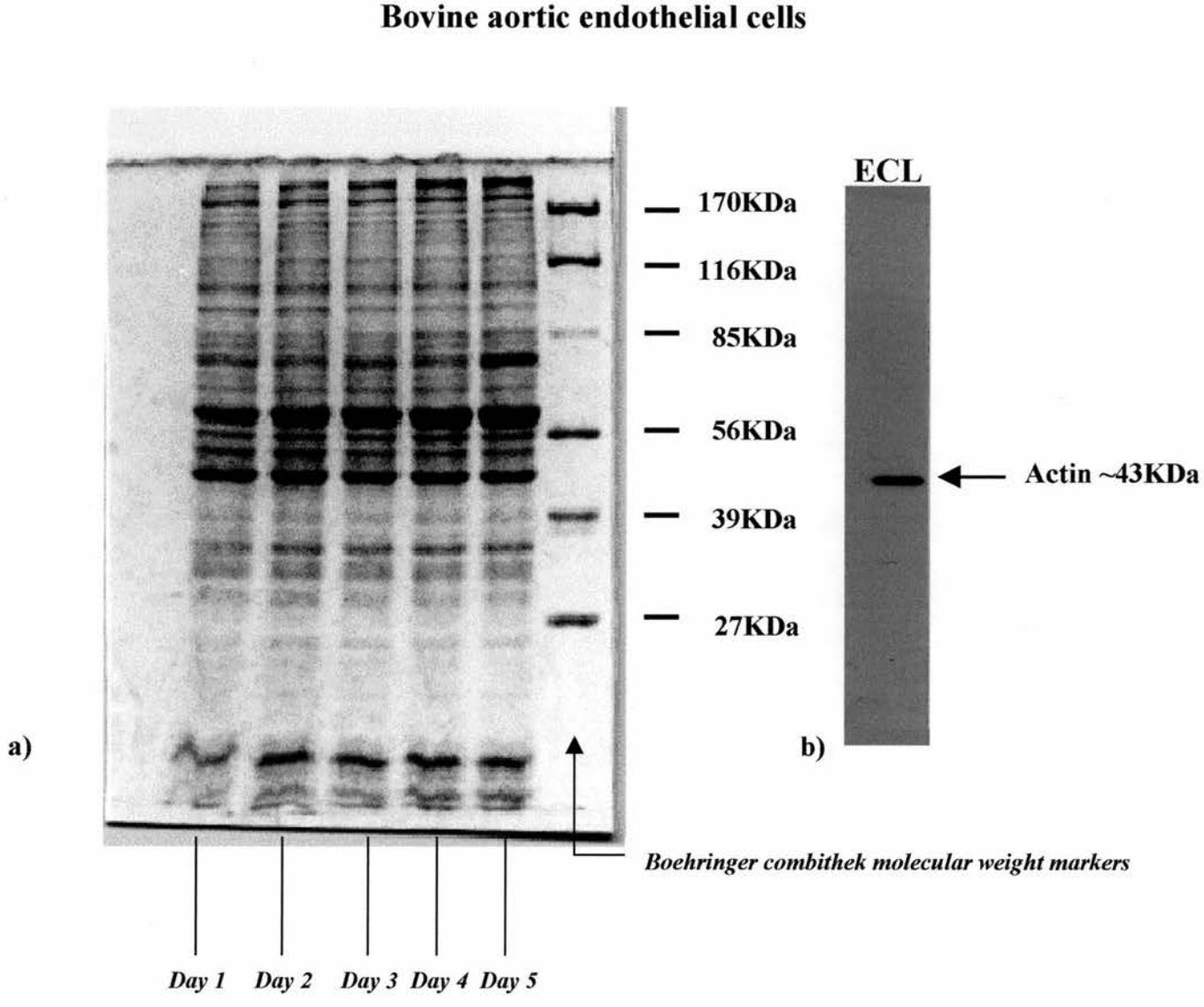

Figure 4.9 8% SDS polyacrylamide gel of BAECs showing expression of actin. Hot lysates were collected from day four cells (p23) and 5µg protein/well was loaded **a)** illustrates the banding pattern from a Coomassie blue stain. **b)** protein bands were visualised via enhanced chemiluminescence (ECL). The membrane was probed with an anti-actin antibody used at 1:2000, secondary antibody was (SAMP) used at 1:1000.

4.4 Discussion

In BAECs the α-1 subunit is readily detectable via immunofluorescence, as demonstrated in Chapter 3. However, experiments by Brown *et al.*, (1996) using cryostat sections and cultured cells, demonstrate that SDS pre-treatment exposes antigenic sites in intracellular compartments leading to the augmentation of α-1 antigen immunoreactivity in various tissues tested (Brown *et al.*, 1996). The aim of these experiments was to attempt to enhance the intensity of the staining in BAECs, and observe the cellular distribution after pre-treatment with 0.1% SDS.

Methods of antigen retrieval were adapted from Brown *et al.*, (1996). Brown used 1.0% SDS to permeabilise (replacing Triton X-100) cryostat sections and cultured cells to enhance staining intensity before indirect immunofluorescence. In this study, 1.0% SDS permeabilisation (as a replacement for 0.1% NP40) for 5 minutes proved to be too harsh on cultured BAECs. Trial and error revealed optimal conditions to be a 10-fold dilution of 1.0% SDS (0.1% SDS) for 10 minutes incubation prior to immunofluorescence. Results from the α-1 staining showed a striking resemblance to actin stress fibres in cultured BAECs. Experiments focused on double labelling the cells to check for co-localisation of the α-1 and actin. However, the binding of TRITC conjugated phalloidin to actin is prevented by pre-treatment with SDS[2] (Brown *et al.*, 1996) and use of FITC conjugated phalloidin (1:200) resulted in too much "*bleed-through*" creating difficulty viewing the α-1 staining under conventional fluorescence microscopy.

[2] Although the binding of Rhodamine-phalloidin to actin is not antibody-antigen binding, prevention of this binding shows that proteins-protein interactions can be adversely affected by SDS pre-treatment (Brown *et al.*, 1996).

In analogous experiments the two proteins appeared to be co-localised, with the pattern of pump staining lining up in parallel arrays like actin stress fibres. It is difficult to say that there is co-localisation of the pump binding directly to actin stress fibres as it appears in Figures 4.3.1 and 4.3.2. However as discussed in Chapter 2.1c, there is interaction between the α-1 subunit and actin via cytoskeletal linking proteins. For instance, actin and spectrin co-localise with the third cytoplasmic domain (CD3) of the Na^+,K^+ ATP α-subunit in some epithelial cells and rat brain, and with anion exchanger 1 (AE-1) in erythrocytes. Na^+,K^+ ATPase and AE-1 are also found to interact with the actin cytoskeleton via the linking protein ankyrin (Cantiello, 1995a; Nelson & Veshnock.1987; Morrow *et al.*, 1989). Brown *et al.*, (1996) found that SDS pre-treatment in various tissues produced an increase in both Na^+,K^+ ATPase and AE-1 staining intensity. A possible reason for this pattern of staining is that SDS pre-treatment has unmasked cryptic antigenic binding sites linking the α-1 subunit to actin. A loss of antigenic binding sites is another possibility for this pattern of staining revealing underlying sites. Brown *et al.*, (1996) found in certain tissues (i.e. mammalian kidney cells) the AE-1 heavily stains within the Golgi apparatus. This pattern of staining was selectively abolished with SDS pre-treatment. Mobasheri (1996) demonstrated in human primary bone osteoblasts, intracellular pools were revealed in the cytoplasm between the nucleus and the plasma membrane, as well as visible patches of pump staining on the nuclear envelope after SDS pre-treatment. This pattern of staining was notably different from the ubiquitously expressed pattern of α-1 staining obtained in osteoblasts permeabilised with Triton–X 100 (Mobasheri, 1996). These examples illustrate that SDS pre-treatment could cause possible antigen loss, revealing pumps only

in precise locations in BAECs, exposing pumps associated with actin stress fibres which are not seen via techniques such as 0.1% NP40 permeabilisation (demonstrated in Chapter 3, Figure 3.6).

Hypotonic lysis of BAECs in this study was adopted from Lamb & Lindsay (1971) and used as a method for analysing pumps in the cell membrane. The cells were observed under phase contrast after introducing the cells to a hypotonic environment. The BAECs appeared distorted compared to their usual appearance in a static monolayer, which was due to cell swelling. "Debris" was detected in the surrounding fluid, and Brownian movement was visible inside the cell. This method proved to expel the contents of the cell, however the Hoechst staining showed that the nucleus was left behind in the majority of the cells. Some cells were detached from the coverslip during this procedure.

Initially, these series of experiments were performed on sub-confluent cells as a precaution, in case bursting cells lead to detachment of not just individual cells, but monolayers of cells. The cells were treated in the hypotonic solution, then double labelled for the α-1 subunit and actin. Cells that remained attached to the coverslip and stained for the α-1 subunit revealed a random pattern of staining, however, the pumps were in clusters, appearing as fewer but larger staining dots. A possible explanation is that when the membrane disrupts from hypotonic bursting it reforms in clumps, changing the pattern of distribution of pumps in the membrane. Therefore instead of visualising individual pumps, one sees clusters of several α-1 subunit fluoresce. An interesting finding was also seen in cells that presumably detached during the hypotonic incubation. These areas

(presumably patches of cell membrane) also stained for pumps. The islands of fluorescing pumps might be patches of the cell membrane left behind as the cell is torn away, or perhaps cytoplasm that has collapsed down onto the coverslip after the cell detaches and is then fixed, leaving behind pumps that were in the cytoplasm.

In addition, patches of actin also stained. Actin staining in sub-confluent cells still showed cells having stress fibres, and "whisker-like" extensions (filopodia) as seen in Figure 4.5 b) & d).

Cells that were in more confluent monolayers were also used for these experiments, but did not become detached from the coverslips as originally suspected. In fact, there appeared to be less cell detachment after hypotonic pre-treatment in more confluent cells. The α-1 subunit ubiquitously stained the plasma membrane as well as having areas of clusters of α-1 subunits fluorescing as large dots. Actin reformed into stress fibres, and also formed small rings of actin. In areas where these rings reformed, the α-1 subunit pumps were found lining the periphery (Figures 4.7 and 4.8 a) & c). Pump staining does not appear to co-localise with actin in any other portion of the cell. The linkage between actin and the plasma membrane involves the recruitment of a variety of cytoskeletal proteins. For example, talin, vinculin and/or α-actinin (Turner *et al.*, 1990; Burridge *et al.*, 1996) are proteins found at focal adhesion sites (illustrated in Figure 4.1). Actin stress fibres bind to focal adhesion sites, which in turn are linked to a family of glycoproteins (integrins) spanning the plasma membrane. Perhaps, after hypotonic pre-treatment and cell refilling there are integrins

spanning the plasma membrane at the sites which rings of actin form. In which case, the ring of pumps which appear to be associated to the actin staining are pumps tethered to the cell membrane.

Part II

Part II

Introduction 1.1

The inner surface of a blood vessel consists of a single layer of squamous epithelial cells measuring from about 0.05 to 1.0 μm in thickness. The cells form a continuous monolayer lining the entire vascular system, which is termed the vascular endothelium. The endothelial cell measures approximately 10 - 15 μm in width, and 25 – 50 μm in length. The cell lining acts as a permeable barrier between blood and the vessel wall (Davies, 1989) and serves to maintain vascular tone and normal vascular function by releasing factors that control platelet adhesion and aggregation, fibrin formation, leukocyte recruitment, smooth muscle contractility and endothelial cell migration and proliferation. (Consigny and Vitali 1998). The cells are constantly exposed to haemodynamic forces i.e. dynamic forces associated with the flow of blood (Chiu, *et al.*, 1998). The cells align with the long axis of the vessel, in accordance with the direction of the shearing force of blood flow (Sacher *et al.*, 1997). Within the ellipsoidal endothelial cell there is an elongated prominent nucleus and various other cellular organelles. Haemodynamic forces elicit changes in cell morphology, physiology and genetic expression (Lansman 1988; Davies, 1995), although the underlying mechanisms are not clearly understood. This section describes the nature of flow in arteries, the range of haemodynamic forces experienced by endothelial cells, and the effect of flow on the sodium pump.

1.2 Types of flow found in arteries

Flow in arteries may be described as the pulsatile motion (Oluwole *et al.*, 1996) of a weakly non-Newtonian fluid (Davies, 1995). In the majority of cases, flow is fully

laminar (Vogel, 1994): that is to say, it is streamlined and the viscosity of the fluid dominates the fluid behaviour. Minor disturbances within the flow do not persist but are dampened through viscous action[1]. Strictly turbulent flow rarely occurs in arteries, although it is characteristic of flow in, for instance, the aorta. The Reynolds number, denoted Re, is a universally applied criterion to determine the point at which a fluid flow changes from principally laminar in character to one that is turbulent (Vogel, 1994). Re is given by:

$$\mathrm{Re} = \frac{Ul\rho}{\mu} = \frac{Ul}{\nu} \qquad 1.$$

where l is a characteristic length scale (in arteries usually taken as the diameter or radius), U is the flow speed, ρ is the fluid density, and μ and ν are the dynamic and kinematic viscosities, respectively. Re is a dimensionless quantity, and the laminar-turbulent transition occurs roughly when Re=2000 for long, straight cylindrical tubing with smooth walls at a considerable distance downstream from the tubes entrance. With roughened tubing, the transition can happen at lower values. In natural systems, other factor may promote the transition from laminar to turbulent flow. These include flow separation, recirculation, and complex flow patterns (eddies). Disturbed laminar flow is found in areas where flow is redirected into branch vessels, around bifurcations of large arteries and where vessels curve significantly such as the aortic arch (Davies, 1989). This is shown schematically in

[1] Vogel (1994) provides an excellent analogy for the distinction between laminar and turbulent flow. In laminar flow, as noted, viscous forces restore disturbances (up to a point). Turbulent flows, on the other hand are characterised by high inertia. Inertial forces reflect the *individuality* of bits of fluid while viscous forces reflect their *groupiness*. The former describes the progress of a milling crowd, the latter of a disciplined march.

Figure 1.1. Atherosclerotic lesions, which will also disrupt flow, tend to develop at these points in the arterial system (Chiu *et al.*, 1998).

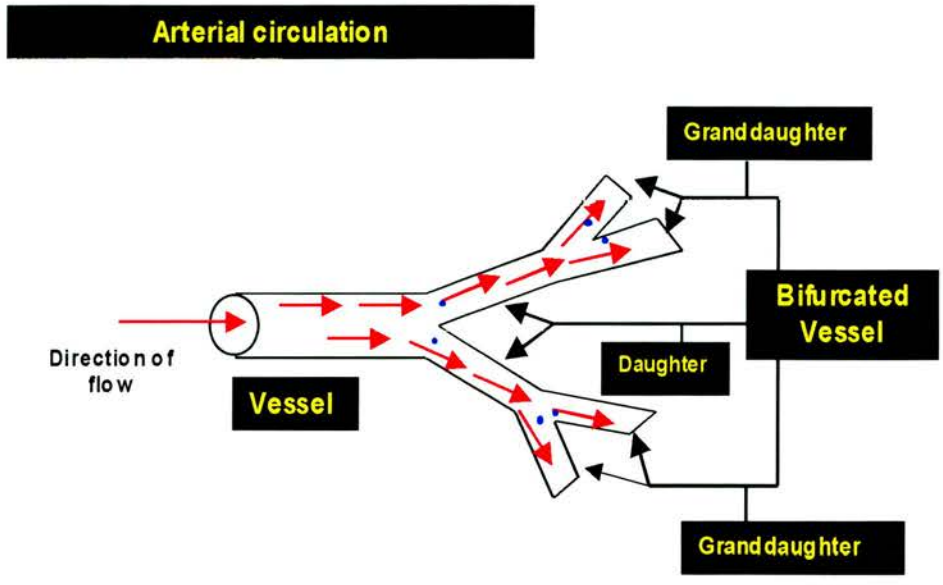

Figure 1.1 The above illustration shows a vessel with two daughter branches and four granddaughter branches. The blue dots indicate areas of turbulence around the bifurcated vessel. In the arterial circulatory system cells align in areas with laminar flow. However, if laminar flow is disrupted for example, in cases of flow separation (bifurcation) areas of turbulent (or chaotic) flow exist. Endothelial cells at sites of bifurcation do not align in the direction of flow as do cells found in areas of laminar flow.

The term weakly non-Newtonian[2] means the relationship between an applied shear stress and the resulting rate of deformation of whole blood is not linear (Easthope and Brooks, 1980). The non-Newtonian behaviour of blood is attributable principally to the plasma viscosity, the flexibility of red blood cells and the degree of cell-cell interaction (Thurston, 1975). It is of interest that experimental studies have indicated that wall shear stress appears to be largely independent of fluid rheology[3] (Dutta and Tarbell, 1996). 112-114

[2] The non-Newtonian properties of blood draw attention to the relationship between viscoscity and velocity In the vascular system. Blood viscosity tends to decrease with increasing velocity (Ballermann, 1998).
[3] Rheology is the study of the deformation or flow characteristics in materials including elasticity, viscosity, and plasticity.

1.3 Haemodynamic forces influencing endothelial cells in laminar blood flow

Endothelial cells are exposed to a number of different forces generated by the movement of blood through the vessel lumen. The situation is complex because arteries are not rigid structures but have varying cross-sectional areas and shapes according to various stimuli (Vogel, 1994). Hence, the forces to which the cells are exposed will also vary in time and in magnitude.

Gradients of flow velocity are an inescapable feature of any moving fluid. Figure 1.3 shows how flow gradients in a cylindrical vessel develop with downstream distance from a source (in this case a reservoir).

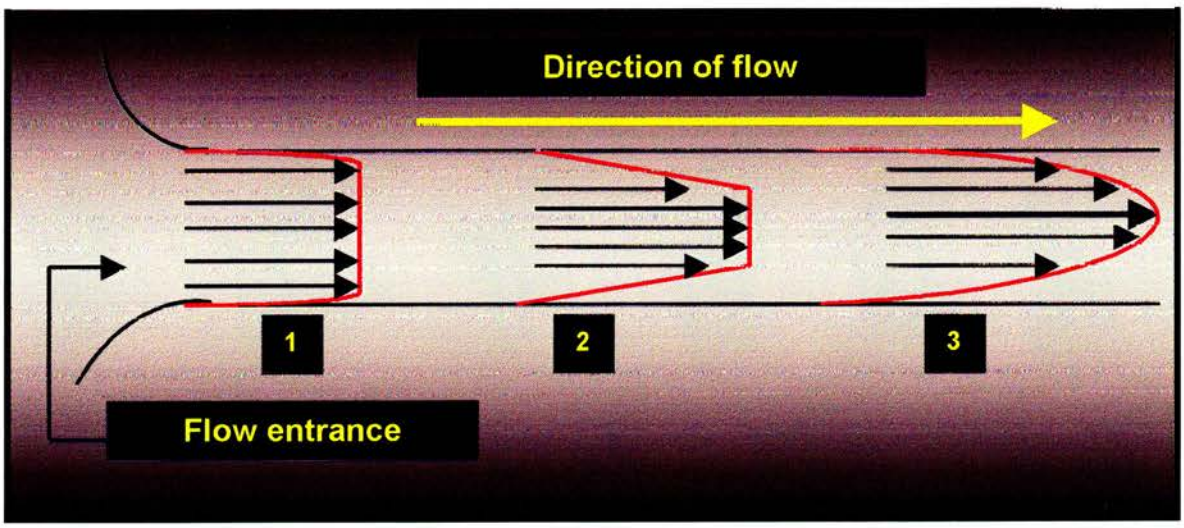

Figure 1.2 The gradual development of a parabolic profile of velocity as fluid enters a cylindrical vessel from a reservoir (taken from Vogel, 1994).

Upon initial entry the fluid speed will be virtually uniform across the vessel (1). The velocity profile is called "slug flow" or "plug flow". A velocity gradient gradually starts to develop at the wall of the vessel (2) thickening downstream until the final velocity profile is achieved. At this stage, the velocity profile is described by a parabolic equation, in which flow velocity increases to a maximum at the artery centreline from zero flow at the artery wall. Thus:

$$U_r = \frac{\Delta p}{4l\mu}(a^2 - r^2) \qquad 2.$$

where $\Delta p/l$ is the pressure drop per unit length, μ is the dynamic viscosity, r is the radial location outward from the centre of the artery (r=0 at the centreline), and a is the artery radius (r=a at the wall). An experimentally determined velocity distribution by Masuda and Fujiwara (1993) is shown in Figure 1.2.

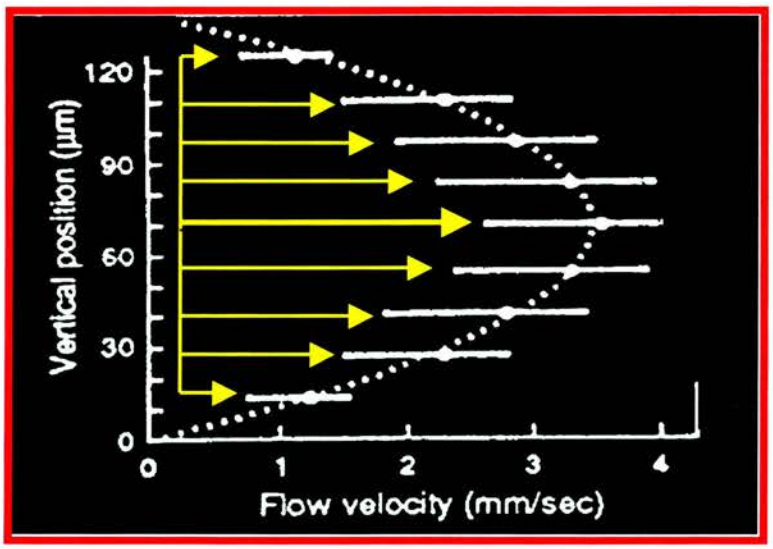

Figure 1.3 Measured distributions of flow velocity between two closely spaced plates in a flow chamber set-up (data from Masuda and Fujiwara, 1993). The lengths of the superimposed yellow arrows are proportional to the flow speeds at their bases; this diagram illustrates the parabolic flow profile.

The presence of a gradient in flow velocity close to the artery wall means that a shear stress, denoted τ, will be exerted on the endothelial surface. The relationship between the velocity gradient in a moving fluid and the fluid shear stress is given by

$$\tau = \mu \frac{dU}{dr} \qquad 3.$$

where τ is the shear stress, μ is the dynamic viscosity, and dU/dr is the local velocity gradient. Shear stress is a force per unit area (units dynes cm^{-2}) and moving blood exerts a *tangential* stress on cell surfaces. Since shear stress is proportional to the product of shear rate and fluid viscosity, an increase in blood flow or viscosity should increase shear stress acting on the endothelial cell layer and therefore elicit vessel dilation. (Koller & Kaley, 1996).

Surface topography and cell geometry influences the magnitude and location of haemodynamic forces acting upon the cell surface. Steeper velocity gradients in faster moving fluids will generate greater shear stresses on the endothelial lining (Davies, 1995; Salwen *et al.*, 1998). Fluid shear stress typically ranges from 0 - 50 dynes cm^{-2} in the human body (Davies, 1997) in relation to the cardiac cycle. Davies, (1996) showed ranges of shear stress in arterial circulation to include negative values through zero (at areas of flow separation) up to approximately 40 – 50 dynes cm^{-2}. Under conditions of dramatically increased cardiac output or hypertension these values may increase to ~ 100 dynes cm^{-2} (Franke, *et al.*, 1984; Davies, 1996). It is interesting to note that wall shear stress within the human circulatory system is, at any given instant, constant throughout (Bevan 1997), in spite of the three order of magnitude variation in vessel diameter (Table 1.1). This arises essentially because

velocity varies in direct proportion with the diameter of the vessel. Hence, from Equation 3, the gradient of velocity is the same everywhere in the system and all the walls will be subjected to similar shear stress.

Blood flow regulates the vascular width through a negative feedback system. The heart serves as the source driving this system that is responsible for fluctuations in flow. For example, when blood flow increases, the vessels dilate, when it decreases, the vascular smooth muscle cells contract. This naturally occurring biosensor is crucial in organ perfusion and peripheral blood flow. Dysfunctions of this sensor can lead to organ insufficiency, hypertension and arteriosclerosis (Siegel *et al.*, 1997).

Vessel	Average radius (mm)
Aorta	12.5
Arteries	2.0
Arterioles	0.03
Capillaries	0.006
Venules	0.02
Veins	2.5
Vena Cavae	15.0

Table 1.1 Average radii of the vessels of the human circulatory system (from Vogel, 1994).

Two distinct haemodynamic forces influence vascular cells. As previously mentioned frictional shear stress acts at the apical surface (tangential stress) and pressure (normal stress) exerts tension and compression within the cells (Dubini *et*

al., 1996). The directions of force can also be thought of as parallel (tangential) and perpendicular (normal). Figure 1.4 illustrates the stresses acting on the luminal

surface of endothelial cells. Cells also experiences tensile stress, which is due to the compliance of the vessel under the pulsatile flow of blood (Salwan *et al.*, 1998). Vessel distension due to pulsatile flow transmits tensile stress to the cell cytoskeleton at points of cell-cell and cell-matrix adhesion, where the cytoskeleton connects to adhesion molecules on other cells or to extracellular matrix molecules via transmembrane proteins called integrins (Davies, 1996, Ballermann, *et al.*, 1998).

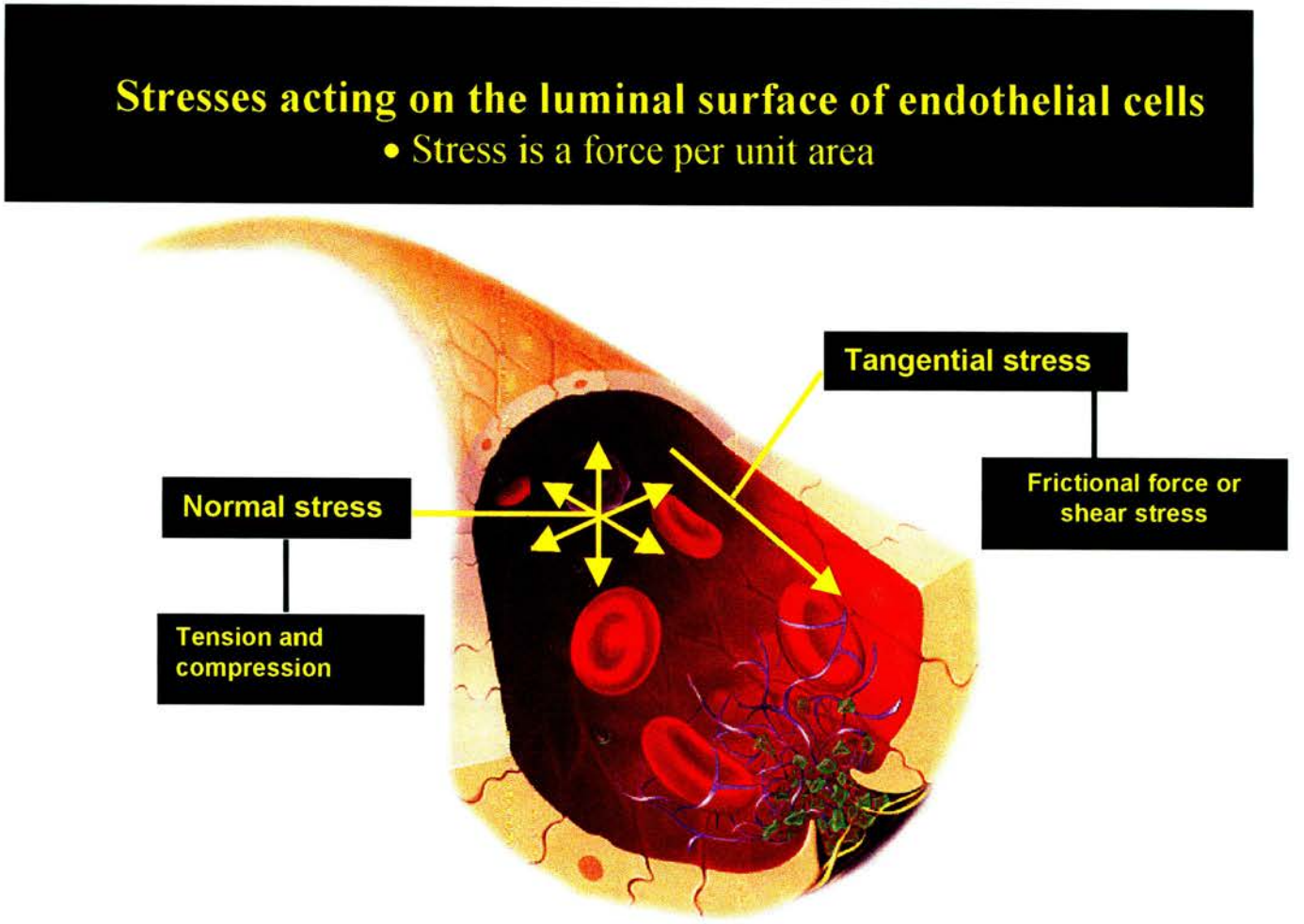

Figure 1.4 Different types of forces exerted on a vessel. Blood pressure acts normal to the cell surface creating a compressive stress within cells, while frictional force of flowing blood generates a shear stress within the cells (Davies, 1996) (Photograph modified from Horowitz, 1997).

Shear stress causes cell deformation (strain)[4]. Tensile strain (or stretch) represents a change in length per unit (original) length. (Davies, 1996) The schematic illustration in Figure 1.5 illustrates the effects of different stresses. Normal stress causes stretch, with cell deformation in all different directions, whereas shear stress is the fluid frictional force acting upon the apical surface of the cell, resulting in unidirectional cell deformation. Shear stress and normal pressure are unrelated forces, however, the application of stress to integrins both yield endothelial cell deformation (strain).

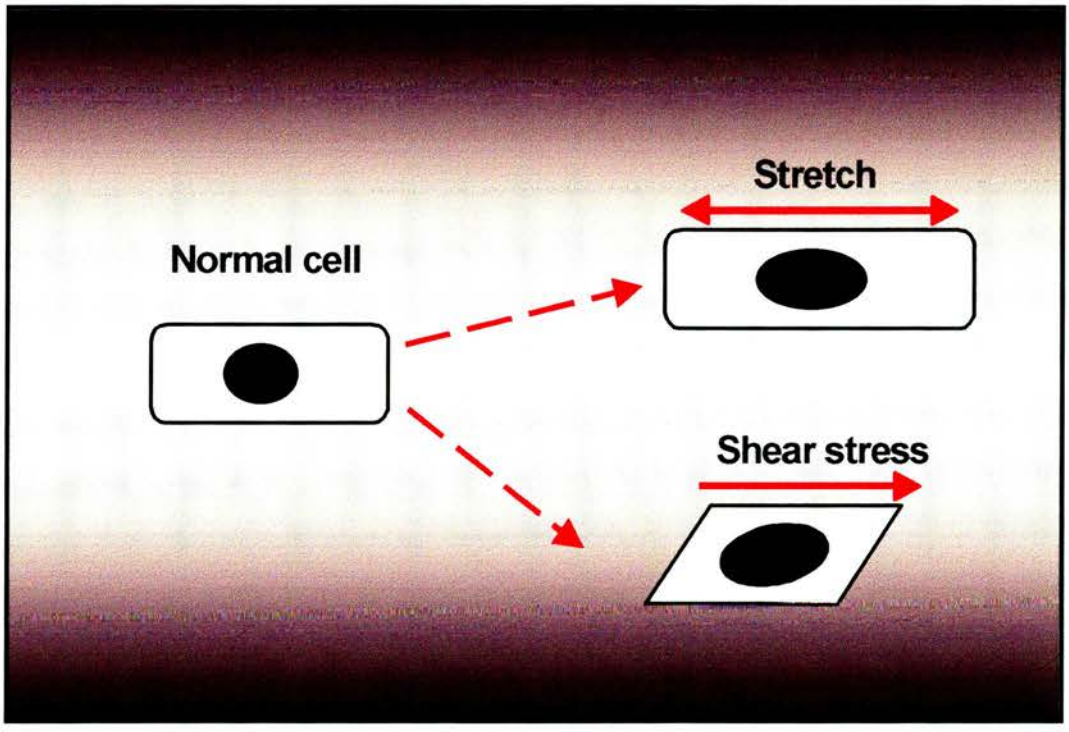

Figure 1.5 Schematic representation of the effects of wall tension and shear stress on endothelial cells (adapted from Ballermann *et al.*, 1998).

1.4 Physiological and biochemical response to fluid shear stress

Force transmission

Molecules of the extracellular matrix (i.e. fibronectin) produce changes of cell shape through binding to the cell surface integrin receptors, which interconnect with actin microfilament

[4] Strain is the dimensional change in the shape of volume of a body as a result of applied shear stress.

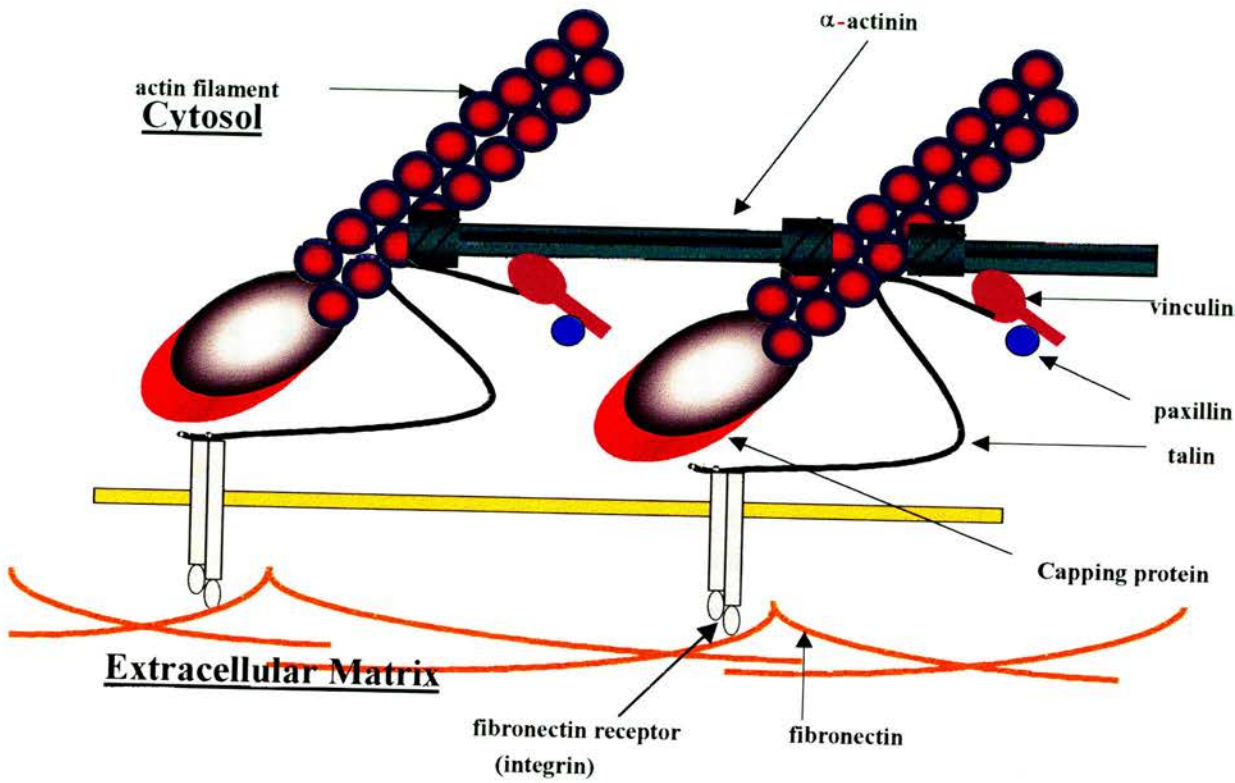

Figure 1.6 This model illustrates the binding of actin to the extracellular matrix. Focal contacts are formed as the transmembrane linker proteins (integrins) bind to glycoproteins on the extracellular matrix.

(Burridge and Wodnicka, 1996). Integrins (Figure 1.6) provide a molecular conduit for force transmission across the cell surface as well as a mechanism for transduction of mechanical signals into biochemical and cytoskeletal response (Sims, *et al.*, 1992). Figure 1.6 illustrates the association of actin to focal adhesion proteins.

Cells that are anchorage-dependent exist in a state of continual tension associated with maintaining their shape. This tension is generated when the cytoskeleton interacts with other regions of the cell. The exact location at which shear stress affects cellular elements to respond is unknown (Masuda and Fugiwara 1992),

however the primary flow sensing event(s) is presumably localised to the luminal surface where shear stress directly acts on the cell membrane. The possible triggers of shear stress-induced mechanotransduction[5] are understood to be the local displacement of sensors at the surface and force transmission by the cytoskeletal elements, which distribute force throughout the cell, followed by force transduction of the transmitted mechanical stress at mechanotransduction sites in underlying isolated areas from the externally applied stress (Davies, 1996). Figure 1.7 A & B shows the possibilities of haemodynamic response mechanisms in endothelial cells, illustrating how the cytoskeleton plays an integral role in transferring stress to different areas in the cell where mechanotransduction may occur. Reorganisation of F-actin stress fibres, intermediate filaments, and microtubules to external forces implicates the cytoskeleton as a principal force transmission element in endothelial cells.

A. Force transmission

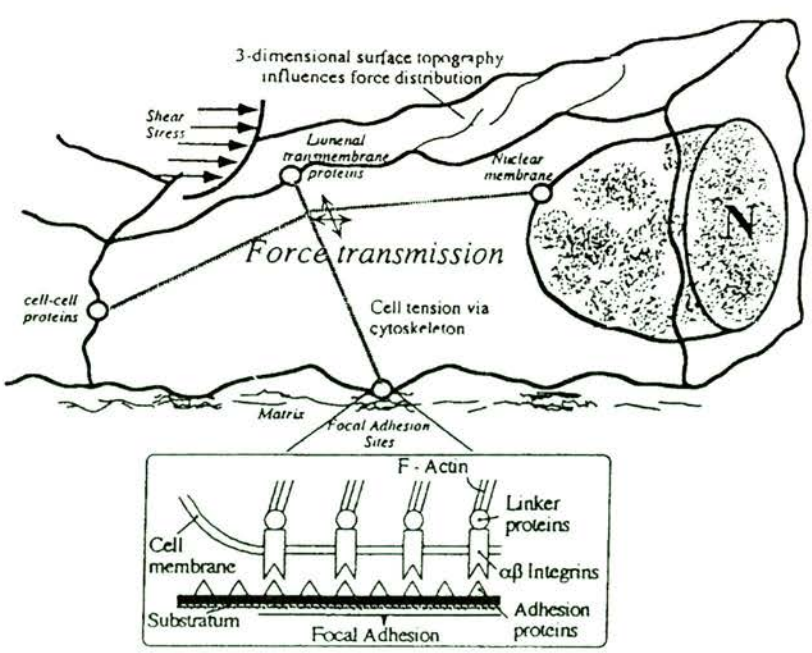

[5] Mechanotransduction is the process of converting a physical force into a cellular response.

B. Force transduction

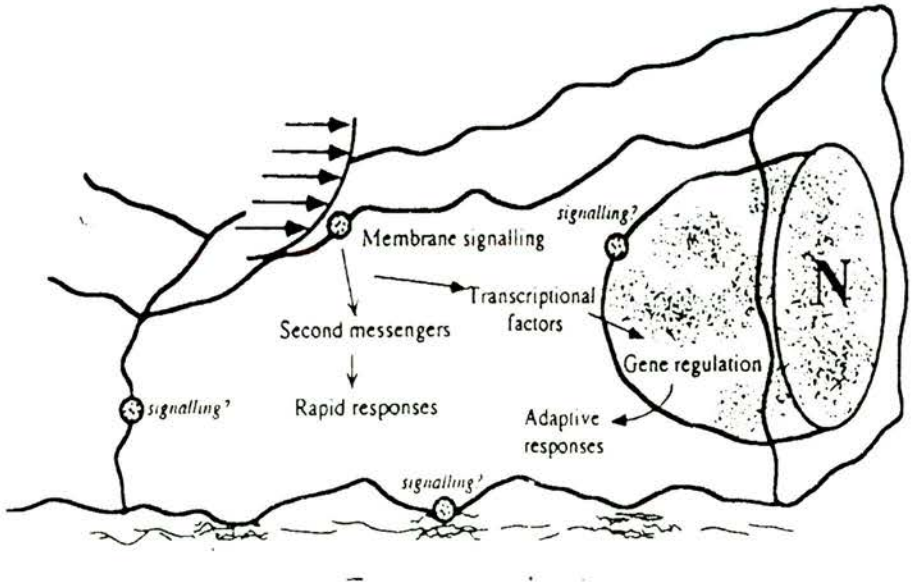

Figure 1.7 A & B break up the different concepts of force transmission (A) and force transduction (B). The cytoskeleton transfers stress to different locations of the endothelial cell where mechanotransduction may occur.

Signal Transduction

Endothelial cells exposed to mechanical forces are shown to respond rapidly, and by predictable biochemical and gene response. *In vivo*, fluid shear stress and circumferential stretch play important roles in maintaining the homeostasis of the blood vessel. *In vitro* experiments using flow chamber apparatus and stretch devices

(Davies, 1995; Chien *et al.*, 1998) help to clarify mechanisms of signal transduction and gene expression in response to the physiological forces experienced by the vessel.

Transmission of shearing forces to the cell first occur at the luminal surface, therefore luminal surface structure is considered to be important in the transmission of signals to the inside of the cell (Davies, 1995; Davies & Tripathi, 1997). Molecules at the plasma membrane of the cell are implicated as mechanotransducers that assist in generating intracellular biochemical signals. Carbohydrate-rich glycoproteins (glycolax) found bordering the cell surface act as either receptors themselves, or are linked to receptors anchored to the plasma membrane Other mechanical sensors at the luminal face may be a molecule or molecular complex with functional dependency on its stressed state (Davies, 1995). One theory of mechanotransduction states that once luminal surface proteins are displaced or activated, biochemical cascades are generated at the cytoplasmic face on the membrane. The proposed model starts with stress activation of mechanoreceptors, leading to the generation of second messengers that activate cytosolic transcription factors, which in turn regulate gene transcription in the nucleus (Davies, 1995).

One of the earliest responses to flow is the activation of inwardly rectifying potassium channels (Davies *et al.*, 1995; Davies *et al.,* 1997). This leads to an increases in intracellular Ca^{+} that activate endothelial nitric oxide syntase (eNOS), increasing nitric oxide production and causing vasodilation (Busse and Mülsch, 1990). The production of nitric oxide in endothelial cells in response to increased shear stress is biphasic, consisting of an initial peak followed by a plateau phase

(Hecker, *et al.*, 1993). The "peak" component can be abolished by the removal of Ca^{+} from the growth medium, whereas the "plateau" phase is Ca^{+} independent.

It is known that fluid shear stress affects gene expression in endothelial cells (Koreanaga *et al.*, 1997). To date approximately 20 have been identified as stress-responsive genes (Tsuboi, 1996). Some genes which are up-regulated by flow include: tissue plasminogen factor (tPA), platelet-derived growth factor (PDGF)-A, nitric oxide syntase (NOS), intercellular adhesion molecule 1 (ICAM-1), transforming growth factor–β1 (TGF-β1) and monocyte chemoattractant protein-1 (MCP-1) Other genes are down-regulated by flow, for instance, angiotensin converting enzyme (ACE) (Khachigian *et al.*, 1996; Korenaga *et al.*, 1997). Endothelial cell response to flow fit into related groups and can be organised on the basis of response time (Davies, 1995; Davies, *et al.*, 1997). A temporal grouping of endothelial cell response to fluid shear stress is illustrated in Table1.2.

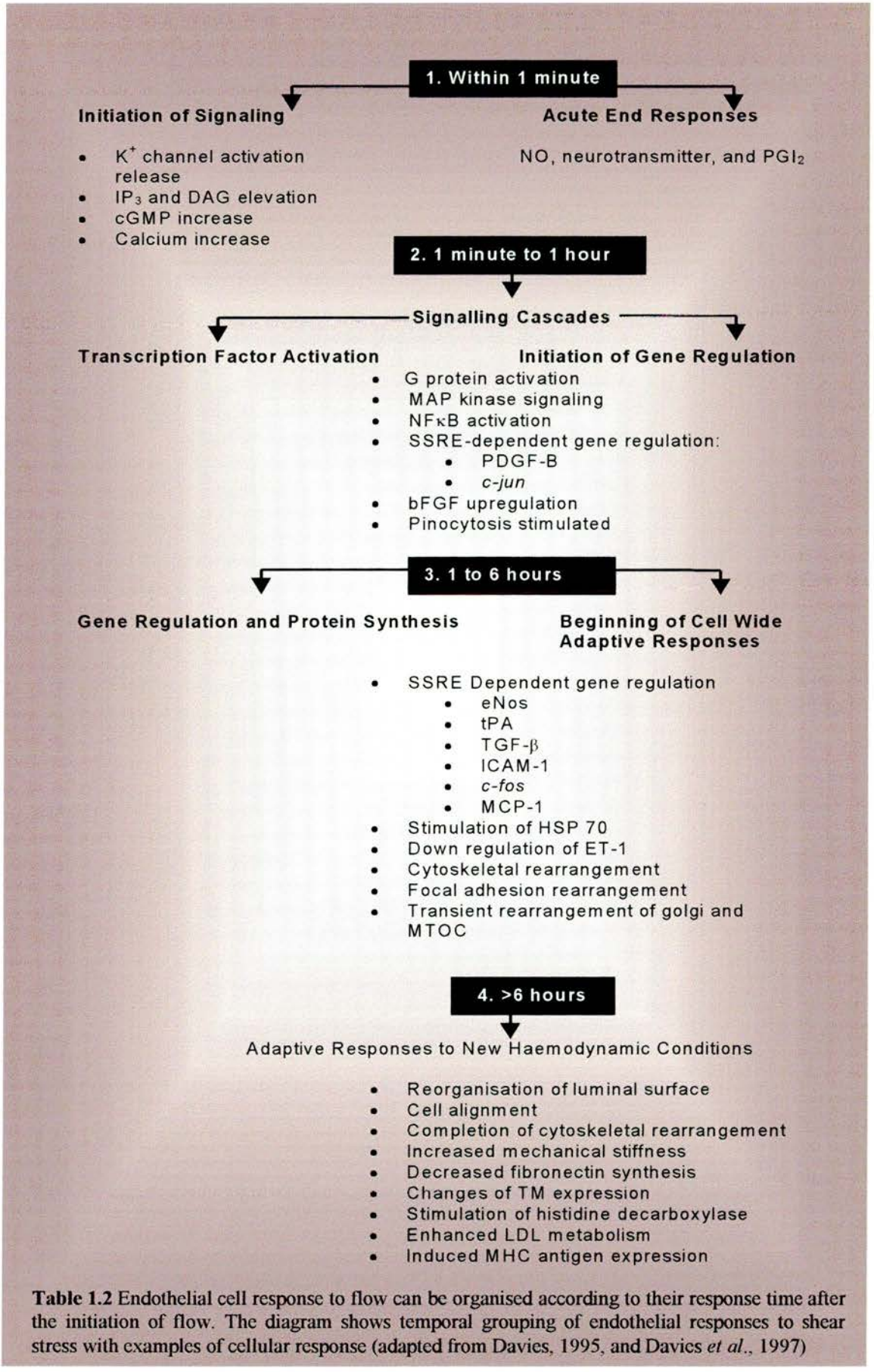

Table 1.2 Endothelial cell response to flow can be organised according to their response time after the initiation of flow. The diagram shows temporal grouping of endothelial responses to shear stress with examples of cellular response (adapted from Davies, 1995, and Davies *et al.*, 1997)

1.5 Components of the cytoskeleton

Another proposition of structural complexity in mechanotransduction involves transmission of stress throughout the cell via the cytoskeleton. In this situation, the membrane molecules can participate to passively transfer stress to the cytoskeleton in an area of the cell or respond to cytoskeletal deformation sites away from the stimulus, for example any point of connection between the membrane proteins and the cytoskeleton. Sites mechanically coupled by the cytoskeleton include: intercellular junctions, abluminal focal attachment sites, nuclear membrane and the luminal surface itself (Davies, 1995).

Morphological changes and possible relationships of the cytoskeletal proteins

The cytoskeleton is a complex network of tension bearing filaments extending through the cytoplasm acting as internal framework for the cell. (Georgantos and Marchesi 1985; Bray, 1992). Is made up of three distinct biopolymers: microtubules, (e.g.tubulin,), microfilaments (e.g. actin) and intermediate filaments (e.g.vimentin, (Knapp *et al.*, 1983, Carraway and Carraway 1992). This complex array of interconnecting filaments serve many functions in the cell such as; shape change and locomotion, cellular responses to environmental stimuli, translation of mRNA into proteins, regulation of gene expression, and the determination of cellular polarity (Zambetti *et al.*, 1991; Ryu *et al.*, 1995).

Experiments using micropipette aspiration reveal a direct relationship between cell shape and mechanical stiffness of the cell surface (Davies, 1989). A three-fold difference is found as cell morphology changes from polygonal to an elongated shape under flow, as well as prominent cytoskeletal changes.

Actin

Cells reorganise shape and cytoskeletal structure in response to fluid mechanical forces. Endothelial cells grown in static culture are polygonal in shape. On exposure to uniform FSS these cells elongate and then undergo realignment in the direction flow (Suciu *et al.*, 1997; Galbraith *et al.*, 1998). During cell realignment, prominent changes occur in filamentous actin (F-actin). Cells grown in static culture contain bundles of actin filaments randomly oriented called stress fibres, as well as dense bands surrounding the periphery of the cell. Upon exposure to FSS the dense peripheral bands re-organise themselves to form near parallel arrays of thick stress fibres (Wong *et al.*, 1983; Franke *et al.*, 1984). Studies by Levesque and Nerem (1985) showed that vascular endothelial cells exposed to high fluid stress in vivo become more ellipsiodal. The formation of stress fibres under flow is an important mechanism that serves to protect the endothelium by maintaining cell - cell contact and cell-substratum contacts (Kim *et al.*, 1989). In regions of low shear stress cells are more polygonal in shape, and these regions of the vasculature are more prone to develop atherosclerosis (Kano *et al.*, 1996). The change in cell alignment is found to be reversible. After the stimulus is removed cells reorient themselves and revert to a more polygonal appearance (Remuzzi, 1984).

Microtubules

The microtubules are cylindrical structures approximately 25 nm in diameter extending throughout the cytoplasm, adding rigidity and elasticity to various parts of the cell. Microtubules are composed of the globular protein tubulin which is found in two forms, α and β. In cross section, the microtubules are made up of 13 protofilaments of alternating α and β subunits (approximately 4 - 5 nm in diameter) (Wolfe, 1993).

These structures are in a state of continual flux from polymerisation to depolymerisation. As polar molecules, microtubules having positive and negative ends, the negative end is embedded in the perinuclear microtubule organising centre (MTOC) while the positive end radiates out towards the edge of the cell (Carraway & Carraway, 1992). To prevent dynamic instability, the positive end can be capped to prevent depolarisation, while the negative end remains protected embedded in the microtubule organising centre. The MTOC is found near the nucleus and close to the Golgi and is composed of a tubulin monomer, γ-tubulin (Coan *et al.*, 1993). The centrosome is located to the side of the nucleus and consists of a pair of L-shaped centrioles, composed of nine microtubule triplets, joined by cross-linking proteins (Stevens & Lowe, 1992). The centrioles are responsible for microtubule nucleation, the process by which microtubules are made and ready to undergo polymerisation (Mogensen *et al.*, 1997).

Microtubules are also found to have an important role in the realignment of vascular cells under flow. Studies by Malek and Izumo, (1996) have shown that treating cells

with nocodazole, a drug that disrupts microtubules, stops the rearrangement of F-actin and prevents the shape change in cells exposed to laminar tangential stress.

Intermediate filaments

Intermediate filaments are named for their diameter that is approximately 8-10nm falling into a middle range (intermediate) being larger then microfilaments (~5nm) and smaller then microtubules (~25nm). Originally they were regarded as disaggregated products of either microtubules or myosin filaments (Lazarides, 1982), however immunological and molecular biological techniques established intermediate filaments as a distinct fibrous system composed of chemically heterogeneous subunits (Goldman & Steinert 1990). The subunit structures have been classified into at least five different classes of tissue or cells specific protein (Steinert, 1984), as shown in Table 1.3.

Type	Subunit	Size (KDa)	Tissue
I	• Acidic keratins	40-60	Epithelial cells
II	• Neurtral-basic keratins	50-70	Epithelial cells
III	• Desmin • Glial fibrillary acidic protein (GFAP) • Vimentin • Peripherin	52 50 53 58	Muscle Astrocytes Fibroblasts and other cells having mesenchymal origin (including endothelial cells) Peripherial nerve axons
IV	• Neurofilament triplet	70 130 180	Neurons
V	• Lamin A • Lamin B • Lamin C	73 69 63	Nuclear envelope (All types)

Table 1.3 The five principle types of intermediate filaments (Adapted from Lazarides, 1982; Sabine, unpublished).

Vimentin (type III) intermediate filaments are a major cytoskeletal constituent of cells of mesenchymal origin (Shah, *et al.*, 1998). Functional implications vary from

maintainance of cell integrity (Lazarides, 1980 Eriksson, *et al.*, 1992) to gene regulation (Traub and Shoeman, 1984).

In subconfluent cells vimentin exists as a dense wavy network of filaments that surrounds the nucleus and extends throughout the cytoplasm. This meshwork of filaments is attached to the nuclear envelope and radiates outward from the nucleus area to the cell periphery where it is associated with the cell membrane. Areas of association are usually concentrated with desmosomes, hemidesmosomes and other types of adhesion sites (Goldman *et al.*, 1996). An interesting reorganisation of the cytoskeleton occurs once cells become confluent and form a continuous monolayer. Intermediate filaments retract from the cell periphery and move towards the nucleus gradually condensing to form a conspicuous, densely stained ring, referred to as the perinuclear ring, which encloses the nucleus, the MTOC and the Golgi complex (Blose & Chacko 1976; Blose & Meltzer 1981; Flitney 1997). The signal that appears to trigger these events is cell-to-cell contacts, similar to that of dense peripherial band formation of actin (Flitney, 1997). The exact function of perinuclear rings is yet to be established, however functional possibilities include a structural pathway for protein synthesis, a cytoplasmic anchor for the nucleus, and involvement in organelle movement (Blose & Meltzer, 1981) and possibly a role in mechanotransduction.

Cells exposed to uniform laminar flow show intermediate filaments undergoing extensive reorganisation within 1-2 hours. Notable differences in intermediate filament (vimentin) reorganisation start with the "unravelling" of the marginal bands

of vimentin forming large "loops" distributed throughout the cytoplasm (Flitney, 1997). After prolonged exposure to fluid shear stress (approximately 8 hours) intermediate filaments are shown to re-align in near parallel arrays in the direction of flow, resembling formation of actin stress fibres (Flitney *et al.,* 1996). A common linker protein is suggested to form a structural link between intermediate filament proteins and microfilaments. The link is a 300kDa intermediate filament associated protein called IFAP300 (Leiska *et al.*, 1985). IFAP300 is found to colocalise with several protein components of specialised focal adhesion sites, including the tips of actin stress fibres, paxillin, talin, and vinculin (Burridge & Chrzanowska-Wodnicka, 1996; Flitney *et al.*, 1996, Flitney, 1997). The association of IFAP300 with focal adhesions sites suggests potential site for the attachment of intermediate filaments to the actin cytoskeleton. However, it is known that IFAP does not directly bind to actin, therefore other adhesion plaque proteins (i.e. paxillin, talin, and vinculin) are implicated as points of attachment.

The above observations suggest that IFAP300 may function as a key link between vimentin and actin components of the cytoskeleton (Flitney *et al.*, 1996). This advocates the possibility that IFAP is involved in the mechanotransduction process, transmitting fluid shear stresses acting at the cell surface to focal adhesion sites via mechanical deformation (strain) of actin and/or vimentin (Wang *et al.,* 1993; Davies, 1995; Flitncy *et al.*, 1996).

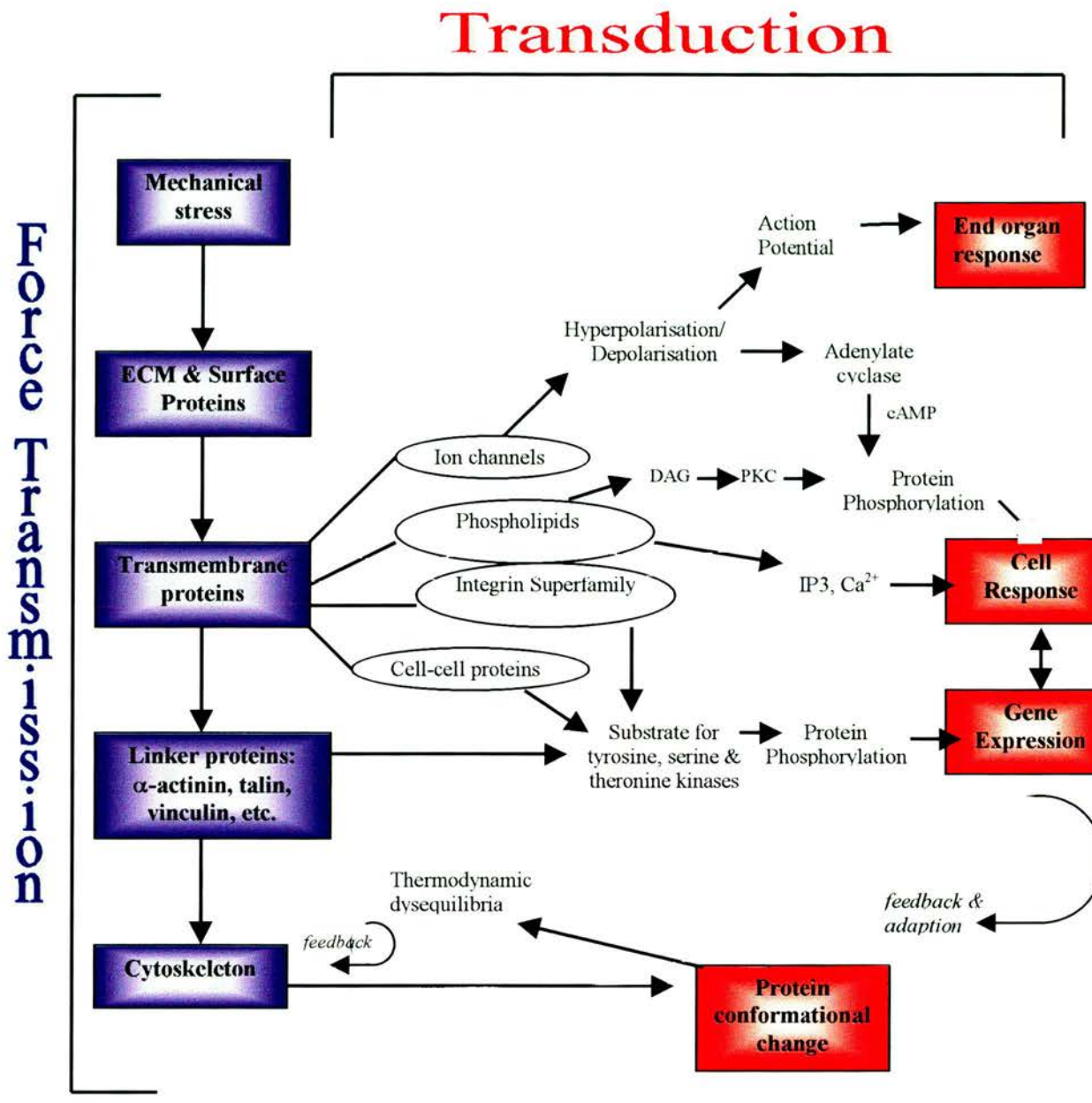

Figure 1.8 Mechanisms of mechanical stress transmission and transduction, illustrating how the physical deformation of a membrane protein or cytoskeletal component can lead to a biochemical response (diagram adapted from Davies & Tripathi, 1997).

The shearing and pulsatile flow forces to which cells are continually exposed are surmised to lead to incessant cell stimulation. *In vitro* experimentation shows cells

elicit many responses at the onset of flow, however through "adaptation" and "signal filtering", sustained stimulation leads to feedback inhibition of mechanotransduction, and selective response to only certain frequencies of stimulus (Davies, 1995). This also draws the distinction between "stress" and "stretch" activated response. For example, endothelial cells exposed to pulsatile flow fail to respond at certain frequencies, possibly due to insufficient duration of the stimulus in order to provoke a response. Conversely, stretch-activated ion channels (or pressure sensitive) do not respond to laminar flow-generated shear stress, however their pressure response permits the influx of a variety of cations (Davies, 1989).

Mechanosensitive ion channels

The role of the cytoskeleton and focal adhesion proteins play a very important role in shear responsive cells. However, there is little evidence for the direct binding of ion channels to the actin cytoskeleton. This association is under scrutiny; and it is questionable whether channel activation is via a direct or indirect linkage due to alterations of tension put forth on the membrane, suggesting a more probable association of ion channels to the underlying cytoskeletal cortex (Davies, 1995). It is however understood that the presence of the cytoskeleton is not directly necessary to activate ion channels, for example, stretch activated ion channels can exclusively use free energy stored in the transmembrane electrochemical gradient and are sensitive to imposed pressure. But interestingly, disruption of actin inhibits their response (Davies & Tripathi, 1997).

Mechanosensitive or stretch activated ion channels are diverse in tissue origin, and have been identified in the following tissues; aortic endothelial cells, the chorid plexus, corneal epithelium, neuroblastoma cells, osteoblasts, Ehrlich ascites tumor cells, opossum kidney cells, *Caenorhabditis elegans* (nematode) muscle cells, *Xenopus* oocytes, amphibian smooth muscle cells, frog diluting segments and basolateral proximal tubule, apical membrane of the *Necturus maculosus* (mudpuppy) renal proximal tubule (Sackin, 1995; Kizer, *et al.*, 1997; Marchenko & Sage, 1997). Although stretch activated channels are found in a variety of tissues and have some similar characteristics, they typically have a medium conductance and are nonselective for monovalent cations (Kizer, *et al.*, 1997).

Osteoblasts (cells responsible for synthesising new bone matrix proteins) are mechanosensitive cells that respond to chronic intermittent mechanical strain by cell reorganisation within the strain field as well as increasing their rate of mitosis. In addition to increasing bone matrix proteins (such as type I collagen), chronic intermittent mechanical strain leads to an increase in stretch activated cation channel open probability and increased sensitivity to activation by strain (Kizer, *et al.*, 1997).

Channel activity has been be studied extensively using a micropipette attached to the cell membrane by suction creating a tight seal, distension of the membrane patch sequestered in the pipette can be controlled by negative pressure (patch clamp technique). It is understood that electrical activity of the membrane, specifically, the opening of cation channels, is related to the degree of membrane stretch (Davies, 1995; Marchenko & Sage, 1997).

ENaC superfamily of ion channels

Most Na^+ -reabsorbing epithelia contain an amiloride blockable Na^+ -specific channel within their plasma membranes referred to as ENaC (Smith *et al.*, 1991; Canessa *et al.*, 1994; Kizer, *et al.*, 1997, Mobasheri, 1999). ENaC is a multimeric protein consisting of three homologus subunits, α, β, and γ (Rossier, *et al*, 1994; Roudier–Pujol, *et al.*, 1996), which serve to control cell volume as well as controlling the entry and reabsorption of Na^+ in a rate-dependent manner (Canessa, *et al.*, 1994). Activity of ENaC is upregulated by vasopressin, aldosterone, hormones involved in the maintenance of Na^+ balance, blood volume, and blood pressure (Rossier *et al.*, 1994; Canessa, *et al.*, 1994). The proteins of each subunit are 30 - 40% homologous that suggests they are derived from a common ancestor (Roudier–Pujol, *et al.*, 1996).

In *C. elegans*, the *mec-4, mec-10, deg-1,* and *unc-105*, a family that encodes members of the degenerin gene family, show a similar homology to the subunits of the vertebrate amiloride sensitive Na^+ -epithelial channel (Driscoll & Chalfie, 1991; Roudier–Pujol, *et al.*, 1996; Waldmann, *et al* 1996). Members of the ENaC superfamily span the membrane twice and have intracellular C- and N- termini with a large extracellular loop containing a conserved cystine-rich region (Mano & Driscoll, 1999). ENaC channels have been implicated in a variety of functions, such as mechanosensing, proprioception, pain sensation, gametogenesis, and epithelial Na^+ transport (Fyfe & Canessa, 1998; Mobasheri, 1999; Mano & Driscoll, 1999).

Molecular and genetic studies of touch avoidance in *C. elegans* have resulted in a molecular model for mechanotransducing complex (Tavernarakis & Driscoll 1997).

mec-4 and mec-10 are postulated to be involved in mechanical signal transduction in the touch reception system (Liu *et al*, 1996) and encode proteins hypothesised to be subunits of a mechanically gated ion channel that are related to subunits of the vertebrate amiloride-sensitive epithelial Na^+ channel (Tavernarakis & Driscoll 1997). Genetic mutations of degenerins in *C. elegans* cause hereditary neurodegeneration (Waldmann, *et al.*, 1996). Clones of mammalian degenerins from human and rat brain function as amiloride sensitive cation channels permeable to Na^+, K^+, and Li^+ (Canessa, *et* al., 1995; Waldmann, *et al.*, 1996). This channel is activated by the same mutations that cause neurodegeneration in *C. elegans*. Continually active muntants of mammalian degenerins cause cell death, like the hyperactive *C. elegans* mutants. This suggests that the gain of function of this novel ion channel in humans might be involved in forms of neuronal degeneration (Driscoll, 1996; Liu *et al.,* 1996; Waldmann, *et al.*, 1996; Roudier–Pujol, *et al.*, 1996).

1.5 Transcriptional regulation of Na^+K^+ -ATPase

The exposure of vascular endothelial cells to fluid mechanical forces can modulate the expression of many genes (examples illustrated in Table1.2, Davies, 1995, Khachigain *et al.*, 1997). In the previous sections, it was discussed that endothelial cells act as mechanotransducers, whereby the transmission of external force induces various cytoskeletal changes and second messenger cascades (Davies, 1995, Oluwole, 1997). This section will look at a break down of Na^+,K^+ -ATPase transcriptional regulation as well as discuss possible regulation of Na^+,K^+ -ATPase under conditions of fluid shear stress.

As discussed in Part I, the genes coding α-1 subunit of Na^+,K^+ -ATPase (*Atp1a1*) is expressed in virtually all tissues. The α-1 gene is ubiquitously expressed, and it shows typical characteristics of most housekeeping genes, i.e. the gene lacks the TATA-box and carries clustered GC-rich domains (Yu *et al.*, 1996) The α-1 subunit is also composed of *cis*-elements to which multiple factors bind (Kawakami *et al.*, 1994). Analysis of the 5'-sequential deletions revealed the *Atp1a1* regulatory element of the gene (ARE) is located (from the transcription initiation site) in the position –102 to –61 (Watanabe *et al.*, 1993; Kobayashi & Kawakami 1995, Kawakami *et al.*, 1996; Kobayashi & Kawakami 1997). The ARE acts as a positive regulatory element in most cells. Elimination of this site drastically reduces transcriptional activity by approximately 80-85% (Kobayashi & Kawakami 1995). It is understood that the core motif of activating transcription factor/cAMP response element (ATF/CRE) in the proximal region of the ARE is required for factor binding and the transcriptional activity of the *Atp1al* promoter (Ahmad & Medford, 1995; Kobayashi & Kawakami 1995 & 1997; Kobayashi *et al.*, 1997). Activating transcription factor-1/cAMP response element binding protein are members of the ATF/CREB family, which belong to the basic leucine zipper superfamily (bZIP, Kobayashi & Kawakami 1995 & 1997; Kobayashi *et al.*, 1997). The Activating transcription factor-1 and CREB are members of the bZIP family of transcription factors that bind to DNA as dimers. Both factors are expressed in a variety of tissues and are believed to play an essential role in some of the housekeeping genes (Ahmad & Medford, 1995; Kobayashi & Kawakami 1995 & 1997; Kobayashi *et al.*, 1997). Studies of the Na^+,K^+ -ATPase α-1 subunit gene have revealed that the gene is subjected to a variety of subtle regulation. The study of mechanisms regulating the rat α-1 subunit gene expression shows that its positive regulation is caused by Sp1

and other *trans*-acting factors which interact with the positive *Atp1a1* regulatory element of the gene (Yu, *et al.*, 1996). Kobayashi & Kawakami (1997) identify in the promoter region the ATF/CRE sites with adjacent GC box. Their findings indicate that both sites are essential for promoter activity. Electrophoretic mobility shift assay indicate that Sp1 and/or Sp3 bind to the GC box and ATF-1/CREB heterodimer binds to the ATF/CRE site. Since the ATF/CRE sites with adjacent GC box is highly conserved in mammalian the Na^+,K^+ -ATPase α-1 subunit genes in other promoters, it is understood that this element is critical for constitutive expression. The Sp1 and Sp3 are ubiquitous transcription factors that bind to the GC box in the zinc finger domains, and along with the assistance of other transcription factors, such as GATA-1, YY1, Stat1, SREBP, is required for Sp1 to function in regulating some promoters (Yu, *et al.*, 1996; Kobayashi & Kawakami, 1997).

Fluid shear stress is found to increase the activities of several different signalling kinases to modulate the phosphorylation of proteins in endothelial cells, for example the proteins in focal adhesion sites and proteins in mitogen-activated protein kinase pathways (Chien, *et al.*, 1998). Located downstream to signalling cascades, are transcription factors such as Sp1, AP1, NFκB, and Egr-1 that are in turn activated as a result of the original stimulus (Davies, 1995; Lin, *et al.*, 1997; Chien, *et al.*, 1998).

The focus of this study has been to examine the characteristics of the sodium pump in cultured endothelial cells. A qualitative approach has been used to examine Na^+,K^+ -ATPase distribution, along with a comparison of pump distribution to actin reorganisation under conditions laminar of fluid shear stress, as well as a semi-

quantitative analysis of pump protein up or down regulation via Western blotting techniques.

2. Methods and Materials II

2.1 Fluid shear stress

Bovine aortic endothelial cells [BAECs] passage 21 - 25 [p21-p25] at days 5 - 7 were used in the following experiments. BAECs were subjected to fluid shear stresses [FSS] of 15 dyn cm^{-2} and 50 dyn cm^{-2}. Changes in cell morphology were examined via immunocytochemical techniques under conditions of uniform laminar flow at different time intervals. In addition, whole cell lysates were collected for gel electrophoresis [see Part I, Chapter 3, and Appendix 1,2 and 4 for details on cell culture, immunocytochemistry and gel electrophoresis] after subjecting cells to uniform laminar shear stresses of 15 dyn cm^{-2} and 50 dyn cm^{-2}. The cells were grown on autoclaved 22 mm^2 borosilicate glass coverslips (BDH) seeded at a density of 2 $x10^4$ cells cm^{-2}, and also on 20 cm^2 glass microscope slides (BDH). Two chambers were specially constructed to fit the exact dimensions of the slides and coverslips, called respectively the *long* and *short* chambers. The chamber design was adapted from Viggers *et al.*, (1986).

The apparatus (Figure 1.9) comprises a conventional parallel plate, laminar flow chamber, within which fluid may be re-circulated under controlled conditions over live cell cultures. There are two fluid reservoirs for tissue culture medium, a peristaltic pumping system (Masterflex) and pressure ports/manometer system for determination of the shear stress over the cell culture.

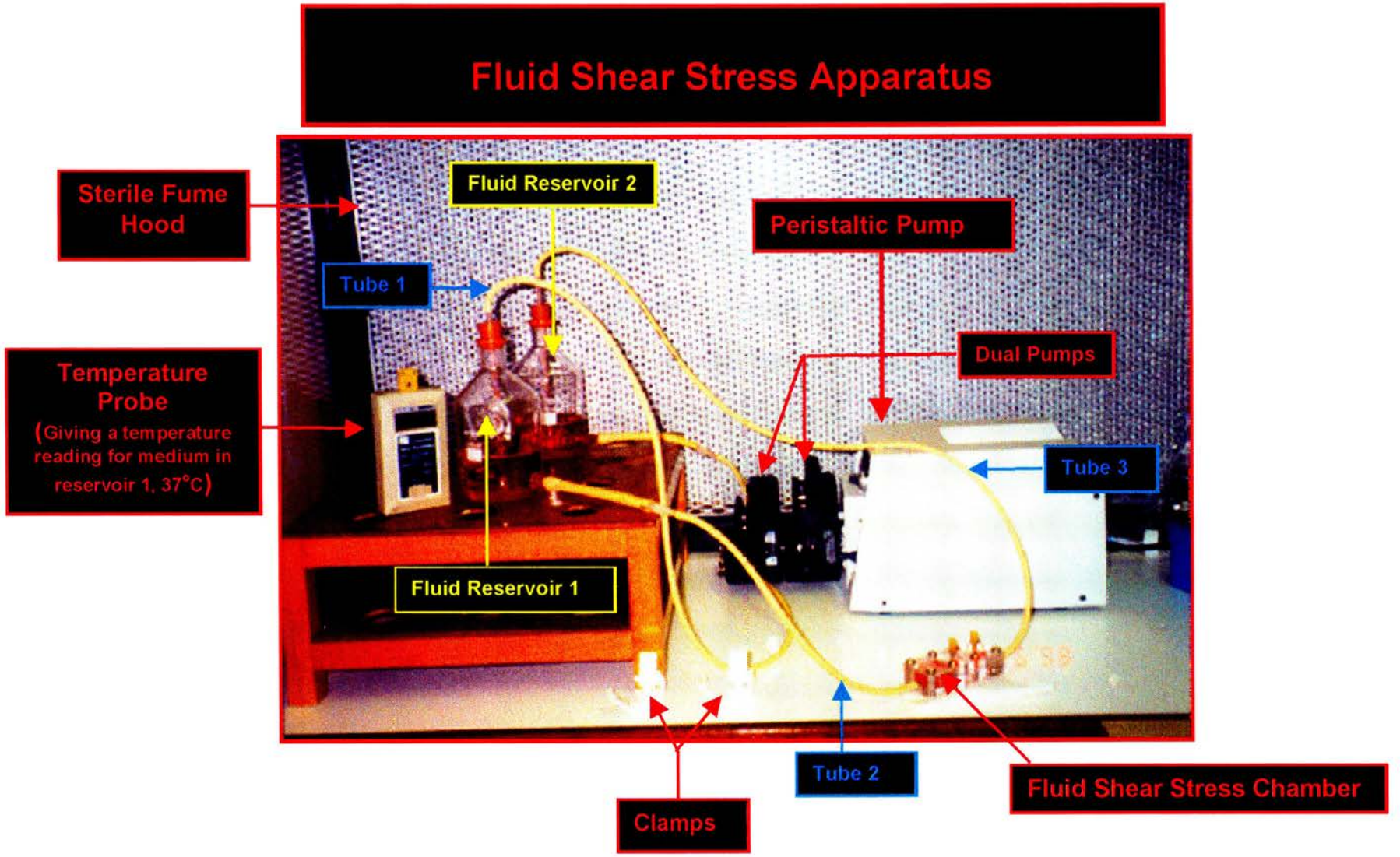

Figure 1.9 This photo illustrates the fluid shear stress apparatus used. Cell medium circulates from the bottom of fluid reservoir 1 though tube 2 and enters the fluid shear stress chamber. Exiting the chamber the medium flows into tube 3 and empties into the top of fluid reservoir 2. The medium then exits from the bottom reservoir 2 into tube 1, tube 1 runs through the peristaltic pump and empties back into the top fluid reservoir 1. This is a closed continuous system used in a sterile fume hood at 37°C. The complete and sterile medium in the reservoirs was supplemented with 25 mM Hepes buffer and was gassed with a mixture of 95% O_2 and 5% CO_2 to maintain the pH at 7.4.

The chamber, which is constructed of perspex, consists of two narrowly spaced plates, an upstream convergent entrance section with a recessed well where the cells are affixed to a coverslip, and an exit region. After the coverslip/slide is positioned in the well, the chamber is assembled and held together by screws.

The dimensions of each of the chambers are summarised in Table 1.4, and each of the chambers is shown in Figure 1.10.

	Chamber 2 (Long)	**Chamber 3 (Short)**
Channel width	2.3 cm	2.0 cm
1/2 Channel height	0.017 cm	0.0284 cm
Distance between pressure ports	8.0 cm	2.9 cm

Table 1.4 Dimensions of each of the experimental flow chambers. The Long chamber is designed for slides, whereas the short chamber is suitable for glass coverslips. Calibration data is discussed in Appendix Part II.

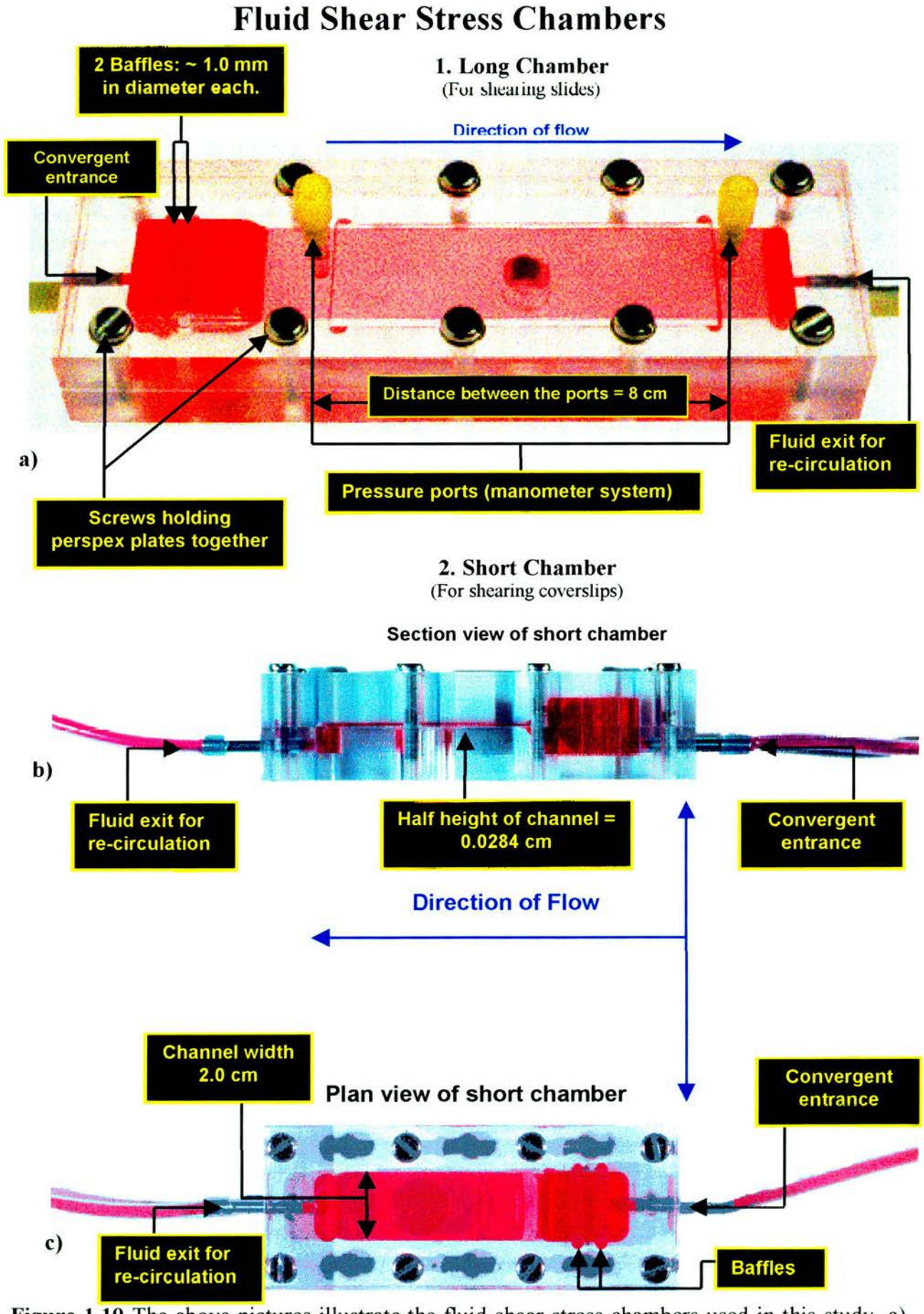

Figure 1.10 The above pictures illustrate the fluid shear stress chambers used in this study. a) illustrates the long chamber used for shearing cells grown on 19.76 cm^2 glass slides, whereas b) and c) illustrate the short chamber used for shearing cells grown on 22 mm^2 glass coverslips (shearing chambers adapted from Viggers *et al.*, 1986).

Over the range of experimental flow rates, flow within each of the chambers is always laminar (on the basis of the magnitude of the Reynolds number, *Re*; see Appendix II for details), and a parabolic velocity gradient may be determined between the plates (e.g. Matsuda and Fujiwara, 1993) as depicted in Figure 1.3 (Part II). Two small baffles with an array of 76 evenly spaced holes approximately 1.0 mm in diameter, which help to ensure the flow remains laminar, are located slightly upstream of the convergent entrance section. One chamber accommodated cells grown on coverslips for morphological studies (chamber 3, short chamber), and the other holds cells grown on slides used for biochemical analysis (chamber 2, long chamber). Measurements of the shear stresses (τ) generated by different flow rates were compared with values calculated from theory (τ^*). Fluid shear stress was determined experimentally from measurements of the absolute pressure gradient along the channel, using the relation:

$$\tau = \frac{(\rho g a h)}{l} \qquad 1.$$

where ρ is the medium density (g cm^{-3}), g is the acceleration due to gravity (cm s^{-2}), h is the difference in pressure (cm water) along chamber, a is the chamber half-height (cm) and l is the distance between pressure measuring ports (cm).

Theoretical fluid shear stresses were calculated from:

$$\tau^* = \frac{3.Q.V}{2.a^2.w} \qquad 2.$$

where Q is the volumetric flow, V is the dynamic viscosity (denoted μ in SI units), a is the channel half weight, and w is the channel width. The flow chamber was also equipped with two pressure ports drilled into the lid surface of the chamber connected to a manometer (Figure 1.10). The units of flow shear stress are dynes cm^{-2} (or dyn cm^{-2}). The chamber has been calibrated for practical purposes in terms of the pump speed (refer to Appendix II).

Supplemented culture medium is re-circulated through the chamber by a peristaltic pump (Figure 1.9). The pulsatile flow generated by the pump is damped as the fluid passses through flasks situated on either side of the chamber (Viggers *et al.*, 1986). The flasks also serve as reservoirs for the medium, and keep system pressures near atmospheric. They also act as a trap for bubbles. The apparatus is set up and used under sterile conditions in a flow hood at 37°C. Because the apparatus is a closed system, the medium is supplemented with 25 mM Hepes (Sigma) buffer in order to help maintain the pH of the complete and sterile DMEM.

3. Results

3.1 Effects of Uniform Laminar Flow

3.1a Effects of fluid shear stress on the distribution of Na^+,K^+ATPase

Figure 1.11 a and b, taken under low power (40x), illustrate the near-cobblestone appearance of sub-confluent cells grown in static culture, and stained with antibody to the α-1 subunit of Na^+,K^+ATPase. The actual appearance of the cells varies and shows inconsistencies in cell size and shape due to the fact that the cells are not fully confluent. Figure 1.11 c shows cells after they have been exposed to laminar flow for 4 hours at 50 dyn cm^{-2}. The photograph was taken under low power (40x) and shows the cells have re-oriented to become more elongate in their appearance and have aligned with the direction of flow. Figure 1.12 a illustrates the same field of view under oil immersion from the same slide preparation as Figure 1.11 b at greater magnification (x100). The α-1 staining of the sodium pump appears as stipple-like dots randomly distributed over the cell, showing no preferred pattern of distribution throughout the cell. However, there are strongly concentrated areas of staining between adjacent cells in areas of confluence (reviewed in Part I, Results section of Chapter 3.3). It is not possible from the view afforded with conventional microscopy to determine whether this is simply apical staining or true lateral staining on the cell periphery. However, it is suggested the density of staining reflects an integrated view of the distribution of pumps through the depth of the cell. In regions of non-confluence cells remain in contact via cytoplasmic processes on which stained sodium pumps are clearly visible.

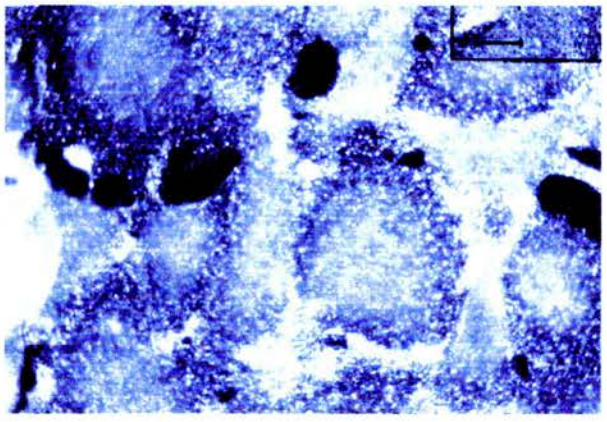

a)

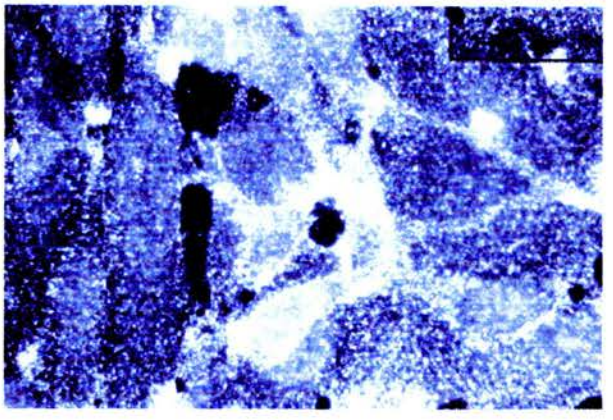

b)

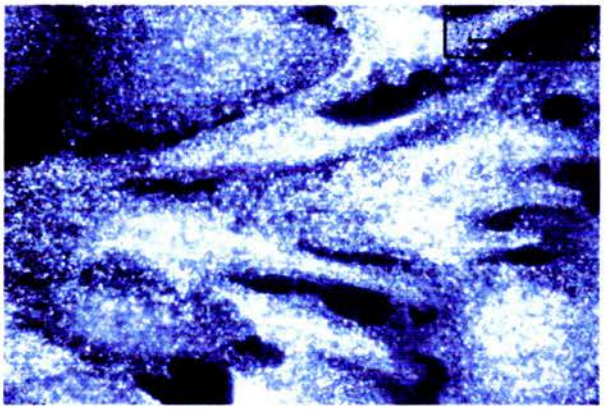

c)

Figure 1.11 a) and b) illustrate near-confluent cells grown in static culture; c) illustrates cells exposed to a laminar shear rate of 50 dyn cm^{-2} for 4 hours.

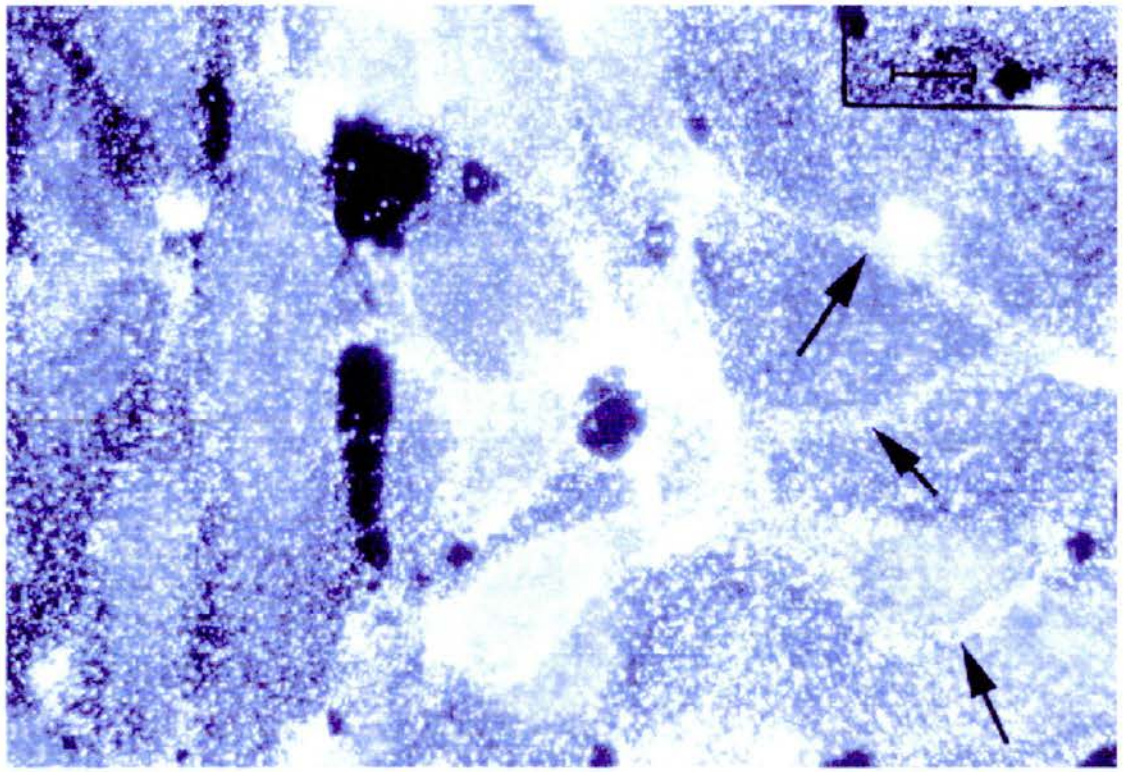

a)

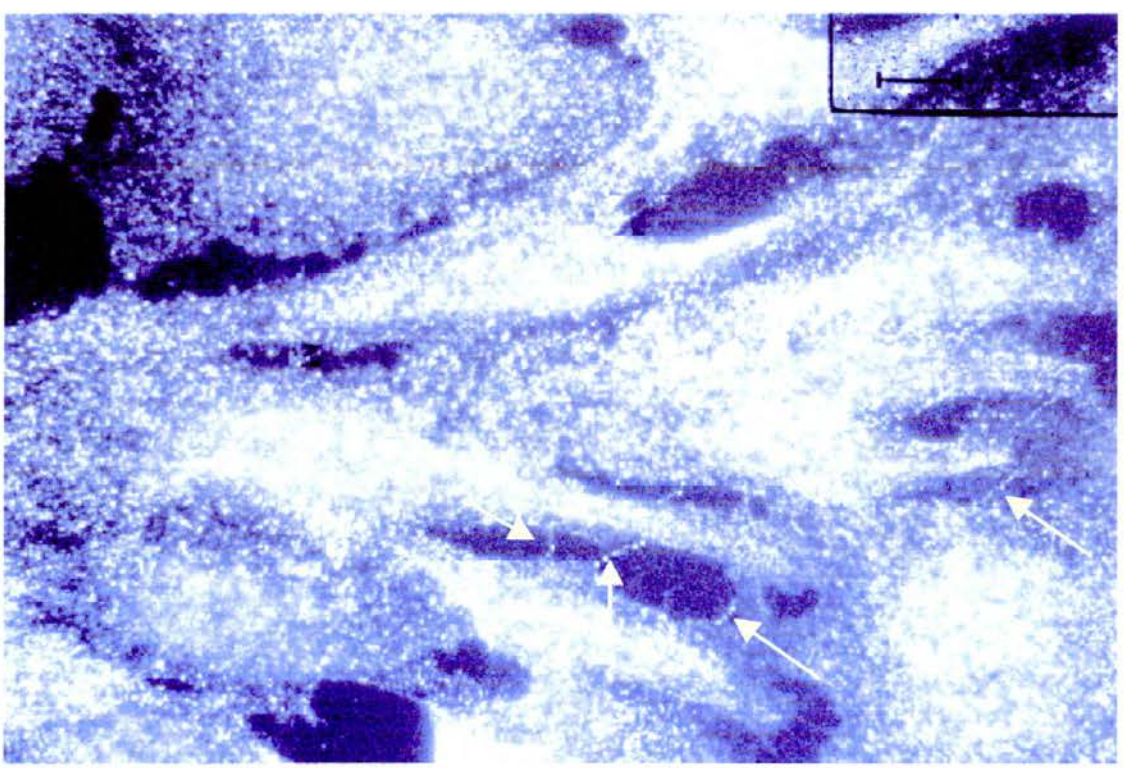

b) **Figure 1.12 a)** magnified (x100) view of 1.11b) illustrating α-1 subunit of Na^+, K^+ATPase distribution in cells grown in static culture, the black arrows illustrate areas of the α-1 subunit densely staining between adjacent cells; b) magnified view of 1.11c) illustrating redistribution of the α-1 subunit of Na^+, K^+ATPase in cells exposed to laminar shear stress of 50 dyn cm^{-2} for 4 hours, the yellow arrows point to areas of sodium pump distribution along cytoplasmic fibres.

Figure 1.12 b shows a magnified view (oil immersion; 100x) of Figure 1.11 c showing a redistribution of sodium pumps in response to flow. Sodium pumps are no longer seen concentrated in areas between adjacent cells but are still observed associated with filopodia. It is interesting to note that cytoplasmic processes still exist following distension and stretching of the confluent layer.

3.1b Actin staining

FITC labelled phalloidin was used to stain actin in BAECs (p8, d13) grown to a confluent monolayer (Review Chapter 3, Results section 3.32, Figure 3.13d). Figure 1.13 a (control) represents a typical actin stain in a static monolayer of cells and demonstres the polygonal shaped cells with dense peripheral bands of actin and random cytoplasmic stress fibre distribution. In response to laminar shear stress of shearing at 15 dyn cm^{-2} for 4 hours (Figure 1.13 b), there is a dramatic increase in the number of cytoplasmic stress fibres. These adopt a near-parallel alignment with their long axis in the direction of flow. This is associated with the disappearance of dense peripheral bands of actin. However the cells still remain in contact with one another via cytoplasmic processes observed under conventional fluorescence microscopy.

Confocal microscopic images show that the distribution of apical surface actin differs from actin at the basal surface. Figure 1.14 a illustrates the apical surface after shearing demonstrating the re-organisation of actin with near parallel arrays of stress fibres in the direction of flow. Confocal images of the basal surface shows actin stress fibres have yet to align with the direction of flow. Figure 1.14 b shows a transitional region, where the stress fibre arrangement is in a criss-crossed pattern oriented in different directions from apical to basal layers. Cell to

cell contacts also appear much stronger at the basal region than apical region. (All the actin photos in this section are courtesy of Dr. E. Flitney.)

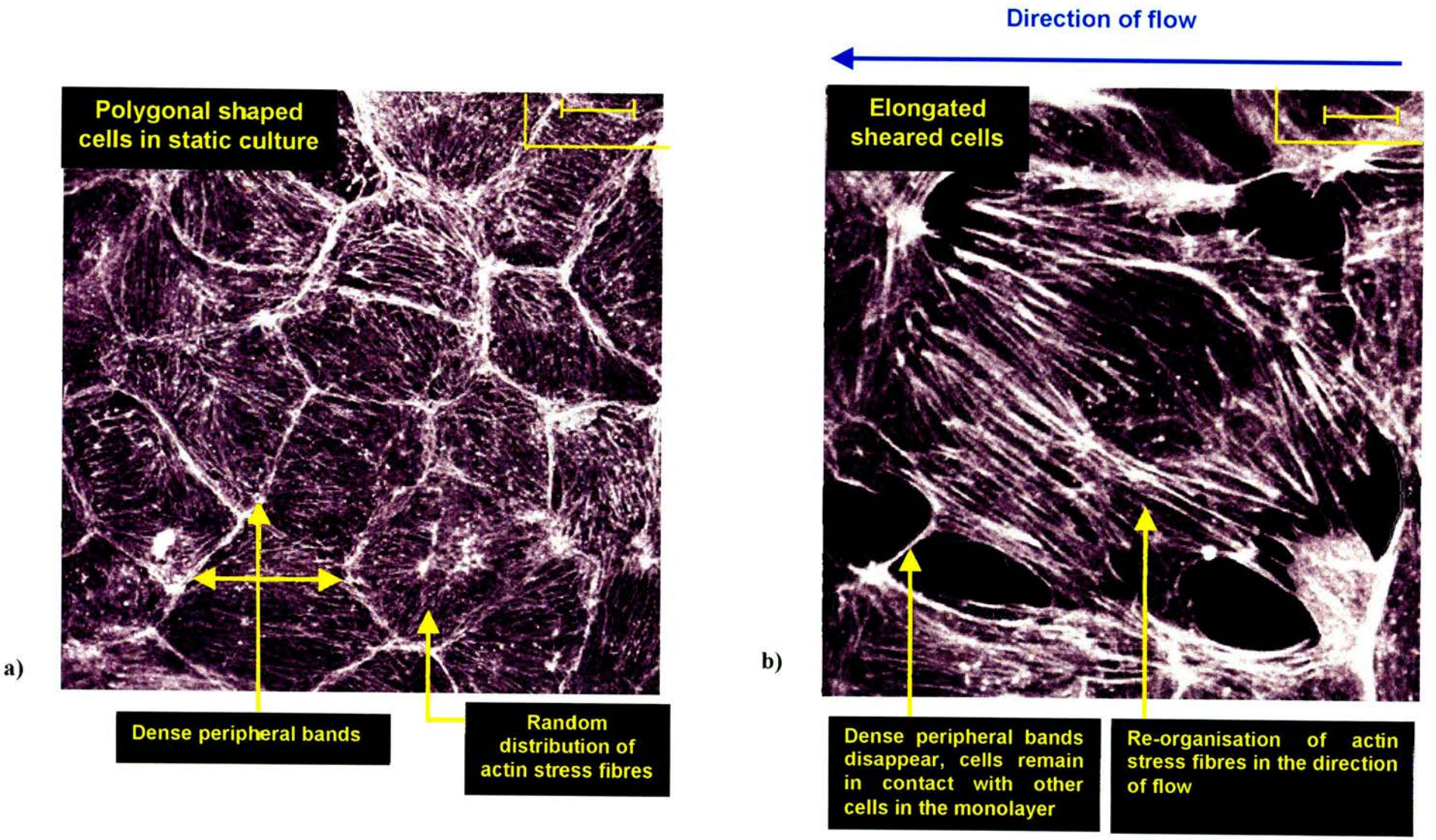

Figure 1.13 Confocal images of BAECs (p8, d13). Photograph a) illustrates a confluent monolayer of cells grown in static culture. The arrows point to dense peripheral bands and stress fibre distribution. Photograph b) illustrates shape change of the cells and F-actin re-organisation in BAECs (p8, d13) that have been sheared at 15 dynes cm^{-2} for 4 hours. In response to flow, the dense peripheral bands disappear and re-organise to create bundles of stress fibres (Photographs courtesy of Dr. E. Flitney). Scale bar = 10 μm.

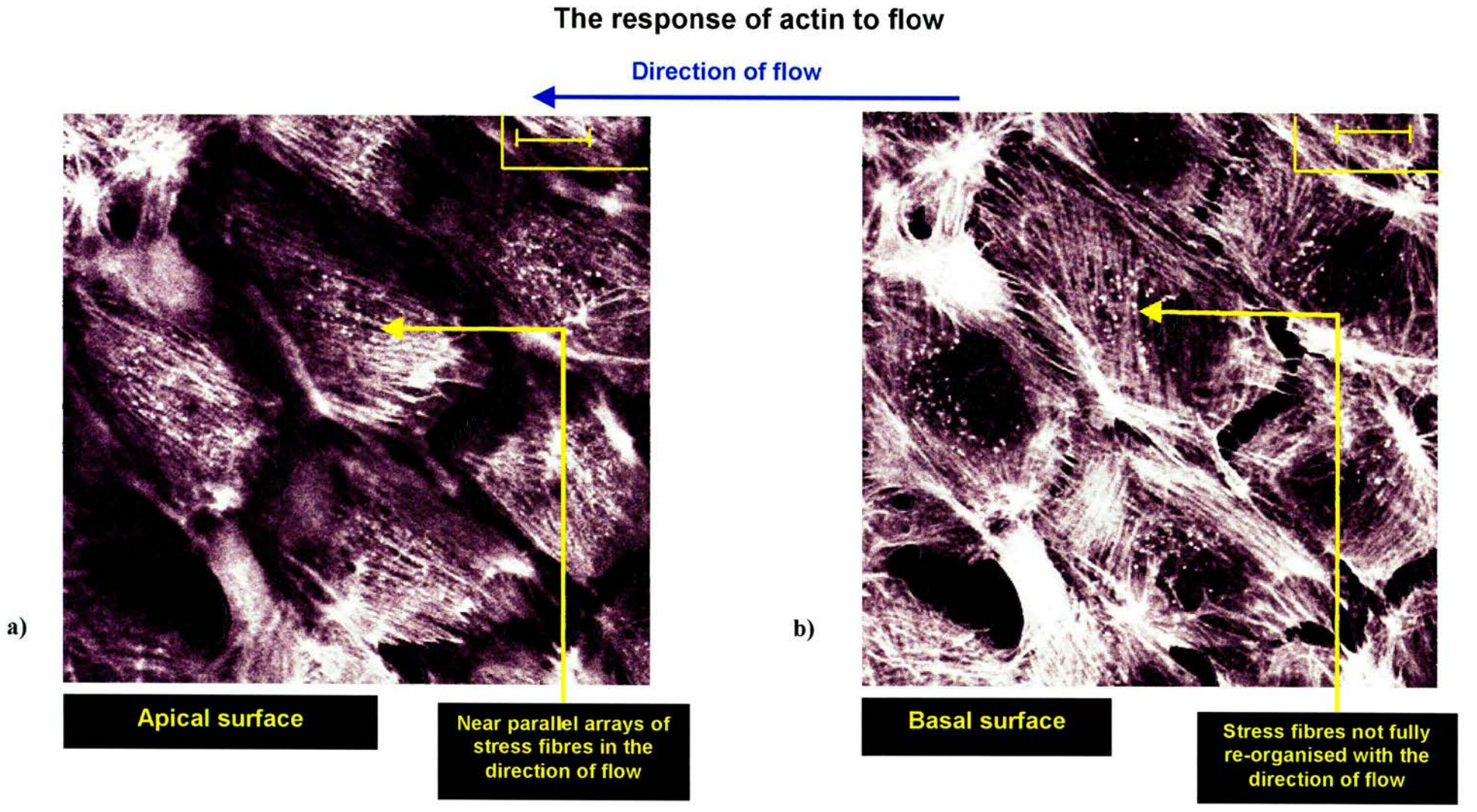

Figure 1.14. Confocal images showing actin stress fibres of BAECs (p8, d13: clonetics) in response to flow. Photograph a) and b) are cells from the same field of view, with the arrows in both photographs pointing to the same cell. Photograph a) illustrates the apical layer of the cell monolayer after a shearing rate of 15 dynes cm^{-2} for 4 hours. Under these conditions actin at the apical layer re-organises in the direction of flow, and dense peripheral bands disappear. Taking micron slices through the cell photograph b) illustrates stress fibres at the basal layer not fully re-organised, with dense peripheral bands are no longer visible. (Photographs courtesy of Dr. E. Flitney). Scale bar = 10 μm.

3.2 Western Blot analysis of sheared cells

Western blot analysis was carried out on sheared and unsheared cells using a monoclonal antibody to the α-1 subunit of Na^+,K^+, ATPase. BAECs were grown on glass microscope slides and split into two groups. One group was exposed to 15 dyn cm^{-2} and the other to 50 dyn cm^{-2} for periods up to 16 hours. Cold lysates from each group were prepared after shearing cells for different time intervals. SDS polyacrylamide gel electrophoresis (6%) was used to separate the proteins after exposure to laminar flow. In both experiments membranes were blocked in 15% Marvel (see page 60) for one hour at room temperature and probed using a monoclonal antibody for the α-1 subunit of Na^+K^+ATPase. Membranes were incubated overnight at 4°C using the primary at 1:100. The secondary antibody (SAMP) was used as at 1:1000 for one hour at room temperature.

Figure 1.15 illustrates a Coomassie blue stain used to check even loading in each well. Obvious changes appear in the molecular weight ranges of 43 KDa and 56 KDa which most likely correspond with actin and vimentin indicated by 'A' and 'B', respectively. In both sets of lysates the intensity of the banding pattern is too weak in the approximate molecular weight range of Na^+K^+ATPase (~112KDa). It is difficult to establish differences in protein levels in each set or if there is a disparity between the two sets as a consequence of different flow velocities. Time course analysis via ECL of Na^+K^+ATPase at the two different shearing rates reveals slight visual

BAEC protein expression after exposure to laminar flow

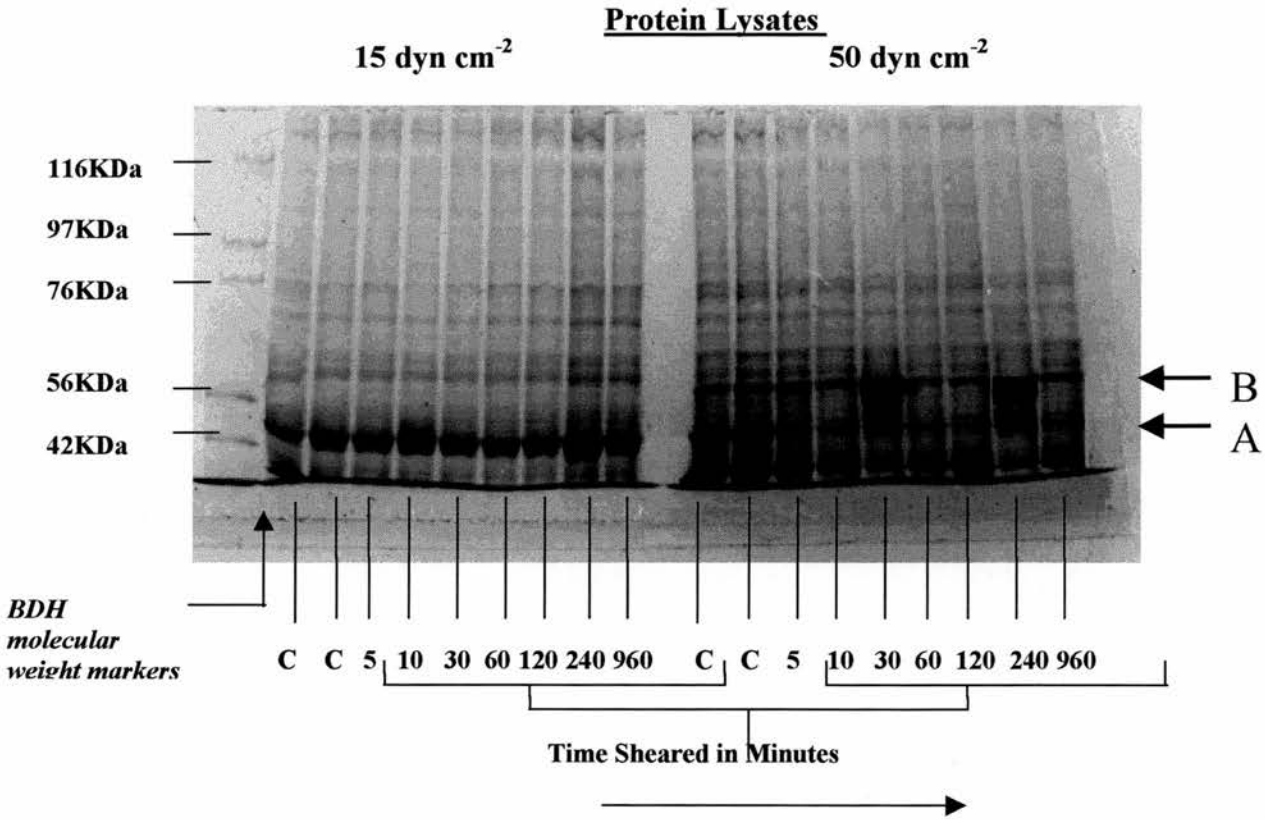

Figure 1.15 Example of a Coomassie blue stain of a 6% SDS polyacrylamide gel. BAECs (p14, d 4) show the difference in protein expression after shearing at 15 dyn cm^{-2} and 50 dyn cm^{-2} at different time intervals. Cold lysates were collected and 20 μg per well was loaded in the first set (15 dyn cm^{-2}), and 18 μg per well in the second set (50 dyn cm^{-2}). The 'A' arrow is ~43KDa, corresponding with actin whereas the arrow 'B' is ~56KDa, vimentin.

ECL:Na^+,K^+-ATPase sheared at 15 dyn cm^{-2}

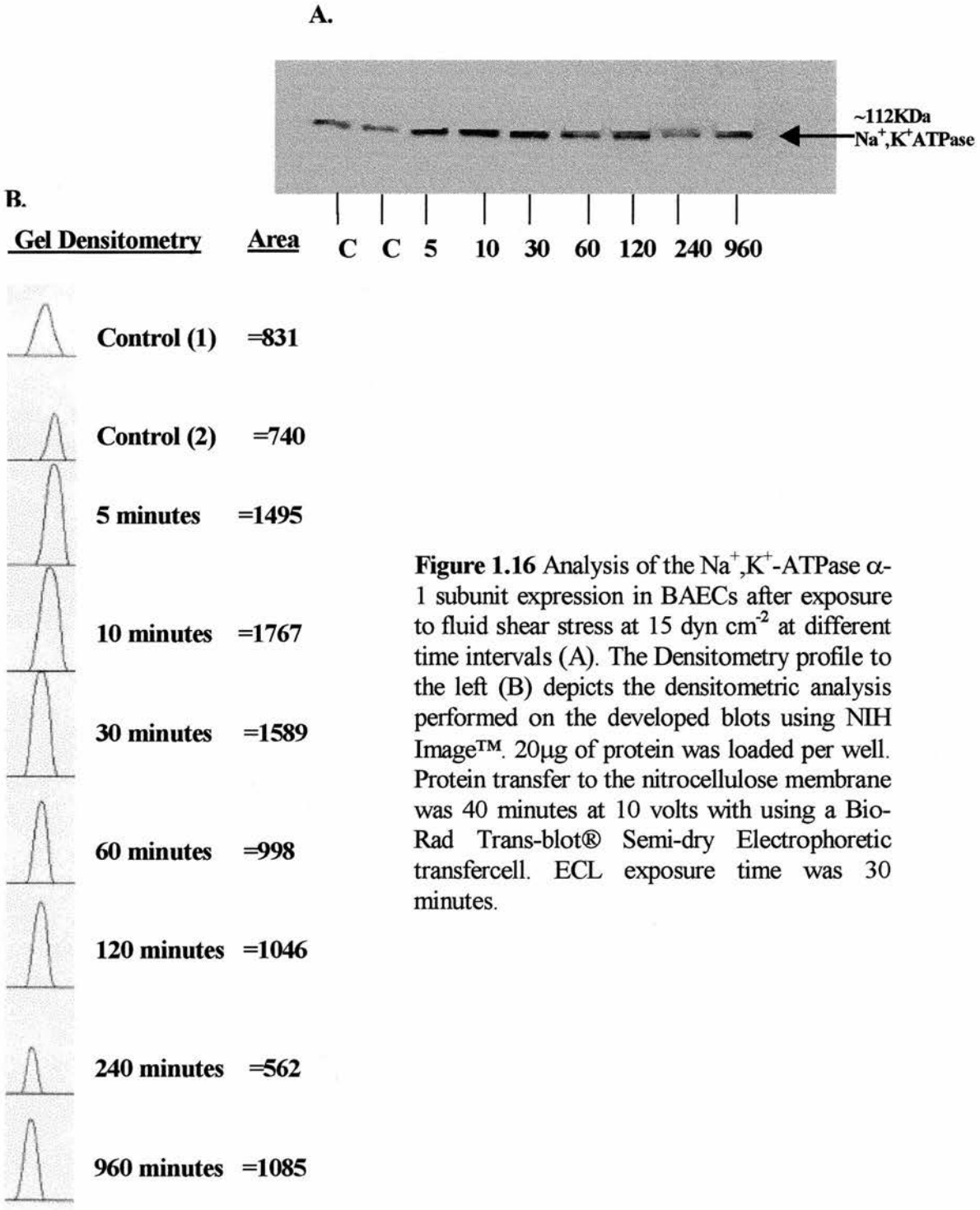

Figure 1.16 Analysis of the Na^+,K^+-ATPase α-1 subunit expression in BAECs after exposure to fluid shear stress at 15 dyn cm^{-2} at different time intervals (A). The Densitometry profile to the left (B) depicts the densitometric analysis performed on the developed blots using NIH Image™. 20μg of protein was loaded per well. Protein transfer to the nitrocellulose membrane was 40 minutes at 10 volts with using a Bio-Rad Trans-blot® Semi-dry Electrophoretic transfercell. ECL exposure time was 30 minutes.

Figure 1.17 illustrates cell lystates sheared at 50 dyn cm^{-2} showing no overall change in the trend with time, except perhaps for a marginal decrease at 960 minutes.

Figure 1.18 compares the effects of flow on protein expression for two differing laminar shear stresses (15 and 50 dyn cm^{-2}). Quantitative analysis obtained by gel densitometry expressed as a percent of the control level is plotted against time for each experiment. The data show in broad terms that higher shear stresses produce a greater Na^+,K^+ATPase α-1 subunit expression in comparison to lower stresses. This is observed for all the time points except for 10 minutes. Statistical analysis, however, reveals that there is **no** significant difference between the two sample groups (ANOVA: df=1, F=7.35×10^{-5}, P=0.993) and therefore the inference is that greater shear stress does not produce a corresponding greater effect. The general trend at the higher stress shows an incremental rise in protein levels relative to the percent of the control, with a maximum level at (*ca.* 183%) at 60 minutes followed by a general decrease with time. A similar bell-shaped trend is noticeable at the lower stress, demonstrating an initial increase in protein that then decreases to the level of the control at 60 minutes and 120 minutes. The trend shows a further decrease to below the level of the control at 240 minutes (*ca.* 70%) rising back up to the level of the control in the last time point (960 minutes). However statistical analysis of the temporal changes shows **no** statistical correlation of the expression of protein levels over time (df=7, F=0.396, P=0.897). This was confirmed for the 50 dyn cm^{-2} at 60 minutes time point (as it shows the largest change with respect to the control) using a two-tailed *t*-test on untransformed data (df=8, F=1.04, P=0.100).

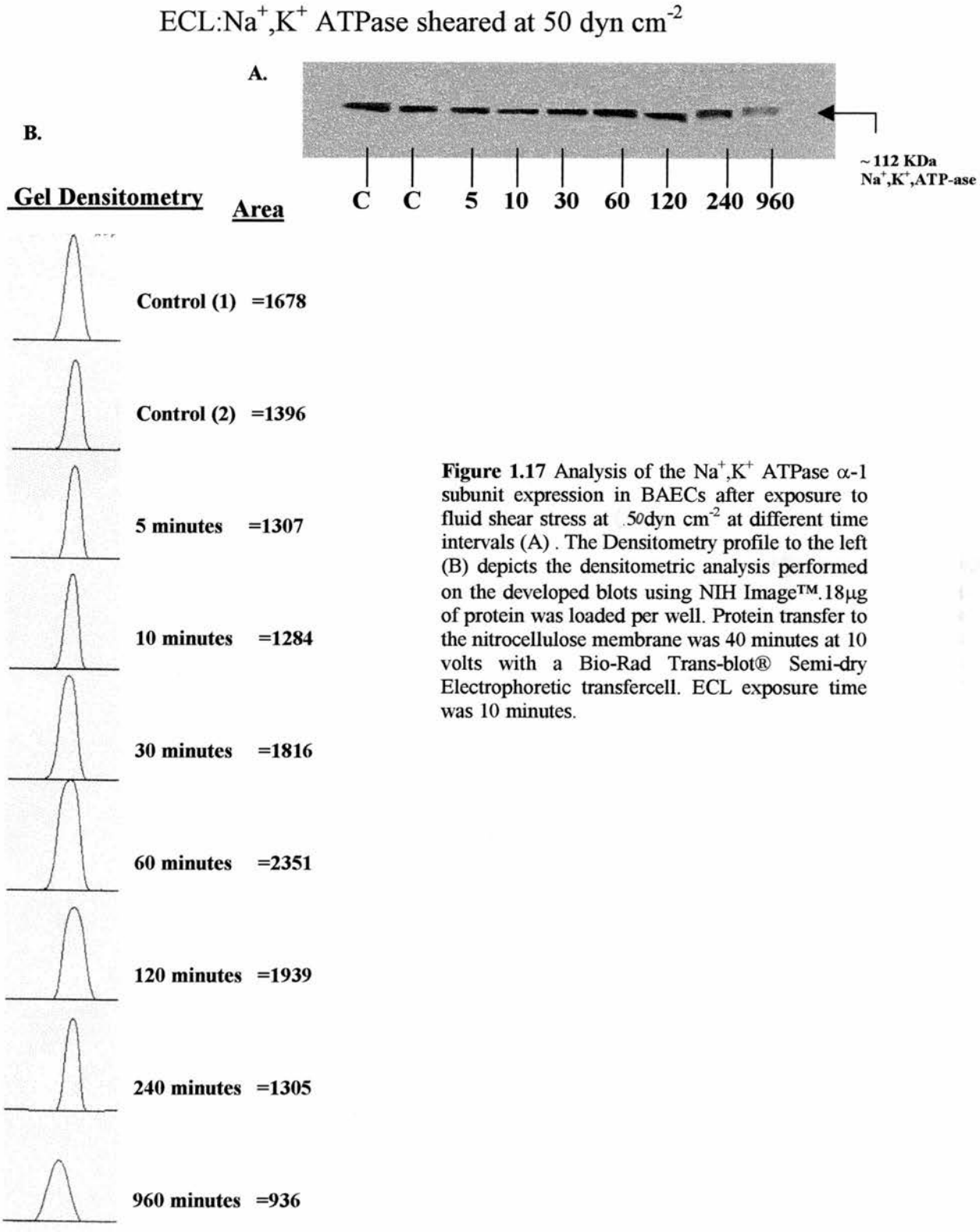

Figure 1.17 Analysis of the Na^+,K^+ ATPase α-1 subunit expression in BAECs after exposure to fluid shear stress at 50dyn cm^{-2} at different time intervals (A) . The Densitometry profile to the left (B) depicts the densitometric analysis performed on the developed blots using NIH Image™.18μg of protein was loaded per well. Protein transfer to the nitrocellulose membrane was 40 minutes at 10 volts with a Bio-Rad Trans-blot® Semi-dry Electrophoretic transfercell. ECL exposure time was 10 minutes.

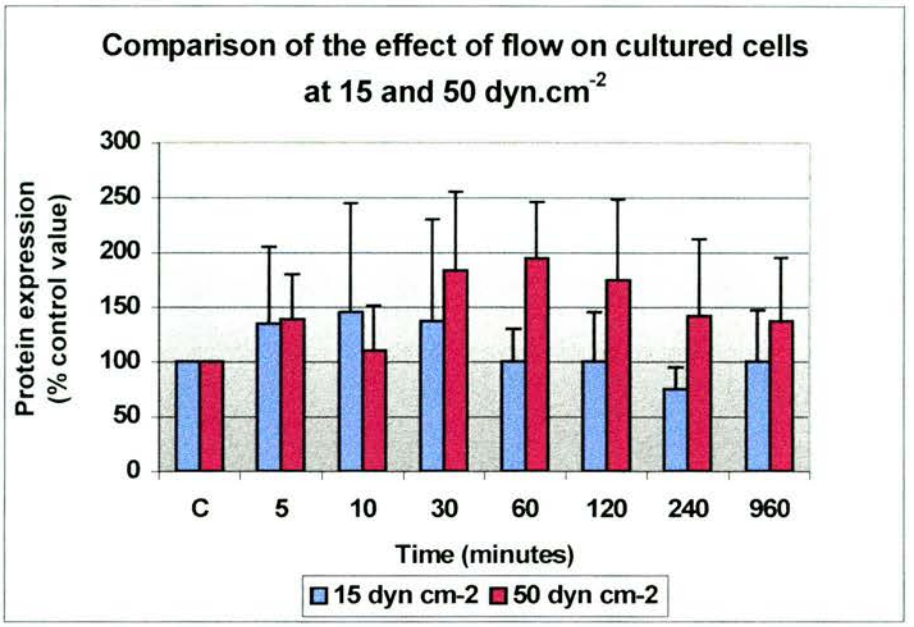

Figure 1.18 The effects of flow on cultured cells at different shear stresses over time (error bars are ± 1 standard deviation; C = control).

BAECs were sheared for a series of different time intervals and different shear stresses 15 and 50 dyn cm^{-2}. Before the cells (sheared on slides) were lysed with cold buffer the slides were returned to their original culture medium used to grow the cells (once slides were in the shearing apparatus the pH of the medium was adjusted and petri dishes stored at 37°C). After shearing the cells incubated for 8 hours at 37°C under static conditions in an attempt to check for elevated levels of protein due to the possibility of activating gene transcription. Protein estimations revealed low levels of protein collected in the samples, most likely due to cell detachment either during the actual shearing process or as a result of environmental change back to static culture. The two sets of protein were run on a 6% polyacrylamide gel. Due to the maximum well capacity (25 µl) 11µg of protein was loaded in the first set 15 dyn cm^{-2} + 8 hours incubation period and only 8µg of protein to the second set 50 dyn cm^{-2}. The results shown in Figure 1.19 at 15 dyn cm^{-2} + 8 hours illustrate electrophoretically separated protein

bands on a typical Coomassie blue stain. The gel does not illustrate any unique patterns of protein expression as a result of the 8 hour incubation period after shearing.

In Western blot analysis trial and error revealed that the optimal conditions when probing for the α-1 subunit was to use the primary antibody at a concentration of 1:200 overnight at 4°C, to block for 1 hour at room temperature with 15% Marvel and to use the secondary antibody (SAMP) at 1:500 for 2 hours at room temperature. Probing for the α-1 subunit of Na^+K^+ ATPase did produce a signal for the 15 dyn cm^{-2} + 8 hour incubation, but proved to be problematic in the 50 dyn cm^{-2} + 8 hour set due to insufficient levels of total protein collected from the lysate. The total well capacity for the standard sized combs used to create the wells in the polyacrylamide gel is a maximum of 25μl, yielding a total of 8μg of protein per well. To correct this problem, larger combs were used to enabling a larger quantity of sample lysate to be loaded. 35μl of protein sample was loaded per well for the 50 dyn cm^{-2} + 8 hour incubation sets providing a total of 11μg of protein per well, consistent with the 11μg of protein loaded per well in the 15 dyn cm^{-2} + 8 hour incubation lysate sets.

BAEC protein expression after exposure to laminar flow + 8 hours

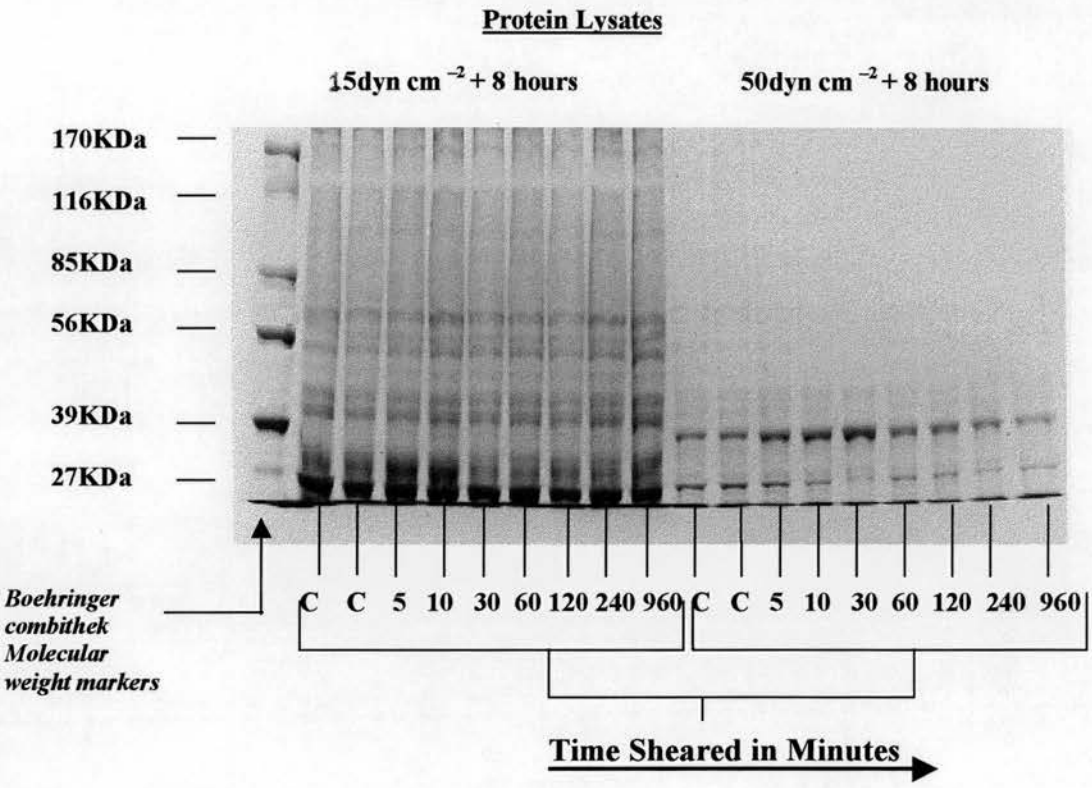

Figure 1.19 Example of a Coomassie blue stain of a 6% SDS polyacrylamide gel. BAECs (p21, d 4) show the difference in protein expression after shearing at 15 dyn cm^{-2} and 50 dyn cm^{-2} at different time intervals Before the cold lysates were collected the cells were returned to static conditions and incubated for 8 hours at 37 C in cell culture medium. 11µg of protein was loaded per well in the first set (15 dyn cm^{-2}), and 8µg of protein per well was added to the second set (50 dyn cm^{-2}).

Densitometry analysis of ECL results showed a overall trend of down regulation of protein α-1 subunit protein with respect to the controls (Figure 1.20).

The signal for the α-1 subunit of the Na^+,K^+ATPase for the 50 dyn cm^{-2} + 8 hour incubation was very weak. However, the result attained from densitometric measurements showed an upregulation from the control with peak intensity at 30 minutes (Figure 1.21).

A comparison of the two shearing rates after an 8-hour incubation period is given in the bar graph in Figure 1.22. In this example, 50 dyn cm^{-2} shear rate plus 8-hour incubation produced a greater overall protein expression and there is a statistically significant difference between the two sample sets (two-way ANOVA without replication: df=1, F= 32.85 P=0.001). Quantitative data obtained by gel densitometry readings expressed as a percent of the control level was plotted against time for each experiment. Here again, the data show in broad terms that higher shear stresses produce a greater Na^+,K^+ ATPase α-1 subunit expression in comparison to lower stresses. This is observed for all time points, and it is also demonstrated that there is a statistical difference between the time points (df=7, F=4.47, P=0.033).

ECL:Na^+,K^+ ATPase sheared at 15 dyn cm^{-2} + 8 hour incubation at 37°C

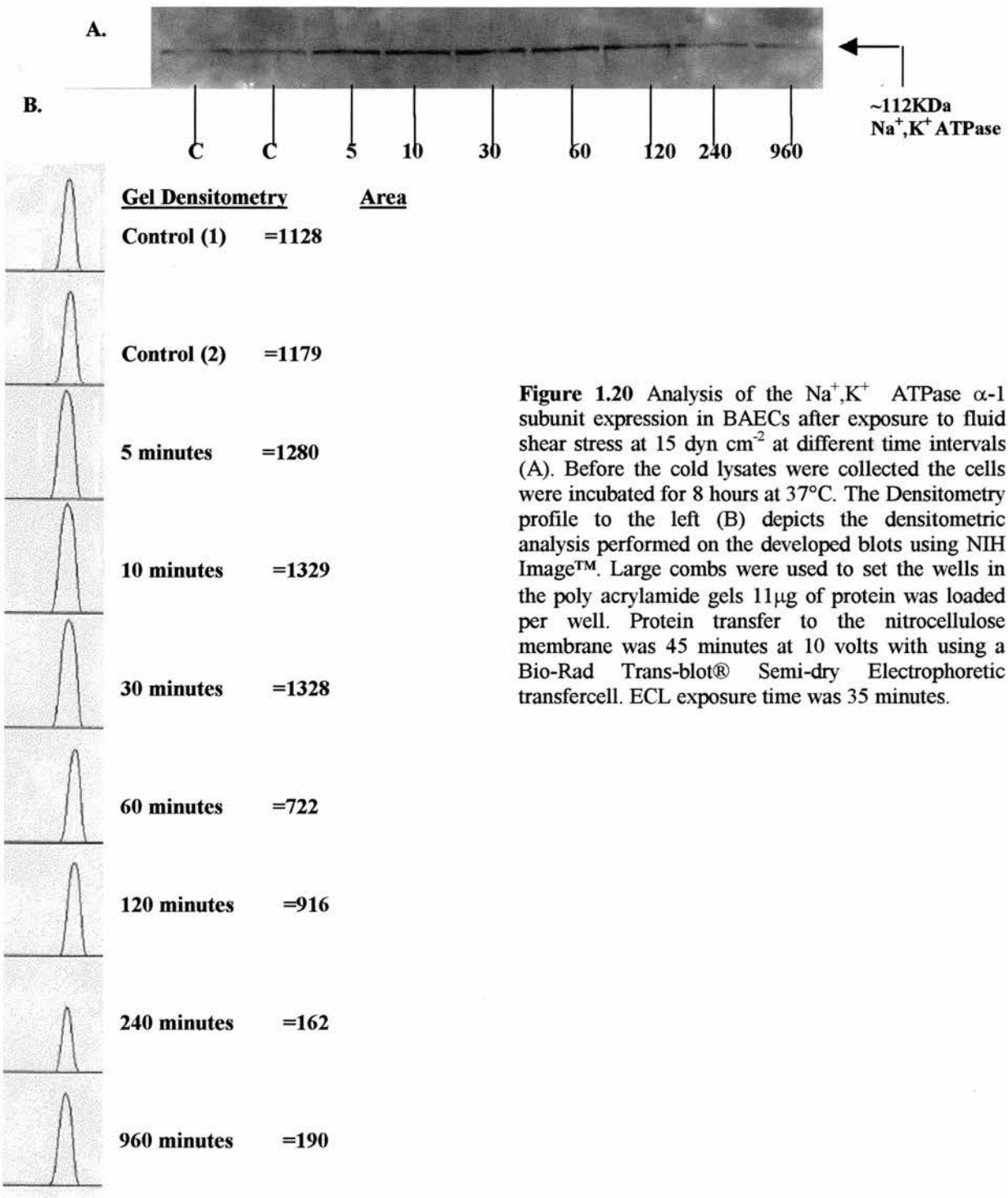

Figure 1.20 Analysis of the Na^+,K^+ ATPase α-1 subunit expression in BAECs after exposure to fluid shear stress at 15 dyn cm^{-2} at different time intervals (A). Before the cold lysates were collected the cells were incubated for 8 hours at 37°C. The Densitometry profile to the left (B) depicts the densitometric analysis performed on the developed blots using NIH Image™. Large combs were used to set the wells in the poly acrylamide gels 11μg of protein was loaded per well. Protein transfer to the nitrocellulose membrane was 45 minutes at 10 volts with using a Bio-Rad Trans-blot® Semi-dry Electrophoretic transfercell. ECL exposure time was 35 minutes.

ECL:Na^+,K^+ ATPase sheared at 50 dyn cm^{-2} + 8 hour incubation at 37°C

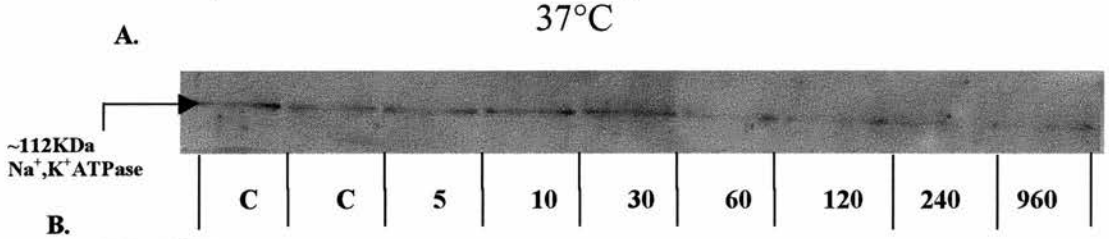

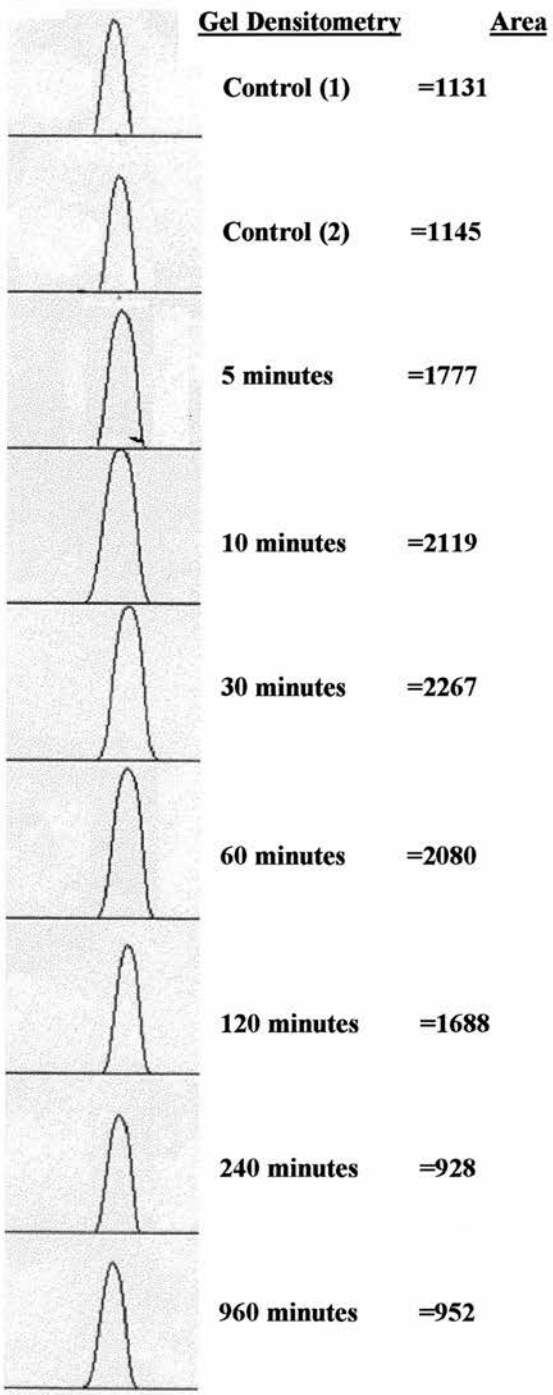

Figure 1.21 Analysis of the Na^+,K^+ ATPase α-1 subunit expression in BAECs after exposure to fluid shear stress at 50 dyn cm^{-2} at different time intervals (A). Before the cold lysates were collected the cells were incubated for 8 hours at 37°C. The Densitometry profile to the left (B) depicts the densitometric analysis performed on the developed blots using NIH Image™. Large combs were used to set the wells in the poly acrylamide gels 11μg of protein was loaded per well. Protein transfer to the nitrocellulose membrane was 45 minutes at 10 volts with using a Bio-Rad Trans-blot® Semi-dry Electrophoretic transfercell. ECL exposure time was 1 hour.

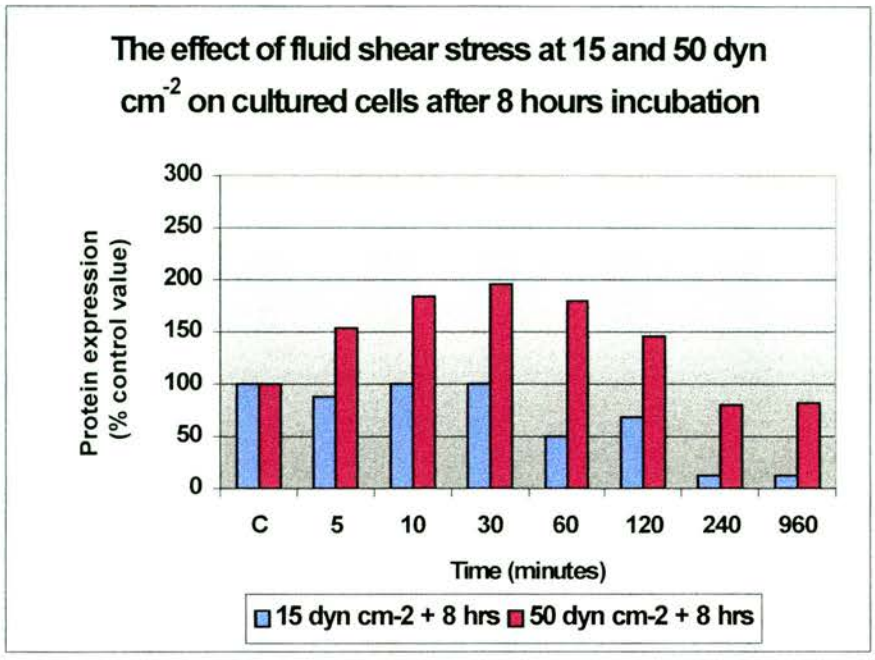

Figure 1.22 A comparison of BAECs sheared at 15 and 50 dyn cm $^{-2}$ plus 8 hour incubation at 37°C.

The data shows a bell shaped trend with a maximum effect (*ca.* 199%) at 30 minutes plus 8-hours relative to the percent of the control group. The 10 and 60 minute plus 8-hour time point have a comparable effect registering densitometry readings (expressed relative to the percent of the control) of *ca.*186% and 182 % respectively. 5 and 120 minutes plus 8-hours incubation are up-regulated from the control in a similar incremental fashion illustrating protein levels of *ca.* 156% and 149%. Time points 240 and 960 plus 8-hour incubation in contrast are down-regulated from the control, but are comparable to each other expressing levels at *ca.* 81.5% and 84%.

The effect at 15 dyn cm^{-2} plus 8-hour incubation shows no effect above the level of the control for any of the time points. There is a small initial decrease at 5 minutes, however 10 and 30 minutes plus 8-hour incubation rise to the

approximate level of the control with both values at approximately 98% relative to the control. At 60 minutes plus 8-hour incubation there is a notable down-regulation to approximately half the level of the control (*ca.* 53%) which then displays a marginal increase to *ca.* 68% at 120 minutes. The last time points 240 and 960 minutes plus 8-hours are well below the control levels having a reading of 12% and 14%, respectively.

4. Discussion

The influence of fluid stresses on cultured endothelial cells has been studied extensively, and it is known that a great many aspects of cell function are influenced by flow stresses (Davies, 1995). A synthesis of the research literature to date (refer to Introduction, Part II) shows that a large volume of work has been done, although little specifically on the sodium pump mechanism with respect to fluid stress. The experiments conducted in this study arose due to an opportunity provided by a new research initiative to understand the effect of shear stress on vimentin intermediate filaments, and fluid stress-induced gene regulation in bovine endothlial cells (Flitney, 1996, unpublished report). Consequently, the experiments are very preliminary in nature. However, they reveal some interesting and novel results, as little is currently known about Na^+·K^+ATPase in relation to fluid shear stress in cultured endothelial cells, and they serve as a useful springboard for future studies in this area.

In this study cultured BAECs were subjected to fluid shear stress by using a parallel plate flow chamber system adapted from Viggers *et al.,* (1986) (Figure 1.10). Parallel plate chambers offer practical advantages over alternative methodologies (e.g. cone and plate systems such as used by Garcia, 1992). They are simpler to manufacture and relatively cheap to construct, and ideal for use with cells on slides or coverslips. They are also relatively easy to calibrate (Appendix 1). A small chamber was used to accommodate coverslips on which cells were exposed to laminar flow at shearing forces of 15 and 50 dynes cm^{-2} for varying time intervals. Cells were then processed for immunofluorescence studies. A larger chamber was used to hold microscope slides in order to grow a

sufficient number of cells to harvest for Western blot analysis (Figure 1.10). The chambers were part of a closed, continuously re-circulating tissue culture medium (maintained at 37°C), driven by a peristaltic pump system (Figure 1.9). This study has demonstrated the utility of laminar flow chambers in studies of the effects of fluid stress influence on bovine aortic endothelial cells.

In the first group of experiments BAECs were labelled for the α-1 subunit of Na^+,K^+ATPase in cells grown in static culture. The control group showed a typical pump staining in day 4 BAECs (Figure 1.11) as previously demonstrated (Chapters Three and Four). Cells were exposed initially to shearing forces of 50 dynes cm^{-2} for 4 hours. Cell re-organisation and alignment in the direction of flow was observed, which previous studies have shown (e.g. Davies, 1995; 1997) and is not unexpected. However, under these shearing conditions there appeared to be a marked change in Na^+,K^+ATPase distribution, in which pumps redistribute from the circumferential regions of cells to become more uniformly distributed throughout the intracellular cytoplasmic region. Redistribution of Na^+,K^+ATPase under conditions of fluid shear has not previously been documented to the author's knowledge. Mechanisms surrounding this phenomenon can therefore, at best, be only speculative. Distribution of Na^+,K^+ATPase in regions of confluence in BAECs grown in static culture show peripheral localisation (Figure 1.12 a), which may simply be a function of a triggering process as subconfluent cells establish cell-cell contacts and attain confluency (Flitney, pers. comm.). Previous work (Figure 3.6 a and b; Chapter 3) clearly shows a non-uniform pattern of staining throughout the cytoplasm for non-confluent cells. The nature or biochemistry of such a triggering process is, as

yet, undiscovered for BAECs. However, in MDCK cells and kidney proximal tubule cells, Morrow *et al.*, (1989) report the strong co-localisation of fodrin and Na^+,K^+ATPase at the basolateral domain only after confluence is achieved. At their own admission, however, their results are circumstantial and 'the molecular mechanisms underlying these changes are poorly understood'.

An interesting association of cytoskeletal re-organisation and Na^+,K^+ATPase with levels of cellular ATP was noted by Mandel *et al.*, (1994) and Bacallao *et al.* (1992). They describe a rapid internalisation of Na^+,K^+ATPase and loss of cortical actin network following ATP depletion induced by treating cells with antimycin and deoxyglucose. These treatments inhibit oxidative and glycolytic energy metabolism. Similar observations have been reported by Rodriguez-Boulan and Nelson (1989). Molitoris *et al.*, (1991, 1992) found that much of the enzyme redistributed to the apical membrane during depletion of ATP, which supports the qualitative observations reported using fluorescence microscopy in this study. Whilst all cells try to maintain cellular homeostasis (Hochachka and McClelland, 1997), particularly with respect to ATP, there is evidence to suggest that under shear stress endothelial cells release ATP (e.g. Milner *et al.*, 1992; Bodin *et al.*, 1992). A logical deduction from these studies is that redistribution of Na^+,K^+ATPase under fluid stress might be, in part, an indirect function of ATP loss as well as the direct influence of the shear forces on the actin cortical network. In other words, fluid shearing results in release of ATP from cells which then produces a loss of cortical actin network which induces internalisation of Na^+,K^+ATPase. Continuous loss of cellular ATP to the recirculating shearing medium in our experimental setup would initiate a positive feedback if the loss of ATP from cells is sufficiently high, since it is known that

exogenous ATP influences the synthesis of new pumps (Aiton and Lamb, 1984). This is unlikely given the ratio of cell numbers to medium volume in the apparatus. Clearly, many different biochemical or biomechanical processes are involved in the process of redistribution and current research has provided no clear answers. Bacallao *et al.* (1992), for example, expressly admit that in spite of their experimental observations 'the mechanisms underlying the re-organisation of the actin network during ATP depletion are unknown' and 'the mechanism [for dissociation of Na^+,K^+ATPase from the cytoskeletal network] is unclear'. An experimental methodology to examine this specific hypothesis and to separate the various factors would be to conduct shearing experiments and measure dissolved ATP in the culture media through time.

Chapter Four remarked on the association of Na^+,K^+ATPase and actin, in which it was ascertained that there is not a direct co-localisation of Na^+,K^+ATPase and actin. However, it is known that there is interaction between the α-1 subunit and actin via specific cytoskeletal components (e.g. actin and spectrin co-localises with the third cytoplasmic domain (CD3) of Na^+,K^+ATPase α-1 subunit in epithelial cells and in the rat brain). With knowledge of the re-organisational effect of fluid shear stress on the cell membrane and underlying cytoskeletal components (Davies, 1995; Ballerman *et al.*, 1998), it would have been interesting to see a change of Na^+,K^+ATPase distribution in the direction of flow, or possibly an indirect or passive association with actin stress fibres. Further experiments based upon greater shear duration or possibly a greater shear magnitude might elucidate this matter further, and this area is certainly deserving of continued investigation.

Confocal images (Figures 1.12 & 1.13) demonstrate BAECs stained for actin. These photographs illustrate the classic re-organisation of actin stress fibres from control group cells in a static monolayer (e.g. Matsuda and Fujiwara, 1992; Davies, 1996), in which there are dense peripheral bands of actin and random arrays of stress fibres distributed throughout the cytoplasm. A shearing rate of 15 dyn cm^{-2} for 4 hours is believed sufficient for cell readjustment to begin and for actin to become re-organised into near-parallel arrays of stress fibres oriented with the direction of flow (Davies *et al.*, 1997). This response usually commences immediately after the shearing stimulus is introduced to the cells and conventional fluorescence microscopy often shows full re-organisation of cells within 1-2 hours (Davies, 1995). Confocal images obtained by Flitney (collaborative research with Dr. R. Goldman, Northwestern University, Chicago, U.S.A.) expand on the current understanding of the actual time it takes for actin to fully re-organise (Flitney, *pers.comm.* 1999). His results suggest it takes longer for actin at the basal surface to re-organise in the direction of flow than the actin at the apical surface, the region of the cell that experiences the shear force. Figure 1.13a & b illustrates this novel idea of apical to basal actin re-organisation, and Figure 1.13b demonstrates a transitory area through a micron-thick slice of the cell showing a criss-cross pattern of apical and basal actin. A longer shearing time or higher shear rate would probably induce full actin re-organisation, however the experimental conditions of 15 dynes cm^{-2-} for 4 hours were not sufficient to elicit a full response of actin throughout the cell. This highlights the importance of **time** in terms of cellular response. Namely, the duration of imposed fluid stresses is as important to the structure and function of cells as the magnitude of flow stresses.

Protein analysis of the sample lysates collected from each shear experiment show an interesting banding pattern on a Coomassie blue stain (Figure 1.14) at ~112KDa. Unfortunately, the protein levels are too weak to ascertain whether there is a difference in Na^{+}·K^{+}ATPase α-1 subunit over time at the different shear stresses. However, the most noticeable difference is around the molecular weight ranges of actin (~43KDa) and vimentin (~56KDa) (Figures 1.14 and 1.18). Both are very abundant cytoskeletal proteins in static culture (Lazarides, 1980; Wong *et al.*, 1983), and show an interesting expression after exposure to the two shear stresses over time in cold lysates. Leaving the cells for 8 hours after shearing proved to be problematic in attaining protein levels comparable to those where the cells are lysed straight away. This is possibly due to cell detachment during shearing, to detachment due to cell re-organisation of sheared cells returning to a cobbled-stone appearance after the stimulus is removed, or simply to the unavoidable disturbance of the slide during the experimental procedure. What might prove interesting in experiments of this type in the future would be to *simultaneously* shear cells in a number of replicate chambers over a time course (e.g. 16 hours). This would reduce the variability in experimental conditions, which occurs here simply due to the duration of the experiments. In addition, benefit could derive from the simultaneous application of both immunofluorescence and Western blot analysis, although of course this would require two sets of apparatus. Other possible experiments would include ^{3}H ouabain binding to assess the number of pumps after shearing, as well as ^{86}Rb flux to assess ion flux across the membrane following shearing.

The series of ECLs obtained from the 15 dyn cm^{-2} and 50 dyn cm^{-2} experiments show up-regulation from the control at several time points (Figure 1.15 & 1.16). Initial up-regulation at the 5 and 10-minute time points could be an expected response due to a mechanical effect triggering gene transcription such as fluid stresses. Also, the simple compositional effect of new medium bathing the apical cell surfaces might trigger a response. Sustained stimulus is a better gauge to what is happening at the transcriptional level. Prolonged stimulus could be enough to switch on or switch off gene transcription and ultimately the expression of protein. The two experiments in Figure 1.17 and 1.21 were designed to assess levels of protein in relation principally to two levels of fluid stress but also in relation to incubation period following cessation of flow stresses. Regrettably, these experiments cannot be statistically compared with each other because there was no replication in the stress plus 8 hours incubation period (Figure 1.21). This was due to time constraints and unforeseen problems associated with this experiment. Nevertheless, the experiments offer some insight into cell response to each variable. Figure 1.17 indicates a slight but consistent trend to both data sets in which protein expression initially increases to a maximum but then decreases through time. This effect is noticeable for cells sheared at both 15 dyn cm^{-2} and 50 dyn cm^{-2}. However, statistical analysis reveals no internal difference between the data sets. This indicates that the expression of Na^+,K^+ATPase within cells is **not** contingent upon external fluid stresses. There is no evidence in the scientific literature that directly suggests or shows that such a relationship should exist. However, predictable and known biochemical and gene responses to fluid stress (Davies, 1995) might provide mechanisms through which Na^+,K^+ATPase expression is controlled in relation to external fluid stresses. It is not possible from these experiments to assess

whether the data reflect a true situation. Notwithstanding the results of the statistical analysis, Figure 1.17 shows for the most part that cells exposed to higher flow stresses do show a trend "albeit marginal" towards up-regulation. This may indicate that additional replication might reveal a true difference in protein expression in relation to flow stress. If this could be proven, future experimentation could focus on identifying the precise mechanisms involved in up/down-regulation.

Experiments in which cells are sheared at different time intervals under two flow stresses and then left for 8 hours (Figure 1.21) were designed to see if gene transcription is switched on or off after the stimulus is removed. Statistical analysis (in this case two-way ANOVA without replication) was used to compare the two data sets and shows clearly that the larger shearing forces (50 dyn cm^{-2}) induced a greater response with more protein expression in comparison to control levels. In purely qualitative terms, the pattern through time (i.e. the bell-shaped distribution) of cells exposed to 50 dyn cm^{-2} is similar here to sheared cells at the same stress and processed immediately (Figure 1.17). That a difference in cell response is evident in this experiment between the two stress levels supports the earlier contention that higher stresses may induce a greater response and that this effect is real. It is of interest that cells exposed to 15 dyn cm^{-2} show no increase over control values (i.e no up-regulation) and decrease markedly (down-regulation) for times in excess of 30 minutes. This contrasts to the corresponding results obtained in the previous experiment (Figure 1.17) in which there is initial up-regulation followed by little (time point 240) or no down-regulation. It appears that the data set in Figure 1.21 for 15 dyn cm^{-2} plus 8 hours is globally shifted downward on the y-axis. This would imply that gene transcription is

switched off during the incubation period causing a down-regulation of protein. This highlights once again the importance of **time** in cellular response.

Part III

Part III

General Discussion

This Chapter presents a collation of the most significant general conclusions reached during the investigations and derived both from experimental results and a study of the literature. Conclusions of a more specific nature are confined to their respective Chapters. Finally, there is a summary of topics recommended for further study under the sub-headings of a) the precise identification of physical linkages and associated mechanisms between the sodium pump and the actin cytoskeleton and b) the effects of fluid stress on the nature and distribution of Na^+, K^+ ATPase.

This project has been a two-part study concerned with aspects of the distribution of Na^+, K^+ ATPase α and β subunits in different cell lines. The principal experimental emphasis was to examine Na^+, K^+ ATPase distribution in relation to cell type, cell morphology and age using immunofluorescence, Western blot analysis, ^3H ouabain assays and various permeabilisation techniques. This formed Part I of the study. Part II of the study focussed on the potential up/down regulation, in addition to changes in Na^+, K^+ ATPase distribution throughout the cytoskeleton, under the influence of laminar fluid shear stress.

The Na^+,K^+ pump is an integral membrane protein found in virtually all cells and is essential to cell life. The enzyme translocates three sodium ions against their electrochemical gradient and is responsible for maintaining ionic balance across

the plasma membrane. The enzyme plays a primary role in controlling cell volume through Na^+ and water reabsorption, in the maintenance of membrane resting potential and intracellular pH through Na+-H exchange (Rindler and Saier, 1981; Skou and Essmann, 1992). Na^+, K^+ ATPase is recycled between two primary locations: the intracellular cytoplasm and the cytoskeleton. Intracellular pumps are generally understood to be non-functional (Lamb, 1988), and once internalised they are either immediately degraded or possibly stored (Fambrough *et al*, 1991). Functional pumps occur only in the plasma membrane. The main function of turnover is to keep an appropriate number of working pumps in the plasma membrane. Understanding sodium pump (re)distribution and numerical abundance within cells - and those factors governing this - will allow a greater understanding of cellular homeostatic mechanisms. Cell morphology, the effect of the external environment and the influence of external tangential fluid stress are amongst those factors considered to influence pump distribution and which were examined in this study.

HeLa cells were initially selected for experimentation, as they are a robust cell line that is relatively easy to culture. In addition, they are known to be very a good physiological model for other cells *in vivo* (Cutler, 1988), and they have a highly sensitive α subunit, which is appropriate for this study. Aspects of HeLa cell morphology were examined using anthroylouabain, a fluorescence derivative of the cardiac glycoside ouabain. Morphology is defined as cells that are either spherical, which is usually associated with actively dividing cells, or flattened. Flattened cells tend to have a more prominent cytoskeletal structure. It was discovered that affinity for ouabain in HeLa cells decreases for cells that are

actively dividing whereas confluent cells exhibit a 3-fold increase in sensitivity to ouabain. The reason for this remains unresolved, however it is understood that during cell division pumps are rapidly internalised from the surface into the cell taking attached ouabain with them. Recovery to the plasma membrane is equally as rapid. Initial findings by Lamb, Lazarus and Flitney (1996), upon which this study was directly based, showed that the dissociation constant K_d for ouabain binding to the sodium pump of HeLa cells is dependent on cell morphology. Results of this study show that rounder cells uptake more anthroylouabain compared to flatter cells, which supports Lamb's observations. It is possible that this may be an artefact of the differing depth of cells, however, laser scanning confocal microscopy reveals this was not the case but a real difference of *ca.* 3-5-fold. The findings reported here (Figures 2.4 and 2.5) coupled with the data of Lamb *et al.*, (1996) highlight the distinction between cell morphology in relation to Na^+, K^+ ATPase distribution. It is evident that conformational changes occur within the cytoskeleton between round and flat cells which induces pump internalisation. Other work has noted the functional interaction between integral membrane proteins and the cytoskeleton (e.g. Koob *et al.*,) and Na^+, K^+ ATPase is known to be tethered to the cell membrane via ankyrin in erthrocytes and MDCK cells (Nelson and Veshnock 1987). Internalisation, then, is most likely due to disruption of the link between membrane proteins and Na^+, K^+ ATPase. Linkage proteins in HeLa cells have not yet been identified, although in epithelial cells and rat brain spectrin has been identified (Cantiello, 1995a). A thorough exploration of cortical linking protein (e.g. spectrin, ankyrin, AE-1 and CD3) structural association in relation to both actin and Na^+, K^+ ATPase in HeLa cells of variable morphology would provide an insight into the exact mechanism underlying the observed pump internalisation.

Follow on studies examined bovine aortic endothelial cells (BAECs) in addition to HeLa cells in order to compare the degree of ouabain binding between young and old cells. BAECs serve as a good model for the study of confluent monolayers of cells sustained longer in growth culture (older cells). It is possible to maintain BAECs for periods of days to weeks due to contact inhibition, which is a property HeLa cells do not exhibit. This was the rationale behind use of BAECs. The results demonstrate that both HeLa cells and BAECs used for experimentation at Day 4 after plating have similar levels of ouabain binding, whereas BAECs harvested at day 14 show less ouabain binding in comparison to younger cells (one way ANOVA $F_{2,56}=8.60$, $p<0.001$). Thus BAECs were confirmed as a good model for future research.

Although less ouabain binding was observed in Day 14 BAECs in comparison to younger cells, confluent monolayers of BAECs did show a very interesting pattern of Na^+, K^+ ATPase α-1 subunit staining revealed via indirect immunofluorescence. Between days 11 and day 14 the primary pattern of staining was heavily concentrated between adjacent cells in the monolayer (Figure 3.7) indicating a large and conclusive redistribution from the cytoplasm to the cell periphery (contrast, for example, Figure 3.6 to Figure 3.7 b). It should be noted that the Na^+, K^+ ATPase may not be confined to the apical surface of cells. The image viewed by conventional microscopy should not be interpreted solely as strong apical staining. Pumps may, for instance, be saturated along the lateral surface through the depth of the cell, which presents the illusion of strong apical staining.

The pattern of staining in this study (Figure 3.7 a and b) strongly resembled the distribution of dense peripheral bands of actin which appear when cells become fully confluent (Figure 3.13 d). Regrettably, it is difficult to state definitively that there is a direct co-localisation between Na^+, K^+ ATPase and the actin in BAECs although it is known that the actin filaments can co-localise with Na^+ channels (implicating to a possible role in regulatory activity). Work by Cantiello (1995) concludes that as Na^+, K^+ ATPase may serve as an important component of transepithelial ion transport response that is functionally controlled by actin.

Considerable uncertainty surrounds the redistribution of pumps to the periphery of the cell in areas of confluence and there is relatively little published material on the subject. One view is that as cells contact one another, a triggering mechanism is activated which redistributes the pumps to the cell periphery (Flitney, pers. comm).

It has also been shown in this study through ouabain binding assays that older (d-14) confluent BAECs have fewer pumps in relation to younger (day 4) cells (Figure 3.15). A possible explanation for these observations is that confluent cells have more cell-cell junctions thus allowing a greater transfer of ions between neighbouring cells. Another possibility is that cells at confluence divide at a slower rate and few, newer sodium pumps are created so the mean age of the sodium pumps in the samples is likely to be older (pers. comm. Mobasheri, Cutler, Lamb).

Detection of the β-1 subunit through immunofluorescence show strong nuclear and juxta-nuclear staining. Laser scanning confocal images confirmed that the pumps were not confined to the nucleus (Figure 3.9). This indicates the majority of the pumps are located at the cell surface. Newly synthesised proteins are moved through an interlocking organelle system characterised by different compartments, and selective transport pathways. These compartments include the endoplasmic reticulum (ER) and Golgi apparatus. Membrane proteins are translated into the (ER) and processed further in the Golgi complex before they are inserted into the membrane (Frambrough *et al.*, 1994). The observed staining from the experiments described in Chapter 3 show possible co-localisation of the β-1 subunit and the Golgi. It is interesting that patterns of staining were markedly different to those observed with the α subunit, and showed only slight association to actin. For example, in young cells the majority of the staining is sequestered to the nuclear and peri-nuclear region (Figure 3.8), whereas in older cells (Figure 3.11) the pattern of staining is still concentrated possibly co-localised to the Golgi. However, there is no appearance of nuclear staining and the pattern of staining is much more diffuse throughout the cytoplasm. Experiments were planned to double label cells with a polyclonal antibody to the Golgi along with an antibody to the β-1 subunit. These would have confirmed the β-1 subunit co-localised with the Golgi, but regrettably the work was not undertaken.

A simple method for antigen retrieval in tissue sections and cell cultures was described by Brown (1996). Many antibodies recognise denatured proteins on western blots, but are poorly reactive by immunocytochemistry. He examined the effect of applying sodium dodecyl sulfate (SDS) to cryostat sections of tissues

and to cell cultures prior to immunostaining. In many cases, a 5-min pretreatment with 1% SDS produced a dramatic increase in staining intensity by indirect immunofluorescence. Among the antibodies tested that showed a positive effect of SDS were an anti-Na/K-ATPase monoclonal antibody. His results revealed that SDS treatment can be used as a simple method of antigen retrieval in cryostat sections and on cultured cells. In some cases, antigens were not detectable without pretreatment with SDS.

Although in this study the monoclonal antibody used reveals sodium pump staining, Brown's experiments highlighted the potential to reveal other sites not detected by the usual immunofluorescence protocol. In these studies pre-treatment with 0.1% SDS and hypotonically bursting the cells were used to expose antigenic sites in intra-cellular compartments leading to the augmentation of α-1 subunit antigen immunoreactivity. Results of the SDS pre-treatment experiment showed α-1 subunit staining having a similar distribution pattern to actin. Hypotonically induced bursting and resealing cells showed areas where actin reformed into circular patterns that were also heavily concentrated with sodium pumps around the periphery of the 'actin circles'. These data support the notion of co-localisation of the α-1 subunit and actin, although they do not provide conclusive proof. This lends weight to the observations and results reported in Chapter 3 concerning possible linkages between the α-1 sub-unit and actin. Notwithstanding this, the mechanisms underlying this association remain unclear. They may, as surmised previously, possibly be due to cortical linking proteins (Cantiello, 1995a) or simply due to passive association.

The inner layer of blood vessels consists of a single layer of squamous epithelial cells that line the entire vascular system forming the vascular enodthelium. These cells are constantly exposed to haemodynamic forces i.e. forces associated with the flow of blood (Davies, 1995). The two principal forces experienced by cells are normal stress, which acts perpendicular to the vessel wall, and tangential stress which creates a frictional drag on cell surfaces parallel to the direction of flow (Figure 1.4). The aim of this study was to examine the effects of tangential fluid stress on BAECs in terms of the changes in Na^+, K^+ ATPase distribution and protein expression. Virtually no previous work specifically on this subject is found in the literature.

BAECs were subjected to steady laminar shear stresses of 15 and 50 dyn cm^{-2} using specialised parallel plate chambers. Immunocytochemical techniques were used to reveal any physical differences in pump distribution after exposure to flow stresses. In addition Western blot analysis was used to explore possible up or down regulation of the α-1 subunit. Distribution of Na^+, K^+ ATPase in regions of confluence in BAECs grown in static culture show peripheral localisation (Figure 1.12 a). This may simply be a function of a triggering process as subconfluent cells establish cell-cell contacts and attain confluency (Flitney, pers. comm.), although the nature of such a triggering process has yet to be discovered for BAECs. Results indicate that under a flow stress of 50 dyn cm^{-2} for 4 hours there is a marked change in Na^+, K^+ ATPase distribution, as well as associated morphological changes in BAECs (specifically reorganisation and alignment of actin stress fibres with the direction of flow). Na^+, K^+ ATPase are redistributed and transfer from the circumferential regions of cells to become

randomly distributed throughout the cytoplasm (Figure 1.12). This phenomenon has, to the author's knowledge, never been observed before.

Fluid stresses exert a drag force on the apical surface of cells. Structural components spanning the cell membrane act as mechanisms for transduction of mechanical signals into biochemical and cytoskeletal response (Davies, 1995). The specific mechanisms surrounding redistribution of Na^+, K^+ ATPase are not known, however this may simply be a mechanical function of fluid shear stress on the cell membrane creating cytoskeletal re-arrangement. It has only been demonstrated circumstantially in this study that there is a link between the α-1 subunit of Na^+, K^+ ATPase and actin rearrangement. However, it is interesting to note that the initial effects of laminar flow result in the rearrangement of dense peripheral bands of actin to elongate near-parallel arrays in the direction of flow (Figure 1.13 a), which are visually coincident with pump redistribution. This is suggestive of a structural association between the two. Redistribution of the pumps may not necessarily be purely a consequence of mechanical stimulation. An interesting association of cytoskeletal re-organisation and Na^+, K^+ ATPase with levels of cellular ATP was noted by Mandel *et al.*, (1994) and Bacallao *et al.* (1992). They describe a rapid internalisation of Na^+, K^+ ATPase and loss of cortical actin network following ATP depletion induced by treating cells with antimycin and deoxyglucose. These treatments inhibit oxidative and glycolytic energy metabolism. This is a biochemically mediated effect. Similar observations have been reported by Rodriguez-Boulan and Nelson (1989). Molitoris *et al.*, (1991, 1992) found that much of the enzyme internalised from the basolateral domain to the cytoplasm although some were found on the apical surface. This

ATP loss to the shearing medium was not determined in this study, however there is evidence which indicates that endothelial cells release ATP under shear stress (e.g. Milner *et al.*, 1992; Bodin *et al.*, 1992). Therefore, it seems possible that redistribution of Na^+,K^+ ATPase under fluid stress might be, in part, an indirect function of ATP loss as well as the direct influence of the shear forces on the actin cortical network. Future experiments may wish to measure the net gain in dissolved ATP through time in the shearing medium (assuming the loss is appreciable) in an effort to separate these two effects.

Protein estimations derived from gel densitometry analysis of ECLs for cells sheared at 15 and 50 dyn cm^{-2} over a time course experiment showed no significant difference with either time or flow stress (two-way ANOVA without replication (15: df=1, F=7.35E^{-5}, p=0.993; 50: df=7, F=0.396, p=0.897). There is no existing work in the literature which suggests that an effect should occur, although there are known biochemical pathways and processes which could potentially facilitate such a response. Additional experiments were designed to expose cells to the same shear magnitude but then incubate them for 8 hours at 37°C to look for down or up-regulation of the sodium pump protein over time. Shearing under a flow stress of 50 dyn cm^{-2} produced a characteristic bell-shaped distribution over time. Statistical analysis showed a significant difference with time and flow stress (two-way ANOVA with replication (50: df=1 F=32.85, p=0.001) indicating possible up-regulation of pump protein after incubation.

Recommendations for future research

The recommendations in this section refer to the main areas in which considerables further work was recognised from this investigation.

Recommendations for future research

The recommendations in this section refer to the main areas in which considerables further work was recognised from this investigation.

Much benefit would be gained from precise identification of physical linkages between the sodium pump and the actin cytoskeleton. This study has provided strong circumstantial evidence for a relationship between the two, but closer inspection of cortical linking proteins e.g. ankyrin, spectrin, CD3 and anion exchange proteins (e.g. AE-1) would provide greater insight into the association in BAECs.

The broad influence of fluid shear stress on cells in relation to the sodium pump is certainly deserving of further attention. The complete lack of previous work in the literature on the subject in itself opens up avenues of future research pertaining to a wide variety of different aspects of sodium pump distribution and function. All of the experiments conducted were very preliminary in nature due to time constraints as well as problems associated with identification of the appropriate experimental conditions. Repetition of these experiments, especially the incubation experiment, would be a useful first step. This would permit comparison of the relative effect of incubation for the same fluid stress, which may point toward mechanisms operating at the transcriptional level. Such research would benefit from a more biochemical approach, as this is a more powerful tool for the identification of genes for Na^+, K^+ ATPase which may be switched on or off under the action of fluid stress.

The mechanisms underlying the redistribution of Na^+, K^+ ATPase in cells exposed to fluid stresses is not known. Benefit may be gained through specific examination of cortical linking proteins currently implicated to be associated with Na^+, K^+ ATPase in sheared cells. This may ultimately prove whether redistribution arises through purely mechanical or biochemical mechanisms, or through a combination of the two.

The focus of this study has been on tangential fluid stresses and yet normal fluid stresses in the vascular system may be equally important. There is, for example, a considerable volume of work on mechanically (not flow) stretch activated sodium channels (Mobasheri, pers. comm.). This would undoubtedly involve the design and construction of new instrumentation but the prospects for furthering our understanding of the processes involved are very exciting.

Conclusions

The main findings of this study may be summarised.

- There is a difference in anthoylouabain uptake between HeLa cells of differing morphologies showing round cells possess a greater degree of anthoylouabain uptake than flatter cells. This was confirmed using confocal microscopy.

- BAEC cells were confirmed as a suitable model for further experimentation through comparative studies with HeLa cells.

- There is a difference in ouabain binding between young (HeLa and BAECs day 4) and old BAECs day 14 found in a fully confluent monolayer.

- Immunofluorescence staining of confluent cells revealed Na^+, K^+ ATPase to be heavily concentrated between adjacent cells. This pattern closely resembled dense peripheral bands of actin that appear when cells become fully confluent.

- BAECs exposed to different pre-treatments (0.1%SDS and hypotonic disruption of the cell membrane) show an interesting association of Na^+, K^+ ATPase and the actin cytoskeleton .
    1. SDS pre-treatment revealed sodium pump staining concentrated in areas where there are dense peripheral bands of actin and areas of near-parallel arrays of intracellular stress fibres.
    2. Hypotonic disruption of the cell membrane produced re-formation of actin into circular patterns and Na^+, K^+ ATPase was observed to display a similar pattern of staining.

- Laminar fluid stresses of 50 dyn cm^{-2} for 4 hours are observed to produce a marked change in Na^+, K^+ ATPase distribution, in addition to a discernible change in cell morphology (alignment with direction of flow) and cytoskeletal protein. Imposed fluid stresses result in redistribution of Na^+, K^+ ATPase.

- There is no statistical dependence of protein expression on either shearing duration or shearing magnitude for cells exposed to laminar fluid stresses of 15 and 50 dyn cm^{-2} in a time course experiment (16 hours).

- There is a statistical increase in protein expression for cells exposed to laminar fluid stresses of 50 dyn cm^{-2} and then incubated for 8 hours in a time course experiment.

Part I

Appendix 1

Cell Culture

Hela Cells purchased from Imperial Labs

Bovine aortic endothelial cells (BAECs) supplied by ECACC, (Centre for Applied Microbiology and Research, Salisbury, Wiltshire. Dulbecco's MEM (Gibco) culture medium diluted 1:10 with distilled H_2O (D H_2O). The buffer sodium hydrogencarbonate ($NaHCO_3$) added drop wise to give a pH of 7.4. This is supplemented with 10% Foetal Calf serum (Globepharm).

Protocol

The medium was decanted off and cells were treated with $2cm^3$ of trypsin. When the cells detached the reaction was neutralised by adding $18cm^3$ of complete, sterile growth medium warmed to 37°C in a hot water bath. Passing the cell suspension through a sterile stainless steel needle (1.1mm internal diameter) using a $10cm^3$ syringe ensured all cells clumped together were separated and suspended in solution. One cm^3 of suspension was taken to estimate the cell number. The appropriate cell concentration was diluted with growth media to continue the next sub-culture of cells. Cells were stored in a sealed box and equilibrated with a 5% CO_2, 95% O_2 mixture to maintain pH at 7.4.and incubated at 37°C.

Cell number estimation

The numbers of trypsinsed cells were measured by using a Coulter Counter connected to a channelyzer. 1cm^3 of cell suspension was added to 19cm^3 of isoton azide free balanced electrolyte solution in Coulter vials.

Trypsin

Trypsin is prepared by dissolving 0.38g EDTA in 500cm^3 (Sigma) Earle's based salt solution w/o calcium or magnesium [EBSS] (Gibco). 2mM EDTA = 0.076/100cm^3 so 180cm^3 EDTA/EBSS added to 20cm^3 raw trypsin (Gibco). Using swinnex - 25 Millipore™ filter millipore solution and aliquot into vials.

- All chemicals used were molecular biology grade

Rederiving cells from liquid nitrogen.

For rederiving HeLa cells that were frozen in 10% dimethyl sulfoxide [DMSO] (Sigma) [solvent to prevent ice crystal formation], vials were warmed in a 37°C water bath. When the cells were nearly thawed, the seal of a Nunc 75cm^3 tissue culture flask was wiped with 70% alcohol. The cells were transferred into the flask (containing approximately 60 cm^3 of DMEM at 37°C) and equilibrated with 5% CO_2, 95% O_2 mixture They were incubated 37°C overnight so that most of the cells settled down and adhered to the sides of the flask. The following day the DMEM was very gently poured off to get rid of any remaining DMSO and fresh DMEM (warmed to 37°C) was added. The cells were incubated at 37°C until ready to be passaged. HeLa cells seeded at 2 x 10^4 cm^{-2} and took 3-4 days to grow before use.

Rederiving BAECs varied slightly. Once cells were thawed, they were placed into a universal container (Sterilin) (sucked up and down a few times in case they have settled) and $10cm^3$ of DMEM (at 37°C) was added drop-wise while shaking. Once $5cm^3$ were added, they were centrifuged at 1000RPM for 10 minutes. Supernatant was decanted off leaving cell pellet. $10cm^3$ medium were added and equilibrated with 5% CO_2, 95% O_2 and incubate at 37°C.

Appendix 2

Anthroylouabain binding

Wash coverslips x2 with $0K^+$ at room temperature aspirate off remaining solution. Add $2cm^3$ $2x10^3$ anthroylouabin (diluted in10 cm^3 of $0K^+$ plus BSA). Let stand for 1 hour at room temperature. Rinse x4 with ice cold $5K^+$, aspirate off any remaining solution. Fix coverslips for 10 minutes in 4% paraformaldehyde. Rinse x2 for 5 minutes with PBSc. Mount using Gelvatol with 100mg cm^3 DABCO.

Anthroylouabain dilution

$788.9\ gl^{-1} = M$ $\quad$ $78.89mg/100cm^3$
$78.89gl^{-1} = 0.1M$ $\quad$ $7.9mg/10cm^3$

Dilute to $5mgcm^{-3}$ in methanol

$$\frac{5mg}{7.9mg} \bullet \frac{x\ cm^3}{10cm^3} = \mathbf{6.3\ cm^3}$$

$5K^+$ Krebs and $0K^+$ Krebs stock solutions

Molar concentrations

NaCl 58.4 gl^{-1}, KCl 74.5gl^{-1}, $MgSO_4$ 246.48gl^{-1}, KH_2PO_4 136gl^{-1}, $CaCl_2$

$100cm^3$ l^{-1} HCl 83.3gl^{-1}, Tris base 166gl^{-1}, NaH_2PO_4 177.9gl^{-1}

$5K^+$ Krebs: 0.1M NaCl, 0.06M KCl, 0.04M $MgSO_4$, 0.01M KH_2PO_4, 0.028M $CaCl_2$ 0.012M HCl, 0.1M Tris base.

$0K^+$ Krebs: K^+ was omitted and replaced by Na^+ salts: 0.1M NaCl 0.04M $MgSO_4$, 0.028M $CaCl_2$, 0.01M Tris, 0.04M NaH_2PO_4

- Make up to 2l with MilliQ™ water

- $2gl^{-1}$ glucose added to both $5K^+$ and $0K^+$ Krebs. Stirred on magnetic stirrer and pH adjusted to 7.4.(Corning, 120 pH meter)

All the above chemicals were obtained from BDH (Analar) and are Molecular Biology Grade.

Appendix 3

Ouabain binding

$5K^+$ Krebs and $0K^+$ Krebs Radioactive solution: See Appendix 2.

- $50cm^3$ $0K^+$ Krebs added to 0.05g BSA. This was left on bench incubator to dissolve, DO NOT shake or stir BSA will froth.

200nmϕ

- $10^3\phi$ = 0.07288g ouabain in $100cm^3$ milli-Q™ water
- $1.0cm^3$ of above solution was taken and made up to $100cm^3$ in $100cm^3$ milli-Q™ water, to equal$10^{-5}\phi$.
- $1.0cm^3$ of the above solution and made up to 50 cm^3 with $0K^+$ with BSA (This is 200nmϕ)

200nmϕ in $0K^+$ Krebs with BSA
$50cm^3$ [$10cm^3$ excess]

[$20cm^3$ $0K^+$ Krebs with BSA]
0.01458gϕ
200nmϕ

(Keep in hot water bath @ 37°C)

$40\mu l^3H\phi$

[$20cm^3$ $0K^+$ Krebs with BSA]
Add

1mMϕ

(Keep in hot water bath @ 37°C)

Calculation of ouabain binding

- Standard: $0.5cm^3$ trypsin added to 1.5 cm^3 $5K^+$ Krebs with FBCS. $0.5cm^3$ aliquoted into each of three pony vials. Add 100 µl of radioactive solution added to each vial and $1.0cm^3$ of scintillant. Only half the isotope was counted the other half was normally used to estimate the number of cells. This must be taken into account when doing the calculations, it is referred to

as the ratio of the total volume on the plate/the actual amount taken for isotope estimation.

$$\textbf{Binding} = \frac{\text{A x ratio x Avagadro's no. [ouabain] x std vol}}{\text{Cell no. x B}}$$

Where: A = counts per minute per plate [remember to subtract the mean value of the blank plates from each of the cell plates]

$$\textbf{Ratio} = \frac{\text{Total solution vol on plate}}{\text{Volume counted for isotope determination}}$$

According to the dilutions above the ratio will be 2.

Avogadro's number = 6.02×10^{23} (molecules/mole)

Ouabain = 2.0×10^{-7}M

Standard volume = volume of the standard counted for determining the specific activity of the isotope (litre e.g. 10^{-4})

Cell number = The number of cells grown on the plate (e.g. 1.2×10^{6})

B = mean standard counts (in cpm)

Appendix 4

Immunofluorescence

Phosphate buffered saline PBSa

	(FW)		
NaCl(Analar)	58.4	0.171M	10g
KCL(Analar)	74.5	0.003M	0.25g
KH_2PO_4(Analar)	136	0.0018	0.25g
$Na_2HPO_4.2H_2O$ (Analar)	178	0.0042	0.747g

Dissolved in 10 litres of distilled water for a x10 stock solution. The pH adjusted to 6.8 so that the final pH with distilled water was 7.4.

Phosphate buffered saline (complete) PBSc

Also used in more recent experiments is Dilute x10 stock PBSa solution 1+9 with distilled water. Add 1.0 cm^3 1M $CaCl_2$ (Analar) to each litre of diluted PBSa.

- Commercially purchased Phosphate buffered saline (Gibco BRL x 10 Concentration catalogue no. 14200-067). The concentrate is stored at room temperature and diluted 100 cm^3 to 1 litre with deionised water and mixed to make working solution for PBSa. To make up PBSc add 1.0cm^3 of M $CaCl_2$ and 0.5cm^3 M $MgCl_2$. Mix by inversion.

Bovine Serum Albumin

1.0g albumin (BDH) added to 100cm^3 PBSc and gently stirred until solution was in clear. Aliquoted into 3.0cm^3 amounts in 5.0 cm^3 Eppendorf tubes (Teklabs) and stored at –20°C. When using to block non-specific binding used at 1:10 dilution i.e. 0.1% in PBSc.

Nonidet P40 10x stock

Take 5.0cm^3 Nonidet P40 and add 495cm^3 PBSc. Dilute 1:10 with PDSc for extraction.

Gelvatol

Add 25g Airvol in 100cm^3 of Na_2HPO_4/0.01M KH_2PO_4/0.14M NaCl; pH 7.

Stock solutions

0.2M Na_2HPO_4	2.84g/100cm^3
0.2M KH_2PO_4	2.72g/100cm^3
4.0M NaCl	23.38g/100cm^3

- Using the stock solutions above 5.0cm^3 0.2M Na_2HPO_4, 5.0cm^3 0.2M KH_2PO_4, and 3.5cm^3 4.0M NaCl taken/100cm^3 and pH adjusted the to 7.2.
- With the solution spinning on magnetic stirrer vinol [poly vinol alcohol resin] (BDH) was added very slowly and agitated for 16 hours at room temperature on magnetic stirrer. 50cm^3 glycerol (BDH) was added and agitated for a further 16 hours and was then centrifuged.

  (Centrifuge J2-21M/E, Rotor: JA20) at 12,000rpm for 15 minutes
- Before use DABCO 100mg cm^3 was added to gelvatol

DABCO = 1,4 diazabicyclo (2.2.2) octane (Sigma D2522)

Hoechst Stain

Glycerol	(Analar)	5.0cm^3
Tris 0.5 pH 9.0	(Analar)	0.5cm^3
p-Phenylenediamine	(Sigma P6001)	20mg

- Made up in 10cm^3 of distilled water. 1.0µl Hoechst 33258 (Sigma B2883) (1:10K dilution). Added used as a mountant for coverslips and sealed with nail polish.

Incubation chamber

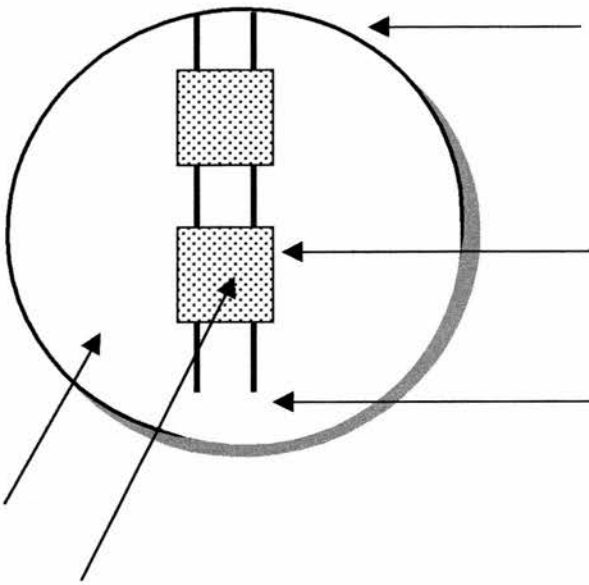

Nunc 90mm diameter Petri dish used for incubating coverslips

$22mm^2$ boroscilicate glass coverslips

Wooden cocktail sticks supporting the glass coverslips in the incubation chamber

Moist filter paper

Cells grown on coverslip to $2x10^4$ cells cm^{-2}

Figure 1.1 A schematic diagram of a typical incubation chamber used in primary and secondary antibody labelling in immunofluorescence.

Appendix 5

Gel Electrophoresis

Lysate preparation

Cells were washed x2 with ice cold PBSa, and ice cold lysis buffer was pipetted over the cells. 1.0cm^3 lysis buffer was used for the 90mm diameter petri dishes and 700µl was used for 19.76 cm^2 glass microscope slides. The cells were set on ice and left to stand for 20 minutes then were scraped with a rubber policeman and pipetted into 2.0cm^3 Eppendorf tube where then were suctioned up and down x 3 through a 1.0cm^3 syringe. They were then centrifuged in a micro-centrifuge for 3 minutes at 12,000rpm the supernatant was retained and the pellet discarded. The lysate was stored at –20°C.

Protein estimation

Using Bio-Rad Protein estimation kit, the samples were measured in a range of 0.1-1.45mg cm ^{3}. The Spectrophotometer (Cecil) was carried out using plastic disposable cuvettes (BDH) and the absorbance measured at 720nm.

BSA Standard Dilutions for Bio-Rad DC Protein Assay

BSA Stock = 1.45 mg cm^3 [Make up 500µl total soultion]

$$\frac{X}{1.45 mg\ cm^3}(500) =$$

STD Dilutions	Stock	1:2 Cold lysis Buffer
0.2mg cm^3	69	431
0.4mg cm^3	138	362
0.8mg cm^3	276	224
1.2mg cm^3	414	86

Bio-Rad protein assay reagent was made first by adding 250µl/sample tube of reagent "A". Reagent "S" was made by adding 20µl $cm^{-3}$of solution "A". Each tube contained 25 µl MilliQ™ water and 25 µl of sample [a 1:2 dilution]. To each tube 250µl of solution "A +S" were added and these were vortexed. 2.0cm^3 of solution "B" were added to each cuvette and then vortexed. Solutions were left to stand a minimum of 15 minutes.

The BSA standards are plotted against the absorbance [@720nm] using Cricket Graph III to show the (linear) relationship between absorbance and the standards. Least squares linear regression analysis of the data provides the equation to calculate protein dilutions for the test samples.

Preparation of the gel plates

The glass plates were first washed in Decon 90 (Decon LTD sussex) and rinsed in distilled water. The were then wiped with 70% acohol and again rinsed with distilled water to ensure there were no other proteins on the plates. Gloves were worn throughout this procedure. Lying the plates flat on paper towels, place the spacers on the larger plate, one on each side, the smaller plate should sit on top.

The Plates are assembled vertically in the MDV2-DC apparatus. The larger plate to the back, the smaller plate to the front and the spacers separating the two are then clamped together in the holding clips and moved onto the rubber seal and clipped into place for pouring the gel. Fit the combs in between the plates [1.0mm width] and mark off 1.0cm below the teeth of the comb to indicate the stopping point at which the resolving gel should be poured. After the solutions are made the seal should be poured first, take 1.0cm^3 of the resolving gel and add 40µl of APS and 4.0 µl of Temed solution polymerised quickly. Pipette half the quantity immediately down the side of the plates, the other half of the quantity down the other side of the plates so the seal is consistent across the bottom. Next add the APS and Temed to the resolving gel [in the quantites stated below] and pour into the plates down one corner, quickly after the solution is poured add about 300µl of 0.1% SDS or n-butanol across the top. This helps prevent oxygen from diffusing into the gel and inhibiting polymerisation. After polymerisation in complete [about 30 minutes] pour off the overlay and rinse the gel several times with deionised water to remove any un-polymerised acrylamide. Drain as much of the residual water off the top of the resolving gel and dry between the plates with a piece of filter paper. Add the appropriate quantities of APS and Temed to the stacking gel and pour the stacking gel on top to the polymerised resolving gel. The combs should be immediately be inserted into the stacking gel, being careful to avoid trapping any air bubbles in between the teeth of the combs. [The combs should be cleaned with 70% ethanol and dried before use.] Lysates should be thawed and up to room temperature before use.

After the stacking gel has polymerised, move gel plates to the electrophoresis apparatus. The smaller plate should be facing the inside of the apparatus. Fill the top and bottom reservoirs with Tris/glycine running buffer and remove any bubbles that become trapped at the bottom of the plates. Remove the teflon combs and rinse out the wells.

With running buffer with a $1.0cm^3$ syringe to remove any left over acrylamide. Fill the wells with 15-20µl of cell lysate and run the gel on 70 volts until the gel front [detected by the bromophenol blue] is through the stacking gel and on 100 volts until the gel front is through the resolving gel. Stop the current before the gel runs off the bottom of the plates. Then remove the plates from the apparatus and put them small face down on clean paper towels, pry the plates apart with a spatula. The gel should be left on the smaller plate. Cut the gel which is going to be used for semi-dry transfer by trimming the sides and the wells off the top, also marking the orientation of the gel by nicking the left hand corner. The gel and "measured to size" nitrocellulose membrane should be soaked in transfer buffer to equilibrate for 20 minutes before semi-dry transfer before it is placed in the transfer blotter. Two pre-soaked blotting papers are used.

The gel is arranged on the anode of the Bio-Rad semi-dry transfer blotter is the in the following manner.

- Pre-soaked blotting paper, roll out any air bubbles with a glass rod
- Pre-soaked Nitrocellulose membrane
- Pre-soaked Gel
- Pre-soaked blotting paper.
- Cathode is placed on top.

This is run for 45 minutes to 1 hour at 10 millivolts. After the protein transfer, the membrane is stained with ponceau red to show the protein bands. This will give you an idea of how good your transfer. At that stage you can also put the gel into Coomassie blue which will stain any proteins left behind. On the ponceau stained membrane, mark the molecular weight markers in pencil, and the gel front. Rf values are calculated by dividing the distance the molecular weight markers bands have moved by the total distance the gel has run [the gel front]. The Rf values were plotted against the log of the molecular weights on Cricket Graph III and regression analysis was used to calculate the approximate molecular weights of the unknown bands.

GEL QUANTITIES FOR MV2-DC MODEL GEL RIG

- All chemicals used are molecular biology grade [MBG]
- Add in the following order

Resolving Gel

	6%	**7.5%**	**8%**
Milli-Q water	16.0cm^3	15.7cm^3	140cm^3
30% Acrylamide	6.0cm^3	8.0cm^3	8.0cm^3
1.5M Tris pH 8.8	7.6cm^3	8.0cm^3	7.6cm^3
10% SDS	0.3cm^3	0.32cm^3	0.3cm^3
10% APS	0.3cm^3	0.16cm^3	0.3cm^3
Temed	0.024cm^3	0.015cm^3	0.18cm^3

Seal

- 1 cm^3 resolving gel 40 µl APS 4 µl Temed. Allow seal to set at the bottom of the plates for 5 minutes before adding resolving gel.
- APS and Temed were added just before pouring resolving gel.

Stacking Gel (5%)

Milli-Q™ Water	6.8cm^3
30% Acrylamide	1.7cm^3
1M Tris	1.25cm^3
10% SDS	0.1cm^3
10% APS	0.1cm^3
Temed	0.01cm^3

* APS and Temed were added just before pouring stacking gel.

SOLUTIONS FOR SDS-PAGE WESTERN BLOTTING

1. **30% Acrylamide**

   Bought ready prepared 29.2% and 0.8% methyl bis acrylamide.

   (Scotlab Easigel). Store at 4°C. Acrylamide is a posionous neurotoxin having cumulative effects, gloves must be worn when handling and proper disposal of acrylamide waste and pipette tips should be enforced.

2. **1.5 M Tris pH 8.8**

   FW: 121.4

   181.5g.Tris (Analar) dissolve in 800cm^3 distilled water.

   pH adjusted with concentrated HCl and volume made up to 1 litre.

   Autoclave.

3. **Tris pH 6.8**

   FW:121.4

   60.5gTris (Analar) dissolved in 800cm^3 distilled water

   pH adjusted with concentrated HCl and volume made up to 1 litre.

   Autoclave.

4. SDS

FW: 288.4 [10%]

10g sodium dodecyl sulphate (Sigma MB grade) dissolve in 100 cm^3 distilled water. SDS may need to be incubated to prevent precipitation.

5. SDS

FW: 288.4 [0.1%]

100 µl of 10% SDS into 9.9 cm^3 distilled water.

6. APS 10%

FW: 228.19 [10%]

100mg of ammonium persulfate (Sigma MB grade) dissolve in 1cm^3 distilled water. (This can be kept up to 2 weeks at 4°C).

7. **TEMED (N'N'N'N' Tetramethylethylenediamine)**

This is prepared commercially and stored at 4°C.

Boehringer Combithek Molecular weight markers

Component	**MW**	**Log_{10} MW**
α2 - Macroglobulin	170,000	5.230
β - Galactosidase	116,353	5.066
Fructose- 6- phosphate	85,204	4.930
Glutamate dehydrogenase	56,000	4.745
Aldoase	39,000	4.593
Triose phosphate isomerase	24,000	4.425

8. 10x Tris/Glycine

	FW		
Tris (Analar)	121.4	0.025 M	60g
SDS (Sigma MB)	288.4	0.1%	20g
Glycine (Sigma MB)	75.07	0.24 M	288g

- pH should be at 8.3 and can be adjusted drop-wise with concentrated HCl.
- Make up to 2 litres with Milli-Q™ water
- Dilute 1:10 for use

9. Transfer Buffer (Semi-dry transfer)

	FW		
Tris (Analar)	121.4	0.025 M	3.0g
Glycine (Sigma MB)	75.07	0.192 M	14.4g
Methanol (Analar)		20%	200 cm^3
SDS (Sigma MB)		0.0375%	3.75 cm^3 of 10% SDS

- Make up to 1 litre in Milli - Q™ water.
- PH should be 8.3 but no alteration is necessary.

10. Coomassie Blue (Protein gel stain)

	FW	
Coomassie Blue R (Sigma)	826.0	1.5g
Methanol (Analar)		900cm^3
Glacial Acetic Acid (Analar)		200cm^3
Distilled water		900cm^3

- Stir on magnetic stirrer and store in brown bottle. Coomassie blue can be re-used several times.

11. **Destain**

Methanol (Analar) 900cm^3

Glacial Acatic cid (Analar) 200cm^3

Distilled water 900cm^3

- Stir on Magnetic stirrer.

12 Ponceau Red stain (x10 Stock solution)

	(FW)	
Trichloroacetic acid (Analar)	163.39	30g
Sulphosalicylic acid (Sigma)	254.2	30g

- Dissolve in 100cm^3 distilled water
- Add 2g Ponceau (S) sigma and mix till dissolved
- For use, dilute 1:10 with distilled water and store at room temp.

0.05%PBS TWEEN [PBS-T] 20

PBS Tween 20 tablets can be commercially purchased from Gibco.

Dissolve 2 tablets of GibcoBRL PBS TWEEN in 1 litre of deionised water. Mix until tablets are fully dissolved on magnetic stirrer.

x1 Laemmli:

Glycerol	1.0cm^3,
1.0M Tris pH 6.8	600µl,
10% SDS	2.0cm^3
10mM Sodum pervanadate	1.0cm^3
Milli-Q™ water	5.4cm^3

3% Beta mercaptoethanol (Sigma)

3% Bromophenol blue (Sigma)

Part II

Appendix 1

Fluid Shear Stress

Viscosity

Viscosity measurements at 35°C measured using a Cannon - Fenske viscometer. Type BS/IP/CF. Readings equal the total seconds it takes the fluid to reach a certain point in the viscometer.

Water: 63, 64, 62, 63, 62 seconds; Mean value: 62.8 seconds

Medium: 66, 68, 67, 68, 68 seconds; Mean Value: 67.4 seconds

Ratio: 67.4/62.8 = 1.07 centipoise

At 35°C the viscosity of the medium equals 1.07 x 0.7194 = 0.7698

At 37°C the viscosity of the medium equals 1.07 x 0.6915 = 0.7399 centipoise.

1 poise = dynes sec cm^{-2}

Table 1 The viscosity (**η, in centipoise**) of water from 0°C to 100°C.

T °C	η	T °C	η	T °C	η	T °C	η
0	1.7870	26	0.8705	52	0.5290	78	0.3638
1	1.7280	27	0.8513	53	0.5204	79	0.3592
2	1.6710	28	0.8327	54	0.5121	80	0.3547
3	1.6180	29	0.8148	55	0.5040	81	0.3503
4	1.5670	30	0.7975	56	0.4961	82	0.3460
5	1.5190	31	0.7808	57	0.4884	83	0.3418
6	1.4720	32	0.7647	58	0.4809	84	0.3377
7	1.4280	33	0.7491	59	0.4736	85	0.3337
8	1.3860	34	0.7340	60	0.4665	86	0.3297
9	1.3460	35	0.7194	61	0.4596	87	0.3259
10	1.3070	36	0.7052	62	0.4528	88	0.3221
11	1.2710	37	0.6915	63	0.4462	89	0.3184
12	1.2350	38	0.6783	64	0.4398	90	0.3147
13	1.2020	39	0.6654	65	0.4335	91	0.3111
14	1.1690	40	0.6529	66	0.4273	92	0.3076
15	1.1390	41	0.6408	67	0.4213	93	0.3042
16	1.1090	42	0.6291	68	0.4155	94	0.3008
17	1.1081	43	0.6178	69	0.4098	95	0.2975
18	1.0530	44	0.6067	70	0.4042	96	0.2942
19	1.0270	45	0.5960	71	0.3987	97	0.2911
20	1.0020	46	0.5856	72	0.3934	98	0.2879
21	0.9779	47	0.5755	73	0.3882	99	0.2848
22	0.9548	48	0.5656	74	0.3831	100	0.2818
23	0.9325	49	0.5561	75	0.3781		
24	0.9111	50	0.5468	76	0.3732		
25	0.8904	51	0.5378	77	0.3764		

From the National Bureau of Standards

The above Table was calculated from the following empirical relationships derived from measurements in viscometers calibrated with water at near 20°C and one atmosphere, modified to agree with the currently accepted value for the viscosity at 20°C of 1.002 cp.

$$0° \text{ to } 20°\text{C: } \log_{10} \eta\tau = \frac{1301}{998.333 + 8.1855(T-20) + 0.00585(T-20)^2} - 3.30233$$

$$20° \text{ to } 100°\text{C: } \log_{10} \frac{\eta\tau}{\eta_{20}} = \frac{1.3272(20-T) - 0.001053(T-20)^2}{T+105}$$

Density

Density bottle volume = $25cm^3$

Density bottle weight = 20.82

Density bottle filled with water = 45.25

Density bottle filled with medium = 44.997

D = m/v [which is expressed in g cm^{-3}]

Water at 36°C

$$D = \frac{44.997 - 20.82}{25}$$

= 0.967g cm^{-3}

Medium at 36°C

$$D = \frac{45.25 - 20.82}{25}$$

= 0.977 g cm^{-3}

The known density of water at 36°C = 0.9936. Therefore,

$$\frac{(\text{Measured medium})(\text{Actual water})}{\text{Measured water}} \qquad \frac{(0.997)(0.9936)}{0.967}$$

=1.004g cm^{-3}

At 37°C the viscosity η of the medium equals 1.07 x 0.6915 = 0.7399 centipoise, and the density = 1.004 g cm^{-3}

Chamber dimensions	**Long chamber**	**Short chamber**
Channel width	2.3 cm	2.0 cm
$\frac{1}{2}$ Channel height	0.0170 cm	0.0284 cm
Distance between pressure ports	8.0 cm	2.9 cm

Two formulas are used to calculate the fluid shear stress:

$$FSS_1 = \tau_1 = \frac{\rho g a h}{l} \qquad \textbf{1.}$$

$$FSS_2 = \tau_2 = \tau^* = \frac{3Q\eta}{2a^2 w} \qquad \textbf{2.}$$

where ρ=medium density (1.004 g.cm^{-3})
g=acceleration due to gravity (980 cm.s^{-2})
h=difference in pressure (cm water) along chamber
a=chamber half-height (cm)
l=distance between pressure measuring ports (cm)
Q=volume flow rate (cm^3.s^{-1})
η=medium dynamic viscosity (0.7399 centipoise)
w=width of channel (cm)

The Reynolds number (Re) is a universal ratio used to establish whether flow is laminar or turbulent.

$$\mathrm{Re} = \frac{\rho l U}{\mu} = \frac{l U}{\upsilon} \qquad \textbf{3.}$$

Where ρ is the fluid density
l is a characteristic length scale
U is flow velocity
μ is the dynamic viscosity
ν is the kinematic viscosity

Flow velocity, U, corresponding to the maximum volume flow rate (9.62 cm^3.s^{-1}) is calculated from Q/A, where A is the chamber cross-sectional area; U=1.23 m s^{-1}. Using a value of ν of 0.7369x10^{-6} m^2.s^{-1} (equivalent to 0.7399 centipoise) and the chamber height as the characteristic length scale, l (which is the appropriate dimension here; see Massey, 1988, p.146), Re=534. The laminar-turbulent transition occurs when Re>1000 in our particular experimental chamber (Massey, 1998).

Graph 1. The relationship between flow rate and flow shear stress in Chamber 2

Settting	Flow rate $cm^3 s^{-1}$	τ_1 dynes cm^{-2}	τ_2 dynes cm^{-2}
0	0.00	0.00	0.00
1	0.04	6.80	5.84
2	1.45	27.81	24.21
3	2.47	48.20	41.24
4	3.59	71.09	59.94
5	4.76	91.69	79.48
6	5.65	105.81	94.34
7	7.00		116.88
8	8.07		134.75
9	8.87		148.10
10	9.62		160.63

1. FSS 1=19.14 x Flow rate r=0.998, n=7, P<0.0001

2. FSS 2=16.69 x Flow rate r=0.999, n=11, P<0.0001

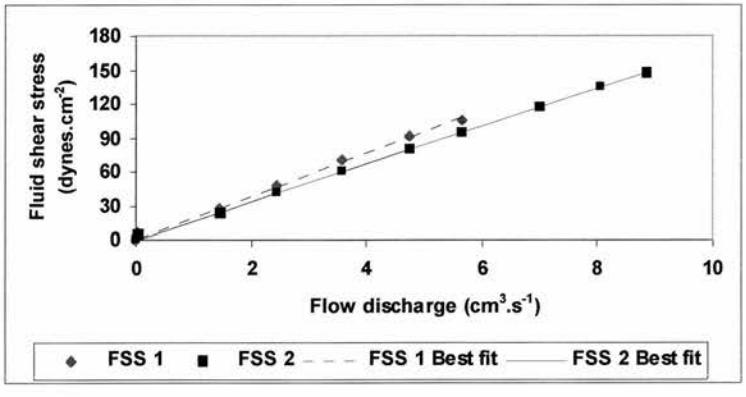

Graph 2: The relationship between flow rate and pressure difference in Chamber 2

Settting	Flow rate $cm^3 s^{-1}$	Pressure difference, ΔP (cm H_2O)
0	0.00	0.00
1	0.04	3.25
2	1.45	13.30
3	2.47	23.05
4	3.59	34.00
5	4.76	43.85
6	5.65	50.00
7	7.00	
8	8.07	
9	8.87	
10	9.62	

1. Pressure difference = 9.11 x Flow rate, r=0.998, n=7, P<0.0001

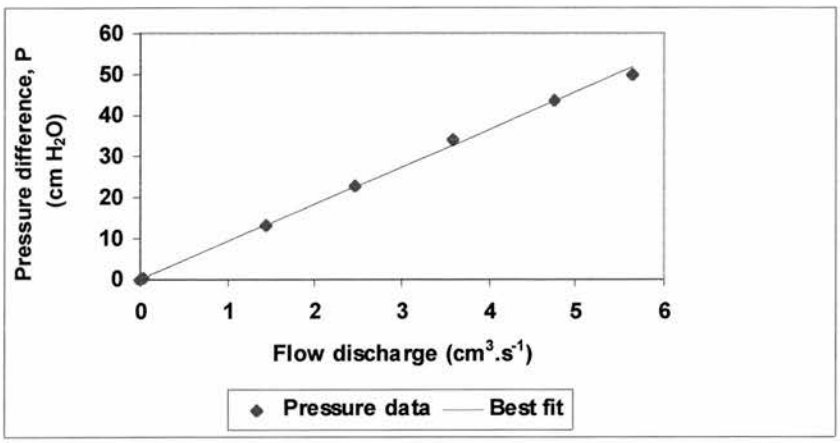

Graph 3. The relationship between flow rate and flow shear stress in Chamber 3

Setting	Flow rate $cm^3\ s^{-1}$	τ_1 dynes cm^{-2}	τ_2 dynes cm^{-2}
0	0.00	0.00	0.00
1	3.00	2.89	2.41
2	1.09	10.50	9.98
3	1.95	18.79	16.99
4	2.80	26.98	24.56
5	4.10	39.51	32.75
6	4.40	42.40	38.87
7	5.30	51.07	48.16
8	6.00	57.81	55.52
9	7.20	69.38	61.03
10	7.90	76.12	66.19

1. FSS 1=9.64 x Flow rate r=0.999, n=11, P<0.0001

2. FSS 2=8.66 x Flow rate r=0.997, n=11, P<0.0001

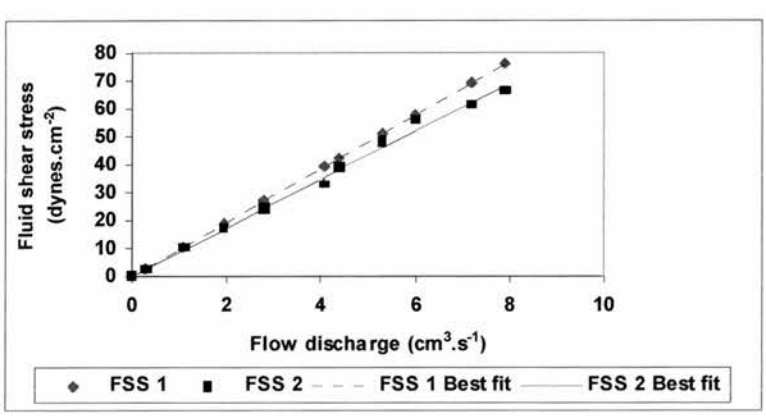

Graph 4:The relationship between flow rate and pressure difference in chamber 3

Settting	Flow rate $cm^3 s^{-1}$	Pressure difference, ΔP ($cm H_2O$)
0	0.00	0.00
1	0.04	0.30
2	1.45	1.09
3	2.47	1.95
4	3.59	2.80
5	4.76	4.10
6	5.65	4.40
7	7.00	5.30
8	8.07	6.00
9	8.87	7.20
10	9.62	7.90

1. Pressure difference = 0.792 x Flow rate, r=0.999, n=11, P<0.0001

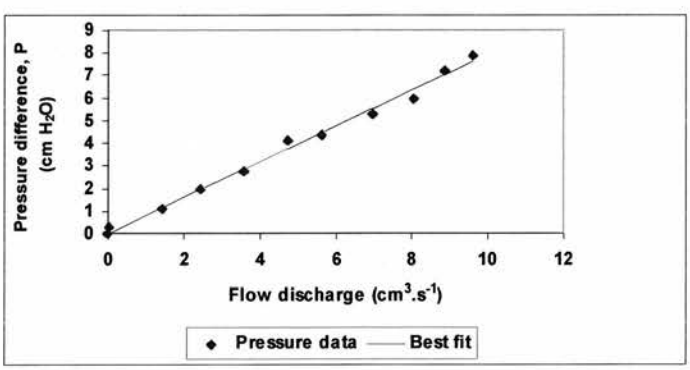

For practical purposes the relationship between pump setting and shear stress for each chamber (using Eq. 2, τ_2 or τ^*) have been tabulated below following regression analysis (see graphs below).

Desired shear stress (dyn cm^{-2})	Pump Setting	
	Chamber 2	***Chamber 3***
0	0.0	0.00
5	0.3	0.75
10	0.6	1.50
15	0.9	2.25
20	1.2	3.00
25	1.5	3.75
30	1.9	4.50
35	2.2	5.25
40	2.5	6.00
45	2.8	6.75
50	3.1	7.50
55	3.4	8.24
60	3.7	8.99
65	4.0	9.74
70	4.3	10.49
75	4.6	11.24
80	4.9	11.99
85	5.2	12.74
90	5.6	13.49
95	5.9	14.24
100	6.2	14.99
105	6.5	15.74
110	6.8	16.49
115	7.1	17.24
120	7.4	17.99
125	7.7	18.74
130	8.0	19.49
135	8.3	20.24
140	8.6	20.99
145	8.9	21.74
150	9.3	22.49
155	9.6	23.23
160	9.9	23.98
165	10.2	24.73

The assistance of Eric Flitney, Jean Melville and Catherine Beers with calibration of the flow chambers is gratefully acknowledged.

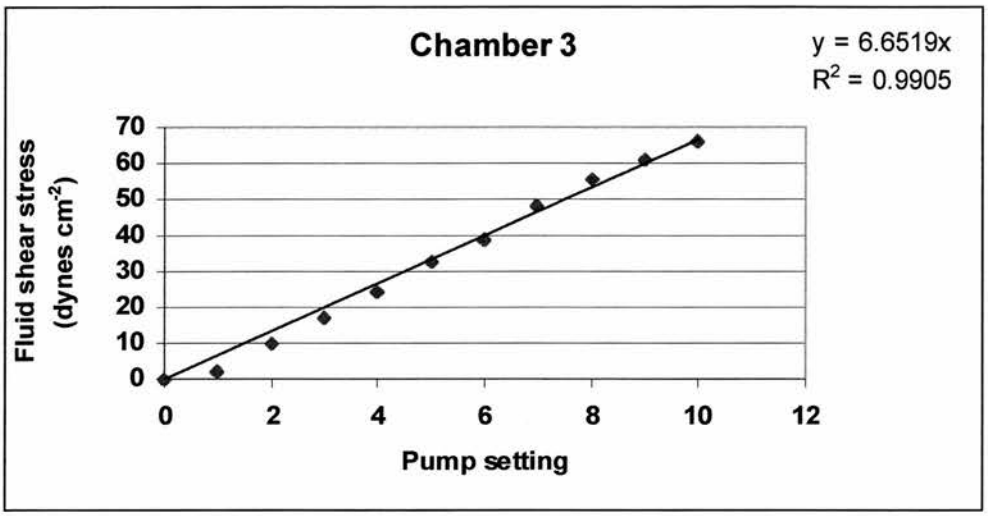
Chamber 3
y = 6.6519x
R2 = 0.9905
Fluid shear stress (dynes cm-2)
70
60
50
40
30
20
10
0
0
2
4
6
8
10
12
Pump setting

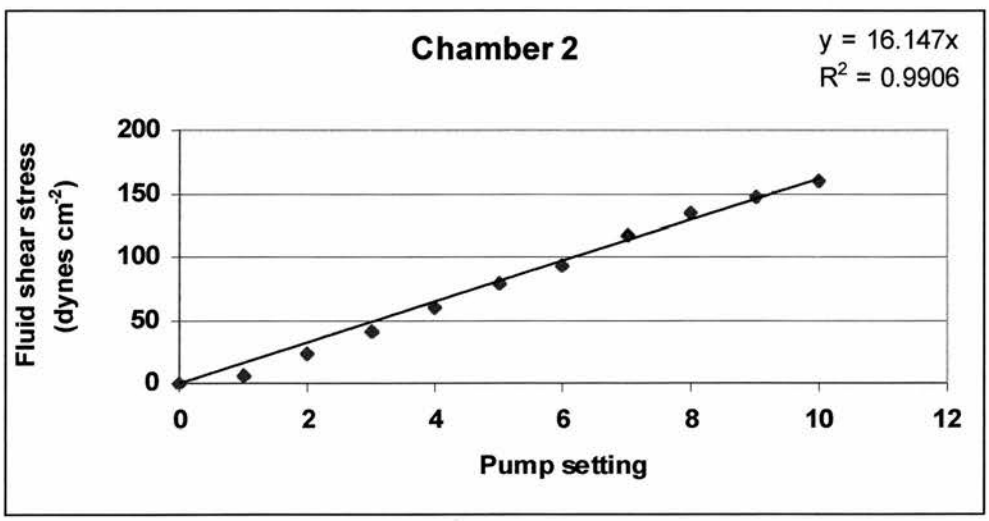
Chamber 2
y = 16.147x
R2 = 0.9906
Fluid shear stress (dynes cm-2)
200
150
100
50
0
0
2
4
6
8
10
12
Pump setting

References

Ahmad, M., Medford, R.M. (1995) Evidence for the regulation of Na^+, K^+ ATPase alpha 1 gene expression through the interaction of aldosterone and cAMP-inducible transcriptional factors. *Steroids*, **60**, 147-52.

Aiton, J.F (1976) The Effects of Serum and Exogenous ATP on the Specific Ouabain Binding and Potassium Fluxes of Cultured HeLa cells. Thesis (Ph.D.) University of St. Andrews.

Aiton, J.F., Lamb, J.F. (1984) Effect of the serum concentration of the growth medium on the sodium pump site density of cultured HeLa cells. *Quart. J. Exp. Physiol.* **69**, 97-115.

Albers, R.W., Koval, G.J. and Seigel, G.J. (1968) Studies on the interaction of ouabain and other cardioactive steriods with sodium-potassium activated adenosine triphosphatase. *Mol. Pharmacol.* **4**, 324-36.

Alberts, B., Bray, D., Lewis, J., Raff, M., Roberts, K. and Watson, J.D. (1989) Molecular Biology of the Cell. Second Edition. Garland Publishing Inc. New York.

Alberts, B., Bray, D., Lewis, J., Raff, M., Roberts, K. and Watson, J.D. (1994) Molecular Biology of the Cell. Second Edition. Garland Publishing Inc. New York.

Allen, D.G., Eisner, D.A., Wray, S.C. (1985) Birthday present for digitalis *Nature*, **316**, 674-5.

Alper, S.L., Stuart, Tilley, A., Simmons, C.F., Brown, D., Drenckhahn, D. (1994) The fodrin-ankyrin cytoskeleton of choroid plexus preferentially colocalizes with apical Na^+, K^+ ATPase rather than with basolateral anion exchanger AE2. *J. Clin. Invest.* **93**, 1430-8.

Amos, L.A., Amos, W.B. (1991) The bending of sliding microtubules imaged by confocal light microscopy and negative stain electron microscopy. *J. Cell. Sci. Suppl.* **14**, 95-101.

Arzamazova, N.M, Arystarkhova, E.A, Gevondyan, N.M., Luneva, N.M., Efremov, R.G., Aldanova, N.A., Nesmeyanov, V.A., Modyanov, N.N. (1988) Sequence analysis of exposed domains of membrane-bound Na^+, K^+ ATPase. Model of transmembrane arrangement. *Prog. Clin. Biol. Res.* **268A**, 57-64.

Avner, E.D., William, E. Sweeney, J.R. and Nelson, W.J. (1992) Abnormal sodium pump distribution during renal tubulogenesis in congenital murine polycystic kidney disease. *Proc. Natl. Acad. Sci. USA.* **89**, 447-451.

Ayrapetyan, S.N., Suleymanyan, M.A., Saghyan, A.A., Dadalyan, S.S. (1984) Autoregulation of the sodium pump. *Cell Mol. Neurobiol.* **4**, 367-83.

Azuma K.K., Hensley C.B., Tang M.J., McDonough A.A. (1993) Thyroid hormone specifically regulates skeletal muscle Na^+, K^+ ATPase α2 and β2-isoforms.
Am. J. Physiol. **265**, C680-7.

Baker, P.F. and Willis, J.S. (1970) Potassium ions and the binding of cardiac glycisodes to mammalian cells. *Nature*, **266**, 521-23.

Baker, P.F. and Willis, J.S. (1972) Binding of the cardiac glycoside ouabain to intact Cells. *J. Physiol.* **224**, 441-62.

Ballermann B.J., Dardik, A., Eng. E., Liu, A. (1998) Shear stress and the endothelium *Kidney Int. Suppl.* **67**, S100-8.

Barlet-Bas, C., Khadouri, C., Marsy, S., Doucet, A. (1990) Enhanced intracellular sodium concentrations in kidney cells recruits a latent pool of Na^+, K^+ ATPase whose size is modulated by corticosteriods. *J. Biol. Chem.* **265**, 7799-803.

Bartolami, S., Planche, M., Pujol, R. (1993) Inhibition of the carbachol-evoked Synthesis of inositol phosphates by ototoxic drugs in the rat cochlea. *Hear. Res.* **67**, 203-10.

Bayer, R. (1990) Topological disposition of the sequences -QRKIVE- and -KETYY in native Na^+, K^+ ATPase. *Biochemistry,* **29**, 2251-6.

Bennett, V., Baines, A.J., Davis, J.Q. (1985a) Ankyrin and synapsin: spectrin-binding proteins associated with brain membranes. *J. Cell. Biochem.* **29**, 157-6.

Bennett, V. (1985b) The membrane skeleton of human erythrocytes and its implications for more complex cells. *Ann. Rev. Biochem.* **54**, 273-304.

Bertorello, A.M. and Katz, A.I. (1995) Regulation of Na^+-K^+ pump activity: pathways between receptors and effectors. *NIPS,* **10**, 253-259.

Bevan, J.A. (1997) Shear stress, the endothelium and the balance between flow-induced contraction and dilation in animals and man. *Int. J. Microcirc. Clin. Exp.* **17**, 248-56.

Bewick, N.L., Fernandes, C., Pitt, A.D., Rasmussen, H.H., Whalley, D.W. (1999) Mechanisms of Na^+-K^+pump regulation in cardiac myocytes during hyposmolar swelling. *Am. J. Physiol.* **276**, C1091-9.

Blose, S.H., & Chacko, S. (1976) Rings of intermediate (100°A) Filament bundles in the perinuclear region of vascular endothelial cells. *J. Cell Biol.* **70**, 459-66

Blose, S.H. (1979) Ten nanometer filaments and mitosis: Maintenance of structural continuity in dividing endothelial cells. *Proc. Natl. Acad. Sci.* **76**, 3372-76.

Blose, S.H. & Meltzer, D.I. (1981) Visualisation of the10nm filaments vimentin rings in vascular endothelial cells *in situ*. *Exp. Cell. Res.* **135**, 229-309.

Boardman, L.J., Lamb, J.F. and McCall, D. (1972) Uptake of [^{3}H]-ouabain and Na pump turnover rates in cells cultured in ouabain. *J. Physiol.* **225**, 619-635.

Boardman, L.J., Huett, M., Lamb, J.F., Newton, J.P. and Polson, J.M. (1974) Evidence for the genetic control of the sodium pump density in HeLa cells. *J. Physiol.* **241**, 771-794.

Boardman, L.J., Hume, S.P., Lamb, J.F., McCall D.Newton, J.P. and Polson, J.M. (1975) Genetic control of sodium pump density. *In*: Lieberman M, Sano T, *Eds*. Developmental and physiological correlates of cardiac muscle. New York, Raven Press pp, 127-138.

Bodin, P., Milner, P., Winter, R., Burnstock, G. (1992)Chronic hypoxia changes the ratio of endothelin to ATP release from rat aortic endothelial cells exposed to high flow. *Proc. R. Soc. Lond. B Biol. Sci.*, **247**, 131-5.

Booyse, F.M., Sedlak, B.J., Rafelson, M.E., Jr. (1975) Culture of arterial endothelial cells: characterization and growth of bovine aortic cells. *Thromb. Diath. Haemorrh.* **34**, 825-39.

Bowen, J.W. and McDonough, A. (1987) Pretranslational regulation of Na^+, K^+ ATPase in cultured canine kidney cells by low K^+. *Am. J. Physiol.* **252**, C179-C189.

Brown, D., Lydon, J., McLaughlin, M., Stuart-Tilley, A., Tyzowski, R., and Alper, S. (1996) Antigen retrieval in cryostat tissue sections and cultured cells by treatment with sodium dodecyl sulfate (SDS) *Histochem.* **105**, 261-267.

Bruck, R., Halpern, Z., Aeed, H., Shechter, Y., Karlish, S.J.D. (1998) Vanadyl ions stimulate K^+ uptake into isolated perfused rat liver via the Na^+/ K^+-pump by a tyrosine kinase-dependent mechanism. *Pflugers Arch.* **435**, 610-6.

Burridge, K., and Chrzanowska-Wodnicka, M. (1996) Focal Adhesions, Contractility, and Signaling. *Ann.Rev. Cell Dev. Biol.* **12**, 463-519.

Busse, R., & Mülsch, A. (1990) Calcium-dependent nitric oxide synthesis in endothelial cytosol is mediated by calmodulin. *FEBS*, **265**, 133-6.

Canessa, C.M., Schild, L., Buell, G., Thorens, B., Gautschi, I., Horisberger, J.D., Rossier, B.C. (1994) Amiloride-sensitive epithelial Na^+ channel is made of three homologous subunits *Nature*, **367**, 463-7

Canessa, C.M., Horisberger, J.D., Schild, L., Rossier, B.C. (1995) Expression cloning of the epithelial sodium channel. *Kidney Int.* **48**, 950-5.

Cantiello, H.F. (1995a) Actin filaments stimulate the Na^+, K^+ ATPase. *Am. J. Physiol.* **269**, F637-F643.

Cantiello, H.F. (1995b) Role of actin cytoskeleton on epithelial Na^+ channel regulation. *Kidney International*, **48**, 970-984.

Caplan, M.J., Palade, G.E., Jamieson, J.D. (1985) Cell surface expression and activation of newly synthesised Na^+, K^+ ATPase in MDCK cells. *In*:

Glynn I.M., Ellory, J.C., *Eds*. The Sodium Pump pp. 147-51.

Carraway, K.L. & Carraway C.A.C. (1992). The Cytoskeleton. Oxford Univ. Pres, Oxford.

Chatterjee, K., Digitalis and Non-ACE inhibitor vasodilators in heart failure (1989) *Cardiology Clinics,* **7**, 99-117.

Chien, S., Shyy, J.Y. (1998) Effects of hemodynamic forces on gene expression and signal transduction in endothelial cells. *Biol. Bull.* **194**, 390-3.

Chiu, J.J., Wang, D.L., Chien, S., Skalak, R., Usami, S. (1998) Effects of Disturbed Flow on Endothelial Cells. *J. Biochem. Eng.* **120**, 2-7.

Chow, D.C. and Forte, J.G. (1995) Functional significance of the β-subunit of the heterodimeric P-type ATPases. *J. Exp.Bio.* **198**, 1-17.

Clausen, T. and Flatman, J.A. (1987) Effects of insulin and epinephrine on Na^+ K^+ and glucose transport in soleus muscle. *Am. J. Physiol.* **252**, E492-E499

Coan, D.E., Wechezak, A.R., Viggers, R.F., Sauvage, L.R. (1993) Effect of shear stress upon localization of the golgi apparatus and microtubule organizing centre in cultured endothelial cells. *J. of Cell Sci.* **104**, 1145-53.

Collins, J.H., Leszyk J. (1987) The γ subunit of the Na^+, K^+ ATPase: a small amphiphillic protein with a unique amino acid sequence. *Biochemistry,* **26**, 8865-8.

Consigny, P.M., Vitali, N.J. (1998) Resistance of freshly adherent endothelial cells to detachment by shear stress is matrix and time dependent. *JVIR,* **9**, 479-85.

Cooper, G.M. (1997) The Cell: A Molecular Approach. Oxford University Press.

Cramb, G., Cutler, C.P., Lamb, J.F., McDevitt, T., Ogden, P.H., Owler, D. and Voy, C. (1989) The effects of monensin on the abundance of mRNA (α) and of sodium pumps in human cultured cells. *Quart. J. Exp. Physiol.* **74**, 53-63.

Cutler, C.P., Cramb, G., Lamb, J.F. (1988) Quantitative analysis of sodium pump-specific mRNA from human endothelial (HeLa) and canine kidney (MDCK) cell cultures. *Prog. Clin. Biol. Res.* **268B**, 59-64.

Crawford, K.M. Ernst, S.A. Meyer R.F., MacCallum, D.K., (1995) Na^+, K^+ ATPase pump sites in cultured bovine corneal endothelium of varying cell density at confluence. *Invest. Ophthalmo. Vis. Sci.* **36**, 1317-26.

Davies, P.F., Olensen, S.P., Clapham, D.E. Morrel, E.M., Schoen, F.J. (1988) Endothelial Communication- State of the art lecture. *Hypertension*, **11**, 563-72.

Davies, P.F. (1989) How do vascular endothelial cells respond to flow? *NIPS,* **4**, 22-25.

Davies, P.F Tripathi, S.C., (1993) Mechanical stress and the cell - an endothelial cell paradigm. *Circulation Res.* **72**, 239-245.

Davies, P.F. (1995) Flow-mediated endothelial mechanotransduction. *Physiol. Rev.* **75**, 519-69.

Davies, P.F. (1997) Mechanisms involved in endothelial responses to hemodynamic forces. *Atherosclerosis,* **131**, 15-17.

(date) and

Davis, J.Q. Bennet, V. The anion exchanger ad the Na^+, K^+ ATPase interact with distinct sites on ankyrin in *in vitro* assays. *J. Biol. Chem.* **265**, 17252-6.

Dean, R.B. (1941) Theories of electrolyte equilibrium in muscle. *Biol. Symp.* **3**, 331-348.

De Tomaso, A.W., Zdankiewicz, P. and Mercer, R.W. (1991) Functional expression of the Na^+, K^+ ATPase on *Spodoptera frugiperda* cell: *In*: The Sodium Pump. pp. 69-73. De Weer, P. and Kaplan J.H. *Eds.* Rockerfeller University Press, New York.

De Weer, P. and Rakowski, R.F. (1984) Current generated by backward-running electrogenic Na pump in squid giant axons. *Nature,* **309**, 450-452.

De Weer, P. (1985) Cellular sodium-potassium transport. *In*: Seldin, D.W., Giebisch, G., *Eds. The Kidney: Physiology and Pathophysiology*, New York, Raven Press pp, 31-48.

Drenckhahn, D., Jons, A, Koob, R., Kraemer, D., Wagner, S. (1993) Cytoskeleton and Epithelial polarity. *Ren Physiol. Biochem.* **16**, 6-14.

Driscoll, M., Chalfie, M. (1991) The mec-4 gene is a member of a family of Caenorhabditis elegans genes that can mutate to induce neuronal degeneration, *Nature,* **349**, 588-93.

Driscoll, M. (1996) Cell death in C. elegans: molecular insights into mechanisms conserved between nematodes and mammals. *Brain Pathol.* **6**, 411-25.

Dutta, A., Tarbell, J.M. (1996) Influence of non-Newtonian behaviour of blood on flow in an elastic artery model. *J. Biomech. Eng.* **118**, 111-9.

Easthope, P.L. and Brooks, D.E. (1980) A comparison of rheological constitutive functions for whole human blood. *Biorheology*, **17**, 235-247.

Edelstein, N.G., Catterall, W.A., Moon, R.T. (1988) Identification of a 33-kilodalton cytoskeletal protein with high affinity for the sodium channel. *Biochemistry*, **27**, 1818-22.

Emmanuel, J.R., Garetz S., Stone L., Levenson, R. (1987) Differential expression of Na+, K+ ATPase α- and β-subunit mRNA's in Rat tissues and cell lines . *Proc Natl. Acad .Sci. USA*, 9030-4.

Erdmann, E., and Hasse W. (1975) Quantitative aspects of ouabain binding to human erythrocytes and cardiac membranes. *J. Physiol.* **251**, 671-82.

Erdmann, E., Philipp, G., Scholz, H. (1980) Cardiac glycoside receptor, Na^+, K^+ ATPase activity and force of contraction in rat heart. *Biochem. Pharmacol.* **29**, 3219-29.

Eriksson, J.E.; Opal, P; Goldman, R.D. (1992) Intermediate filament dynamics. *Curr Opin. Cell Biol.* **4**, 99-104.

Evans, R.M. (1988) The steroid and thyroid hormone receptor superfamily. *Science,* **240**, 889-95.

Fambrough, D.M., Wolitzky, B.A., Taormino, J.P., Tamkun, M.M. Takeyasu, K., Somerville, D., Renaud, K.J., Lemas, M.V., Lebovitz, R.M., Kone, B.C., *et al* (1991) A cell biologist's perspective on sites of Na^+, K^+ ATPase regulation. *In*: The Sodium Pump. pp. 17-30. De Weer, P. and Kaplan J.H. *Eds*. Rockerfeller University Press, New York.

Fambrough, D.M., Lemas, M.V., Hamrick, M., Emerick, M., Renaud, K.J., Inman, E.M., Hwang, B. and Takeyasu, K. (1994) Analysis of subunit assembly of the Na^+, K^+ ATPase. *Am. J. Physiol.* **266**, C579-C589

Fortes, P.A.G. (1988) Anthroylouabain: a specific fluorescent probe for the cardiac glycoside receptor. *Biochemistry*, **16**, 531-5.

Felsenfeld, D.P., Sweadner, K.J. (1988) Fine specificity mapping and topography of an isozyme-specific epitope of the Na^+, K^+ ATPase catalytic subunit. *J. Biol. Chem.* **263**, 10932-42.

Féraille, E., Carranza, M.L., Rousselot, M., Farve, H. (1997) Modulation of Na^+, K^+ ATPase activity by a tyrosine phosphorylation process in the rat proximal convoluted tubule. *J. Physiol.* **498**, 99-108.

Feschenko, M.S. and Sweadner, K.J. (1995) Structural basis for species-specific differences in the phosphorylation of Na^+, K^+ ATPase by protein kinase C. *J. Biol. Chem.* **270**, 14072-77.

Fortes, P.A. (1977) Anthroylouabain: a specific fluorescent probe for the cardiac glycoside receptor of the Na^+, K^+ ATPase. *Biochemistry*, **16**, 531-40.

Flitney, F.W., Goldman, R.D. Skalli, O., Mercurius, K.O., Davies, P.F. (1996) Dynamic properties of intermediate filaments in cultured endothelial cells: the effects of controlled fluid shear stress. In: The Biology of Nitric Oxide, (Moncada, S., Stamler, J., Gross, S. & Higgs, E.A.) 5:251.

Flitney, F.W. (1997) BHF Grant Application.

Franke, R.P., Gräfe, M., Schnittler, H., Seiffge, D. Mittermayer, C. Drechahn, D. (1984) Induction of human vascular endothelial stress fibres by fluid shear stress. *Nature*, **307**, 648-9.

Fyfe, G.K., And Canessa, C.M. (1998) Subunit composition determines the single site channel kinetics of the epithelial sodium channel. *J. Gen. Physiol.* **112**: 423-32.

Galbraith, C.G. Skalak, R. Chien, S. (1998) Shear Stress Induces Spatial Reorganization of the Endothelial Cell Cytoskeleton. *Cell Motility and the Cytoskeleton*, **40**, 317-30.

García-Añoveros, J., Ma, C., Chalfie, M. (1995) Regulation of Caenorhabditis elegans degenerin proteins by a putative extracellular domain [published erratum appears in *Curr. Biol.* **5**, 441-8

Garcia, N. (1991) Focal and regional responses of endothelium to disturbed flow *in vitro* PhD. Thesis. Harvard-MIT Division of Health Sciences and Technology.

Geering, K. (1990) Subunit assembly and functional maturation of Na^+, K^+ ATPase. *J. Membr. Biol.* **115**, 109-21.

Geering, K. (1991) The functional role of the beta-subunit in the maturation and intracellular transport of Na^+, K^+ ATPase. *FEBS Lett.* **285**, 189-93.

Ghosh, S., Freitag, A.C., Martin-Vasallo, P., Coca-Prados, M. (1990) Cellular distribution and differential gene expression of the three alpha subunit isoforms of the Na^+, K^+ ATPase in the ocular ciliary epithelium. *J. Biol. Chem.* 1990 **265**, 2935-40.

Ghosh, S., Hernando, N., Martín-Alonso, J.M., Martin-Vasallo, P., Coca-Prados, M. (1991) Expression of multiple Na^+, K^+ ATPase genes reveals a gradient of isoforms along the nonpigmented ciliary epithelium: functional implications in aqueous humor secretion. *J. Cell Physiol.* **149**, 184-94.

Giannella, R.A., Orlowski, J., Jump, M.L. and Lingrel, J.B. (1993) Na^+, K^+ ATPase gene expression in rat intestine and Caco-2 cells: Response to thyroid hormone. *Am. J. Physiol.* **265**, G775-G782

Gick, G.G., Ismail-Beigi, F., Edelman, I.S. (1988) Thyroidal regulation of rat renal and hepatic Na^+, K^+ ATPase gene expression, *J. Biol. Chem.* **263**, 16610-8

Girardet M., Geering, K., Gaeggeler, H.P., Rossier, B.C. (1986) Control of transepithelial Na+ transport and Na^+, K^+ ATPase by oxytocin and aldosterone, *Am. J. Physiol.* **251 Pt 2**, F662-70.

Glynn, I.M., Karlish, J.D. (1975) The sodium pump, *Ann. Rev. Physiol.* **37**, 13-55.

Glynn, I.M. (1985) The Na^+-K^+-transporting adenosine triphosphatase. *In:* The Enzymes of Biological membranes *Eds*: Martonosi, A.N. Plenum Press, New York pp, 35-114.

Glynn, I.M., Karlish, S.J. (1990) Occluded cations in active transport, *Ann. Rev. Biochem.* **59**, 171-205.

Glynn, I.M. (1993) All hands to the sodium pump. Annual Review prize Lecture. *J. Physiol.* **462**, 1-30.

Georgatos, S.D., and Marchesi, V.T. (1985) The binding of vimentin to human erythrocytes membranes: a model system for the study of intermediate filaments-membrane interactions. *J.Cell Biol.* **100**, 1955-61.

Goldman, R.D. & Steinert, P.M. (Editors) (1990) Cellular and Molecular Biology of Intermediate Filaments.

Goldman, R.D., Khoun, S., Chou, Y.H., Opal, P. & Steinert, P.M. (1996) The function of intermediate filaments in cell shape and cytoskeleton integrity. *J.Cell Biol.* **134**, 971-83.

Goldshleger, R., Tal, D.M., Karlish, S.J. (1995) Topology of the alpha-subunit of Na^+, K^+ ATPase based on proteolysis. Lability of the topological organization. *Biochemistry,* **34**, 8668-79.

Good, P.J., Richter, K. and Dawid, I.B. (1990) A nervous system-specific isotype of the beta subunit of the Na^+, K^+ ATPase expressed during early development of Xenopus laevis. *Proc. Natl. Acad. Sci. U.S.A.* **87**, 9088-9092.

Georgatos, S.D. and Marchesi, V.T. (1985) The binding of vimentin to human erythrocyte membranes: a model system for the study of intermediate filament-membrane interactions. *J. Cell Biol.***100**, 1955-61

Griffiths, N.M., Ogden, P.H., Cormack, R., and Lamb, J.F. (1991) Discrepancy between the short and long term effects of ouabain on the sodium pump of human cells. *Br. J. Pharmacol.* **104**, 419-427.

Guiramand, J., Lenoir, M., Pujol, R., Récasens, M. (1990) Ototoxic and nephrotoxic drugs inhibit agonist-induced inositol phosphateformation in rat brain synaptoneurosomes. *Toxicol. Lett.* **51**, 331-8.

Hammerton, R.W., Krzeminski, K.A., Mays, R.W., Ryan, T.A., Wollner, D.A., Nelson, W.J. (1991) Mechanism for regulating cell surface distribution of Na^+, K^+ ATPase in polarized epithelial cells. *Science*, **254**, 847-50.

Hall, A.C., Starks, I., Shoults, C. and Rashidbigi,S. (1996) The cellular physiology of articular cartilage. *Exp. Physiol.* **81**, 535-45.

Harris, W.E., Stahl, W.L. (1988) Origin of the gamma polypeptide of the Na^+, K^+ ATPase. *Biochim. Biophys. Acta*, **942**, 236-44.

Hecker, V., Mülsch, A., Bassenge, E., Förstermann,U., Busse, R. (1994) Subcellular Localization and characterization of nitric oxide synthase(s) in endothelial cells: physiological implications. *Biochem. J.* **299**, 247-252.

Hernando, N., Martin, Vasallo P., Ghosh, S., Ghosh, P.K., Swaroop, A., Coca Prados, M. (1994) Nucleotide sequence of a cDNA for the beta 2 subunit isoform of Na^+, K^+ ATPase from human retina. *Biochim. Biophys. Acta.* **1189**, 109-11.

Herrera, V.L., Emanuel, J.R., Ruiz-Opazo, N., Levenson, R., Nadal-Ginard, B. (1987) Three differentially expressed Na^+, K^+ ATPase alpha subunit isoforms: structural and functional implications. *J. Cell. Biol.* **105**, 1855-65.

Hinson, J.P., Dawnay, A.B. and Raven, P.W. (1995) Why we should give a qualified welcome to ouabain: a whole new family of adrenal steroid hormones. *J. Endo.* **146**, 365-68.

Horisberger, J-D., Lemas, V., Kraehenbühl, J-P. and Rossier, B.C. (1991) Structure-Fuction relationship of Na^+, K^+ ATPase. *Ann. Rev. Physiol.* **53**, 565-584.

Horowitz, B., Hensley, C.B., Quintero, M., Azuma, K.K., Putnam, D. and McDonough, A.A. (1990) Differential regulation of Na^+, K^+ ATPase $\alpha 1$, $\alpha 2$ and $\beta 1$ subunit mRNA and protein levels by thyroid hormone. *J. Biol. Chem.* **265**, 14308-14.

Hug, T., Koslowsky, T., Ecke, D., Greger, R., Kunzelmann, K. (1995) Actin-dependent activation of ion conductance in bronchial epithelial. *Pflugers Arch.* **429**, 682-90.

Hunter, M. (1990) Stretch-activated channels in the basolateral membrane of single proximal cells of frog kidney. *Pflugers Arch.*, **416**, 448-53.

Isenmann, S., Brandner, S., Sure, U., Magyar, J.P., Schachner, M., Aguzzi, A. (1994) [Morphology and development of neural transplants of AMOG-deficient mice]. *Verh Dtsch Ges Pathol.* **78**, 433-7.

Ismail-Beigi, F., Edelman, I.S. (1970) Mechanism of thyroid calorigenesis: role of active sodium transport. *Proc. Natl. Acad. Sci. U S A* **67**, 1071-8.

Jaisser, F., Horisberger, J-D. and Rossier, B.C. (1992) The β subunit modulates potassium activation of the Na, K-pump. *Annals of the New York Academy of Science*, **671**, 113-19.

Jaisser, F., Jaunin, P., Geering, K. Rossier, B.C. and Horisberger, J-D. (1994) Modulation of the Na, K-pump function by β subunit isoforms. *J. Gen. Physiol.* **103**, 605-23.

Jewell, E.A. and Lingrel, J.B. (1991) Comparison of the substrate dependence properties of the rat Na^+, K^+ ATPase alpha 1, alpha 2, and alpha 3 isoforms expressed in HeLa cells. *J. Biol. Chem.* **266**, 16925-30.

Jordan, C., Püschel, B., Koob, R., Drenckhahn, D. Identification of a binding motif for ankyrin on the alpha-subunit of Na^+, K^+ ATPase. *J. Biol. Chem.* 1995, **270**: 29971-5.

Jorgensen, P.L. (1975) Isolation and characterisation of the components of the sodium pump. *Q. Rev. Biophys.* 7, 239-74.

Jorgensen, P.L. (1982) Protein structure and conformation of the pure Na^+, K^+ ATPase *Biochim. Biophys. Acta.* **694**, 27-68

Jorgensen, P.L. (1986) Structure, function and regulation of Na^+, K^+ ATPase in the kidney. *Kidney Int.* **29**, 10-20.

Jorgensen, P.L., Collins, J.H. (1988) Localization of tryptic and chymotryptic cleavage sites in alpha-subunit of Na^+, K^+ ATPase. *Prog. Clin. Biol. Res.* **268A**, 85-92.

Kano, Y., Katoh, K., Masuda, M., Fujiwara, K. (1996) Macromolecular composition of stress fiber-plasma membrane attachment sites in endothelial cells in situ. *Circ. Res.* **79**, 1000-6.

Karlish, S.J., Jorgensen, P.L., Gitler, C. (1977) Identification of a membrane-embedded segment of the large polypeptide chain of Na^+, K^+ ATPase. *Nature*, **269**, 715-7.

Kawakami, K., Ohta, T., Nojima, H., Nagano, K. (1986) Molecular cloning and sequence analysis of human Na^+, K^+ ATPase beta-subunit. *Nucleic Acids Res*, **11**, 2833-44.

Kawakami, K., Masuda, K., Nagano, K., Ohkuma, Y., Roeder, R.G. (1996) Characterization of the core promoter of the Na^+, K^+ ATPase alpha 1 subunit gene. Elements required for transcription by RNA polymerase II and RNA polymerase III in vitro. *Eur. J. Biochem.* **237**, 2, 440-6.

Kawamura, M. Nagano, K. Evidence for essential disulfide bonds in the beta-subunit of Na^+, K^+ ATPase. (1984) *Biochim. Biophys. Acta*; **774**, 188-92.

Kennedy, D.G., Aronson, J.K., Bloomfield, J.G., Grahame-Smith, D.G. (1990) The effects of a low extracellular concentration of potassium on the activity and numbers of Na+/K+ pumps in an EB-virus transformed human lymphocyte cell line. *Biochim. Biophys. Acta*, **1027**, 218-24

Khachigian, L.M., Lindner, V, Williams, A.J., Collins, T. (1996) Egr-1-induced endothelial gene expression: a common theme in vascular injury. *Science*, **271**, 1427-31.

Kim, D.W. Gotlieb, A.I., Langille, B.L. (1989) In vivo modulation of endothelial f-actin microfilaments by experimental alterations in shear stress. *Arteriosclerosis,* **9**, 439-45.

Kimelberg, H.K., Kettenmann, H. (1990) Swelling-induced changes in electrophysiological properties of cultured astrocytes and oligodendrocytes. I. Effects on membrane potentials, input impedance and cell-cell coupling. *Brain Res.* **529**, 255-61.

Kizer, N., Guo, X.L., Hruska, K. (1997) Reconstitution of stretch-activated cation channels by expression of the a-subunit of the epithelial sodium channel cloned for osteobalsts. *Prod. Natl. Acad. Sci.*. **94**, 1013-1018.

Klip, A., Ramlal, T., Cragoe, E.J. Jr. (1986) Insulin-induced cytoplasmic alkalinization and glucose transport in muscle cells. *Am. J. Physiol*, **250 Pt 1**, C720-8.

Knapp, L.W. Oguin, W.M., Sawyer, R.H. (1983) Drug-induced alterations of cytokeratin organization in cultured epithelial cells. *Science*, **219**, 501-3.

Kobayashi, M., Kawakami, K. (1995) ATF-1CREB heterodimer is involved in constitutive expression of the housekeeping Na^+, K^+ ATPase alpha 1 subunit gene. *Nucleic Acids Res.* **23**, 2848-55.

Kobayashi, M., Shimomura, A., Hagiwara, M., Kawakami, K. (1997) Phosphorylation of ATF-1 enhances its DNA binding and transcription of the Na^+, K^+ ATPase alpha 1 subunit gene promoter. *Nucleic Acids Res.* **25**, 877-82.

Kobayashi, M., Kawakami, K. (1997) Synergism of the ATF/CRE site and GC box in the housekeeping Na^+, K^+ ATPase alpha1 subunit gene is essential for constitutive expression. *Biochem. Biophys. Res. Commun.* **241**, 169-74.

Koob, R., Zimmermann, M., Schoner, W., Drenckhahn, D. (1988) Colocalization and coprecipitation of ankyrin and Na^+, K^+ ATPase in kidney epithelial cells. *Eur. J. Cell Biol.* **45**, 230-7.

Koller, A. Kaley, G. (1998) Shear stress-induced dilation of arterioles. *Am J Physiol.* **274**, Pt 2, H382-3.

Korenaga, R., Ando, J., Kosaki, K., Isshiki, M., Tadaka, Y., Kamiya, A. (1997) Negative transcriptional regulation of VCAM-1 gene by fluid shear stress in murine endothelial cells. *Am. J. Physiol.* **273**, 1506-15.

Kyte, J., Doolittle, R.F. (1982) A simple method for displaying the hydropathic character of a protein. *J. Mol. Biol.* **157**, 105-32.

Lamb, J.F. and Lindsay, R. (1971) Effect of Na^+, metabolic inhibitors and ATP on Ca^{2+} movement in L cells. *J Physiolol.* **218**, 691-708.

Lamb, J.F., Newton, J.P. (1972) Effect of cycloheximide and actinomycin D on Na pump density in Hela cells. *J. Physiol.* (Lond), **231**, 11P-12P.

Lamb, J.F., McCall, D. (1972) Effect of prolonged ouabain treatment of Na, K, Cl andCa concentration and fluxes in cultured human cells *J. Physiol.* (Lond), **225**, 599-617.

Lamb, J.F, Boardman, L.J., Newton, J.P., Aiton, J.F., (1973) Effect of calf serum on sodium pump density in HeLa cells. *Nat. Rev. Biol*, **242** 115-7.

Lamb, J.F. Regulation of sodium pump abundance in animal cells. (1988) *Prog. Clin. Biol. Res*, **273**, 361-8.

Lamb, J.F., Flitney, E.F., Lazarus, C., (1996) Interaction of the sodium pump and the cytoskeleton in cultured human cells. (*J. Physiol*) in press.

Lansman, J.B. (1988) Going with the flow. *Nature*, **331**, 481-2.

Published update

Lavoie, L., Roy, D., Ramlal, T., Dombrowski, L., Martin Vasallo, P., Marette, A., Carpentier., J.L., Klip, A. (1996) Insulin-induced translocation of Na^+, K^+ ATPases subunits. *Am. J. Physiol.* **270**, Pt 1, C1421-9.

Lazarides, E. (1980) Intermediate filaments as mechanical integrators of cellular space. *Nature*, **283**, 249-56.

Lazarides, E. (1982) Intermediate Filaments: A chemically heterogeneous, developmentally regulated class of proteins. *Ann. Rev. Biochem.* **51**, 219-50.

Leberer, E., Härtner, K.T., Brandl, C.J., Fujii, J., Tada, M., MacLennan, D.H., Pette, D. (1989) Slow/cardiac sarcoplasmic reticulum Ca^{2+}-ATPase and phospholamban mRNAs are expressed in chronically stimulated rabbit fast-twitch muscle. *Eur. J. Biochem*, **185**, 51-4.

Lecuona, E., Luquín, S., Avila, J., García Segura, L.M., MartínVasallo, P. (1996) Expression of the beta 1 and beta 2(AMOG) subunits of the Na^+, K^+ ATPase in neural tissues: cellular and developmental distribution patterns *Brain Res. Bull.* **40**, 167-74.

Lescale-Matys, L., Putnam, D.S. and McDonough, A.A. (1993) Na^+, K^+ ATPase α1- and β1-subunit degradation: evidence for multiple specific rates. *Am. J. Physiol.* **246**, C583-C590.

Levesque, M.J., Nerem, R.M. (1985) The eleongation and orientation of cultured endothelial cells in respose to shear stress. *J. Biomech. Eng.* **107**, 341-47.

Leiska, N., Yang, H-Y. & Goldman, R.D. (1985) Purification of the 300KDa intermediate filament-associated protein and its in vitro recombination with intermediate filaments. *J. Cell Biol.* **101**, 802-13.

Lin, M.H., Akera, T. (1978) Increased Na^+, K^+ ATPase concentrations in various tissues of rats caused by thyroid hormone treatment. *J. Biol. Chem.* **253**, 723-6.

Lin, M.C., Almus-Jacobs, F., Chen, H.H., Parry, G.C., Mackman, N., Shyy, J.Y., Chien, S. (1997) Shear stress induction of the tissue factor gene. *J. Clin. Invest.* **99**, 737-44.

Lingrel, J.B., Orlowski, J., Shull, M.M. and Price, E.M. (1990) Molecular genetics of Na^+, K^+ ATPase. *Prog. Nucleic. Acid. Res. Mol. Biol.* **36**, 37-89.

Lingrel, J.B. (1992) Na^+, K^+ ATPase: isoform structure, function, and expression. *J. Bioenerg. Biomembr.* **24**, 263-70.

Lingrel, J.B., Van-Huysse, J., O'Brien, W., Jewell-Motz, E., Askew, R. and Schultheis, P. (1994) Structure-function studies of the Na^+, K^+ ATPase. *Kidney Int.* **44**, S32-S39.

Liu, J., Schrank, B., Waterston, R.H. (1996) Interaction between a putative mechanosensory membrane channel and a collagen. *Science*, **273**: 361-4.

Lo, C.S., Edelman, I.S. (1976) Effect of triiodothyronine on the synthesis and degradation of renal cortical Na^+, K^+ ATPase. *J. Biol. Chem.* **251**, 783-40.

Lo, C.S., Lo, T.N. (1980) Effect of triiodothyronine on the synthesis and degradation of the small subunit of renal cortical Na^+, K^+ ATPase. *J. Biol. Chem.* **255**, 2131-6.

Lytton, J. (1985) Insulin affects the sodium affinity of the rat adipocyte Na^+, K^+ ATPase. *J. Biol. Chem.* **260**, 1075-80.

Lytton, J., Lin, J.C. and Guidotti, G. (1985) Identification of two molecular forms of Na^+, K^+ ATPase in rat adipocytes. *J. Biol. Chem.* **260**, 1177-1184.

Magyar, J.P., Bartsch, U., Wang, Z.Q., Howells, N., Aguzzi, A., Wagner, E.F., Schachner, M., (1994) Degeneration of neural cells in the central nervous system of mice deficient in the gene for the adhesion molecule on Glia, the beta 2 subunit of murine Na^+, K^+ ATPase. *J. Cell Biol.* **1127**, 835-45.

Malek, A.M., & Izumo, S. (1996) Mechanisms of endothelial cell shape change and cytoskeletal remodelling in response to fluid shear stress. *J. Cell Sci.* **109**, 713-26.

Mandel, L.J., Doctor, R.B., Bacallao, R. (1994) ATP depletion: a novel method to study junctional properties in epithelial tissues. II. Internalization of Na^+, K^+ ATPase and E-cadherin. *J. Cell. Sci.* **107**, 3315-24.

Mano, I., Driscoll, M. (1999) DEG/ENaC channels: a touchy superfamily that watches its salt. *Bioessays*, **21**, 568-78.

Marchenko, S.M. and Sage, S.O. (1997) A novel mechanosensitive cationic channel from the endothelium of rat arota. *J. Physiol.* **498**, 419-25.

Marín, J. and Angeles Rodríguez-Martinéz, M. (1997) Role of vascular nitric oxide in physiological and pathological conditions. *Pharmacol. Ther.* **75**, 111-134.

Martin-Vasallo, P., Dackowski, W., Emanuel, J.R., Levenson, R. (1989) Identification of a putative isoform of the Na^+, K^+ ATPase beta subunit. Primary structure and tissue-specific expression. *J. Biol. Chem.* **264**, 4613-8.

Martinez-Fong, D. Mullersman, J.E., Purchio, A.F., Armendariz-Borunda, J., Martinez-Hernandez, A. (1994) Nonenzymatic glycosylation of poly-L-lysine: a new tool for targeted gene delivery. *Hepatology*, **20**, 1602-8.

Mason, D.T., Zelis, R., Lee, G., Hughes, J.L., Spann, J.F. Jr., Amsterdam, E.A. (1971) Current concepts and treatment of digitalis toxicity. *Am. J. Cardiol.* **27**, 546-59.

Masuda, M. and Fujiwara, K. (1992) Morphological responses of single endothelial cells exposed to physiological levels of fluid shear stress. *Frontiers Med. Biol. Enging.* **5**, 79-87.

Masuda, M. and Fujiwara, K. (1993) The biased lamellipodium development and microtubule organizing centre position in vascular endothelial cells migrating under the influence of fluid flow. *Biol. Cell*, **77**, 237-245.

Massey, B.S. (1989) Mechanics of Fluids, Sixth edition. T.J.Press LtD, Padstow, Cornwall. pp 599.

Maunsbach, A.B., Skriver, E., Jorgensen, P.L. (1988) Analysis of Na^+, K^+ ATPase by electron microscopy. *Methods Enzymol.* **156**, 430-41.

McCormick, S.D. (1990) Fluorescent labelling of Na^+, K^+ ATPase in intact cells by use of a fluorescent derivative of ouabain: Salinity in teleost chloride cells. *Cell Tissue Res.* **260**, 529-33.

McDonough, A.A., Geering, K. and Farley, R.A. (1990) The sodium pump needs its beta subunit. *FASEB J.* **4**, 1598-1605.

McGrail, K.M., Phillips, J.M., Sweadner, K.J. (1991) Immunofluorescent localization of three Na^+, K^+ ATPase isozymes in the rat central nervous system: both neurons and glia can express more than one Na^+, K^+ ATPase. *J. Neurosci.* **11**, 381-91.

Mercer, R., (1993) Structure of Na^+, K^+ ATPase. *Interl. Review of Cyto.* **137**, 139-68.

Mircheff, A.K. (1989) Isolation of plasma membranes from polar cells and tissues: apical/basolateral separation, purity, function. *Methods Enzymol.* **172**, 18-34.

Milner P; Bodin P; Loesch A; Burnstock G (1992) Increased shear stress leads to differential release of endothelin and ATP from isolated endothelial cells from 4- and 12-month-old male rabbit aorta. *J. Vasc. Res.* **29**, 420-5.

Mobasheri, A., Smith, A.L., France, S.J., Urban, J.P.G. and Hall, A.C. (1995) Autoradiographic localisations of the Na^+, K^+ ATPase in isolated bovine articular chondrocytes; correlation of density with tissue [Na^+]. *J. Physiol.* **489**, 65P 9 (abstract).

Mobasheri, A. (1996) The effect of the extracellular environment on sodium pump density in cartilage. Thesis (Ph.D.) Oxford University.

Mobasheri, A., Killick, R., Trujillo, E., Alverez ce la Rosa, D., Marín, J., Canessa, C.M., Martín-Vasallo, P. (1999) Subunits of the sodium channel in avian and human chondrocytes. *J. Physiol.* **518**, P.117 (*Abstract submitted).*

Moczydlowski, E.G., and Fortes (1980) Kinetics of cardiac glycoside binding to the sodium, potassium adenosine triphosphatase studied with a fluorescent derivative of ouabain. *Biochemistry*, **19**, 969-77.

Mogensen, M.M., Mackie, J.B., Doxey, S.J., Stearns, T., Tucker, J.B (1997). Centrisomal deployment of γ-tubulin and pericentrin; evidence for a microtubule-nucleating domain and a minus-end docking domain in certain mouse epithelial cells. Cell motility and the cytoskeleton, **36**, 276-90.

Molitoris, B.A., Geerdes, A., McIntosh, J.R. (1991) Dissociation and redistribution of Na^+, K^+ ATPase from its surface membrane actin cytoskeletal complex during cellular ATP depletion. *J. Clin. Invest.* **88**, 462-9.

Molitoris, B.A., Dahl, R., Geerdes, A. (1992) Cytoskeleton disruption and apical redistribution of proximal tubule Na^+, K^+ ATPase during ischemia. *Am. J. Physiol.* **263** (Pt 2), F488-95.

Morrow, J.S., Cianci, Ardito, T., Mann, S., Kashgarian, M. (1989) Ankyrin links fodrin to the alpha subunit of the Na^+, K^+ ATPase in madin-darby canine kidney cells and in intact renal tubule cells. *J. Cell Biol.* **108**, 445-465.

Müller-Husmann, G., Gloor, S., Schachner, M. (1993) Functional characterization of beta isoforms of murine Na^+, K^+ ATPase. The adhesion molecule on glia (AMOG/beta 2), but not beta 1, promotes neurite outgrowth. *J. Biol. Chem.* **268**, 26260-7.

Nelson, W.J., Veshnock,P.J. (1987) Ankyrin binding to Na^+, K^+ ATPase and implications for the organization of membrane domains in polarized cells. *Nature*, **328**, 533-6.

Nelson, W.J., Hammerton, R.W., McNeill, H. (1991) Role of the membrane-cytoskeleton in the spatial organization of the Na^+, K^+ ATPase in polarized epithelial cells. *Soc. Gen. Physiol. Ser.* **46**, 77-87.

Noguchi, S., Mishina, M., Kawamura, M., Numa, S. (1987) Expression of functional Na^+, K^+ ATPase from cloned cDNAs. *FEBS Lett*, **225**, 27-32.

Oh ,V.M., Taylor, E.A., Ding, J.L., Boon, N.A., Aronson, J.K.,Grahame-Smith, D.G. (1987) Enhancement of specific [^{3}H]ouabain binding and ouabain sensitive ^{86}rubidium influx in intact human lymphocytes by a dialysable factor in human and fetal calf serum. *Clin. Sci.* **72**, 71-9.

Orlowski, J., Lingrel, J.B. (1988) Tissue-specific and developmental regulation of rat Na^+, K^+ ATPase catalytic alpha isoform and beta subunit mRNAs. *J. Biol. Chem.* **263**, 10436-42.

Oluwole, B.O., Du, W., Mills, I., Sumpio, B.E. (1996) Gene regulation by mechanical forces. *Endothelium*, **5**, 85-93.

Oluwole, B.O., Du, W., Mills, Sumpio, B.E. (1997) Gene regulation by mechanical forces. *Endothelium*, **5**, 85-93.

Overton, E. (1902) Beiträge zur allgemeinen muskel und nervenphysiologie II. Ueber die unenthehrliehkeit von natrium (oder lithium) ionen für den contractionsact des muskels. *Pflügers Arch.* **92**, 346-86.

Paccolat, M.P., Geering, K., Gaeggler, H.P. Rossier, B.C. (1987) Aldosterone regulation of Na+ transport and Na^+, K^+ ATPase in A6 cells: role of growth conditions. *Am. J. Physiol.* **252**, c468-76.

Pedemonte, C.H., Kaplan, J.H. (1992) A monosaccharide is bound to the α-subunit. *Biochemistry*, **31**, 10465-10470.

Palade, G. (1975) Intracellular aspects of the process of protein synthesis. *Science,* **189**, 347-358.

Paller, M.S. (1994) Lateral mobility of Na^+, K^+ ATPase and membrane lipids in renal Cells. Importance of cytoskeletal integrity. *Membrane Biol.* **142**, 127-35.

Perrone, R.D. and McLaughlin, M.L. (1989) Cyst function in polycystic disease: nongradient cyst. *Clin. Nephro.* **32**, 113-18.

Pollack, L.R., Tate, E.H., Cook, J.S. (1981) Turnover and Regulation of Na^+, K^+ ATPase in Hela cells. *J. Cell Physol.* **241**, C173-83.

Pressley, T.A. (1988a.) Ion concentration-dependant regulation of Na, K-pump abundance. *J. Membr. Biol.* **105**, 187-195.

Pressley, T.A. (1988b.) Ismail-Beigi F, Gick G.G., Edelman, I.S. Increased abundance of Na^+, K^+ ATPase mRNAs in response to low external K^+. *Am. J. Physiol.* **255**, C252-260.

Pressley T.A (1992). Phylogenetic conservation of isoform-specific regions within alpha-subunit of Na^+, K^+ ATPase *Am. J. Physiol.*, **262**, C743-51

Price, E.M., Lingrel, J.B., (1988) Structure-function relationships in the Na^+, K^+ ATPase α subunit: Site directed mutagenesis of glutamine-111 to arginine and asparagine-122 to aspartic acid generates a ouabain resistant enzyme. *Biochemistry*, **27**, 8400-8.

Price, E.M., Rice, D.A., Lingrel, J.B., (1989) Site-directed mutagenesis of a conserved, extracellular aspartic acid residue affects the ouabain sensitivity of sheep Na^+, K^+ ATPase. *J. Biol. Chem.* **264**, 21902-6.

Rapeport, W.G., Aronson, J.K, Grahame-Smith, D.G., Carver, J.G. (1985) Increased specific [^{3}H]-ouabain binding to lymphocytes after incubation with acetylstrophantidine for 3 days. *Br. J. Clin. Pharmac.* **20**, 277-8.

Rapeport, W.G., Aronson, J.K., Grahame-Smith, D.G., Harper, C. (1986) The effects of serum, lithium, ethacrynic acid, and a low external concentration of potassium on specific [^{3}H]-ouabain binding to human lymphocytes after incubation for 3 days. *Br. J. Clin. Pharmacol,* **22**, 275-9.

Rapoport, R.M., Schwartz, K., Murad, F. (1985a) Effects of Na^+, K^+ -pump inhibitors and membrane depolarizing agents on acetylcholine-induced endothelium-dependent relaxation and cyclic-GMP accumulation in rat aorta. *Euro. J. Pharmacol.* **110**, 203-9.

Rapoport, R.M., Schwartz, K., Murad, F. (1985b) Effect of sodium-pump inhibitors and membrane-depolarizing agents on sodium nitroprusside-induced relaxation and cycle guanosine monophosphate accumulation in rat aorta. *Circ. Res.* **57**, 164-70.

Redondo, J., Perió, C., Rodríguez -Mañas, Salaices, M., Marín, J., Sánches – Ferrer, C.F. (1995) Endothelial stimulation of sodium pump in cultured vascular smooth muscle. *Hypertension,* **26**, 177-85.

Redondo, J., Rodríguez Martínez, M.A., Alonso, M.J., Salaices, M., Balfagón, G. Marín, J. (1996) Endothelium stimulates the vascular smooth muscle cell Na/K pump of normotensive and hypertensive rats by a protein kinase C pathway. *J. Hypertens.* **14**, 1301-7.

Remuzzi, A., Dewey, C.F. Jr., Davies, P.F., Gimbrone, M.A. Jr. (1984) Orientation of endothelial cells in shear fields in vitro. *Biorheology*, **21**, 617-30.

Richter, H.P., Jung, D., Passow (1984) Regulatory changes of membrane transport and ouabain binding during progesterone-induced maturation of Xenopus oocytes. *J. Membr. Biol.* **79**, 203-10.

Rindler, M.J. and Saier, M.H. Jr. (1981) Evidence for Na+/H+ antiport in cultured dog kidney cells (MDCK). *J. Biol. Chem.* **256**,10820-5.

Rodriguez-Boulan, E., and Salas, P.I.J. (1989) External and Internal signals for epithelial cell surface polarization. *Annu. Rev. Physiol.* **51**, 741-54.

Rossier, B.C., Canessa, C.M., Schild, L., and Horisberger, J.D. (1994) Epithelial Sodium Channels. *Current Opin. Nephrol. And Hyperten.* **3**, 487-96.

Rossier, B.C., Geering, K., Kraehenbuhl, J.P. (1987) Regulation of the sodium pump; how and why? *TIBS,* **12**, 483-9.

Roudier-Pujol, C., Rochat, A., Escoubet, B., Eugène, E., Barrandon, Y., Bonvalet, J.P., Farman, N. (1996) Differential expression of epithelial sodium channel subunit mRNAs in rat skin. *J. Cell Sci.* **109**, Pt 2, 379-85.

Russo, J.J., Sweadner, K.J. Na^+, K^+ ATPase subunit isoform pattern modification by mitogenic insulin concentration in 3T3-L1 preadipocytes (1993) *Am. J. Physiol.* **264**, 2 Pt 1, C311-6.

Ryu, G.H., Kim, J. Ruggeri, Z.M., Han, S.H. Kim, J.H., Min, B.G. (1995) Effect of shear stress on fibrinogen adsorption and its conformational change. *ASAIO J.* **41**, M384-8.

Sabine, V. (1997) An immunofluorescence study on the effects of cytochalasin d on the cytoskeleton of cultured endothelial cells. BSc. *Unpublished*, St. Andrews University.

Sackin, H. (1995) Mechanosensitive channels. *Ann. Rev. Physiol.* **57**, 333-53.

Salwen, S.A., Szarowski, D.H., Turner, J.N. Bizios, R. (1998) Three-Dimensional changes of the cytoskeleton of vascular endothelial cells exposed to sustained hydrostatic pressure. *Med. Biol. Eng.Comput.* **36**, 520-27.

Sargeant, R.J., Liu, Z., Klip, A. (1995) Action of insulin on Na^+, K^+ ATPase and the Na(+)-K(+)-2Cl- cotransporter in 3T3-L1 adipocytes. *Am. J. Physiol.* **269**, Pt 1, C217-25.

Shainskaya, A. and Karlish, S.J. (1994) Evidence that the cation occlusion domain of Na^+, K^+ ATPase consists of a complex of membrane-spanning segments. Analysis of limit membrane-embedded tryptic fragments. *J. Biol. Chem.* **269**, 10780-9.

Scheiner-Bobis, G., Farley, R.A. (1994) Subunit requirements for expression of functional sodium pumps in yeast cells. *Biochim. Biophys. Acta*, **1193**, 226-34.

Schmalzing, G., Kroner, S., Schachner, M., Gloor, S., (1992) The adhesion molecule on glial (AMOG/β2) and α1 subunits assemble to functional sodium pumps in *Xenopus* oocytes. *J. Biol. Chem.* **267**, 20212-6.

Schwartz, A.L., Lindenmayer, G.E., Allen, J.C. (1975) The sodium-potassium adenosinetriphosphatase: Pharmacological, physiological and biochemical aspects. *Pharmaco. Rev.* **27**, 3-134.

Schwartz, A., Grupp, G., Wallick, E., Grupp, I.L. Ball, W.J. Jr. (1988) Role of the Na^+, K^+ ATPase in the cardiotonic action of cardiac glycosides. *Prog. Clin. Biol. Res.* **268B**, 321-38.

Shah, V., Braverman, R., Prasad, G.L. (1998) Suppression of neoplastic transformation and regulation of cytoskeleton by tropomyosins Somat Cell *Mol. Genet.* **24**, 273-80.

Shamraj, O.I., Grupp, I.L., Grupp, G., Melvin, D., Gradoux, N., Kremers, W., Lingrel, J.B., De Pover, A. (1993) Characterisation of Na^+, K^+ ATPase, its isoforms, and the inotropic response to ouabain in isolated failing human hearts. *Cardiovasc. Res.* **27**, 2229-37.

Shamraj, O.I. and Lingrel, J.B. (1994) A putative fourth Na^+, K^+ ATPase alpha-subunit gene is expressed in testis. *Proc. Natl. Acad. Sci. U S A*, **91**, 2952-6.

Shull, G.E., Schwartz, A., Lingrel, J.B., (1985) Amino-acid sequence of the catalytic subunit of the Na^+, K^+ ATPase deduced from a complementary DNA. *Nature*, **316**, 691-695.

Shull, G.E., Lane, L.K., Lingrel, J.B. (1986a) Amino-acid sequence of the beta-subunit of the Na^+, K^+ ATPase deduced from a cDNA. *Nature*, **321**, 429-31.

Shull, G.E., Greeb, J. Lingrel, J.B., (1986b) Molecular cloning of three distinct forms of the Na^+, K^+ ATPase alpha-subunit from rat brain. *Biochemistry*, **125**, 8125-32.

Shull, G.E., Lingrel, J.B. (1986c) Molecular cloning of the rat stomach H^+,K^+ATPase. *J. Biol. Chem.* **261**, 16788-91

Shull M.M.,and Lingrel, J.B. (1987) Multiple genes encode the human Na^+,K^+ ATPase catalytic subunit. *Proc. Natl. Acad. Sci. U S A*, **84**, 4039-43.

Sims, J.R. Karp, S, Ingber, D.E. (1992) Altering the cellular mechanical force balance results in integrated changes in cell cytoskeletal and nuclear shape. *J. Cell Sci.* **103**, Pt 4, 1215-22.

Siegel, G., Malmsten, M., Klüssendorf, D., Hofer, H.W. (1997) Vascular smooth muscle, a multiply feedback-coupled system of high versatility, modulation and cell-signaling variability. *Int. J. Microcirc. Clin. Exp.* **17**, 360-73.

Skou J.C. (1957) The influence of some cations on adenosine triphosphatase from peripheral nerves. *Biochim. Biophys. Acta.* **23**, 394-401.

Skou, J.C., Essman, M. (1992) The Na^+, K^+-ATPase. *J. Bioenerg. Biomembr.* **24**, 249-61.

Smith, J.B., Rozengurt, E. (1978) Serum stimulates the Na^+, K^+ pump in quiescent fibroblasts by increasing the Na^+ entry. *Proc. Natl. Acad. Sci. USA* **75**, 5560-4.

Smith, P.R., Saccomani, G., Joe, E.H., Angelides, K.J., Benos, D.J. (1991) Amiloride-sensitive sodium channel is linked to the cytoskeleton in renal epithelial cells. *Proc. Natl. Acad. Sci.* U S A, **88**, 6971-5.

Steinert, P.M., Jones, J.C.R. and Goldman, R.D. (1984) Intermediate Filaments. *J. Cell Biol.* **99**, 22s-27s.

Strous ,G.J., van Kerkhof, P.,van Bokhoven, A., Schwartz, A.L., de Pont, J.J. (1988) Effect of primaquine on the topology of Na^+, K^+ ATPase and the receptor for asialoglycoproteins. *Prog. Clin. Biol. Res.* **268B**, 437-42.

Suciu, A., Civelekoglu, G., Tardy, Y., Meister, J.-J. (1997) Model for the alignment of actin filaments in endothelial cells subjected to fluid shear stress. *Bulletin of Mathe. Biol.* **59**, 1029-46.

Sweadner, K.J. (1989) Isozymes of the Na^+, K^+ ATPase. *Biochim. Biophys. Acta.* **988**, 185-220.

Sweadner, K.J. (1995) Na^+, K^+ ATPase and its isoforms. *Neuroglia Eds*: H. Kettenmsann & B.R. Ransom, Oxford Univ. Press, New York pp, 259-272.

Takeyasu, K., Lemas, V., Fambrough, D.M.(1990) Stability of Na^+, K^+ ATPase alpha-subunit isoforms in evolution. *Am J Physiol.* **259**, 4 Pt 1, C619-30.

Tamkun, M.M. and Fambrough, D.M. (1986) The Na^+, K^+ ATPase of chick sensory neurons. *J.Biol.Chem.* **261**, 1009-19.

Taormino, J., Fambrough, D.M.(1990) Pre-translational regulation of the Na^+, K^+ ATPase in response to demand for ion transport in cultured chicken skeletal muscle. *J. Biol. Chem*, **265**, 4116-23.

Tavernarakis, N., Driscoll, M. (1997) Molecular modeling of mechanotransduction in the nematode Caenorhabditis elegans. *Ann. Rev. Physiol.* **59**, 659-89.

italics

Thurston, G.B., (1975) Elastic effects in pulsatile blood Flow. *Microvas. Res.* **9**, 147-157.

Traub, O., Ishida, T., Ishida, M., Tupper, J.C., Berk, B.C. (1999) Shear stress-mediated exracellular signal-regulated kinase activation is regulated by sodium in endothelial cells. *J. Biol.Chem.* **274**, 20144-50.

Tsuboi, M., Eguchi, K., Kawakami, A., Matsuoka, N., Kawabe, Y., Aoyagi, T. Maeda, K., Nagataki, S. (1996) Fas antigen expression on synovial cells was down-regulated by interleukin 1 beta. *Biochem. Biophys. Res. Commun.* **218**, 280-5.

Turner, J.R., Tartakoff, A.M. (1990) On the relation between distinct components of the cytoskeleton: an epitope shared by intermediate filaments, microfilaments and cytoplasmic foci. *Eur. J. Cell. Biol.* **51**, 259-64.

Unkles, S., McDevitt, T., Voy, C., Kinghorn, J.R., Cramb, G., Lamb, J.F. (1988) The effect of groeth in monensin on internal sodium, alpha sub-unit mRNA and sodium pump density in human cultured cells. In: Skou, J.C. Norby, J.G., Maunsbach, A.B., Esmann, M. eds. The Na^+, K^+ ATPase, Part B*: Cellular Aspects*. New York: Alan R. Liss, 157-162.

Vaughan, G.L., and Cook, J.S. (1972) Regeneration of cation-transport capacity in HeLa cell membranes after specific blockade by ouabain. *Proc. Natl. Acad. Sci. U S A*, **69**, 2627-31.

Verrey, F., Schaerer, E., Zoerkler, P., Paccolat, M.P., Geering, K., Kraehenbuhl, J.P., Rossier, B.C. (1987) Regulation by aldosterone of Na^+, K^+ ATPase mRNAs, protein synthesis, and sodium transport in cultured kidney cells. *J. Cell Biol.* **104**, 1231-7.

Verrey, F., Kraehenbuhl, J.P., Rossier, B.C. Aldosterone induces a rapid increase in the rate of Na^+, K^+ ATPase gene transcription in cultured kidney cells. (1989) *Mol. Endocrinol.* **3**, 1369-76.

von Heijne, G. (1995) Membrane protein assembly: rules of the game. *Bioessays*, **17**, 25-30.

Waldmann, R., Champigny, G., Voilley, N., Lauritzen, I., Lazdunski, M. (1996) The mammalian degenerin MDEG, an amiloride-sensitive cation channel activated by mutations causing neurodegeneration in *Caenorhabditis elegans*. *J Biol Chem*, **271**, 10433-6

Wang, N., Butler, J.P. and Ingber, D.E. (1993) Mechanotransduction across the cell surface and through the cytoskeleton. *Science*, **260**, 1124-27.

Wilson, P.D., Sherwood, A.C., Palla, K., Du, J., Watson, R., Norman, J.T. (1991) Reversed polarity of Na^+, K^+ ATPase: mislocation to apical plasma membranes in polycystic kidney disease epithelia. *Am. J. Physiol.* **19260**, F420-30.

Wolfe, S.L. (1993) Molecular and Cell Biology. Wadsworth Pub. Comp., California.

Wolitzky, B.A., Fambrough, D.M. (1986) Regulation of the Na^+, K^+ ATPase in cultured chick skeletal muscle. Modulation of expression by the demand for ion transport. *J. Biol. Chem.* **261**, 9990-9.

Wong, M.K., Gotlieb, A.I. (1986) Endothelial cell monolayer integrity. I. Characterization of dense peripheral band of microfilaments. Arteriosclerosis, **6**, 212-9.

Wong, A.J. Pollard, T.D. (1983) Actin Filament Stress Fibers in Vascular endothelial cells in vivo. *Science,* **249**, 867-69.

Watson, A.J., Levine, Donowitz, M., Montrose, M.H. (1993) Serum regulates Na+/H+ exchange in Caco-2 cells by a mechanism which is dependent on F-actin *J. Biol. Chem.* **267**, 956-62.

Woolfson, R.G., Poston, L. Graves, J.E. (1993) Effects of sodium-transport inhibition in human resistance arteries. *J. Cardiovasc. Pharmacol.* **2**, 1-3.

Yu, X., Chamberland, H., Lafontaine, J.G., Tabaeizadeh, Z. (1996) Negative regulation of gene expression of a novel proline-, threonine-, and glycine-rich protein by water stress in *Lycopersicon chilense*. Genome, **39**, 1185-93.

Vander, A.J., Sherman, J., Luicand, D. (1998) Human Physiology: the Mechanisms of the Body. Boston, Mass., WCB/McGraw-Hill.

Vogel, S. (1994) Life in Moving Fluids: The physical biology of flow. Princeton University Press, N.J., 467pp.

Yoda, A., Yoda, S. (1988) Interaction between ouabain and the phosphorylated intermediate of Na^+, K^+ ATPase. *Mol. Pharmacol. Res.* **192**, 93-101. **22**, 700-8.

DIWEDD